STRUCTURAL AND METABOLIC STUDIES ON NORMAL AND PATHOLOGICAL BONE

by

Robert A. Dodds

Thesis presented for the degree of
Doctor of Philosphy in Brunel University

Department of Biochemistry

January, 1985

Division of Cellular Biology
The Mathilda and Terence Kennedy Institute
of Rheumatology, Hammersmith, London W6 7DW.

Brunel University, Uxbridge

Department of Biochemistry.

Robert A. Dodds

Structural and Metabolic Studies on Normal and Pathological Bone

1985

Abstract

Bone is refractory to most conventional biochemical procedures. However because it is now possible to cut sections (e.g. 10μm) of fresh, undemineralized adult bone, this tissue can be analyzed by suitably modified methods of quantitative cytochemistry. A new substrate for assaying hydroxyacyl dehydrogenase activity demonstrated that bone cells may use fatty acids as a major source of energy: detailed analysis of the activities of key enzymes indicated that the paradox of 'aerobic glycolysis' of bone could be explained by fatty acid oxidation satisfying the requirements of the Krebs' cycle and directing the conversion of pyruvate to lactate The influence of glucose 6-phosphate dehydrogenase (G6PD) activity in aerobic glycolysis has been considered. The inverse relationships between this activity and that of Na-K-ATPase led to the development of a new method for the latter, based on a new concept in cytochemistry ('hidden-capture' procedure).

A major feature of fracture-healing is increased periosteal G6PD activity. The association with the vitamin K cycle has been investigated by feeding rats with dicoumarol which not only inhibited bone-formation but also G6PD activity. The stimulation of this activity in fracture-healing has been linked with ornithine decarboxylase (ODC) activity, for which a new method has been developed. Rats deficient in pyridoxal phosphate (cofactor for ODC) had decreased G6PD responses and also appeared to become osteoporotic. Studies on osteoporotic fractures in the human showed the presence of relatively large apatite crystals close to the fracture-site, and disorganized glycosaminoglycans (demonstrated by the new method of 'induced birefringence').

ACKNOWLEDGEMENT

I gratefully acknowledge Dr. J. Chayen, for giving me the opportunity to do this thesis and for his advice and inspiration given to me along the way.

I am indebted to Dr. Lucille Bitensky for all her help, advice and persistence.

I would like to thank all my colleagues in the Cell Biology Division, past and present, but special thanks go to Dr. Nigel Loveridge, Dr. Brian Henderson, Mr. Jack Johnstone, Dr. Jane Dunham, Dr. Neil Kent, Dr. Menachem Nahir and Dr. John Hart, with whom I had the pleasure of working. I thank them for their advice and encouragement.

I would also like to thank Mr. L. Klenerman and Mr. A. Catterall for their help in the clinical aspects of the thesis.

Many thanks go to: Ann Lewtas for her efficiency and understanding in the typing of this thesis, and to Miss J. McClelland for typing the legends.

I thank Lorraine for all her patience and understanding and also for typing the bibliography.

CONTENTS

CHAPTER I.

GENERAL INTRODUCTION

Bone is a major tissue-component of the body. Although a great deal of work has been done on its various biomechanical and bioelectrical properties, it has proved to be remarkably recalcitrant to other forms of investigation. Thus sections of bone are studied by histopathologists for diagnostic purposes: these sections are usually of pieces of bone, ground down to a thickness suitable for histological examination; or of methacrylate - embedded bone; or of decalcified bone that has been embedded in paraffin wax. Such special bone investigations are normally done only in a few, specialized laboratories. One of the major centres for this type of work is that of Professor R. Burkhardt, in Munich which reported that, unfortunately, such methods have not been successful for the application of enzyme or immuno-histochemistry, as would be required for extending the diagnostic use of such bone biopsies (Bartl et al, 1978).

As regards the chemistry on bone, a great deal of work has been done on the components of the matrix, including studies on collagen, the glycosaminoglycans, and the mineral component of bone (as reviewed in Bourne, 1976). Relatively little has been done on the metabolism of the various types of bone cells in intact bone, largely because bone does not readily lend itself to conventional biochemical investigations.

Thus the refractoriness of bone to conventional procedures of study has impeded advances in knowledge of its metabolism and of the possible interaction between the various cells and the matrix. Consequently, the demonstration that fresh, undemineralized adult bone could be sectioned, by suitably modified but relatively conventional cryostat microtomy (Johnstone et al, 1972; Johnstone, 1979), opened the way to detailed analysis of this tissue. The earlier studies, in this laboratory, concentrated on major changes during fracture-healing (Shedden et al, 1976; Dunham et al, 1977). Following these studies, it was found (Hauschka et al, 1978) that mineralization might involve a cycle of events in which vitamin K_1 played a major role. This finding, discussed in detail in Chapter III, was a major stimulus for the investigations detailed in this thesis. Thus it was first demonstrated that elevated production of NADPH was associated with the early deposition of bone (Chapter VII). Dicoumarol was used to inhibit the vitamin K_1-cycle to test whether or not this cycle was operative in the fracture-healing in the rat. The results (Chapter VIII) were in accord with this hypothesis, but they showed that dicoumarol also influenced the production of NADPH which, together with vitamin K_1, was apparently essential for bone-formation.

These finding led to the enquiry as to what chemical stimulus might be involved in the increased production

of NADPH. From other studies in progress in this laboratory there seemed a fair possibility that putrescine, produced by ornithine decarboxylase (ODC) activity (discussed in Chapter IV) might be at least one of the material stimulators of glucose 6-phosphate dehydrogenase (G6PD) activity, and of the increased production of NADPH. Two lines of approach were investigated. The first involved trying to develop a cytochemical assay of ODC activity (Appendix II). For the second, the rats were kept on a diet that was deficient in vitamin B_6, so that they were expected to be deficient in pyridoxal phosphate, which is the essential cofactor for ODC activity. The results of this study (Chapter IX) were in accord with the hypothesis. However, the results involved such an overwhelming change in the nature of the bone that they open new lines of investigation, particularly in regard to osteoporosis.

The problem of osteoporosis is one of the major challenges in bone pathology and in rheumatology. Of particular moment are the hitherto unexplained fractures of the neck of femur, often induced by minimal trauma, in osteoporotic subjects. Such fractures have been investigated in some detail (Chapter X). Simple inspection of the sections taken from the fracture site showed the presence of unexpectedly large crystals, apparently of apatite. The development of a method involving the induced birefringence of the glycosaminoglycans (GAGS) showed that whereas they appear to be

orientated close with the collagen in the normal bone, they were disorientated in the fractured bone. The results required detailed investigation (Kent et al, 1983) so that the proposed enzymatic studies, akin to those done on fracture-healing in the rat, had to be delayed. However it was found that the circulating levels of vitamin K_1 were depressed in these patients (Hart et al, 1984) so that it is likely that studies in these fractures on the activity of glucose 6-phosphate dehydrogenase, generating NADPH for the vitamin K-cycle, may be of interest.

CHAPTER II

THE STRUCTURE AND BIOCHEMISTRY OF BONE

The Cells

The Osteocyte. Osteocytes, which develop from osteoblasts, are spidery shaped cells, found within the bone matrix in lacunae from which anastomosing canaliculi radiate. They have as many as fifty long, fine branching cytoplasmic processes (Bélanger, 1971) which, in newly formed bone, fully occupy the canaliculi. With maturity these cells become flatter and the processes gradually retract.

The functional role of osteocytes is not known but they probably play a role in maintaining the matrix. It has been suggested (as reviewed by Bélanger, 1971) that osteocytes may facilitate the exchange of materials between tissue fluids and bone matrix and that they possibly synthesize and resorb the surrounding matrix.

Osteoblasts. The osteoblasts are responsible for the synthesis and secretion of components of bone matrix (e.g. collagen,proteoglycans and glycoproteins) (as reviewed by Cameron, 1972). Newly synthesized, not yet calcified matrix is termed osteoid; calcium phosphate crystals are then deposited in the osteoid, changing it to bone matrix (as reviewed by Pritchard, 1972). Osteoblasts are found on the surfaces of bone tissue usually as a single layer. It is claimed (Owen, 1983) that below the osteoblast layer there may be a mixed

population of proliferating cells, often termed osteoprogenitor cells. These cells develop into osteoblasts and osteoclasts. The current theory is that there may be two types of osteoprogenitor cells: preosteoblasts and preosteoclasts (as reviewed by Owen, 1971, 1983; Ascenzi, 1976) that have differentiated along divergent lines from a fixed mesenchymal precursor. Morphological studies indicate that osteoblasts, like chondrocytes, secrete membrane-bound matrix vesicles which are strongly implicated in the calcification mechanisms (as reviewed by Anderson, 1976).

Osteoclasts. Osteoclasts are large, motile, multinucleated cells found upon bone surfaces (often in shallow pits called the lacunae of Howships), which are undergoing resorption, as shown by the solubilization both of mineral and of the organic components of bone. They are believed also to engage in the elimination of the resulting debris formed during bone resorption. However the processes involved are still not well understood. Reviews of the osteoclasts themselves and the process of bone resorption are given by Hancox (1972), Cameron (1972), Marks and Walker (1976) and Reynolds (1983). Osteoclasts contain numerous membrane-bound vesicles, thought to be lysosomes. Vaes (1969) has reviewed the evidence that hydrolases associated with the lysosomes of osteoclasts are essential for the resorption of organic components of bone matrix, and

possibly contribute to the solubilization of the mineral. The hydrolytic enzymes will be discussed briefly in another section.

The Organic Matrix of Bone

Collagen. Collagen is the principle organic component of bone (as reviewed by Herring, 1972; Stockwell, 1979). Its composition is distinctive: one-third of its total amino acids consists of glycine, one-ninth is alanine, and two-ninths proline and hydroxyproline. The basic unit of collagen is the polypeptide α chain; upon denaturation, the collagen macromolecules (tropocollagen) dissociate into three α chains. The tropocollagen molecule of bone consists of two α_1 and one α_2 chains coiled around each other in a right-handed helix. This is in the form of a long thin rod of about 2800 Å in length and 14 Å in diameter, and has a molecular weight of about 300,000. The tropocollagen molecules are organized into fibrils forming native collagen. This long helical molecule gives bone both its tensile properties and overall shape (as discussed later).

The Glycosaminoglycans. Glycosaminoglycans (GAGs) are long unbranched polysaccharide chains which contain many acidic groups (carboxylate and sulphate groups). They do not exist as free chains but as proteoglycans in which the chains are covalently linked by the terminal sugar residue to a protein. On the basis of different

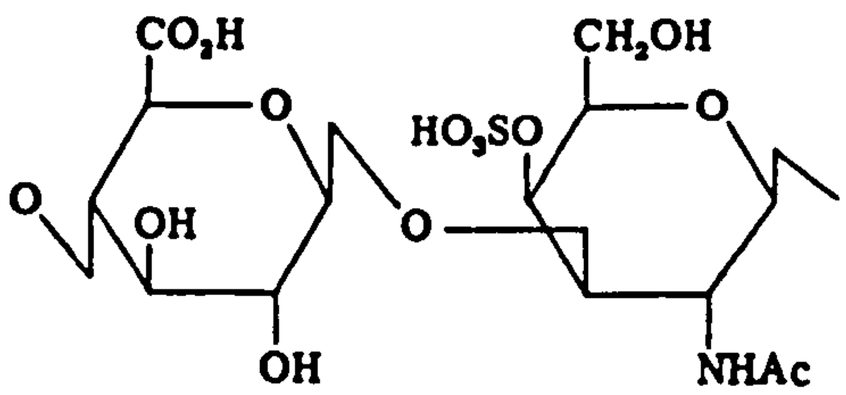

(I)

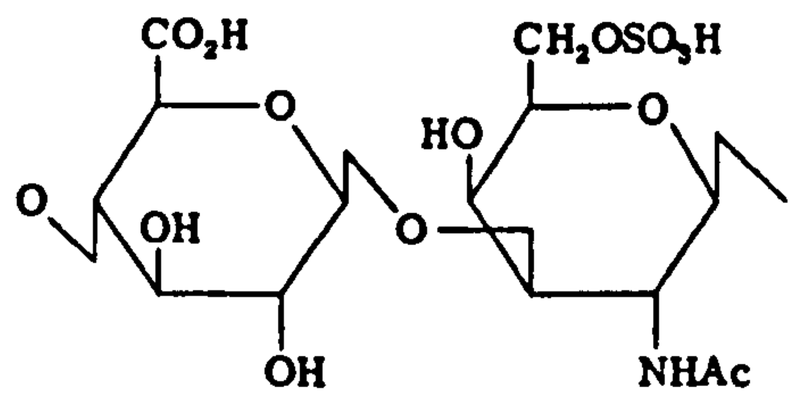

(II)

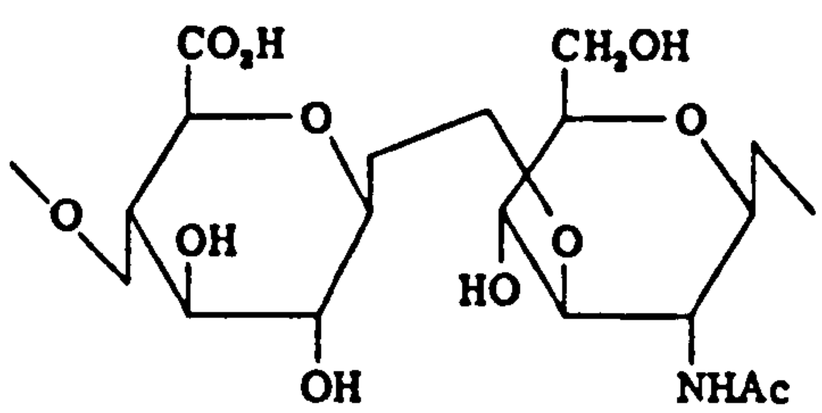

(III)

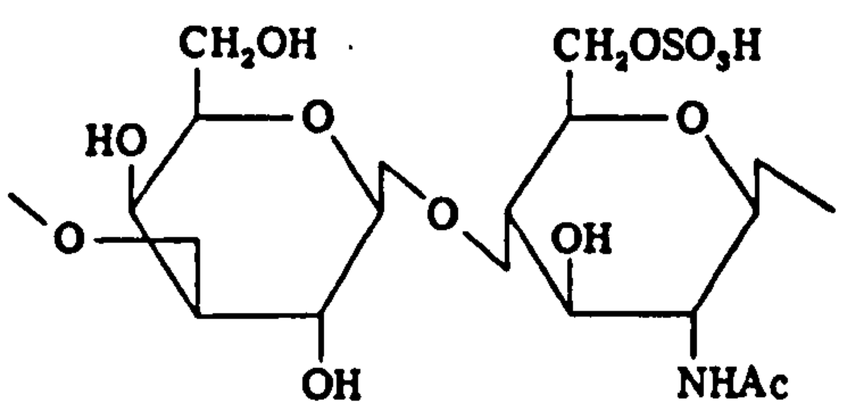

(IV)

Fig. II. 1. The structure of the repeating disaccharides units that occur in glycosaminoglycans. I : chondroitin 4-sulphate II : chondroitin 6-sulphate III : hyaluronateand IV : keratan sulphate.

repeating disaccharidge units, there are seven types of GAGs (Table II, 1; taken from Hardingham, 1981). Fig. II.1 gives the structures of the repeating disaccharide units of the GAGs: chondroitin 4-sulphate, chondroitin 6-sulphate, hyaluronic acid, and keratan sulphate. Cartilage has an extremely high proteoglycan content and the details of their structure have been studied in detail and are better understood than in bone (as reviewed by Muir and Hardingham, 1975; Hardingham, 1981). Fig. II.2 is a schematic model of the aggregation of cartilage proteoglycans (taken from Hardingham, 1981).

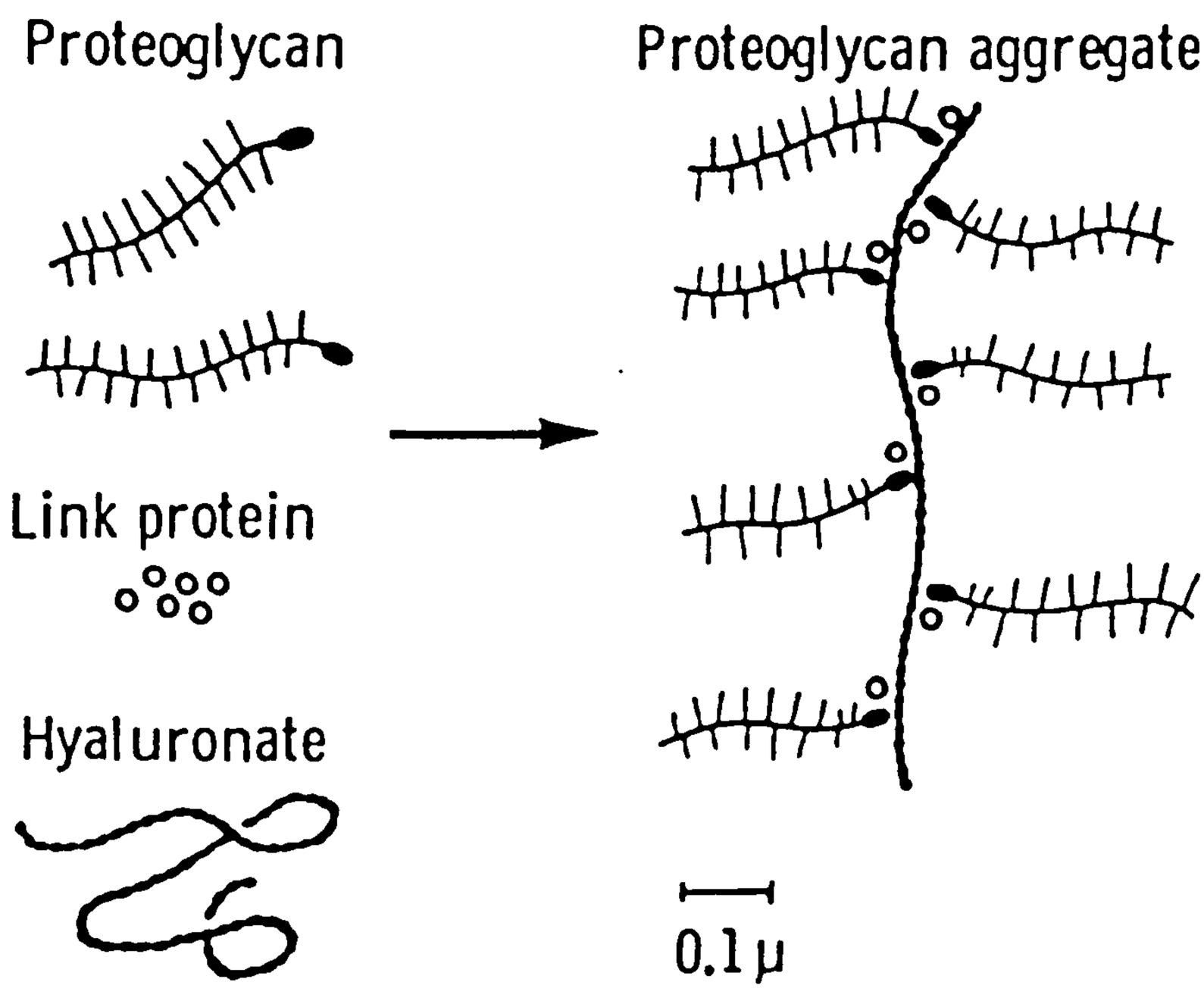

Fig. II. 2 Diagrammatic representation of a model of the structure of proteoglycans. (From Hardingham, 1981).

Table II. 1. Composition of mammalian glycosaminoglycans. From Hardingham, 1981.

	Disaccharide repeating unit			
	Hexuronic acid	Hexosamine*	Sulphate	Linkage to protein
Hyaluronic acid	D-Glucuronic acid	D-Glucosamine	—	?
Chondroitin 4-sulphate	D-Glucuronic acid	D-Galactosamine	*O* Sulphate	-Gal Gal Xyl Ser
Chondroitin 6-sulphate	D-Glucuronic acid	D-Galactosamine	*O* Sulphate	-Gal Gal Xyl Ser
Dermatan sulphate	L-Iduronic acid or D glucuronic acid	D-Galactosamine	*O* Sulphate	-Gal Gal Xyl Ser
Keratan sulphate	D-Galactose	D-Glucosamine	*O* Sulphate	(*a*) skeletal: -GalNAc Ser(Thr) / AcNeu Gal (*b*) corneal: -GalNAc-Asn Gal Gal Xyl Ser
Heparan sulphate	D-Glucuronic acid or L iduronic acid	D Glucosamine	*O* Sulphate and *N* sulphate	
Heparin	D Glucuronic acid or L iduronic acid	D Glucosamine	*O* Sulphate and *N* sulphate	-Gal Gal Xyl Ser

* Always *N*-acetylated, except when *N* sulphated.

In this model the protein backbone is composed of a globular region with intramolecular disulphide bridges that form a specific site for binding to hyaluronate and to a link protein. Next to this region is an extended polypeptide rich in keratan sulphate chains. The largest portion is again a long polypeptide containing a proportion of the chondroitin sulphate chains; it is proposed that this region is of variable length.

Other Bone Proteins. Apart from collagen, discussed briefly above, bone contains several other proteins most of which are, as yet, but poorly defined. For example, a specific bone sialoprotein has been reported (Herring, 1972). The most characteristic bone peptide is osteocalcin, which will be considered in detail in Chapter III . It is clear that other, glutamate-rich peptides also occur; unlike osteocalcin, these are not readily removed from bone and are not yet characterized. The non-collagenous proteins of bone has been the subject of a recent study (Delmas et al, 1984).

The Nature of the Mineral

The mineral component of bone contains calcium, phosphate and carbonate, with fluoride and sometimes aluminium as minor components. The characteristic mineral is hydroxyapatite, which is commonly written as 3 $Ca_3 (PO_4)_2$ Ca $(OH)_2$ (Merck, 1968); or

Ca_{10} $(PO_4)_6$ $(OH)_2$; it is related to apatite ($3Ca_3$ $(PO_4)_2$ Ca F_2). A calcium carbonate may also be mixed together with the hydroxyapatite (Robinson, 1952).

There have been many studies on the crystalline nature of the hydroxyapatite in bone (Robinson, 1952; Carlstrom, 1955; Bernard, 1969; Bocciarelli, 1970; Engstrom, 1972; Voegel and Frank, 1977 and Jackson et al, 1978). Most investigators seem to agree that the size of the crystals of normal bone is about 100 nm (range 500 - 50 nm). It is noteworthy that x-ray crystallographic analysis of the crystal structure requires prior heating to at least 400° C, preferably above 600° C, to give clear x-ray diffraction patterns. Thus it is not impossible that the normal state is poorly crystalline until the hydroxyapatite is influenced by other factors, such as temperature or age (as discussed in Chapter IX).

Bone Tissue

Periosteum and Endosteum

The internal and external surfaces of mammalian bones are covered by layers of connective tissue named endosteum and periosteum respectively (Fig. II.3).

The periosteum consists of two layers being very fibrous externally but more cellular near the bone tissue. The periosteal cells resemble fibroblasts and are able to divide and differentiate into osteoblasts

a

b

c

d

e'

f

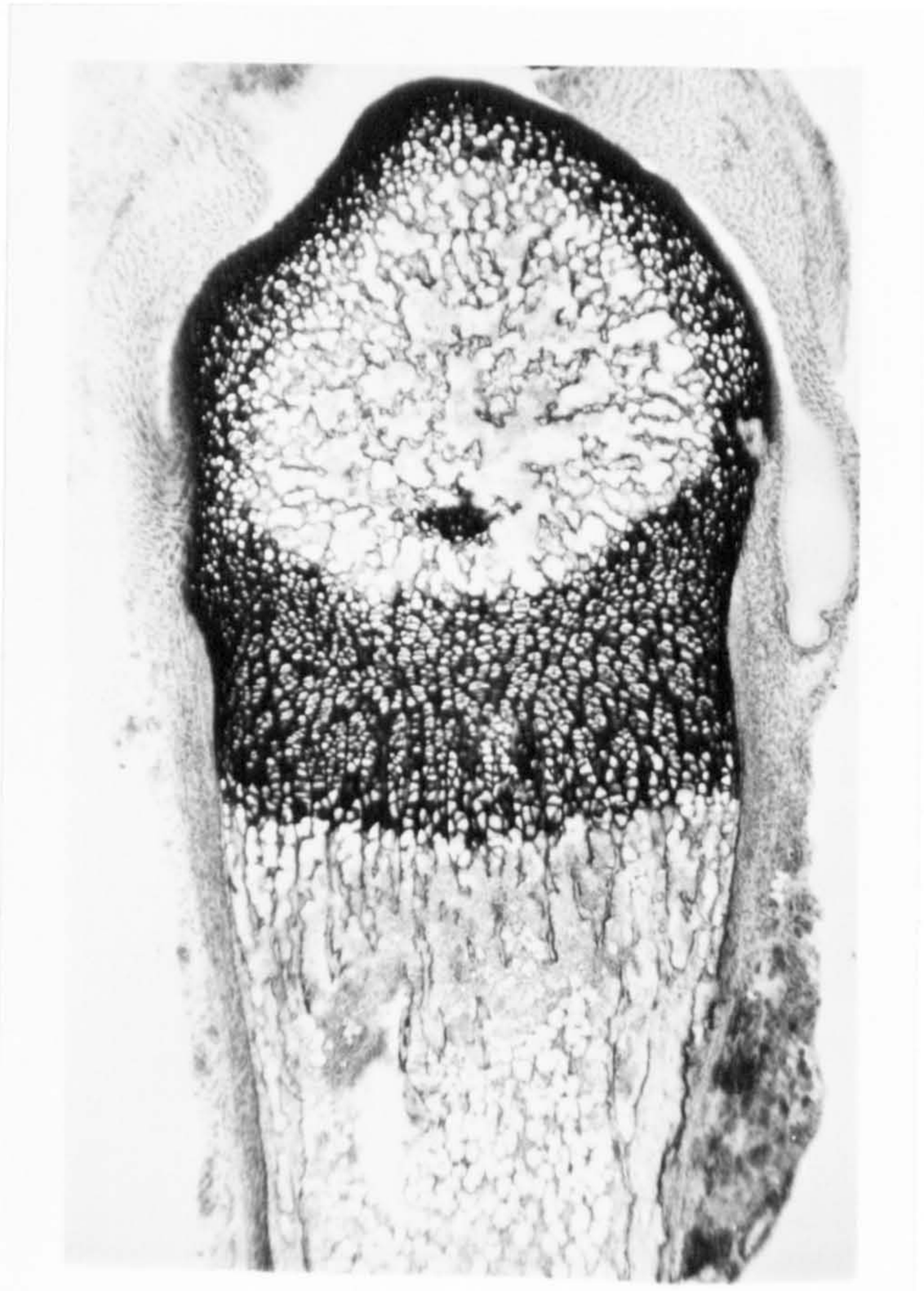

Fig. II . 3. Cryostat section of the rat metatarsal head and shaft.

(a) articular cartilage (b) epiphyseal cancellous bone

(c) epiphyseal growth plate (d) metaphyseal trabeculae

(e) cortical bone of shaft (f) bone marrow cavity.

Toluidine bone, X 35.

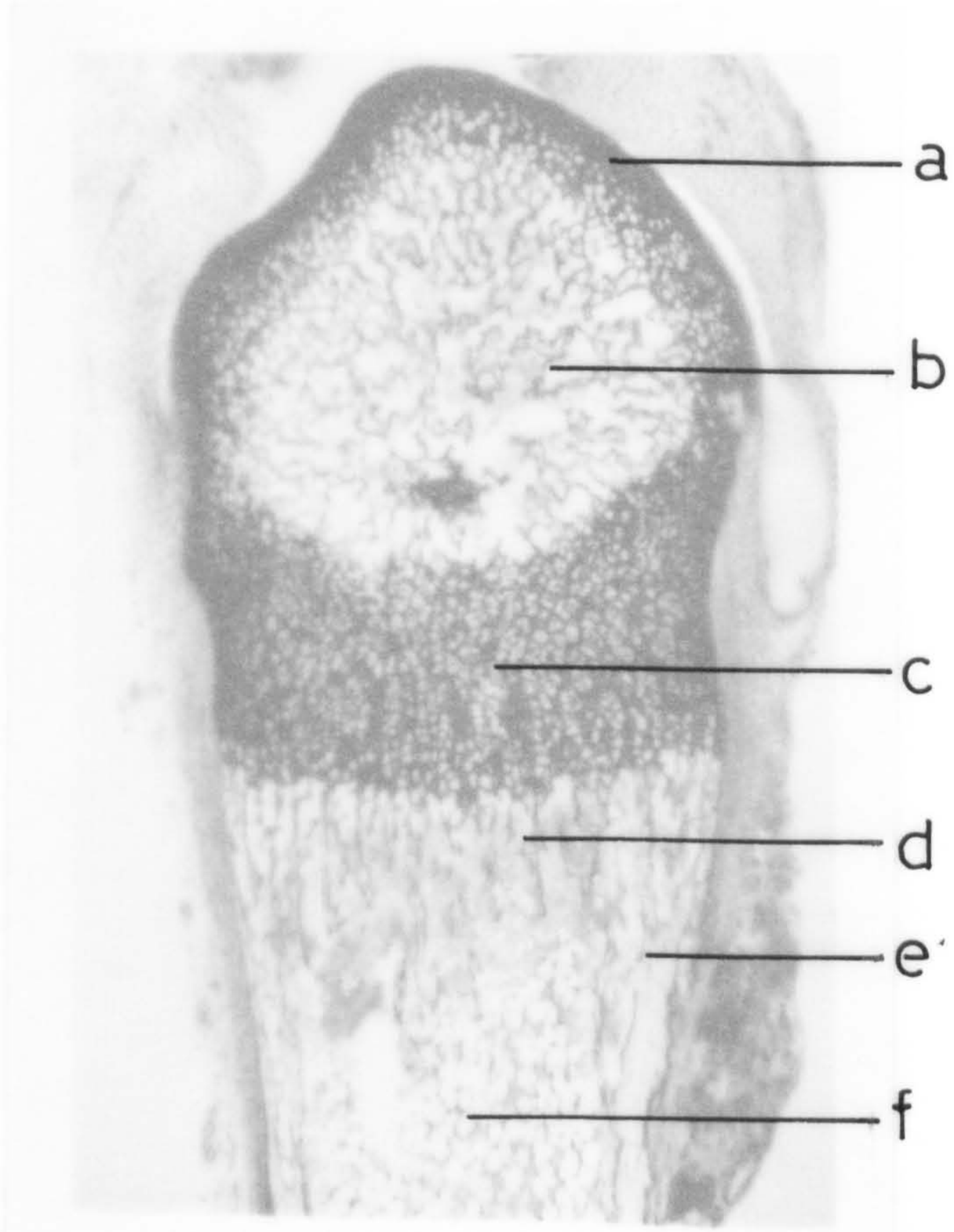

Fig. II . 3. Cryostat section of the rat metatarsal head and shaft.

(a) articular cartilage (b) epiphyseal cancellous bone

(c) epiphyseal growth plate (d) metaphyseal trabeculae

(e) cortical bone of shaft (f) bone marrow cavity.

Toluidine bone, X 35.

and chondrocytes. These cells have an essential role in bone growth and fracture repair (as discussed in Chapter VII and reviewed by Ham and Harris, 1971).

The end osteum is much thinner, consisting of only one layer; it also plays an important role in bone growth.

Types of Bone Tissue.

The structure and histology of bone have been extensively reviewed (e.g. Pritchard, 1972; Junqueria, 1977). Macroscopically there are two distinguishable types of bone in the mature mammalian skeleton: the spongy (cancellous) bone and the hard compact cortical bone. Cancellous bone consists of fine irregular trabeculae, which branch and unite with one another forming a meshwork of interconnecting cavities filled with marrow. The cortical bone shows dense areas without cavities.

In long bone, the extremities (called the epiphyses) are composed of cancellous bone covered by a thin layer of cortical bone (Fig. II.3). The cylindrical part of the bone, called the diaphysis, is mainly compact, cortical bone, with a small amount of cancellous bone in the bone marrow cavity (not present in the rat metatarsal; Fig. II.3). Likewise, the short bones have a core of cancellous bone completely encased by cortical bone.

Within the cavities of cancellous bone and the marrow cavity of the diaphysis of long bones exists

bone marrow: the red bone marrow from which the blood cells form; and the yellow bone marrow, consisting mainly of large fat cells.

Woven Bone. The first bone to appear in embryonic development or in the early fracture callus is immature. It forms very rapidly and rather erratically. The collagenous fibres are arranged in an irregular array. The bone consists of anastomosing trabeculae that resemble a honey-comb. The intertrabecular spaces contain small blood vessels and osteogenic cells. The cells next to the bone are osteoblasts, forming a regular, one-cell thick 'epithelium'. If such bone is laid down on a scaffolding of calcified cartilage, as in the growth plate, and developing fracture callus, the core of the bone may contain remnants of this calcified cartilage.

As soon as the woven bone is formed it is remodelled, some of the trabeculae being removed altogether by osteoclasts, while others are further thickened by the osteoblasts laying down extensive osteoid on the surface of the woven bone, prior to its mineralization. This remodelling gives rise to secondary bone, namely the cortical and cancellous bone.

Compact Cortical Bone

Secondary bone, whether cortical or cancellous, characteristically shows collagenous fibres arranged in lamallae, 3 - 7 μm thick, which are parallel or concentrically curved around a vascular canal. The

whole complex of concentric lamellae, surrounding a canal containing blood vessels, nerves and loose connective tissue, is called the Haversian system or more correctly the osteon. Rat 'cortical bone' does not have the classical Haversian systems but contains long fibres of collagen often termed fibre bone.

Cortical bone arises partly (a) by thickening of woven bone whereby osteoblasts produce layer after layer of bone inwards on the surfaces of the vascular tunnels of the woven bone, until the canals are reduced to narrow canals containing the blood vessels; (b) partly by direct, primary formation of solid bone on the periosteal and endosteal surfaces of an existing bone surface: this bone persists as concentric lamellae; and (c) partly by the remodelling of existing cortical bone, whereby tunnels, containing blood vessels and marrow, are eroded and then replaced, as successive lamellae of bone are deposited, progressively inward, until the tunnel is reduced to a narrow canal around the blood vessels. Resorption cavities appear continuously during growth of bone and even in adult bone, and are replaced by third, fourth, and higher orders of osteons. Therefore it is common to find developing osteons, that have large vascular canals lined with plump osteoblasts, and eroding osteons that have large irregular canals, lined with osteoclasts. Osteons that escape destruction become "interstitial lamellae" that fill in between new systems. Cortical bone may

also arise from the consolidation of cancellous bone.

Being essentially cylindrical, osteons, in sections, may appear with circular, elliptical or parallel-sided profiles, according to the plane of the section. In general, most osteons have their long axis almost parallel with the long axis of the bone. The circular profiles that appear are what are classically called Haversian systems. Secondary Haversian systems (i.e. sections of secondary osteons) are larger than primary osteons (around 100 μm in diameter) and, unlike primary osteons, their organization does not conform with adjacent osteons. They are bound externally by a clear cement line. Osteons run somewhat obliquely: they tend to spiral clockwise on the right and anticlockwise on the left and pass at an angle of about 30° from the periosteal to the endosteal lamellae. They branch, either anastomosing with neighbouring osteons, or ending blindly. (I am indebted to Mr. A. Catterall, FRCS., for his advice on this histology).

Within the osteon, osteocytes are arranged regularly and orientated with respect to the central vascular canal. The long axis of the spidery osteocyte conforms with the long axis of the osteon, its fine processes running in a radial fashion; the canaliculi of osteocytes anastomose freely with those of their neighbours. As mentioned earlier there is evidence suggesting that the normal mechanism of internal bone resorption occurs under the influence of mature osteocytes (reviewed by

Bélanger, 1971).

Cancellous Bone.

Cancellous bone of the adult mammal is very similar to that of cortical bone except that, rarely, are there complete osteons. Instead, the trabeculae consist of irregular haphazard fragments of osteons (Fig. II.3 shows the cancellous bone in the epiphyseal end of the rat metatarsal). They have very irregular indented outlines resulting from extensive resorption and deposition. Where new bone is being added to the trabeculae of the cancellous bone, the surfaces are covered with plump active osteoblasts. Similarly, osteoclasts are present where the trabecular surface is being eroded.

The Growth of Bone.

The growth of bone is fully discussed by Sissons (1971) and Stockwell (1979). There are two types of bone formation. The first is known as membranous ossification, which concerns the direct appositional formation of bone on a pre-existing surface, for instance periosteal and endosteal bone growth in the long bones. The second type is known as endochondrial ossification, which occurs only when an epiphyseal plate is present, or as described in Chapter VII, in new bone formation during fracture healing.

During active growth of bone, endochondrial ossification is the mechanism concerned with the rapid development in length and mass of the bone. The epiphyseal plate, or cartilaginous growth-plate is siutated between

the epiphysis and the shaft of a long bone (Fig. II.3). The chondrocytes are arranged in columns that are parallel to the long axis of the bone (Fig. II.4). Five zones are recognized, corresponding to the various phases of the maturation process.

1. resting zone (hyaline cartilage);
2. proliferative zone, with stacks of flattened cells;
3. hypertrophic zone, with enlarged chondrocytes;
4. degenerative zone, with calcified matrix;
5. ossification zone, with the appearance of bone material.

There are two surfaces to the growth plate: the epiphyseal surface and the metaphyseal surface (Fig. II.3). Endochondrial ossification consists of the coordinated sequence of multiplication, growth and degeneration of chondrocytes in this growth plate followed by the vascularization of the degenerated hypertrophic chondrocytes by capillaries and undifferentiated cells originating from the periosteum.

In the hypertrophic zone, the matrix is reduced to a thin septum between the chondrocytes. It is these thin septa that are calcified with thedeposition of hydroxyapatite, following the degeneration of the chondrocytes. The invading undifferentiated cells that originated from the proliferating periosteum form osteoblasts: they form a layer over the septa; these osteoblasts

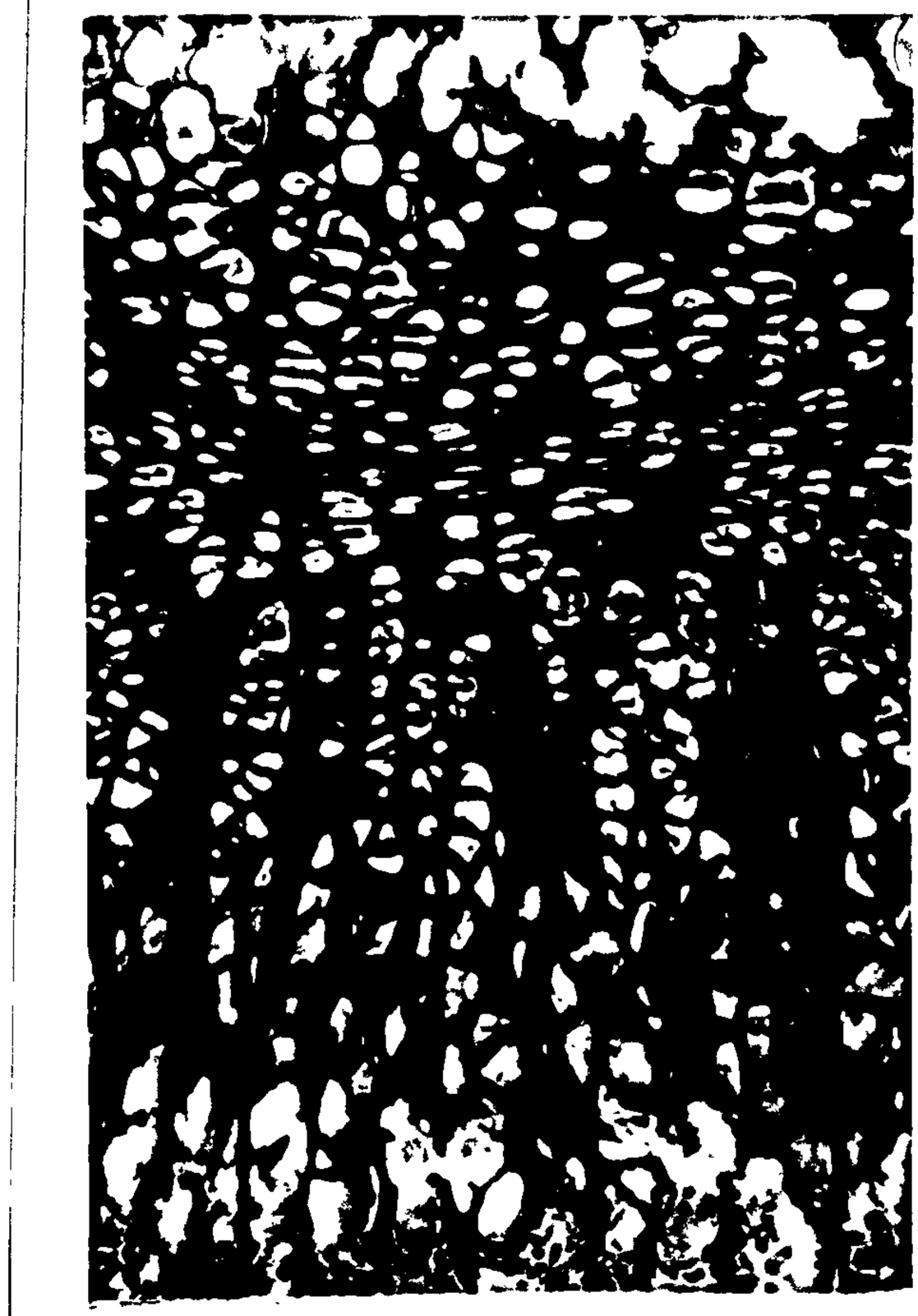

Fig. II. 4. Cryostat section of the rat epiphyseal growth plate; the resting zone is at the top of the plate and the ossification zone appears on the lower end. Toluidine blue; X 220.

lay down the bone matrix. This bone matrix calcifies and some of the osteoblasts are imprisoned as osteocytes. In this way a network of bone trabeculae is formed on the framework of the unresorbed septa. Thesemetaphyseal bone trabeculae extend continuously into the receding zone of hypertrophic cartilage, and thus increase the length of the bone shaft. This new bone tissue is extensively remodelled: simultaneously with the laying down of new bone on the calcifying matrix, the central trabeculae are continually resorbed; and there is a progressive reduction of the trabeculae in this region. The peripheral metaphyseal trabeculae contribute to the diaphyseal development by being incoporated into the diaphysis. The shaft bone that eventually replaces the metaphyseal trabeculae is almost devoid of trabecular structure and, in contrast to the cancellous bone of the metaphysis, consists of compact bone (described earlier). In the rat, the 'compact bone' of the shaft does not show the classicaly arranged osteons, but exists in a simple lamellar form. While these changes occur, bone is being laid down immediately beneath the periosteum on the shaft of the bone, this being the final stage in endochondrial ossification (membranous ossification). The bone increases in width as a result of this bone formation by the periosteum. Simultaneously, bone is resorbed from the internal surface, increasing the diameter of the bone marrow cavity. Similarly, at the metaphysis, owing to endosteal bone formation, bone is also deposited on the internal surface, and again there is continued resorption, around this area

on the external surface. It is the partial resorption of newly formed bone, coupled to the laying down of new bone, that permits the shape of the bone to be maintained as it grows. In man the growth plate stops growing at around 20 years of age: it is completely replaced by cancellous bone. Thus the extremities of long bones (epiphyses) are composed of cancellous bone. As discussed earlier, remodelling is considerably active in this cancellous bone when compared to cortical bone. In our laboratory, growth-plate closure has not been seen in the rat, although there appears to be a close relationship between the rate of growth of an epiphyseal plate and its thickness, in that younger rats have a thicker growth plate.

Even in adult life, bone (both cancellous and cortical) is subject to an almost continuous process of structural remodelling, involving successive cycles of bone deposition and resorption. The maintenance of normal bone structure depends on a balance between these two processes.

Enzyme Biochemistry of Bone.

Relatively little work has been done on the metabolic biochemistry of bone. The paucity of information is due, to a large extent, to the refractory nature of the material and the sparse distribution of cells of different types. The practical difficulties encountered when conventional biochemical procedures are applied to bone have been considered by Hekkleman (1973) in a critical review of the enzyme biochemistry of bone.

The position is, if anything, even worse when histochemistry has been used since virtually all such studies have involved chemical fixation, followed by decalcification and embedding in paraffin wax, (Some biochemical and histochemical work, to which these structures do not fully apply, has been done on calvaria in embryos and very young animals). Thus the histochemical reports (e.g. Balogh et al, 1961, and reviewed by Fullmer, 1966) must be viewed with considerable scepticism.

In our laboratory, the ability to cut serial sections of adult unfixed, undemineralized bone (Johnstoneet al, 1972 and as discussed in this thesis) have overcome these difficulties, in that such sections can be examined by conventional methods of quantitative cytochemistry; in this way, biochemical activities can be related to histology, so avoiding the problems of tissue heterogeneity.

The Enzymes of Bone

Approximately 90% of the citrate present in the body of mammals is located in bone (Dixon and Perkins, 1952). Citrate has a strong affinity for calcium ions, forming a chelate complex. Several authors have shown that citrate is produced in bone. Dixon and Perkins (1952) demonstrated the presence of an enzyme presently known as citrate synthetase. This enzyme is responsible for the synthesis of citrate from oxaloacetate and acetyl-coenzyme A. Dixon and Perkins (1952) were, however, unable to detect the enzyme isocitrate dehydrogenase, the enzyme responsible for the breakdown of citrate

in the Krebs' cycle. They suggested that the production of citrate could possibly result from a block of the enzyme isocitrate dehydrogenase. In 1959, Van Reem did demonstrate the presence of isocitrate dehydrogenase activity in diaphyseal bone, and thus discounted Dixon and Perkins earlier hypothesis.

An alternative explanation for the citrate production was described by Hekkelman (1973); it involves the inhibition, by calcium ions, of aconitase, the enzyme converting citrate into isocitrate in the Krebs' cycle. Hekkelman (1973) showed that the inhibition occurred by the formation of a calcium-citrate complex, which decreased the available substrate for the enzyme; moreover, the complex acts as a competitive inhibitor. Hekkelman (1973) also put forward another hypothesis: if the Embden-Meyerhoff pathway has a capacity far larger than that of the Krebs' cycle, lactate, and probably citrate will accumulate.

Bone produces a considerable amount of lactate, from glucose under aerobic conditions: this is known as aerobic glycolysis (Neuman, 1977; Brommage et al, 1977). This phenomena has been discussed fully in Chapter VI.

Cohn and Forscher (1962) used radioactively labelled substrate in studies on the relative capacity of the Krebs' cycle, glycolysis and pentose shunt in rabbit epiphyseal-metaphyseal bone slices. The yield of $^{14}CO_2$ and ^{14}C-lactate was assayed. They found that lactic acid wwas the major metabolic end-product of

glucose metabolism and that only minor amounts of labelled Krebs' cycle acids were formed. Approximately 15% of the lactate was formed from the pentose shunt and the remainder from the Embden-Meyerhof pathway. They showed that although the major portion of the $C^{14}O_2$ evolved by slices arose from the Krebs' cycle, the latter pathway seemed to play a minor role in the overall metabolism of the bone.

Hekkelman (1973) described a study in which the activities of a number of catabolic enzymes was determined in extracts of kidney, liver, brain and diaphyseal limb bone. The enzymes studied were: aconitase, isocitrate dehydrogenase, glucose 6-phosphate dehydrogenase and 6-phosphogluconate dehydrogenase. They found that aconitase and isocitrate dehydrogenase activities were low in bone when compared with other tissues, whilst the pentose shunt enzymes showed comparable activities. The ratios of the pentose shunt pathway enzymes over the Krebs' cycle enzymes were considerably higher in bone than in the other tissues (except brain). These results indicated the presence of a relatively high amount of the enzymes of the pentose shunt pathway in bone tissue.

Both osteoblasts and osteocytes possess the ability to synthesize collagen, and a great deal of work has been devoted to elucidating this process, particularly in relation to the post-transcriptional modification of proline, in protocollagen, to the characteristic amino acid of collagen, namely hydroxyproline. Almost

all this work has been done on tissues other than bone.

Hydrolytic enzymes play a critical role in bone resorption (reviewed by Vaes, 1969). Evidence suggests that the hydrolases, associated with the lysosomes of bone, are essential to the resorption of the organic components of the bone matrix, and possibly the solubilization of the mineral component. The hydrolytic enzymes of bone cells have not been extensively studied by standard biochemical methods, probably because of the difficulty of preparing valid homogenates or extracts from this hard tissue (as previously discussed). A summary of the information provided by histochemistry on hydrolytic enzymes in bone cells is presented in table II.2. As shown in Table II 2. acid phosphatase activity is present in all types of bone cells but is particularly active in the osteoclasts. Acid phosphatase activity is also observed extracellularly in subosteoclastic resorption zones. In direct contrast, there was negligible alkaline phosphatase activity in the osteoclasts whereas this enzyme was extremely active in the osteoblasts and to a lesser extent present in the osteocytes. Quantitative biochemical studies of several hydrolytic enzymes have been made on homogenates of bone (calvaria) from infant rats (reviewed by Vaes, 1969). The most important hydrolytic activities on numerous substrates were evidenced at acid pH values, especially those enzymes which degrade proteoglycans and their derivatives (hyaluronidase, β-glucuronidase,

Table II. 2. Distribution and hydrolytic enzymes in bone cells, as visualized by histochemistry. (From Vaes, 1969)

Distribution of hydrolytic enzymes in bone cells, as visualized by histochemistry.

Enzyme	*Osteoclasts*	*Osteoblasts*	*Osteocytes*	*References*
(a) Acid hydrolases				
Acid phosphatase	+ +	+	+	2–7, 10–12, 14, 19–22
Phosphoamidase	+ +	+	0	5, 15
β-glucuronidase	+ +	+	+	4, 5, 9, 22
β-galactosidase	+ +	+	+	16
β-glucosidase	+	+	+	17
(b) Other hydrolases				
Protease (gelatinase)	0	0	+	1
Alkaline phosphatase	0	+ +	+	2–4, 6, 11, 12
Aminopeptidase	+ +	+	+	2, 3, 13, 22
5′-nucleotidase	0	+	+ +	2, 8
Adenosine triphosphatase	+	+	+	2, 7, 18

Symbols 0: no activity; + : activity; + + : more activity.

References cited in Vaes (1969)

1 Bélanger and Migicovsky (1963)
2 Burstone (1960a)
3 Burstone (1960b)
4 Cabrini (1961)
5 Cabrini et al. (1962)
6 Changus (1957)
7 Doty et al. (1968)
8 Gibson and Fullmer (1967)
9 Gubisch and Schlager (1961)
10 Handelman et al. (1964)
11 Jeffree (1960)
12 Jeffree (1962)
13 Lipp (1959)
14 Schajowicz and Cabrini (1958)
15 Schajowicz and Cabrini (1964)
16 Schlager (1959)
17 Schlager (1960)
18 Severson et al. (1967)
19 Susi et al. (1966)
20 Tonna (1958)
21 Vaes and Jacques (1965a)
22 Warner (1964)

N-acetyl-β-glucosaminidase, and β-galactosidase); for the proteolytic actively measured with denatured haemoglobin as substrate (acid protease or 'cathepsin'); for the hydrolysis of deoxyribonucleic acid; and for the hydrolysis of ribonucleic acid and of phosphate monoesters (either phenylphosphate or β-glycerophosphate).

Alkaline phosphatase (non specific) has an extremely high specific activity in bone when compared with other tissues. Many hypotheses have been put forward concerning its function (especially its involvement in the calcification process) (as reviewed by Walker, P.G., 1973; Bourne, G.H., 1976). However, its function is still obscure.

CHAPTER III.

OSTEOCALCIN: A VITAMIN K-DEPENDENT CALCIUM-BINDING PROTEIN.

Vitamin K_1 has been associated with the blood clotting process and prothrombin since 1935 (as reviewed by Price, 1983). However it was not until the seventies that the molecular function of vitamin K was shown to be the post-translational γ-carboxylation of all glutamic acid residues in the first 40 N-terminal residues of prothrombin (Fig. 111.1) (Stenflo and Suttie, 1974; and as reviewed by Bell, 1978). The evidence suggests that the role of γ-carboxyglutamate residues in prothrombin as well as the other vitamin K-dependent blood coagulation factors is to promote their binding to the phospholipid vesicles released by blood platelets which have aggregated on the exposed collagen surfaces of damaged blood vessels. It is generally thought that the function of the Gla in this interaction is to serve as a Ca^{2+} chelator (Nelsestuen, 1978) by virtue of its two carboxy groups. The production of these calcium-binding γ-carboxyglutamate (Gla) residues was shown to be effected by a microsomal mixed-function oxidation -carboxylation reaction in which vitamin K_1, or a similar naphthoquinone substituted at the 3 position (Olsen et al, 1978), is reduced by NAD (P) H (Stenflo and Suttie, 1977; Suttie et al, 1978).

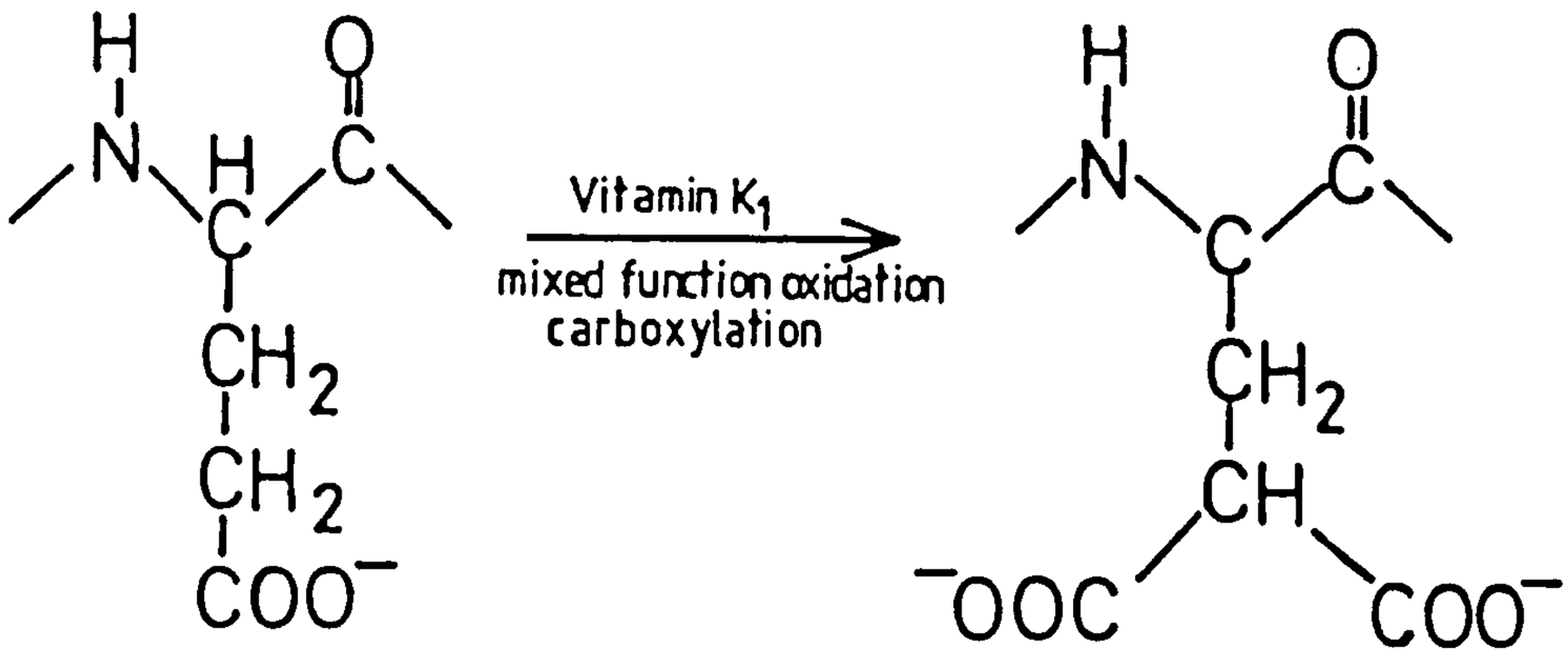

Fig. III. 1 The transformation of glutamate residues to γ-carboxy-glutamate(Gla) residues.

The reoxidation of the quinol is required for the process in which a proton is abstracted from the γ-methylene of a glutamate residue (Stenflo and Suttie, 1977). The resulting carbanion fixes carbon dioxide to form the γ-carboxyglutamate residue (Hauschka et al, 1978; Olsen et al, 1978). This is known as the vitamin K_1 cycle (Fig. III.2). The vitamin K_1 antagonists dicoumarol and warfarin are believed to inhibit to conversion of the epoxide to the quinone. Their structures are shown in Fig. III.3. When it was discovered that Gla was stable under conditions of alkaline protein hydrolysis, research into the presence of Gla in various Ca^{2+} binding proteins and tissue extracts led to the independent discovery by two groups of workers (Hauschka et al, 1975; Price et al, 1976a) of a hitherto unknown polypeptide, rich in Gla residues, in the bones of the chicken and the calf. This polypeptide, which could be extracted intact (Price, 1983), was called 'osteocalcin'.

- Distribution of Gla residues in Tissues.

One of the difficulties of evaluating the significance of osteocalcin, and of Gla residues generally, has been the fact that, initially, the presence of these residues was considered as indicative of the presence of osteocalcin. This has confused the issue because it now seems apparent that Gla residues can occur in other proteins in bone. It is therefore

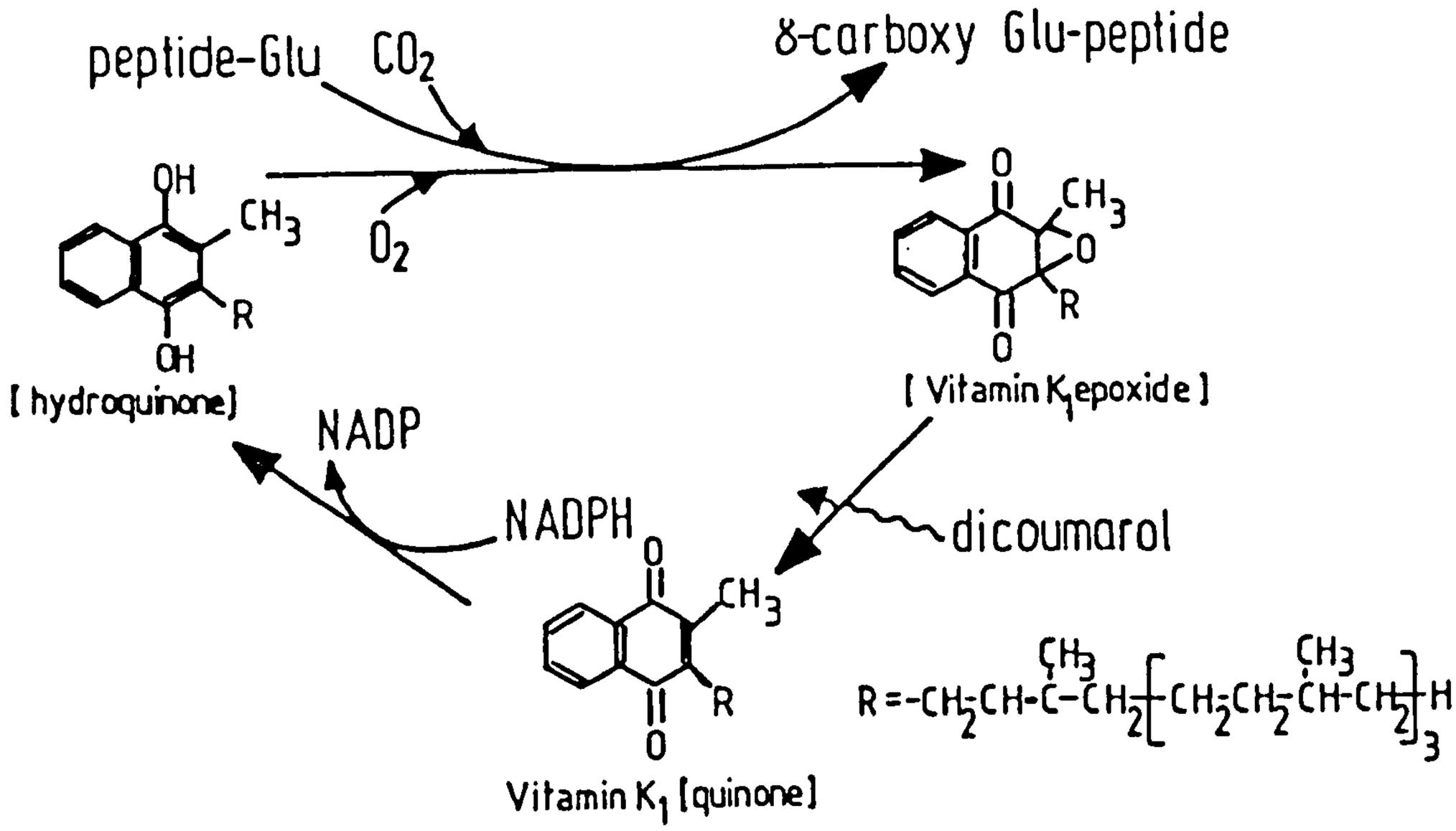

Fig. III. 2 Diagrammatic representation of the vitamin K cycle.

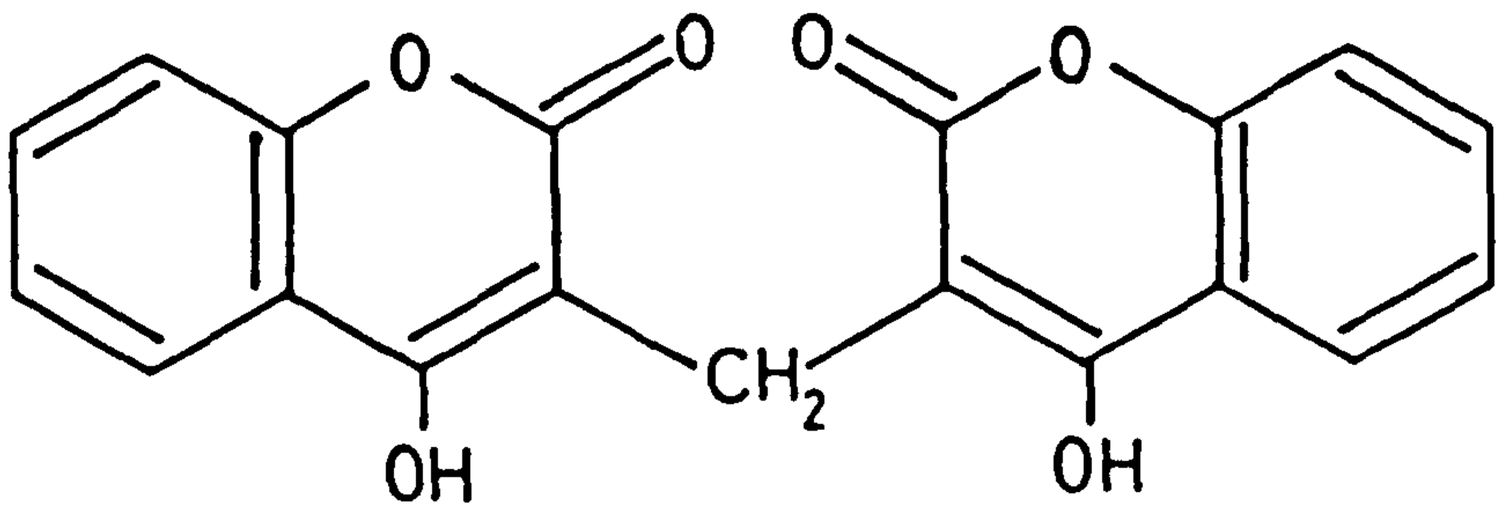

Dicoumarol

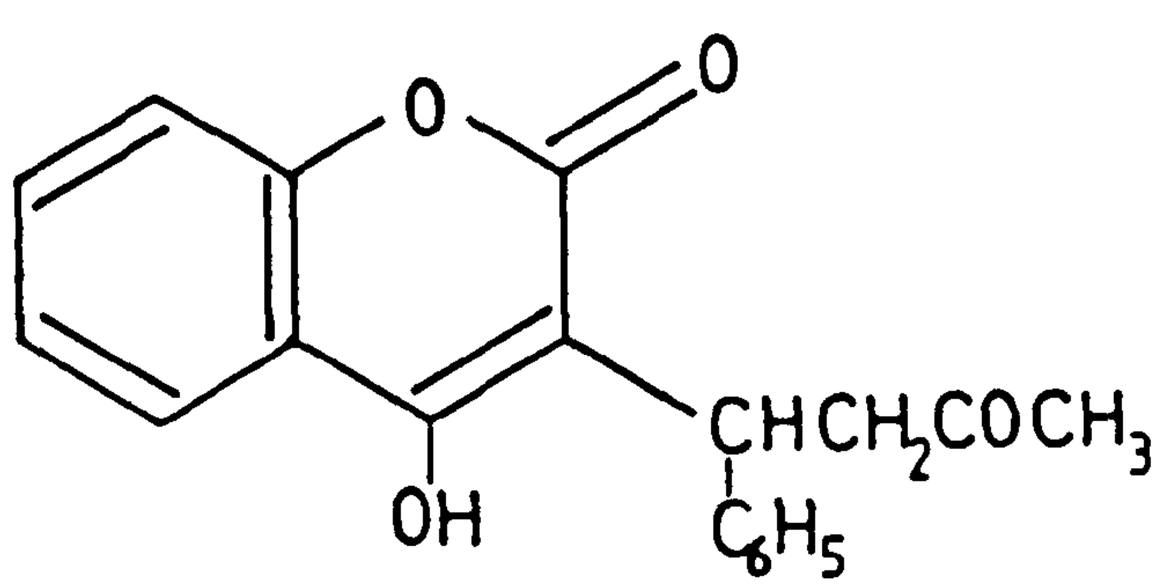

Warfarin

Fig. III. 3 Structural formulae of dicoumarol and warfarin.

necessary, in evaluating published reports, to distinguish whether they refer to the distribution of Gla residues, to the isolated osteocalcin, or to radioimmunoassay results ostensibly based on antibodies to osteocalcin.

The polypeptide, osteocalcin, which is extracted from bone by EDTA, comprises about 1% of the total protein of chicken and bovine bones and about 20% of the non-collagenous protein (Lian et al, 1978). The distribution of Gla in calcified tissue, dentine, and in some soft tissues is shown in Table III.1. The significant finding was that the epiphysis had low concentrations of Gla residues compared to the diaphysis and metaphysis, despite being the site of high bone turnover. Cartilage also had low levels of Gla residues. Thus the concentration of Gla apparently correlated with the degree of mineralization (Hauschka et al, 1978).

Characterization

The molecular weights of calf and chicken "osteocalcin" are low: 5800 and 6500 daltons, respectively (Price et al, 1976b ; Hauschka and Gallop, 1977). It is also a very acidic protein.

The covalent structure has been determined for "osteocalcin" from calf, swordfish, human, chicken, and monkey bone (Poser et al, 1980; Price et al, 1976 b ; Price et al, 1977; Carr et al, 1981 and Hauschka et al, 1982) and the N-terminal sequence has been reported for rat "osteocalcin" (Otawara et al, 1981).

Table III.1 . γ - carboxyglutamic acid content of various 3 week chick tissues.

Tissue	Relative Gla content
Long bone diaphysis	100 ± 3
Long bone metaphysis	67
Long bone epiphysis	23
Long bone articular cartilage	18
Long bone marrow	<1
Mandible	66
Calvarium	56
Sternum keel bone	51
Sternum cartilage	22
Tracheal cartilage	17
Tendon	<1
Brain	<1
Kidney	14
Liver	10

Long bone diaphysis = 68.9 ± 2.4 residues Gla/10^5 amino acid residues.

From Hauschka et al, 1978.

A direct comparison of these structures reveals a remarkable degree of conservation (as reviewed by Price, 1983) (Fig. III.4). The commonest feature is 3 Gla residues and an associated disulphide bond. Because of this sequence homology there are sufficient similarities for most antibodies, currently used for clinical assays, to have been raised against bovine osteocalcin (as reviewed by Price, 1983).

Osteocalcin was found to be distinctly different from the vitamin k-dependent blood coagulation factors by molecular weight, amino acid composition and sequence (Hauschka et al, 1975; Hauschka and Gallop, 1977; Price et al, 1976).

Interaction of Osteocalcin with Ca^{2+} and Hydroxyapatite

Osteocalcin binds Ca^{2+}, although the strength of this association is relatively weak. Calcium binding studied by equilibrium dialysis of chicken osteocalcin demonstrated two distinct classes of calcium binding sites with an average dissociation constant of 0.8 mM (as reviewed by Hauschka et al 1978; Price 1983). Analysis of Ca^{2+} binding to calf osteocalcin showed three distinct binding sites with an average dissociation constant of 3 mM (Poser and Price, 1979). This Ca^{2+} binding to osteocalcin is lost following thermal decarboxylation of γ-carboxyglutamate to glutamate.

Osteocalcin has a much greater affinity for hydroxyapatite. The dissociation constant for osteo-

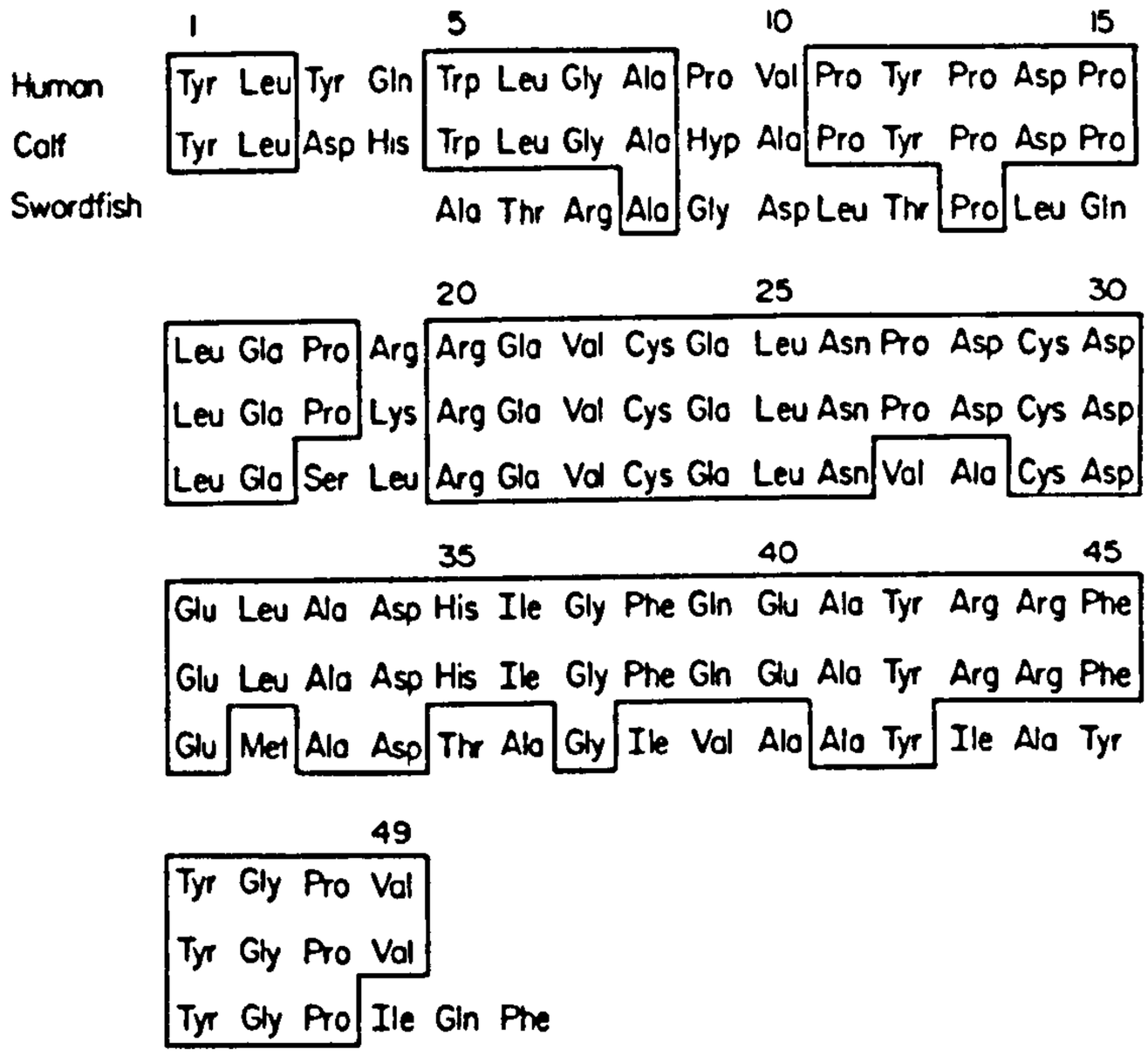

Fig. III. 4 The amino acid composition of osteocalcin derived from human, cow and swordfish. The points of dissimilarity are shown as open symbols. (From Price, 1983).

calcin binding to hydroxyapatite is around 10^{-7}M (as reviewed by Price, 1983). The affinity of osteocalcin for hydroxyapatite is greatly reduced after thermal decarboxylation of the osteocalcin (Poser and Price, 1979). The decarboxylated osteocalcin also exhibits a shift in isoelectric focussing position from pH 4.0 to pH 4.5. This change in the property of the protein after decarboxylation of Gla to Glu is important, as will be discussed later, in determining at what point the protein is decarboxylated in bone primary culture. The affinity of osteocalcin for hydroxyapatite is selective in that it binds only weakly with amorphous calcium phosphate (Price et al, 1976a).

Brushite ($CaHPO_4 2.H_2O$) is an important mineral phase in embryonic bone (as reviewed by Hauschka et al, 1978), which undergoes metamorphosis to hydroxyapatite. Hauschka et al (1978) showed that the in vitro transition of brushite to hydroxyapatite is strongly inhibited by low ($\sim$ 2 μM) concentrations of osteocalcin. However caution should be taken in relating these in vitro properties of osteocalcin to its still obscure in vivo functions.

Biosynthesis

There is good evidence that that the polypeptide, osteocalcin, is synthesized by bone. The most direct evidence has been obtained by the analysis of proteins labelled with ^3H proline in the primary culture of 1mm thick cross-sectional wafers of calf trabecular and

cortical bone (Nishimoto and Price, 1979). It was demonstrated that ^{3}HPro is incorporated into a protein which is identical to osteocalcin in molecular weight, electrophoretic mobility, and isoelectric focussing position. The osteocalcin labelled with ^{2}HPro is cleaved by trypsin into the same peptides as purified bovine osteocalcin. This labelled osteocalcin exhibits a shift in isoelectric focussing position from pH4.0 to pH 4.5 after thermal decarboxylation of Gla to Glu, demonstrating that this protein is not only synthesized, but fully carboxylated in bone in primary culture.

Further evidence that osteocalcin is synthesized in bone has been obtained by the SDS gel-electrophoretic analysis of proteins labelled with ^{14}C in γ-carboxy-glutamate during incubation of chick bone microsomes with $^{14}CO_2$ and vitamin K_1 (Lian and Friedman, 1978). However they showed vitamin K-dependent formation of γ -carboxyglutamic acid in endogenous proteins only in microsomal preparations from chick embryos treated with sodium warfarin for 5 days prior to killing. A 4 to 5 fold increase in ^{14}C- γ-carboxyglutamate formation into the microsomal endogenous proteins in warfarin-treated embryos was found compared with that found in untreated embryos. This clearly demonstrated that precursor protein accumulated in bone microsomes. This finding supported previous studies that demonstrated in vivo formation of ^{14}C- γ-carboxyglutamate in embryonic chick organ cultures by incubation in a medium supplemented

with ^{14}C-$NaHCO_3$ (Lian et al, 1976). While little vitamin K-dependent carboxylation of endogenous protein could be shown in bone microsomes prepared from normal bone, the presence of carboxylase activity was demonstrated using a synthetic peptide, Phe-Leu-Glu-Glu-Val, as substrate (Lian and Friedman, 1978).

There is some evidence that indicates that osteoblasts synthesizeosteocalcin. Firstly osteocalcin has been shown to have a residue of 4-hydroxyproline in its structure (Price et al, 1976b). This indicates the presence of prolyl hydroxylase in cells synthesizing osteocalcin, an enzyme that is used as a marker for osteoblasts in culture. Osteocalcin is synthesized by clonal osteosarcoma cells that display common features of the osteoblast phenotype. These clonal osteosarcoma cells form fully mineralized osteosarcomas when implanted into rats (Nishimoto and Price, 1980; Majeska et al, 1980; Nishimoto and Price, 1981). Analysis of the proteins synthesized by these osteosarcoma cells indicates the presence of a precursor of osteocalcin (Price, 1983).

Developmental Appearance of Osteocalcin (or Gla residues) in Mineralizing Tissues.

Two methods have been used to investigate the developmental appearance of osteocalcin in calcifying tissues.The first depends on the chemical detection of carboxyglutamate residues, assumed to be indicative of the presence of osteocalcin; the second has involved the direct radio-immunoassay of osteocalcin. These

two assays have presented conflicting evidence. In the early studies by Hauschka et al (1978) it was shown, by the chemical analysis of γ-carboxyglutamate, that Gla is first detectable in growing chick embryos when the first histologically detectable mineral deposition occurs (Fig. III.5). Interference with the vitamin K status of the chick by injecting warfarin into these developing chick embryos, or by feeding young chicks either with a vitamin K deficient diet or with one containing added dicoumarol, depressed the rate of Gla formation in the forming bone. Although gross macroscopic abnormalities were not observed in bones of chicks fed either with dicoumarol or with vitamin K deficient diets, there was microscopic evidence of impaired calcification (Hauschka et al, 1978). The direct chemical analysis of γ-carboxyglutamate in the developing rat and chicken (Hauschka and Reid, 1978a; Price et al, 1980a) and in bone induced by subcutaneously implanting demineralized powder of collagenous bone matrix into rats showed that the content of skeletal γ -carboxyglutamate residues rises when mineral first accumulates in bone (Hauschka and Reddi, 1980). In contrast, analysis by immunoassay for the detection of osteocalcin in demineralization extracts of calcifying tissues or in transverse sections of rat tibia in 2 and 4 week rats showed that the protein did not appear coincidently with the accumulation of mineral but much later, at about the

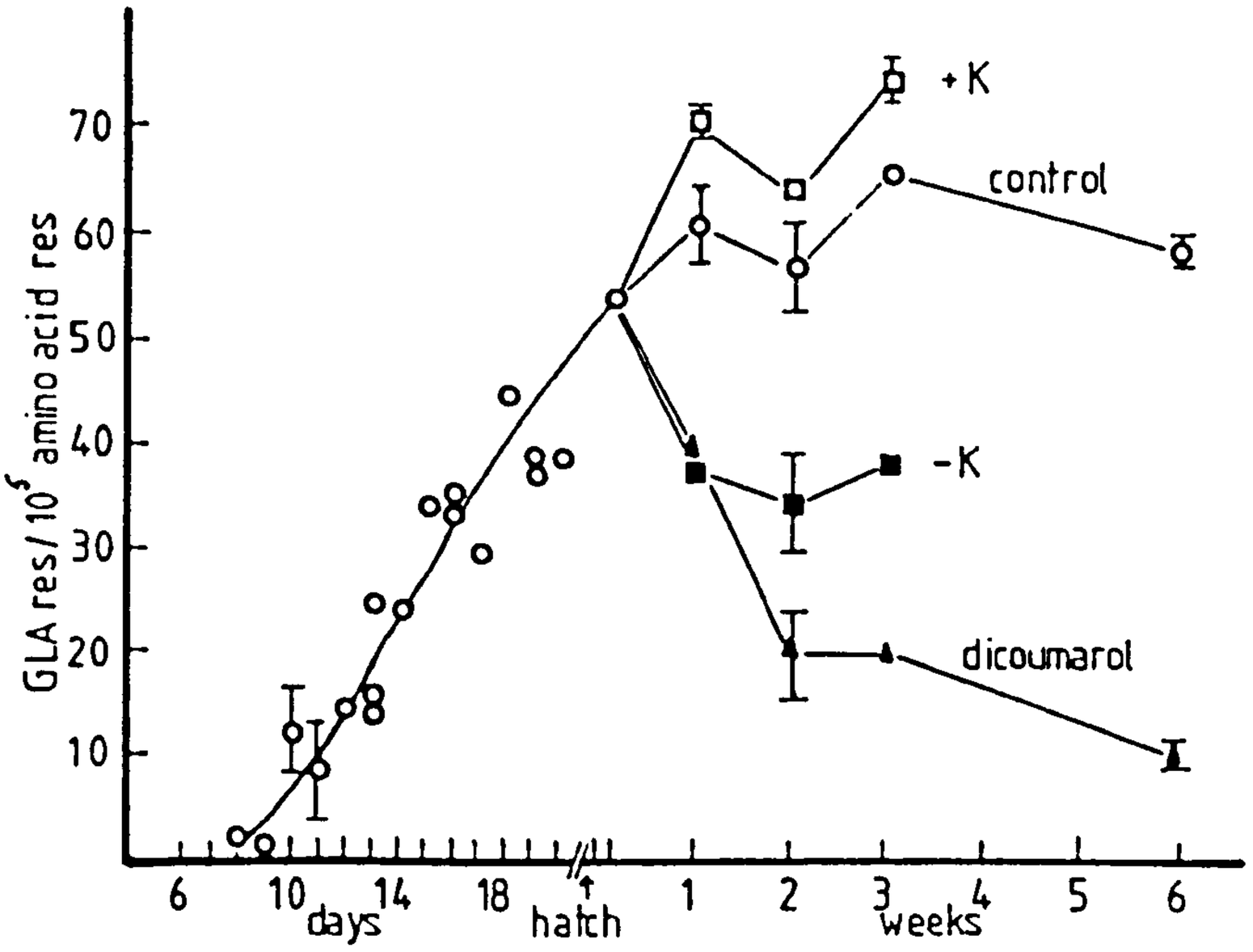

Fig. III. 5 The content of γcarboxyglutamate residues in chick limbs from the embryonic stage to six weeks of age. The effect of adding vitamin K (+K) or removing it (-K) from the diet and the effect of dicoumarol is also shown.

(From Hauschka et al, 1978)

same time as the initial mineral phase was maturing into hydroxyapatite (Price et al, 1981a). This discrepancy is probably due to the presence of other Gla containing proteins, associated with the collagenous bone matrix, that are not extracted by the acid or EDTA demineralization procedures (Price, 1980a: Table III.2). These other Gla-containing components appear in close temporal association with the accumulation of mineral, explaining the results of Hauschka et al (1978) whereas, osteocalcin as detected by immunoassay, appears much later. For example, in new born rats the amount of Gla is at 33%, while bone osteocalcin (as determined by radioimmuno-assay) is at 1% of adult levels (Price et al, 1980a).

The first mineral phase in rat, calf and human is almost devoid of osteocalcin, as determined by radio-immunoassay (Price et al, 1980 a,b); Price et al, (1981 a). The overall level of osteocalcin in bone rises rapidly with subsequent development in all three species, approaching adult levels by 14 days of age in rats, and by the gestational age of 9 months in the calf and 15 weeks in humans.

The Nature of Circulating Osteocalcin.

Sensitive radioimmunoassays have now detected a protein that is apparently identical to osteocalcin and which is present in plasma and serum (Price and Nishimoto, 1980; Price et al, 1980b ; Patterson-Allen et al, 1982). It deserves to be noted that the

Table III. 2 The γ-carboxyglutamic acid concentration in newborn and adult limb bone was determined by amino acid analysis after alkaline hydrolysis of three fractions: the intact bone, the formic acid extracted proteins, and the insoluble collagenous residue. For comparison data are expressed as micromoles of γ-carboxyglutamate per g of original bone sample.

Bone fraction	Adult	Newborn
	μmol Gla/g	
Whole bone	0.67	0.25
Extracted protein	0.57	<0.04
Insoluble residue	0.09	0.21

antibody developed by Price and co-workers does not discriminate between 'osteocalcin' that contains Gla residues and 'osteocalcin' that lack Gla residues, for example, after oxidative removal of the γ-carboxy group (Price et al, 1980a ; Price and Nishimoto, 1980). The antibody developed by Patterson-Allen and co-workers has not been decisively characterized, although it was shown to respond to osteocalcin that contained Gla residues; it also responded to some other peptides that were equally rich in Gla-residues but which were not osteocalcin. However it was not shown to be specific for Gla-residues.

Price and co-workers (Price and Nishimoto, 1980; Price and Williamson, 1981, Price et al, 1981b) have used the ability of their 'osteocalcin' to bind hydroxy-apatite to indicate the presence of Gla residues. Thus they showed that the osteocalcin-like peptide, present in the circulation, has the same molecular weight as has osteocalcin that is extracted from bone and the same affinity for hydroxyapatite.

The osteocalcin present in the circulation arises from new cellular synthesis and not from the release of extracellular bone matrix osteocalcin during bone resorption (Price et al, 1981b). This was shown by two experiments. The first experiment analysed serum osteocalcin in rats treated with warfarin and showed that 3 hours after a single dose of warfarin, serum osteocalcin had lost its ability to bind to hydroxy-apatite (Price et al, 1981). This is best explained

by the fact that warfarin had inhibited the vitamin K_1-dependent γ-carboxylation of newly synthesized osteocalcin. Osteocalcin extracted from the bone of these rats was normal and was able to bind hydroxyapatite normally. Thus the abnormal serum osteocalcin in these animals could not have come from extracellular bone matrix osteocalcin during bone resorption. The level of circulating osteocalcin from these warfarin-treated rats was found to be 4-fold greater than that of circulating osteocalcin in control rats at day 30, the levels decreasing thereafter. This could be due to the fact that the osteocalcin which would normally accumulate in bone now appears in the circulation (Price and Williamson, 1981) (see later in the section 'The effects of warfarin on bone'). Secondly, administration of vitamin K_1 to chronically warfarin-treated rats caused serum levels of fully γ-carboxylated osteocalcin (as judged by binding to hydroxyapatite) to return to normal within 15 hours. Since the total osteocalcin level in the bones of these rats was approximately 1.5% of normal after 15 hours of vitamin K-administration, again it seems clear that the osteocalcin in serum must have arisen from new cellular synthesis (Price et al, 1981b).

The turnover of osteocalcin must be reasonably fast, since, as seen in the first experiment outlined above, the serum osteocalcin loses its ability to bind to hydroxyapatite within 3 hours of a single dose of

warfarin (Price et al, 1981b), and as fully reviewed by Price, 1983).

Circulating levels in the human

As shown in Table III.3, there appears to be no consensus on the circulating levels of osteocalcin. For example, two groups showed that levels in women are higher than in man and two groups showed the reverse. Equally some showed levels increasing with age and others showed them to decrease with age. This confusion is unfortunate because osteocalcin may be a useful indicator of bone metabolic activity, so that circulating osteocalcin levels could provide a valuable measurement for the diagnosis of metabolic bone diseases (as discussed below).

The discrepancies between the circulating levels of osteocalcin with age and sex are probably due to the characteristics of the populations studied. Price et al (1980 b) and Gundberg et al (1982) reported lower levels of circulating osteocalcin in females. Epstein et al (1984) and Couch et al (1984) however showed higher levels of osteocalcin in women than in men. In all these studies the mean values of circulating levels of osteocalcin were taken from a wide range of ages in both groups. However, the ranges and means of ages differed in these studies. The mean age of female subjects studied by Price et al (1980 b) was 44. The mean age of the males studied was not indicated, nor the range of ages in both groups. In a personal communication by Price and as described by

Table III. 3. The results in some recent publications on the circulating levels of osteocalcin.

Circulating levels of 'osteocalcin'				
♀ : ♂	Change with age	Osteoporosis	Author	
↓	↓	↑(♀)	Price et al,	1980
-	↑	↑	Delmas et al,	1983 a,b
↓	↑	No change	Gundberg et al,	1983
↑	↑	↑	Epstein et al,	1984
↑	↑(♀)	—	Couch et al	1984

Delmas et al (1983a), only half of the normal women in their study were over 30 years of age (34 out of 62) and only 4 of them were older than 70 years of age. They reported however that circulating levels of osteocalcin fell with age in women, with no significant variation with age in men. Gundberg et al (1982) measured circulating levels of osteocalcin in males and females whose ages ranged from 1 to 65 years. This group reported extremely high levels (10 - 40 ng/ml) in growing children, declining to the normal adult levels at about the age of puberty. The mean age of the adults studied in this group of subjects was 37 years in both males and females. However quite surprisingly mean values for the circulating levels of osteocalcin in adults were obtained by measuring in the age range 12 to 65 in males and in the age range 17 to 65 in females. Thus two male children with levels as high as 35 ng/ml were included in the male adult level of circulating osteocalcin. In this study, however, it did appear that levels were increasing with age after 30 years but there was no apparent difference between male and female levels. Epstein et al (1984) measured the level of circulating osteocalcin in adults ranging from 30 to 90 years. The mean age of their subjects was much higher than in the two previously mentioned surveys: 57 and 67 years for females and males respectively. They showed that circulating osteocalcin increased with age in both men and women. The difference between women aged 30 and those aged 80 was much greater than that between men

of the same ages. Delmas et al (1983a) also reported that circulating levels of osteocalcin increased with age in women, but they did not measure osteocalcin in men.

Price et al (1980 b) showed that circulating levels of osteocalcin were elevated dramatically in patients with metabolic bone diseases whic' are characterized by increased bone turnover, such as Paget's disease, hyperparathyroidism, and metastatic bone disease: Circulating osteocalcin levels were found to be correlated with circulating alkaline phosphatase levels, although there were discrepancies (Price et al 1980 b). Gundberg et al (1983) also showed significant increases in circulating osteocalcin in patients with Paget's disease. Price et al (1980 b) reported that in patients with osteoporosis the mean concentration of circulating osteocalcin was slightly higher than in normal women; however it is not clear whether this 'osteocalcin' had its full complement of Gla-residues. Unfortunately, these two groups were not of similar ages, the mean age of the controls being 44 years whereas that of the osteoporotics was 60 years. For all that, Epstein et al (1984) showed that age-matched osteoporotic patients had significantly raised levels of circulating osteocalcin as defined by radioimmunoassay (17.3 ng/ml). Epstein et al (1984) pointed out that it was interesting that the increase in circulating osteocalcin with age occurred most noticeably at the age when a reduction in bone

mass or postmenopausal osteoporosis becomes evident in women and also when osteoporosis is most common in the male population. Similar levels were reported in osteoporotic patients by Delmas et al (1983b). However, Gundberg et al (1983) showed only a slight elevation of circulating osteocalcin in patients with osteoporosis.

Circulating levels of osteocalcin and alkaline phosphatase levels fall appreciably in patients with Paget's disease, following long-term treatment with salmon calcitonin (Deftos et al, 1982). In the same study these workers showed that circulating levels of osteocalcin fell following parathyroidectomy in women with primary hyperparathyroidism. Treatment with salmon calcitonin also reduced circulating levels of osteocalcin in patients with bone cancer. Again, in this study, although circulating levels of osteocalcin and circulating alkaline phosphatase were generally correlated, there were dissociations between the two. Thus measurement of the circulating level of osteocalcin may be a more specific index of bone turnover than is the measurement of the circulating levels of alkaline phosphatase. This, however, will depend on reliable immunoassays which yield equivalent results in different laboratories.

Correlations between circulating osteocalcin and other biochemical factors and bone mass.

Both Delmas et al (1983a) and Epstein et al (1984) have correlated circulating levels of osteocalcin with age, iPTH, ionised calcium, alkaline phosphatase, 1,25 - $(OH)_2D$, midshaft bone mass, distal bone mass, lumbar spine bone mass, urinary hydroxyproline, urinary cAMP and creatinine clearance. The results are summarized in Table III.4. In the study by Delmas et al (1983a, done only on women, the results suggest that overall bone turnover increases in women with ageing and may indicate that age-related bone-loss does not result primarily from decreased bone formation. The measurements by Epstein et al (1984) were consistent with the findings of Delmas et al (1983a).

Urinary γ-Carboxyglutamate.

In humans, free γ-carboxyglutamate residues are excreted in the final breakdown of all vitamin K_1-dependent proteins (Shah et al, 1978). Total alkaline hydrolysis of whole urine yields free Gla derived from all the urinary constituents. Gundberg et al (1982) showed that 80% - 99% of total urine Gla is excreted as free Gla in normal subjects. Less than 5% protein-bound Gla was found. Thus this indicates that the measurement of free urinary Gla is an adequate assessment of the breakdown of Gla-containing proteins. Levy and Lian (1979) showed that the excretion of Gla

Table III. 4. Some recent publications on the correlation between circulating levels of osteocalcin, other biochemical factors and bone mass. Upper table from Epstein et al, 1984; lower table from Delmas et al, 1983a.

-	Correlation coefficient with BGP	
	Women	Men
Age	0.41(p<0.001)	0.29(p<0.01)
iPTH	0.37(p<0.001)	0.20(NS)
Ionised calcium	-0.10(NS)	0.07(NS)
Alkaline phosphatase	0.31(p<0.001)	0.26(p<0.05)
1,25-$(OH)_2D$	-0.20(p<0.10)	-0.18(NS)
Midshaft mass	-0.43(p<0.001)	-0.57(p<0.001)
Distal mass	-0.40(p<0.002)	-0.39(p<0.01)

NS = not significant

Correlation Coefficients Between Age, Biochemical,and Densitometric Variables

		BMD					Urinary	Serum
	Age	Lumbar spine	Mid-radius	Distal radius	Urinary cAMP	Serum iPTH	H-proline	Alk.Phos.
Serum BGP	0.44*	-0.45*	-0.40*	-0.46*	0.17[1]	0.36*	0.39*	0.43*
Serum alkaline phosphatase	0.31*	-0.34*	-0.26*	-0.30*	0.16[1]	0.27*	0.38*	
Urinary hydroxyproline	0.29*	-0.18[1]	-0.23[2]	-0.25*	0.25*	0.26*		
Serum iPTH	0.39*	-0.20[2]	-0.32*	0.32*	0.15[1]			
Urinary cAMP	0.38*	-0.05	-0.14	-0.16[1]				
BMD								
Lumbar spine	-0.47*							
Midradius	-0.67*							
Distal radius	.67*							

* p <0.001
[1] p <0.05
[2] p < 0.01

decreased in human subjects treated with warfarin. Thus urinary Gla measurements may reflect bone turnover. Gundberg et al (1982) measured urinary Gla in patients with Paget's disease or with osteoporosis, and compared them to levels of circulating osteocalcin in these patients. They found that urinary Gla excretion was increased in patients with osteoporosis, by up to 150% of the normal level. However (as mentioned earlier) circulating levels of osteocalcin were not significantly different from normal in this study. In Paget's disease, this pattern was reversed in that circulating levels of osteocalcin were increased 3-fold, while urinary Gla-excretion was consistently normal. This normal level of excreted Gla was shown regardless of the extent of the disease. Gundberg et al (1982) had previously shown high levels of urinary Gla in growing children. These levels decreased with age until they normalized at puberty. These changes in urinary Gla, as a function of age, closely resembles those of circulating osteocalcin (as discussed earlier). From these results, Gundberg et al (1982) suggested that, with epiphyseal closure, urinary Gla and circulating osteocalcin levels decline and that in the adult these parameters most likely represent the coupling of bone resorption and new synthesis during normal bone turnover. Gundberg et al (1982) suggested that the increased Gla excretion in patients with osteoporosis may reflect an imbalance between bone resorption and bone formation, in contrast

to the normal levels of urinary Gla in Paget's disease where there is tight coupling between bone formation and bone resorption (i.e. no net loss of bone). Certainly these results suggest that measurements of urinary Gla and circulating osteocalcin may provide important insight into the metabolic disorders of bone.

The Effects of Warfarin on Bone.

To investigate the physiological role of osteocalcin and other Gla-containing proteins, several workers have focussed on the effects of the vitamin K_1 antagonists, dicoumarol and warfarin, on bone and calcification. These anticoagulants are believed to inhibit the conversion of the epoxide to the quinone in the vitamin K_1 cycle, preventing the post-translational conversion of glutamate residues to γ-carboxyglutamate residues (Whitlon et al, 1978); they are not believed to inhibit the biosynthesis or secretion of osteocalcin or the other Gla-containing proteins.

Warfarin has been used for long-term anticoagulation for 25 years, and has been shown to cause nasal hypoplasia, stippled epiphyses and distal extremity hypoplasia in the offspring of women treated with Coumadin during pregnancy (Hall et al, 1980). However Piro et al (1982) showed that treatment with Coumadin (related to warfarin and dicoumarol) appeared to have no detrimental effect on cortical bone-mass in adults receiving long-term therapy. The effects of anti-coagulant therapy on bone-repair was studied by Stinchfield

et al (1956) who found fibrous tissue and immature bone in the healing fractures of rabbits and dogs given dicoumarol at a dose equivalent to the clinical dose for humans. Hähnel et al (1978) made an histological and histochemical investigation of the epiphysis of the tibia and humerus in rats after 8 weeks of coumarin administration. They showed reduced cellularity in the zones of resting cartilage, of young proliferative cartilage, and especially in the bone of the epiphysis. There was also degenerative fibrillation of the ground substance. However there were no differences with regard to the width of the epiphyseal plates, or the width of metaphyseal trabeculae. It is of interest though, that in these studies by Stinchfield et al (1956) and Hähnel et al (1978), they found very similar, if not more pronounced effects, with heparin administration. Hauschka et al (1976) and Hauschka et al (1978) showed no gross morphological abnormalities in bones of dicoumarol treated chicks, but there was histological evidence of deficient calcification. Price and Williamson (1981) developed a procedure by which the levels of osteocalcin (measured by radioimmunoassay) in rat bone can be reduced to 2% of normal values. In this procedure newborn rats are maintained on a ratio of a lethal dose of warfarin and sufficient vitamin K_1 to prevent bleeding and death. In this way the rats can be maintained in a chronically vitamin K-deficient state. As described earlier, because the

radioimmunoassay for rat osteocalcin does not discriminate between carboxylated and non-carboxylated 'osteocalcin', this low level of 'osteocalcin' in warfarin-treated rats reflects the suppression of the normal developmental accumulation of osteocalcin in bone; since the biosynthesis of the Glu-osteocalcin is unimpaired, this lack of binding of the 'osteocalcin' within the bone could account for the raised levels of circulating 'osteocalcin' in warfarin-treated animals. The γ-carboxyglutamic acid levels in alkaline hydrolysates of whole bone, from 52 day-old warfarin-treated rats containing approximately 2% of normal levels of osteocalcin, was 0.16 μmol Gla/g of bone compared to normal levels of 0.67 μmol Gla/g of bone at the same age. Of great interest was the finding that over 80% of the Gla which does remain in the bones of these warfarin-treated rats, is associated with the collagenous bone matrix; this Gla-material is not extracted after formic acid demineralization procedures (Price and Williamson, 1981). In the same study Price and Williamson (1981) showed that 17-day old rats, placed on warfarin, took over 4 weeks to reach this 2% level, and similarly required over 4 weeks to return to the normal level again. This is in direct contrast to results from studies on circulating osteocalcin, in which the Gla content changes dramatically within 3 hours of warfarin treatment (see earlier) to a normal level (Price et al, 1981b).

Using this protocol Price and Williamson (1981) showed

Warfarin had no effect on the length, mass and gross morphology of femurs and tibias, although no results were shown.. They also studied the degree of mineralization in bones of warfarin-treated rats in acid extracts of powdered femurs, by measuring phosphate levels. No differences were observed. Price and Williamson (1981) concluded that osteocalcin had no major role in the growth, morphology or mineralization of rat bone. Price and Williamson (1981) looked for a role of osteocalcin in skeletal or serum calcium homeostasis, by placing the warfarin-treated rats on a Ca^{2+} -deficient diet and then measuring bone and serum Ca^{2+} levels. No differences were observed between experimental and control rats. These authors then studied the repair of fractures in young rats, in which the radius was fractured at 17 days of age. No significant differences or abnormalities were observed in the repair of fractures in rats fed warfarin from birth. The evidence of repair was obtained radiologically. No histological observations were made in this study. Finally Price and Williamson (1981) showed that demineralized bone matrix from control or warfarin treated rats implanted subcutaneously over the thorax of 1 month old rats showed identical abilities to induce host mineralization, as determined by osteocalcin and phosphate levels measured in each group.

More recently Price et al (1982) maintained rats on warfarin for 8 months, using this same protocol, and

showed growth plate closure and cessation of longitudinal growth of the tibia.

Finally, I have studied the effects of dicoumarol on the healing of closed fractures of metatarsals in the rat (Chapter VIII). A detailed histological and metabolic study has been made.

SUMMARY

Gamma-carboxylation, by the vitamin K_1 cycle, of glutamate residues in existing proteins, results in calcium-binding Gla residues (Olsen et al, 1978; Stenflo and Suttie, 1977; Suttie et al, 1978). The major Gla-protein isolated from bone is osteocalcin (or bone Gla-protein) (Hauschka et al, 1975; Price et al 1976a): it contains 47-51 amino acids of which 3 are Gla, and is readily extracted by EDTA when the bone is decalcified, leaving other Gla-containing proteins within the bone (Price et al, 1980a). Such results indicate that the primary binding of calcium, during mineralization, may be to the latter proteins, and that osteocalcin binds to pre-formed hydroxyapatite (Hauschka et al, 1978; Hauschka and Reid, 1978b; Hauschka and Reddi, 1980; Price et al, 1980a; Price et al 1981a).

The radioimmunoassay (RIA) of osteocalcin does not distinguish between the peptide with Gla or with glutamate (Price et al, 1980a; Price and Nishimoto, 1980). Conseq-uently some discrepancies have been reported, depending

apparently on whether the results are based on RIA or on the chemical demonstration of Gla. True Gla-containing osteocalcin strongly binds hydroxyapatite, and inhibits the transformation of brushite to hydroxy-apatite (Hauschka et al, 1978). Warfarin (or dicoumarol and related compounds) inhibits the reduction of the vitamin K epoxide back to the naphthoquinone, so antag-onising the vitamin K cycle (as discussed by Whitlon et al, 1978). Thus it can influence only the new form-ation of Gla-residues so that the newly formed osteocalcin contains glutamate and not Gla residues.

The role of osteocalcin and of the other Gla-containing proteins has been tested in vitamin K-deficient animals. The protocol used by Price and Williamson (1981) in which rats were maintained on a lethal dose of warfarin and sufficient vitamin K_1 to prevent bleeding and death, showed no defects in bone metabolism. In this protocol the levels of osteocalcin were reduced to 2% of normal. However it was of great interest to find that over 80% of the Gla which remained in these warfarin-treated rats, was associated with the collagenous bone-matrix, and could be extracted only after deminer-alization with formic acid (Price and Williamson, 1981). This non 'bone Gla-protein' was shown to be associated with the first stages of mineralization (Hauschka et al, 1978; Hauschka and Reid, 1978b; Hauschka and Reddi, 1980) unlike osteocalcin (as detected by RIA) which appears in calcifying tissues after the initial mineral phase has matured to hydroxyapatite (Price et al, 1980a; Price et al, 1981a).

CHAPTER IV

POLYAMINES

The polyamines spermidine and spermine, and their precursor 1,4 diaminobutane (putrescine) are ubiquitous organic cations of low molecular weight, found in a wide variety of eukaryotes and prokaryotes, their relative amounts differing markedly in different cell types. Their structures are shown in Fig. IV.1. The metabolism and possible roles of these cations have been extensively reviewed (Tabor and Tabor, 1976; Maudsley, 1979; Heby, 1981; Pegg and McCann, 1982; Allen, 1983). Briefly the main lines of evidence are as follows. Firstly, several micro organisms have an absolute requirement for polyamines for normal growth and DNA-synthesis. Secondly, the concentration of the polyamines, and the activities of the enzymes involved in their biosynthesis, increases rapidly when resting cells are induced to proliferate. This increase precedes increases in RNA, DNA and protein. Despite extensive research, the precise physiological function of the polyamines is not understood.

Polyamine Metabolism

The pathway for mammalian polyamine synthesis is shown in Fig. IV.2. In mammalian tissues 1,4 diaminobutane (putrescine) is derived by decarboxyation of ornithine by the action of ornithine decarboxylase

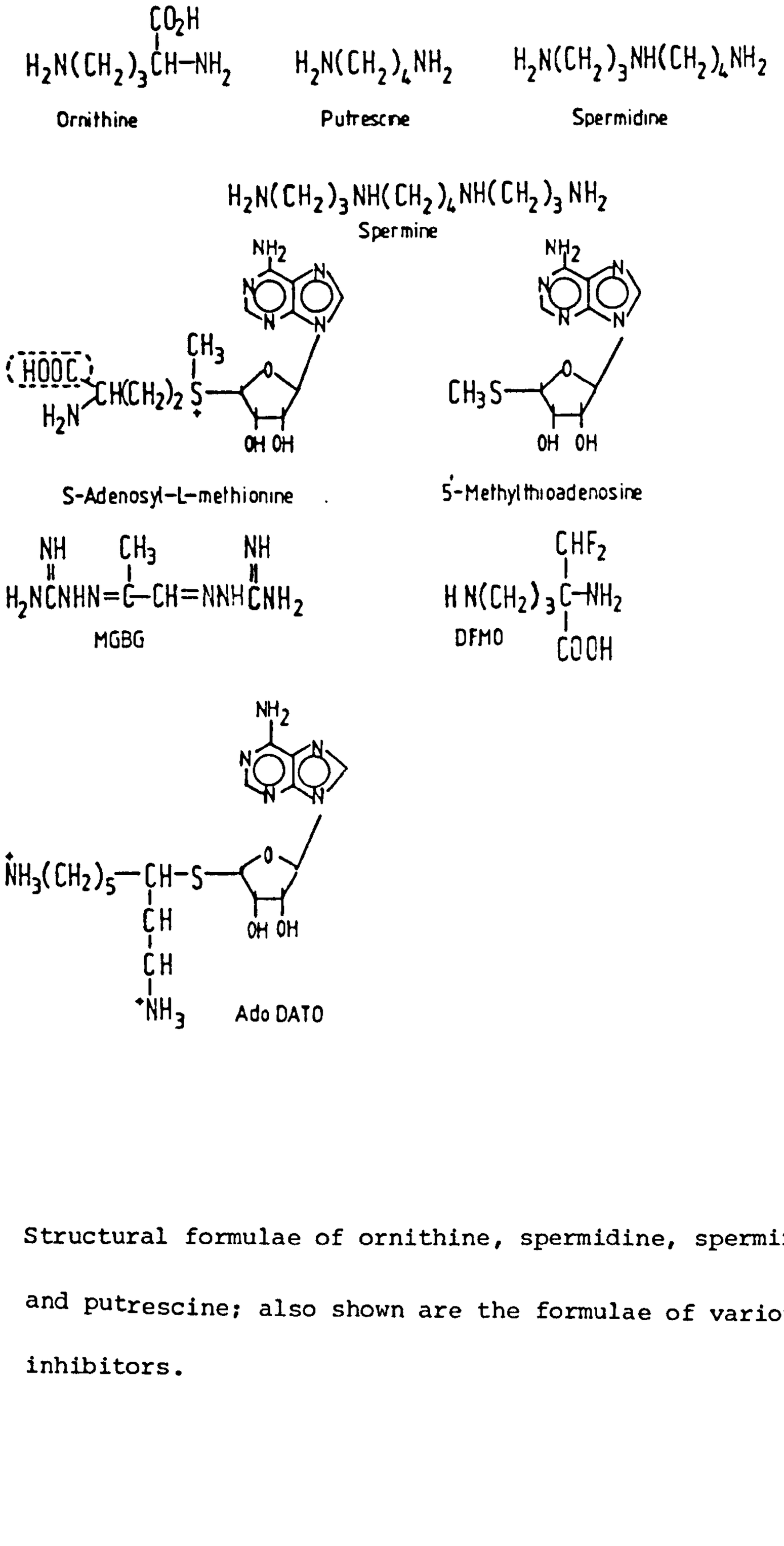

Fig. IV. 1 Structural formulae of ornithine, spermidine, spermine and putrescine; also shown are the formulae of various inhibitors.

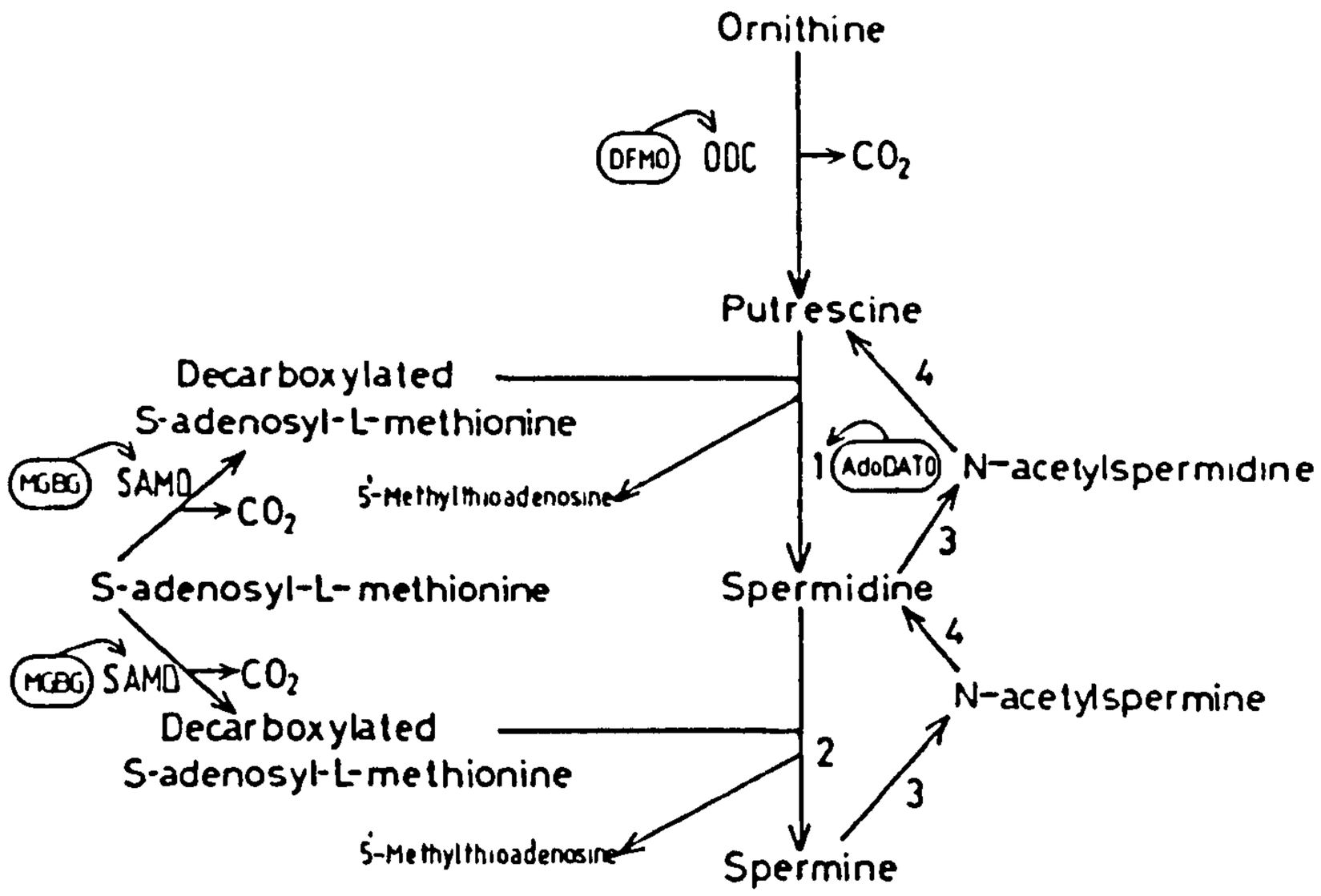

Fig. IV. 2 Diagrammatic representation of the pathway of polyamine synthesis; ODC: ornithine decarboxylase; SAMD: S-adenosyl methionine decarboxylase; 1 : spermidine synthase; 2: spermine synthase; 3: spermine or spermidine N-acetyl transferase; 4: polyamine oxidase. The inhibitors are shown encircled and their site of action is indicated.

(ODC). In many micro-organisms and higher plants putrescine can also be produced by decarboxylation of arginine, but the enzyme arginine decarboxylase is lacking in all mammalian cells. Ornithine is available for these reactions from the plasma (Allen, 1983) and can also be formed by the enzyme arginase within the cell. It has been suggested that arginase, which is more widely distributed than the other enzymes of the urea cycle, is present in extra hepatic tissues to ensure the availability of ornithine for polyamine synthesis (Pegg and McCann, 1982). Ornithine decarboxylase requires pyridoxal phosphate as a coenzyme and is subject to feedback inhibition and repression by 1,4-diaminobutane (putrescine) or spermidine (cited by Tabor and Tabor, 1976). This enzyme is present in very low amounts in quiescent cells but its concentration and activity increase dramatically after a variety of stimuli: hormonal, drugs, tissue regeneration, and growth factors (as reviewed by Tabor and Tabor, 1976; Pegg and McCann, 1982; and Allen, 1983).

To convert 1,4 diaminobutane (putrescine) into spermidine an amino propyl group, derived from methionine is added by the action of S-adenosyl-L-methionine decarboxylase (SAMD). This converts S-(5'-adenosyl)-3-methionine to S-(5'-adenosyl)-3-methyl-thiopropylamine (Fig. IV.2). No other reactions are known to utilize decarboxylated S-adenosyl methionine (Pegg and McCann, 1982). The production of decarboxylated S-adenosylmethionine is normally low and is the rate-

limiting step in spermidine formation. The donated aminopropyl group is transferred to putrescine by spermidine synthase to form spermidine (N-(3-aminopropyl) buta-1,4 diamine). The residual group 5'-methylthioadenosine is rapidly degraded by a phosphorylase to yield adenine and 5'-methylthioribose-1-phosphate. Adenosine 5-monophosphate is formed from adenine, catalysed by the enzyme adenine phosphoribosyltransferase. Kamatani and Carson (1981) estimated that almost 90% of the de novo synthesis of adenine is formed from polyamine synthesis. The 5'-methylthioribose-1-phosphate is converted back to methionine.

Spermine (N, N'-bis (3-aminopropyl) buta-1,4-diamine) is formed by another aminopropyl transfer from S-(5'-adenosyl)-3-methylthiopropylamine, to the amino-butyl group of spermidine, catalysed by spermine synthase (Pegg and McCann, 1982) (Fig. IV.2).

The spermidine synthase and spermine synthase reactions are irreversible. However spermine can be converted into spermidine, and spermidine into putrescine by the actions of enzymes, spermine-N'-acetyltransferase and polyamine oxidase (Pegg et al, 1981) (Fig. IV.2). This polyamine interconversion is thought to be of physiological importance in regulating the levels of spermidine and spermine (Pegg et al, 1981; and reviewed by Pegg and McCann, 1982). The degradation of polyamines involves distinct polyamine oxidases, and is discussed by Pegg and McCann (1982; also Allen, 1983).

Inhibition of Polyamine Synthesis

Many inhibitors of the enzymes involved in polyamine biosynthesis, particularly the rate-limiting enzyme ornithine decarboxylase, are now available. Table IV.1 shows some of the many polyamine synthesis inhibitors effective in producing polyamine deficiency in eukaryotic cells (taken from Heby, 1981). Fig. IV.1 shows the structures of the more widely used inhibitors. Briefly ornithine decarboxylase is inhibited competitively by α-methylornithine and α-hydrazino- δ-aminovaleric (HAVA) and irreversibly by inhibitors such as α-difluoromethyl ornithine (DFMO), α-ethynlornithine, and 5 hexyne-1,4-diamine. These irreversible inhibitors are highly specific and significantly reduce putrescine synthesis in vivo (reviewed by Pegg and McCann, 1982; and Allen, 1983).

SAM-decarboxylase (SAMD) is strongly inhibited by methylglyoxal-bis (guanylhydrazone) (MGBG) which is also significantly inhibits polyamine synthesis in vivo. Administration of MGBG to rats, or exposure of stimulated lymphocytes to this drug prevented incorporation of labelled putrescine into spermidine, and lead to an accumulation of putrescine in the cells (cited by Pegg et al, 1973).

However, all the currently available inhibitors have some drawbacks when they are used to study the role of polyamines in cellular physiology. One test of specificity of the action of putative inhibitors of ODC or of SAMD has been to show that the metabolic

Table IV. 1 Some of the inhibitors of polyamine synthesis (From Heby, 1981)

Target enzyme	Inhibitor	Mechanism of action
Ornithine decarboxylase (ODC)	*Substrate analogs.*	
	a) DL-α-Hydrazinoornithine	Reversible and competitive
	b) DL-α-Methylornithine	Reversible and competitive
	c) DL-α-Hydrazino-α-methylornithine	Reversible and competitive
	d) *trans*-3-Dehydro-DL-ornithine	Reversible and competitive
	e) DL-α-Difluoromethylornithine	Catalytic irreversible
	Product analogs:	
	f) *trans*-1,4-Diamino-2-butene	Reversible and competitive
	g) 1,4-Diaminobutanone	Reversible and competitive
	h) 5-Hexyne-1,4-diamine	Catalytic irreversible
	i) *trans*-Hex-2-en-5-yne-1,4-diamine	Catalytic irreversible
	j) Homologous diamines with 3-12 C atoms (1,3-diaminopropane to 1,12-diaminododecane)	Indirect, e.g., by induction of ODC-inhibitory protein (ODC-antizyme)
	k) 1,3-Diamino-2-propanol	Indirect
S-Adenosyl-methionine decarboxylase (SAMDC)	a) Methylglyoxal-bis(guanylhydrazone); 1,1'-[(methylethanediylidene)dinitrilo]diguanidine; (MGBG)	Reversible and competitive with respect to the substrate (S-adenosyl-L-methionine)
	b) 1,1'-[(Methylethanediylidene)dinitrilo]bis-(3-aminoguanidine); (MBAG)	Initially reversible and competitive with respect to the substrate, but subsequently irreversible
	c) S-Adenosyl-DL-2-methylmethionine	Reversible and competitive with respect to the substrate
Spermidine synthase	α,ω-Diamines with 3-12 C atoms (1,5-diaminopentane is most active)	Reversible and competitive with respect to one of the substrates (putrescine)
Spermine synthase	α,ω-Diamines with 3-12 C atoms (1,3-diaminopropane and 1,5-diaminopentane are most active)	Reversible and competitive with respect to one of the substrates (spermidine)

effects are reversed by the addition of polyamines to the cells, so indicating that the effect of the inhibitors is solely on the supply of polyamines. However, this is not entirely adequate because MGBG has been found also to inhibit diamine oxidase: this effect may not be discernable merely by supplementing the cells with polyamines. Moreover it must be borne in mind that substances, such as MGBG, that resemble polyamines in that they are strongly basic molecules, may have polyamine-like effects of their own, apart from inhibiting the relevant decarboxylase. Thus, for example, MGBG is taken up into cells by the same active transport system as are polyamines (as reviewed by Pegg and McCann, 1982).

The most studied ODC inhibitor has been α(-difluoro-methyl)-ornithine. This compound brings about extensive depletion of putrescine and spermidine in cultured mammalian cells, resulting in the cells growing at a markedly reduced rate (Mamont et al, 1978). This has been confirmed by many workers (as reviewed by Pegg and McCann, 1982). The growth-inhibitory effects are reversed by supplementation by spermidine or by putrescine (cited by Pegg, 1983). However this inhibitor has very little effect on the spermine content. This could be because there is sufficient residual ODC activity to maintain spermine levels. The small amount of putrescine that is produced even in the presence of the inhibitor is very efficiently converted into spermine

(Mamont et al 1981). To add to the problem, as a consequence of the fact that ODC has an extremely high rate of turnover, the concentration of inhibitor must remain high, to prevent accumulation of newly synthesized active ODC. Thus this inhibitor depletes both spermidine and putrescine but is not useful for studying the effects of depleting spermidine by itself (Pegg et al, 1982b).

Thus to have a better understanding of the physiological role(s) of the polyamines in cells it was necessary to study the effects of the selective accumulation of putrescine, spermidine, or spermine. Pegg et al (1982b) studied the effects of the specific inhibitors of the amino-propyl transferases, spermidine synthase and spermine synthase (Fig. IV.2). Spermidine synthase is strongly inhibited by the analogue, S-adenosyl-1,8-diamino-3-thiooctane (AdoDATO) (Pegg et al, 1982b)(Fig. IV.1) and when mammalian cells (transformed mouse fibroblasts or rat hepatoma cells) were exposed to this inhibitor there were profound changes in the intracellular polyamine content. Putrescine levels were increased and spermidine levels decreased. This is consistent with the potent and specific inhibition of spermidine synthase (Fig. IV.2).

The spermine content of the cells also increased when the cells were exposed to AdoDATO, probably because spermine synthase was now able to use a larger concentration of the available 3-(5' adenosyl)-3-methyl thiopropylamine, the levels of which also increased due to the increase

in SAMD in response to the decline in spermidine since SAMD is apparently also regulated by the content of spermidine.

The growth of mouse fibroblasts was markedly reduced as a result of the inhibition by AdoDATO. This inhibition of growth was reversed by the addition of spermidine, not putrescine. They also showed that replenishment of either putrescine or spermidine was able to restore normal cellular content of spermidine in cells exposed to DFMO (the ODC inhibitor). As mentioned previously the effect of DFMO on cellular polyamines is to decrease the content of putrescine and spermidine to virtually zero levels, with a decrease in cell growth. But there is no change in spermine content. Spermine production stems from the efficient conversion of extremely low levels of putrescine into spermine (Pegg and McCann, 1982). The combination of DFMO with AdoDATO lowered the spermine content of the transformed mouse fibroblasts by 80% probably by preventing the conversion of the residual putrescine into spermidine (Pegg et al, 1982b). The cellular content of putrescine and spermidine were reduced by more than 95% in these mouse fibroblasts. This is the lowest level of polyamines achieved with inhibitors. The cells grew very slowly as a consequence. It was possible to substantially increase the growth rate of these cells with addition of spermidine.

One important finding in this study by Pegg et al (1982 was that significant changes in polyamine levels could be produced by concentrations of AdoDATO that had very little, or no effect on the growth of the cells, implying that the changes were not secondary to changes in growth rate.

The results by Pegg et al (1982b) using the inhibitors AdoDATO and DFMO confirm previous studies, that mammalian cells require certain levels of polyamines for optimal growth, but are able to survive and grow in spite of large variations of these levels.

The disadvantage of using reversible inhibitors of ODC activity is that they increase the actual concentration of ODC and thus reduce the inhibition (cited by Pegg et al, 1982b). The increase is due to the stabilization of the enzyme-protein which therefore prolongs its otherwise short half-life.

Mamont et al (1976) nevertheless clearly demonstrated that inhibition of ODC by α-methylornithine, in proliferating HTC cells caused a rapid fall in the levels of putrescine followed by a huge decrease in spermidine. The decrease in spermidine paralleled inhibition of DNA synthesis and cell proliferation. Again, addition of polyamines resulted in proliferation of the cells. There were no deleterious effects on the cells with the inhibition by α-methylornithine.

As mentioned previously, ODC shows an absolute requirement for pyridoxal phosphate (Raina and Jänne, 1975). Eloranta et al(1976) and Pegg (1977) showed that polyamine concentrations were decreased in rats fed on a diet deficient in vitamin B_6 (discussed in Chapter IX).

Some potential physiological roles of polyamines.

Hölttä et al (1979) demonstrated that the activation of human peripheral blood lymphocytes by phytohaemagglutinin invitro resulted in a striking increase in the concentrations of putrescine, spermidine and spermine. This enhanced accumulation of polyamines was almost totally abolished by DFMO and in the presence of MGBG, the accumulation of spermidine and spermine was largely prevented whereas the accumulation of putrescine was enhanced. The inhibition of the polyamine accumulation was associated with a marked suppression of DNA synthesis, which was partially or totally reversed by addition of low concentrations of the polyamines. These authors also showed that a distinct inhibition of protein synthesis preceded that of DNA synthesis in the cultures where the polyamine accumulation is prevented. The synthetic rates of DNA and protein were inhibited by up to 90% by the combination of these inhibitors (Hölttä et al, 1979). This clearly shows the importance of polyamines in cell growth. In these and other studies it is difficult to elucidate whether

each polyamine exerts different effects in bringing about resumption of cell proliferation, since rapid conversion of putrescine into spermidine and spermine and of spermidine into spermine occurs. However exogenous spermine fully reversed the inhibition of DNA, protein and RNA synthesis. Hölttä et al (1979) did not rule out the possibility that polyamines could directly regulate the metabolism of nucleic acids. Thus the inhibition of general protein synthesis may be reflected in the altered nucleic acid synthesis in polyamine-depleted cells.

Regulation of polyamine biosynthesis

Part of the evidence that polyamines are important for normal cellular growth stems from the rapid and large increase in ornithine decarboxylase activity (ODC) that occurs in virtually all biological systems stimulated to grow (reviewed by Tabor and Tabor, 1976; Maudsley, 1979; Heby, 1981; Pegg and McCann, 1982; Allen, 1983). This increase in ODC activity, which can be very rapid, arises either from de novo synthesis or from the liberation of latent ODC activity (e.g. from an antizyme-ODC complex). In vivo, its half-life is less than 1 hour (as reviewed by Allen, 1983), implying that rapid inactivation of the enzyme must occur. ODC activity may also be subject to some form of feedback inhibition and repression by putrescine or spermidine.

Fong et al (1976) showed that the 'feed back' inhibition may involve the induction of a macromolecular inhibitor, the so-called 'antizyme'. Despite the fact that this 'antizyme' has been well characterized (Cannellakis et al, 1981) its precise role is not clear ever since the discovery of posttranslational modifications of ODC in mammalian and non-mammalian systems to an inactive form of ODC. Two posttranslational modifications have been found: a phosphorylated ODC (Kuehn and Atmar, 1982; Sekar et al, 1982) and an ODC-putrescine conjugate. ODC from rat liver is capable of being post-translationally modified on its γ-glutamyl side-chains by the addition of 4 moles of putrescine, a reaction catalysed by a transglutaminase (Russell and Manen, 1982; and reviewed by Allen, 1983). A polyamine-dependent kinase has been reported in many cell types that specifically phosphorylates ODC (Kuehn and Atmar, 1982; Sekar et al, 1982).

Despite the fact that these post-translational modifications lead to a loss of ODC activity, Russell and Manon (1982) showed that when the ODC-putrescine conjugate was added to a preparation of rat liver nuclei (in vitro), there was a subsequent increase in RNA polymerase I activity. Allen (1983) put forward a hypothetical regulatory role for ODC incorporating a role for the ODC-putrescine conjugate.

In mammalian cells, SAM decarboxylation is also regulated by polyamines. The enzyme is activated by

putrescine and inhibited by spermidine so that the supply of S-(5'-adenosyl)-3-methylthiopropylamine is regulated by the requirement for spermidine and the availability of putrescine (Pegg, 1984). A detailed review of polyamine and ODC regulation is given by Canellakis et al (1979).

Polyamine synthesis and the cell cycle

Polyamines and their biosynthesis are closely associated with the cell cycle (reviewed by Tabor and Tabor, 1976; Maudsley, 1979; Heby, 1981; Pegg and McCann, 1982; Allen, 1983). Early studies suggested that some cells required exogenous polyamines to achieve maximum growth-rate (as reviewed by Heby, 1981). Heby et al (1982) showed that cellular putrescine, spermidine, and spermine increased progressively as the cell cycle proceeded from G_1 to mitosis, in a manner reflecting the order of biosynthesis of these polyamines. Heby et al (1982) also showed that spermidine levels of cells in culture showed a direct linear correlation with their growth rate. They interpreted this result as indicating that the accumulation of spermidine is directly associated with cell replication. They also showed that a high content of putrescine and spermidine increased and that a low content restrained, the growth-rate; they concluded that putrescine and spermidine played a part in the regulation of the cellular growth-rate (Heby, 1981; Heby et al, 1982). However, Allen

(1982) pointed out that the accumulation of polyamines in cells during the cell cycle may be accounted for by the concurrent increase in cell volume. For all that, in a study using Chinese hamster ovary (CHO) fibroblasts synchronised by mitotic detachment, Heby and Anderson (1980) (as reviewed by Pegg and McCann, 1982) found that polyamine synthesis started in mid G_1 and polyamines began to accumulate towards the end of the G_1 phase. Polyamine synthesis peaked as DNA synthesis (S phase) began. The levels of putrescine, spermidine and spermine, and ODC activity decreased markedly during mid-S but rose again towards the end of the S-phase. Just before cell division, ODC activity and the level of polyamines reached a second peak, falling rapidly after mitosis. It was concluded that the two peaks of ODC activity and polyamine-accumulation may be connected with the preparation of cells for DNA synthesis and division. Similar results, using rat hepatoma cells, were reported by McCann et al (1975). However it has been reported that cells in G_1, that have been rendered unable to synthesize polyamines, have enough polyamines to allow some DNA synthesis to occur (as reviewed by Allen, 1983).

Jänne et al (1975) studied the effect of polyamines on the in vitro transcription of DNA and chromatin. They showed that physiological levels of spermidine and spermine stimulated transcription by DNA-dependent RNA polymerases by increasing the rate of RNA-chain

elongation whereas higher concentrations inhibited chain-elongation. They suggested that this mechanism indicated a possible role for these polyamines as intracellular regulators of transcription.

The effects of polyamine depletion, induced by the use of inhibitors of polyamine synthesis, on the stages of the cell cycle have been investigated and reviewed by Pegg and McCann (1982) and Allen (1983). Briefly, non-transformed cells, depleted of polyamines, eventually arrest in G_1 whereas transformed cells similarly depleted of polyamines, are able to progress to S or G_2. Sunkara et al (1979 a,b) partly resolved this difference between normal and transformed cells and postulated that polyamines may play a role in stabilizing cellular structures, as for example during the mitotic process. Evidence for this stems from the finding that transformed cells (CHO and HeLa) depleted of polyamines by MGBG or α-methylornithine, had altered chromosome condensation and reduced cytokinesis (Sunkara et al, 1979, a,b). Hölttä and Pohjanpelto (1983) showed that CHO cells, depleted of polyamines in this manner, undergo mitosis at a reduced rate.

In a wide variety of animal tumours there is a general pattern of increased putrescine and spermidine synthesis; this is also observed in other types of hyperproliferative conditions, such as the skin abnormality, psoriasis.

Polyamines and Differentiation

There is a lot of good evidence that polyamines play a role in mammalian cell differentiation, and that interference with polyamine biosynthesis can influence differentiation (reviewed by Heby, 1981; Pegg and McCann, 1982). For example DFMO has profound effects on embryonic development in a wide variety of species (cited by Pegg and McCann, 1982).

Polyamines have been implicated in the complex process of bone differentiation. Briefly, Rath and Reddi (1981) showed enhanced polyamine synthesis during osteogenesis, using a matrix-induced endochondrial bone formation model. Takano et al (1982) showed a requirement for polyamines during the differentiation of rabbit costal chondrocytes in culture and that exposure to HAVA blocked glycosaminoglycan synthesis in these cultured chondrocytes. These effects were reversed by the addition of putrescine. An important finding by these authors was that these effects were observed in non-proliferating culture and thus indicated that polyamines are not required solely for cell growth. In Chapter IX the effects of vitamin B_6 deficiency on fracture healing are studied.

CHAPTER V

METHODS

The main procedures used in these studies were (A) those for preparing sections; and (B) those for measuring the amount of chromogenic product produced per cell. The use of quantitative polarized light microscopy is discussed in Chapter X. The materials and methods used for each study are given in the relevant chapters in this thesis.

A. Preparatory Procedures.

1. Chilling.

The basis of the chilling procedures has been discussed by Chayen and Bitensky (1968). It depends on chilling to -70°C, to produce supercooling (Lynch et al, 1966) and then sectioning in a cryostat with the cabinet temperature at -25°C and with the knife cooled further by packing solid carbon dioxide around its shaft, to dissipate the heat of the cutting onto the knife and away from the tissue (e.g. Chayen, 1980).

These procedures were developed for soft tissues. For bone, I found it necessary to coat the specimen with a 5% solution of polyvinyl alcohol (PVA) before it was chilled. This was beneficial as it prevented the bone from cracking during the chilling procedure. The 5% PVA also successfully filled the marrow spaces in the bone especially in the large human pieces and in doing so, bound the sparse trabeculae. Finally

when the bones were mounted on chucks prior to sectioning (Chayen et al, 1973), the pieces were embedded in a solution of 5% PVA: the original coating protects the tissue from thawing. This embedding of the bone in the 5% solution of PVA greatly enhances the ease with which sections can be cut.

2. Sectioning.

For this work, a tungsten carbide-tipped knife, set in a special Jung 1130 heavy duty rotary microtone (in a Bright's cryostat) was used to section fresh, unfixed, undemineralized bone (as described fully by Johnstone et al, 1972; Johnstone,1979). As in the soft tissue procedure, the knife was cooled with solid carbon dioxide and the cabinet was maintained at -25 to -30°C.

In conventional soft tissue cryostat microtomy, the sections were flash-dried off the knife (Chayen et al, 1973). This was possible with the small sections of rat growth-plate described in Chapter VI. However with the larger pieces of bone used in the various studies in this thesis, it was necessary to lightly press the slide against the knife to pick the section off. It proved beneficial to coat the knife with a thin layer of low temperature oil: this prevented the section from sticking to the knife.

3. Cytochemical reactions.

The procedures were the same as for cryostat

sections of fresh tissue (Chayen et al, 1973). Details of the reactions are given in the relevant chapters and in the Appendix.

A major difference is the fact that the Gomori calcium-trapping method for alkaline phosphatase activity cannot be applied to sections of undemineralized bone because of the calcium-content of the bone. It was replaced by the naphthol phosphate method (described by Chayen et al, 1973) as was used by Shedden et al (1976). The substrate, α-napthol acid phosphate (sodium salt) was used at a considerably lower concentration (1/5th) compared with that used for other tissues, because of the exceptionally high alkaline phosphatase activity in growing bone.

The use of Alcian blue to stain for glycosaminoglycans (GAGs) by the critical electrolyte method of Scott and Dorling (1965; and as described by Chayen et al, 1973) is described fully in Chapter X.

B. Measurement.

The chromogenic reactions were measured by scanning and integrating microdensitometry by means of a Vickers M85 or M85A microdensitometer. The theory of the procedure has been described by Chayen (1978; 1980); possible pitfalls have been discussed by Bitensky (1980). For the studies on bone a x40 objective was used and a flying spot that had a diameter of 0.4 μm in the plane

of the section. In Chapter XI(Development of a Method for Measurement of Na^+ K^+-ATPase) a x100 objective was used in part of the study. Details of the exact procedures used for each study are given in the relevant place.

CHAPTER VI.

OXIDATIVE METABOLISM OF NORMAL BONE: THE PARADOX OF 'AEROBIC GLYCOLYSIS'.

PART I. CYTOCHEMICAL STUDIES ON FATTY ACID OXIDATION.

Introduction

Although many cytochemical methods have been developed for assaying the activity of enzymes that oxidize sugar-based substrates, virtually no methods exist for those that are involved in the oxidation of fatty acids. Yet fatty acids are oxidized to carbon dioxide and water in almost all tissues of the vertebrates (Lehninger, 1976); in some, fatty acids comprise around half, or more, of the substrates for the production of energy. Thus even in rat liver, up to about 40% of the energy-production comes from fatty acids; in well oxygenated cardiac tissue, fatty acid oxidation accounts for 60%-70% of the total oxidative activity, increasing in certain conditions (Neely et al, 1972) or becoming suppressed in anoxic conditions (Neely and Morgan, 1974).

There was no information as to whether cells of bone, or of the associated cartilage of the growth plate, oxidize fatty acids as a source of energy or not. It was therefore of some moment to develop a method for assaying fatty acid oxidation to test this question.

Consequently, Part I of this Chapter will be devoted firstly to a description of the development of a quantitative cytochemical assay of the activity of one of the enzymes involved in fatty acid oxidation, based largely on the method developed by Chambers et al (1982) and done during that work, and secondly to the validation of this method as applied to bone and to the growth plate. In the second part of this Chapter, the peculiar metabolic paradox of 'aerobic glycolysis' in bone and cartilage will be considered.

Oxidation of Fatty Acids.

Briefly the oxidation of fatty acids is as follows. Fatty acids enter the cell and are activated by formation of a CoA derivative. These acyl CoA derivatives are unable to permeate through the mitochondrial membrane into the mitochondria, to the site of fatty acyl CoA oxidation. The acyl group is transferred to the carrier molecule carnitine. The movement of the acyl carnitine across the membranes of the mitochondria is mediated by acyl transferases (Fritz, 1963; Fritz and Yue, 1963). Then the acyl group from the fatty acyl carnitine is transferred to intramitochondrial CoA, occurring on the inner surface of the inner membrane of the mitochondrion, releasing carnitine. The acyl CoA derivatives are oxidized by a sequence of reactions in which the fatty acyl chain is shortened by β-oxidation, involving the removal of two carbon atoms at a time. The intermediates in these reactions are CoA derivatives.

This shortening of the fatty acid chain by two carbon atoms requires 4 steps:

(1)

(fatty acyl-CoA-thioester)

$$\overset{(3)}{R\ CH_2}\ \overset{(2)}{CH_2}\ CH_2\ COSCoA + FAD$$

$$\xrightarrow[\text{dehydrogenase}]{\text{acyl CoA}} RCH_2\ CH = CHCOSCoA + FADH_2$$

(α,β- unsaturated acyl-CoA)

(2)

$$R\ CH_2\ CH = CH\ COSCoA + H_2O$$

$$\underset{\text{transferase}}{\overset{\text{enoyl CoA}}{\rightleftharpoons}} \overset{(3)}{R\ CH_2\ CH\ OH}\ \overset{(2)}{CH_2}\ COSCoA$$

(β-hydroxyacyl-CoA)

(3)

$$RCH_2\ CHOHCH_2\ COSCoA + NAD^+$$

$$\underset{\text{dehydrogenase}}{\overset{\beta\text{ hydroxyacyl CoA}}{\rightleftharpoons}} \overset{(3)}{RCH_2\ CO}\ \overset{(2)}{CH_2}\ COSCoA + NADH + H^+$$

(β-ketoacyl-CoA)

(4)

$$\overset{(3)}{RCH_2\ CO}\ \overset{(2)}{CH_2}\ COSCoA + HSCoA$$

$$\underset{\text{acetyltransferase}}{\overset{\text{acetyl CoA}}{\rightleftharpoons}} RCH_2\ CO\ SCoA + CH_2\ COSCoA$$

(fatty acyl-CoA)

The long-chain saturated fatty acyl-CoA product, having two fewer carbon atoms than the original fatty acid, becomes the substrate for another β-oxidation.

Thus at each passage through this spiral the fatty acid chain loses a two-carbon fragment as acetyl CoA. During the dehydrogenation steps the hydrogen atoms removed enter the respiratory chain. Each molecule of $FADH_2$ donates a pair of reducing equivalents to ubiquinone of the respiratory chain: two molecules of ATP are generated from ADP and phosphate during the transport of the reducing equivalents to oxygen and the coupled phosphorylations. Similarly each molecule of NADH formed donates a pair of reducing equivalents to the NADH dehydrogenase of the respiratory chain: the subsequent transport of the reducing equivalents to oxygen results in the formation of 3 ATP molecules from ADP and phosphate. Thus 5 molecules of ATP are formed per molecule of acetyl-CoA removed during each β -oxidation. The other product, acetyl CoA then enters the Krebs' cycle and is oxidised to CO_2 and H_2O.
The overall equation (Lehninger, 1982) for the complete oxidation of palmitic acid (16 carbons) for example is:

$$\text{Palmitic acid} + 23O_2 + 129\ Pi + 129\ ADP \longrightarrow 16\ CO_2 + 145\ H_2O + 129\ ATP$$

i.e. 35 ATPs from 7 cycles of β-oxidation and 96 from 8 oxidations of acetyl CoA by the Krebs' cycle. Two molecules of ATP are utilized to form palmitoyl CoA.

About 40% of the standard free energy of oxidation of palmitic acid is recovered as high-energy phosphate.

Development of the Method

Background

In conventional biochemistry the activity of βhydroxyacyl-coenzyme A dehydrogenase (step 3) is assayed by measuring the reversal of the reaction, i.e. the reduction of aceto-acetyl-coenzyme A by NADH. However this substrate is very expensive and has now been taken off the market because of the carcinogenic properties of the intermediates used in its synthesis. Even when this substrate was used, the less expensive N-acetyl cysteamine derivative was often used instead of coenzyme A. The aceto-acetyl-cysteamine was about 5 times less efficient so that increased concentrations of the substrate had to be used to compensate (Biochemica Catalogue, 15336EHAB). Unfortunately this reaction, involving the oxidation of NADH, cannot be linked to a cytochemical chromogenic reaction. These problems were overcome by the synthesis of a new substrate (by Mr. G.T.B. Frost, Sigma), namely DL-S-β-hydroxybutyryl-N-acetyl cysteamine. The reaction is thus:

$CH_3\ CH_2\ CH_2\ COO\text{-cysteamine} + NAD^+ \rightleftharpoons$

hydroxybutyryl cysteamine

$CH_3\ CO\ CH_2\ COO\text{-cysteamine} + NADH$

acetoacetyl cysteamine

and the reducing equivalents from the NADH can easily be transferred directly or indirectly by way of an intermediate electron acceptor (e.g. PMS or menadione) to a tetrazolium salt. The resulting reduced tetrazolium, a formazan, is a purple precipitate that can be measured

quantitatively using a scanning and integrating micro-densitometer.

Materials and Methods

Metatarsals were removed from 50 g female Wistar rats, killed by cervical dislocation. The metatarsals were cut in half and the distal half, with the epiphyseal plate,was removed. Two metatarsals from each of six rats were used in this study. The bones were dipped in 5% polyvinyl alcohol before being chilled in n-hexane at -65 to 70°C. These techniques have been fully described by Chayen et al (1973) and in Chapter V. The bones were sectioned (10 μm) on a Jung 1130 rotary microtome set in a Bright's cryostat (cabinet temperature -25 to 30°C, with the knife cooled with solid carbon dioxide: Johnstone et al, 1972; Johnstone, 1979).

The reaction-medium contained 0.6% (10 mM) chloroform purified neotetrazolium chloride (Serva) in a 30% (w/v) solution of polyvinyl alcohol (grade G04/140; Wacker Chemicals Ltd., Walton-on-Thames, Surrey, U.K.) in glycyl-glycine buffer (50 mM; pH 8.0). Two intermediate electron-acceptors were studied, namely phenazine methosulphate and menadione (2-methyl-1-4 naphthoquinone). The reaction medium also contained NAD as the required co-factor. Sodium nitroprusside was included to inhibit the effects of any acetyl cysteamine liberated by non-enzymic hydrolysis of the substrate. Sodium nitro-prusside forms a complex with any cysteamine released during the reaction. The reaction-medium also contained either the substrate DL-S-hydroxybutyryl-N-acetyl cysteamine or cysteamine

(β-mercaptoethylamine) for control experiments. The hydroxybutyryl cysteamine substrate is a viscous liquid, and about 90 - 95% pure. The menadione and the substrate were first dissolved in a small volume of ethanol to give a final concentration of alcohol in the reaction-medium of 1%.

The reactions were done at 37° C in an atmosphere of nitrogen, since oxygen competes with neotetrazolium chloride for reducing equivalents.

Measurement. The coloured formazan produced in the sections was measured with a Vickers M85 scanning and integrating microdensitometer with a x40 objective and a flying spot that had a diameter of 0.4 μm in the plane of the section, and at a wavelength of 585 nm (Butcher and Altman, 1973). The mask encompassed one cell of each type studied. Thus the results were expressed as units of extinction (M.I.E. x100) per cell; correction had to be made for the time of reaction.

The cell types that were measured were as follows:

1. chondrocytes in the (a) hypertrophic zone
   (b) proliferating zone
   (c) resting zone
2. osteoblasts in the metaphysis
3. osteocytes in the metaphysis

Results

Initial work on the cytochemical demonstration of β-hydroxyacyl CoA dehydrogenase activity had been done on dog cartilage (Nahir, 1983). The concentrations of the reactants used in that study were used as a basis for the present optimization experiments on rat bone. The basic reaction-medium contained 30% PVA (G04/140 grade) in 0.05 M glycyl-glycine buffer, pH 8.0, to which was added 0.6% neotetrazolium chloride; 5 mM sodium nitroprusside; 3 mM menadione; and 2 mM NAD^+. The final pH after the addition of the substrate (or cysteamine as a control) was pH 8.5. The reaction-medium was saturated with nitrogen and warmed to 37° C. Preliminary experiments showed that, in bone, 45 minutes reaction-time gave an adequate level of activity for microdensitometric measurements.

Optimal Concentrations of Reactants

Concentrations of substrate and cysteamine. Measurements made in osteoblasts and chondrocytes, in the growth plate, with increasing concentrations of substrate produced typical substrate-activity graphs with a rapid initial rise in activity at lower concentrations (up to 5 - 10 mM) and a much slower rise in activity at higher concentrations, up to 100 mM (Fig. VI.1).

Because of the small differences found at higher concentrations, and also the high cost of the substrate, 37 mM was taken as an adequate compromise.

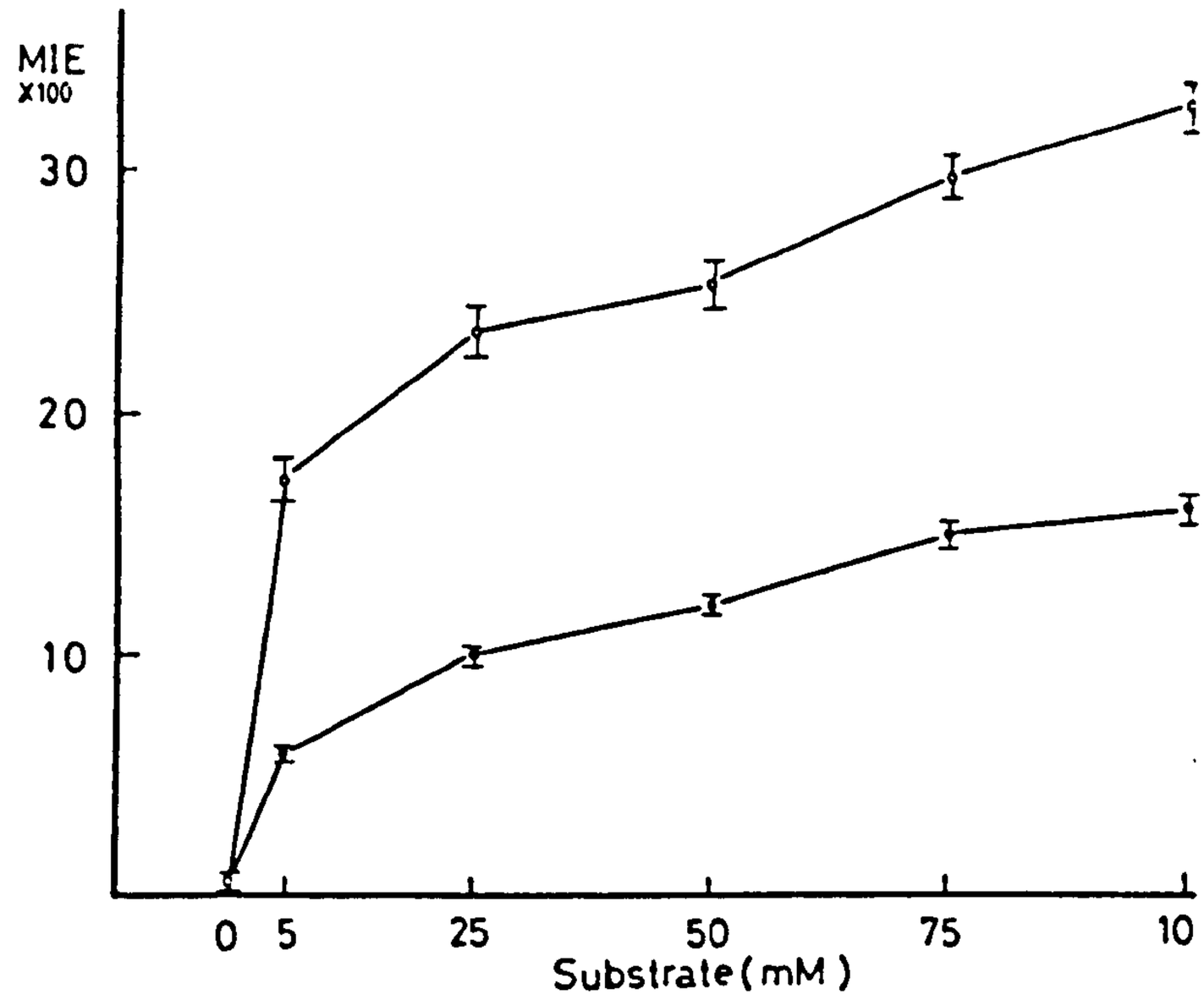

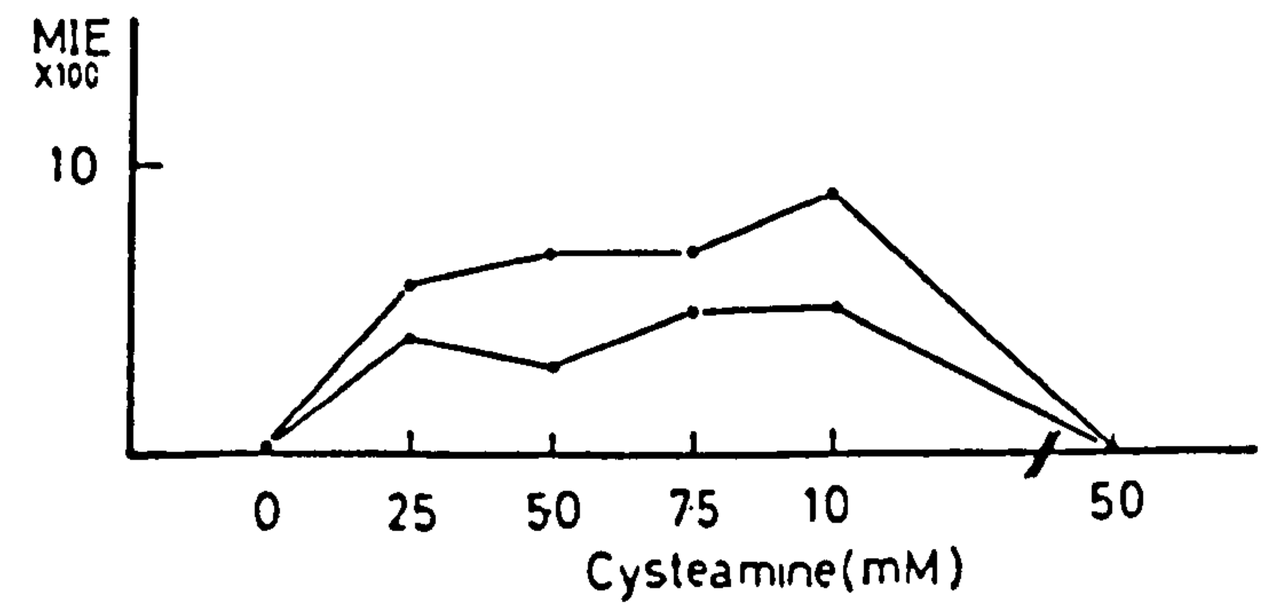

Fig. VI. 1 Upper graph. The activity of hydroxyacyl dehydrogenase (MIE x 100; mean ± SEM) in osteoblasts (open circles) and chondrocytes (closed circles) with increasing concentrations of the substrate.

Fig. VI. 2 Lower graph. Sections of growth plate incubated with increasing concentrations of cysteamine (in place of the substrate DL-S-β hydroxybutyryl-N-acetyl cysteamine); this 'activity' would indicate the maximum 'non-specific' reduction of the tetrazolium salt by spontaneous hydrolysis of the substrate to yield free cysteamine. Chondrocytes: lower; osteoblasts: upper.

The substrate can be hydrolysed at the pH of the reaction medium (8.5) to yield free N-acetyl-cysteamine, that in the presence of an intermediate electron acceptor, could reduce the neotetrazolium chloride. The amount of cysteamine liberated in the reaction-medium over a period of 90 minutes, measured spectrophotometrically (Jocelyn, 1972), gave values equivalent to 3.1, 4.0 and 2.7 mM of free cysteamine (in 3 separate determinations).

When sections were reacted with various concentrations of cysteamine instead of the substrate, the "activity" recorded was maximal with 2.5 mM cysteamine. This level of activity persisted up to 10 mM, but at higher concentrations the "activity" dropped. At 50 mM no activity was recorded (Fig. VI.2).

Because the greatest concentration that was actually found in the reaction-medium did not exceed 5 mM, this concentration was used for 'control' reactions.

Optimal concentration of NAD^+. Fig. VI.3 shows the graph relating activity to various concentrations of cofactor, measured in osteoblasts and chondrocytes. The activity was broad with around 2 mM NAD^+ giving maximum activity. Higher concentrations showed little sign of inhibition.

Optimal pH. The optimal pH was pH 8.5 for osteoblasts and pH 8.0 for chondrocytes (Fig. VI.4). In the final method the pH of the medium was adjusted to pH 8.9 before

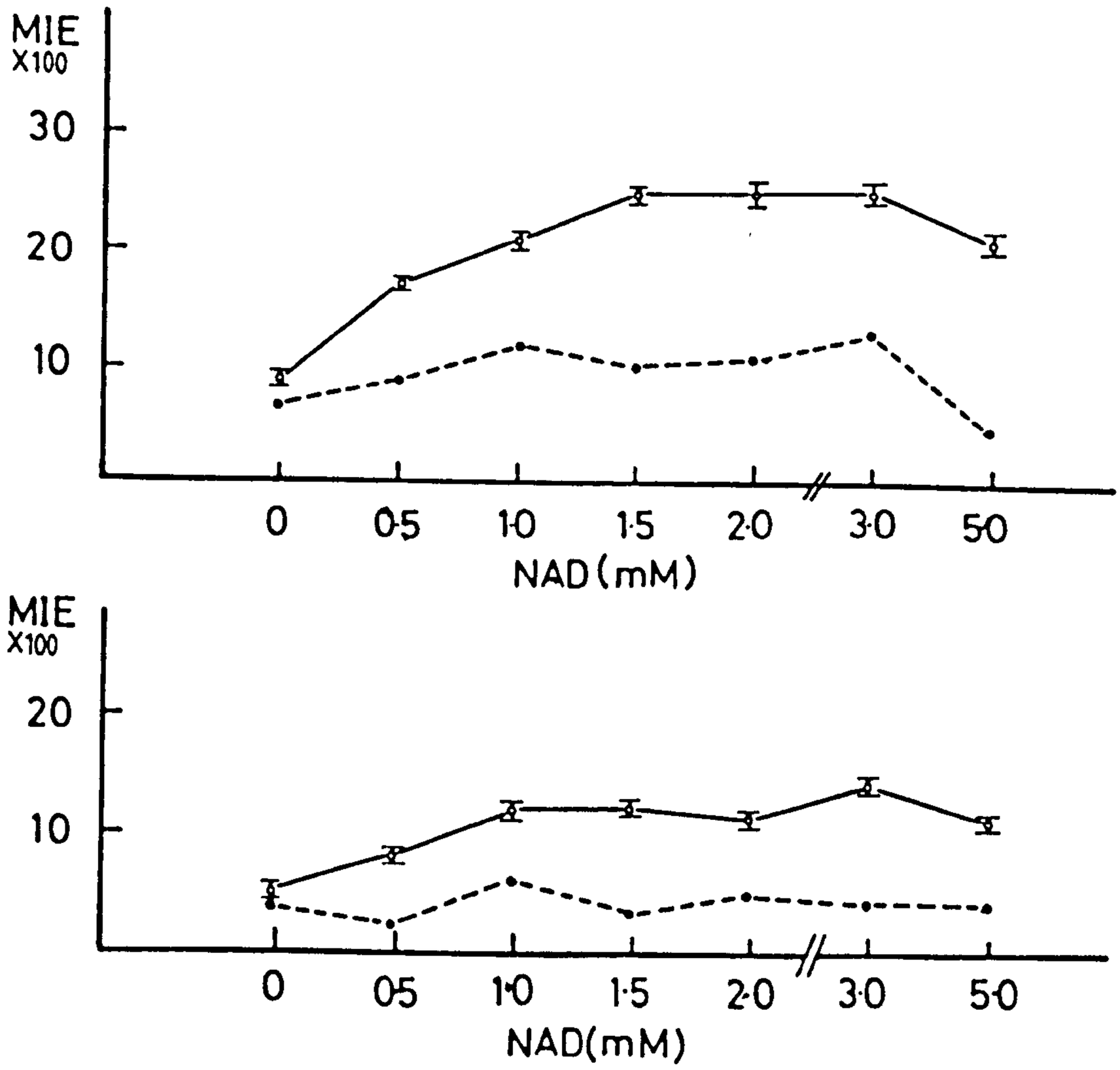

Fig. VI. 3 Activity of hydroxyacyl dehydrogenase (MIE x 100; mean ± SEM; solid line) in osteoblasts (upper graph) and chondrocytes (lower graph) with increasing concentrations of NAD. The activity recorded with cysteamine in the place of the substrate is indicated by the dotted line.

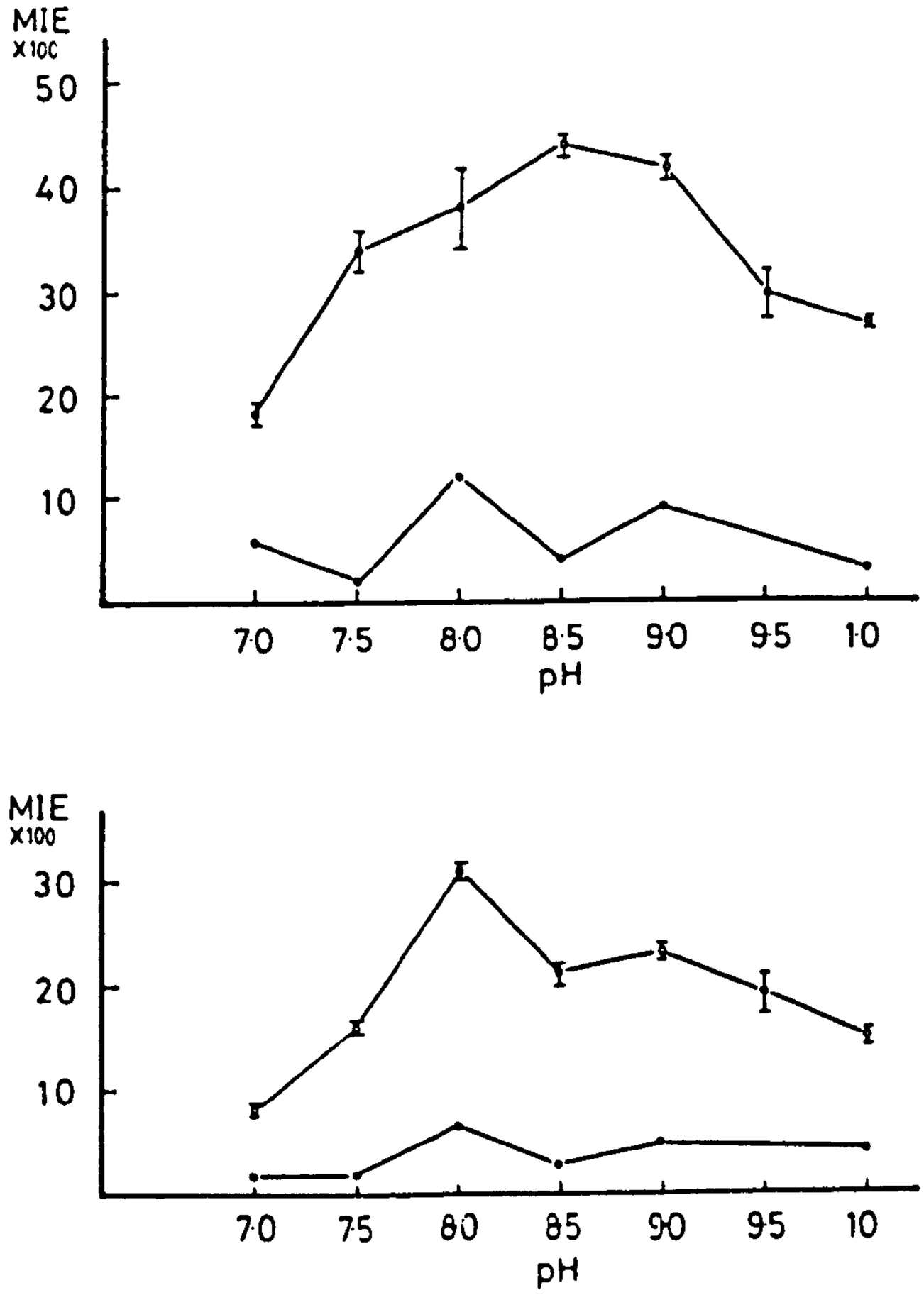

Fig. V1. 4 The hydroxyacyl dehydrogenase activiety (MIE x 100: mean ± SEM; open circles) at various pH values measured in osteoblasts (upper graph) and chondrocytes (lower graph). Cysteamine in place of the substrate: filled circles.

the substrate, or cysteamine, was added to it and brought down to pH 8.5 with 1 M HCl.

Optimal concentration of neotetrazolium chloride (NT). The concentration of this final hydrogen-acceptor had a strong influence on the activity recorded. Measurements in the osteoblasts showed mean extinction of 0.29 with 0.6% NT (10 mM); maximal (0.32) at 0.9% NT (15 mM): there was some inhibition (extinction of 0.23) at 1.2% NT (20 mM). A concentration of 0.6% NT was used in all subsequent studies (Fig. VI.5).

Optimal concentration of nitroprusside. Nitroprusside increased activity in osteoblasts and in chondrocytes up to a concentration of 5 mM with considerable inhibition at higher concentrations (Fig. VI.6). There was total inhibition of activity when 50 mM nitroprusside was used. A concentration of 5 mM was used in all subsequent studies.

Optimal concentration of menadione or of phenazine methosulphate (PMS). Menadione is the preferred intermediate hydrogen-acceptor for this reaction (Chambers et al, 1982). Menadione forms an adduct with thiols (Olson et al, 1978) so that it might be expected to react with any cysteamine liberated by the spontaneous hydrolysis of the substrate. Increasing the concentration of menadione (Fig. VI.7) up to 3 mM, increased the activity

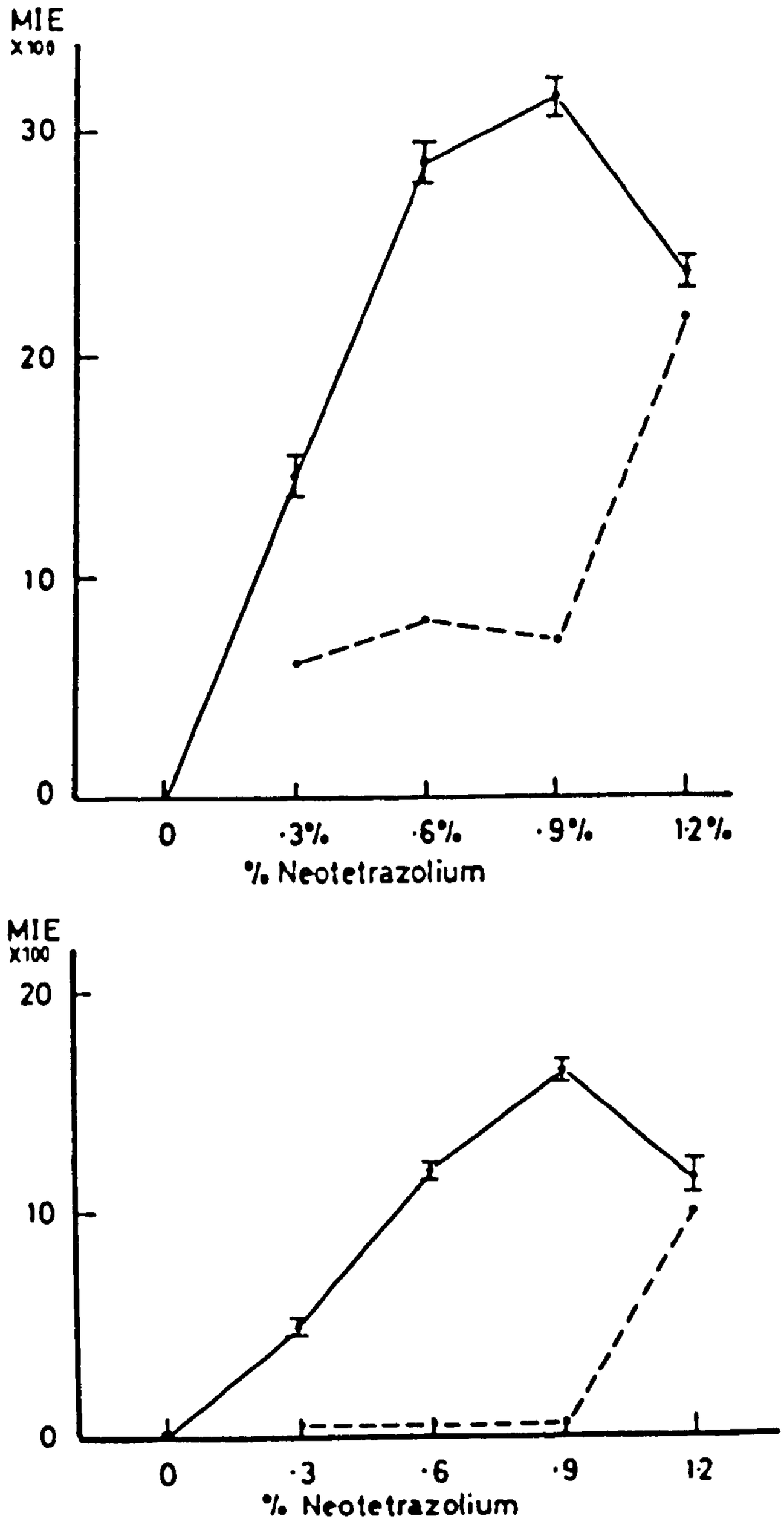

Fig. VI. 5 Hydroxyacyl dehydrogenase activity (MIE x 100; mean ± SEM) with different concentrations of neotetrazolium chloride measured in osteoblasts (upper graph) and chondrocytes (lower graph). The activity with cysteamine in the place of the substrate is shown by the dotted line.

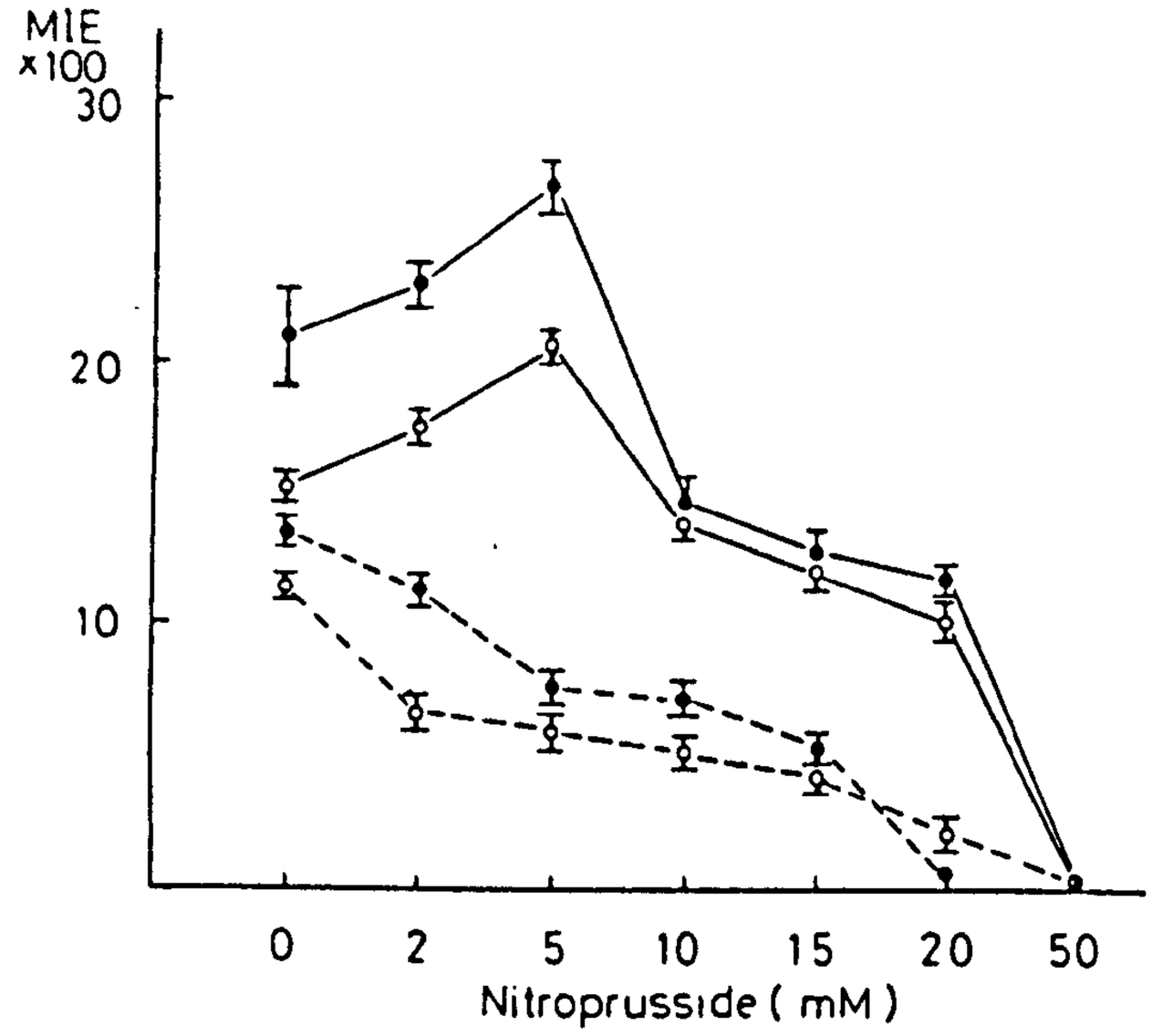

Fig. VI. 6 The effect of increasing concentrations of sodium nitroprusside on the activity of hydroxyacyl dehydrogenase (MIE x 100; mean ± SEM) in osteoblasts (closed circles) and chondrocytes (open circles); cysteamine in place of substrate is shown by the dotted line.

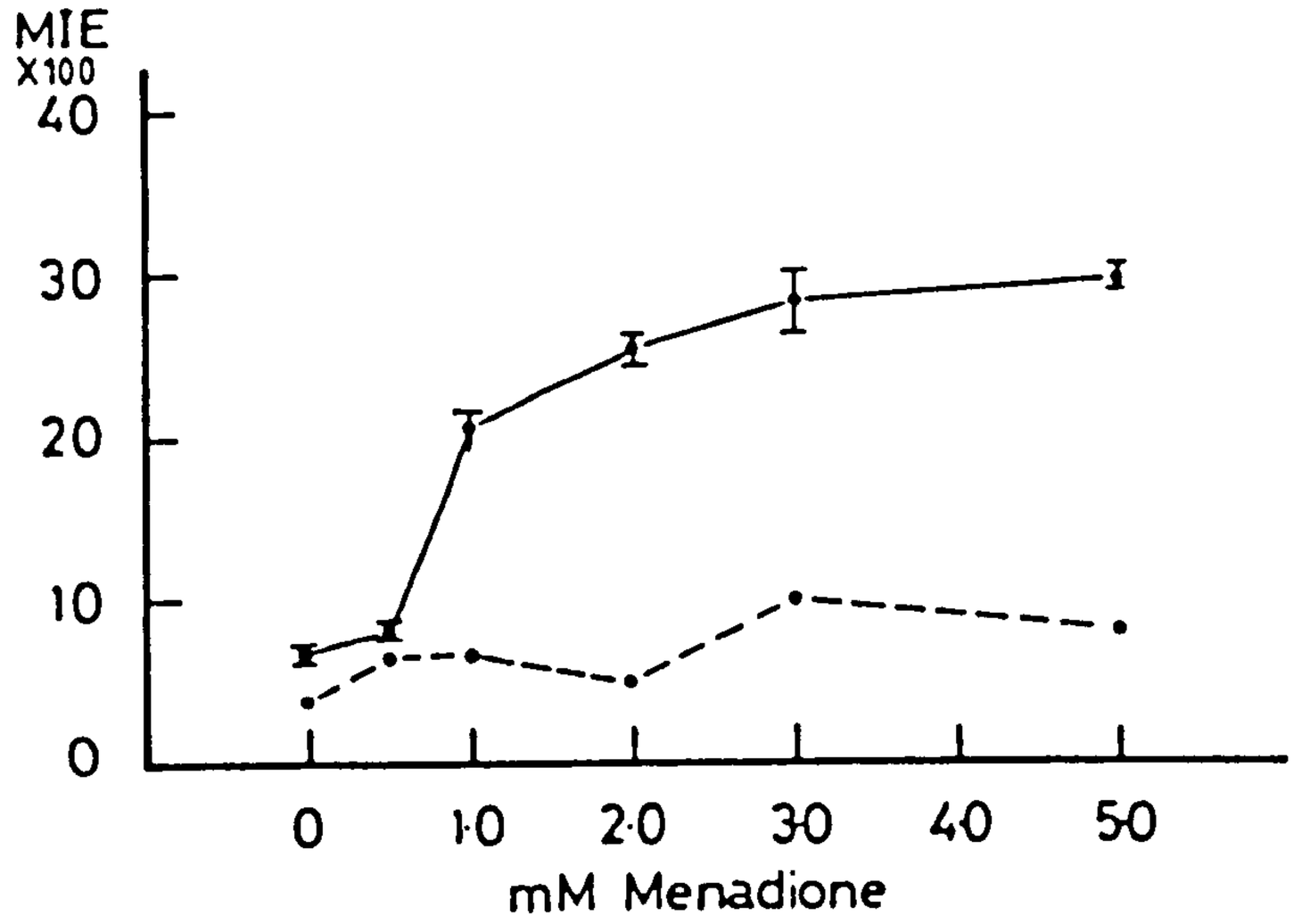

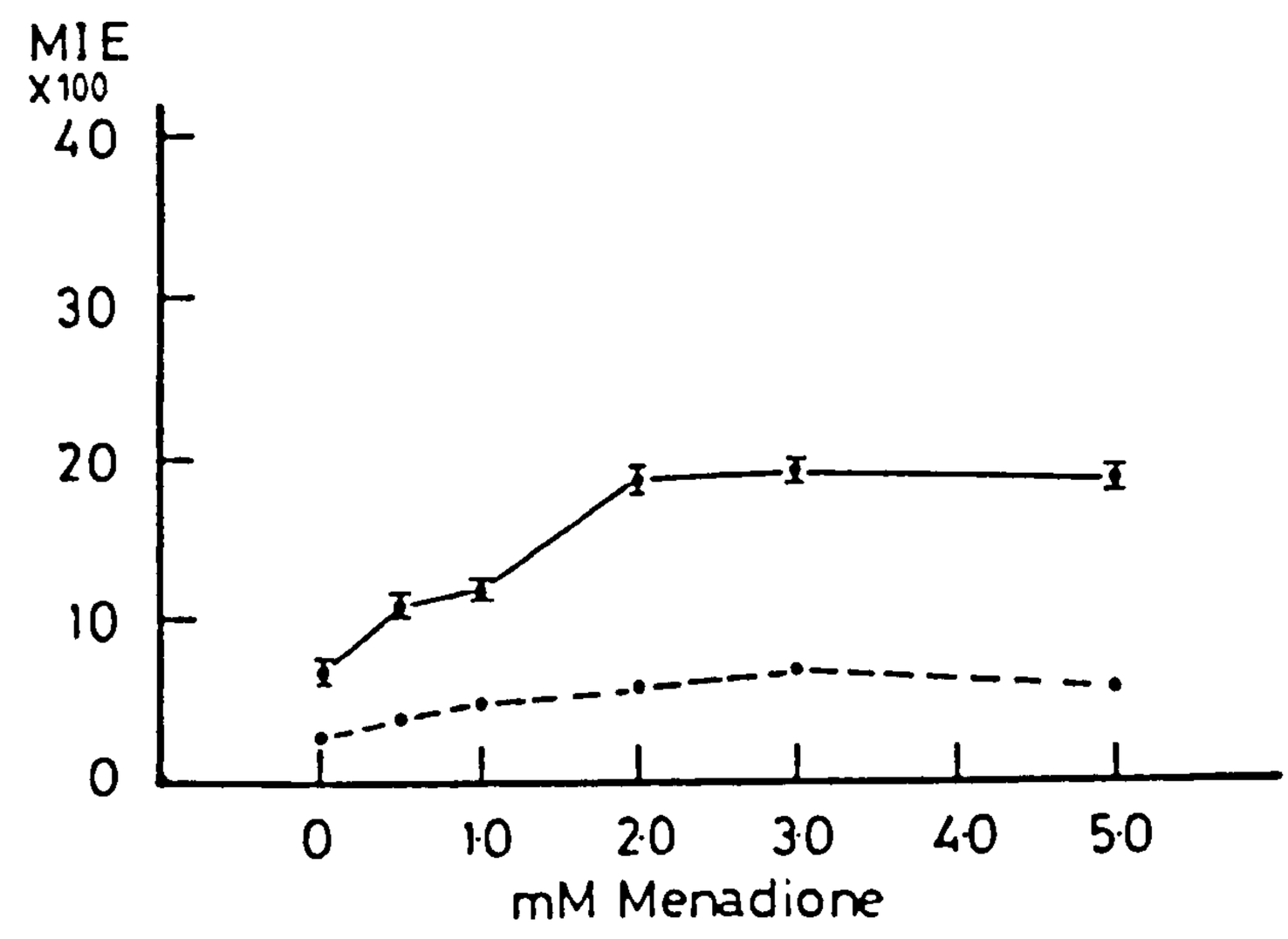

Fig. VI. 7 The effect of increasing concentrations of menadione on the activity of hydroxyacyl dehydrogenase (MIE x 100; mean ± SEM) in osteoblasts (upper graph) and chondrocytes (lower graph); cysteamine in place of substrate is shown by the dotted lines.

in the osteoblasts and chondrocytes. There was no further increase, or inhibition, at concentrations up to 5 mM.

A concentration of 3 mM was used in all subsequent studies.

Fig. VI.8 shows a graph of enzyme activity with various concentrations of the intermediate hydrogen-acceptor, phenazine methosulphate (PMS). Maximal activity was found at a concentration of 1 mM.

Linearity of response. The reaction was linear with time over the first 45 minutes (Fig. VI.9). Over the subsequent 20 minutes there was only a small increase in activity. With longer reaction times there was no increase in activity.

Cell-types that show activity. When sections of bone were incubated in the final reaction-medium for 45 minutes at 37° C there was β-hydroxyacyl dehydrogenase activity in all the cell-types of normal bone, including the osteocytes deeply embedded in adult bone; with most cytochemical procedures, these cells show remarkably little metabolic activity.

Discussion

With the development (by Mr. G.T.B. Frost) of this new substrate, namely DL -S-β-hydroxybutyryl-N-acetyl cysteamine and this method for measuring fatty acid oxidation, it has been possible to demonstrate, for the first time, that all the cells of the growth plate, even the differentiated osteocytes, are capable of oxidizing fatty acids.

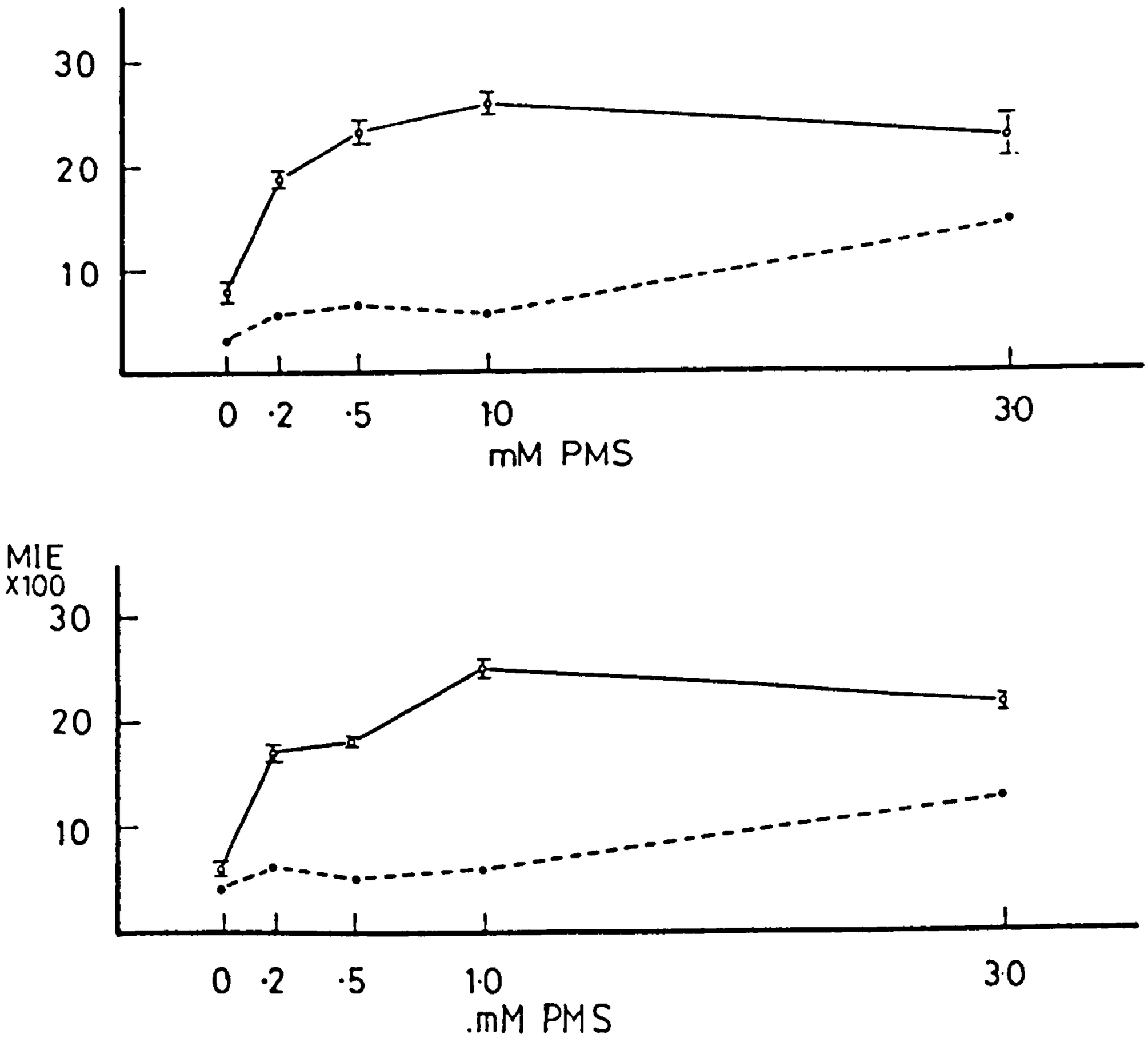

Fig. VI. 8 The effect of increasing concentrations of phenazine methosulphate (in place of menadione) on hydroxyacyl dehydrogenase activity (MIE x 100; mean ± SEM) measured in osteoblasts (upper graph) and chondrocytes (lower graph). Dotted lines: cysteamine in place of the substrate.

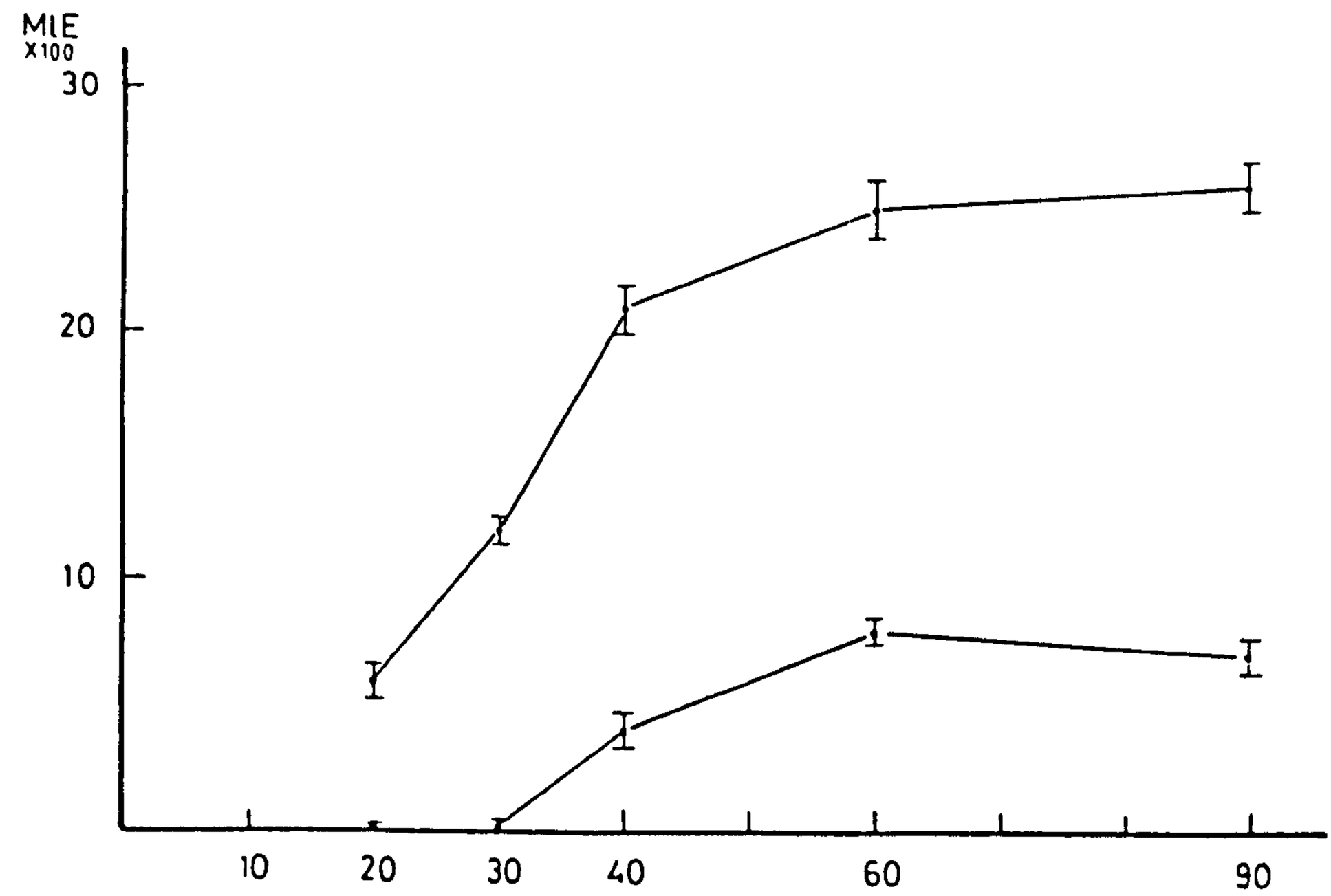

Fig. VI. 9 Hydroxyacyl dehydrogenase activity (MIE x 100; mean ± SEM) with increasing times of incubation measured in osteoblasts (upper line). Lower line: activity with cysteamine in place of the substrate.

PART II. OXIDATIVE METABOLISM OF BONE AND CARTILAGE

Introduction

Bone and cartilage are capable of producing considerable amounts of lactic acid from glucose (Hekkelman, 1973; Neuman, 1977; Stockwell, 1979; Maroudas, 1980). Cartilage is very avascular and therefore relatively anaerobic which could explain the high glycolytic activity. However, bone is a highly vascular tissue so this argument cannot apply. Also, bone and cartilage show the phenomenon of "aerobic glycolysis": that is a high rate of formation of lactic acid from glucose, even when studied, in vitro, at high oxygen tensions in the medium, effectively defying the Pasteur effect. This phenomenon of aerobic glycolyses is not peculiar to bone and cartilage, but occurs in many cell-types, e.g. in erythrocytes, renal medulla, striated muscle, tissues of the foetus, intestinal mucosa, retina and particularly in growing malignant cells (Krebs, 1972; Eigenbrodt and Glossmann, 1980).

In bone it is believed that lactate production is the principle mechanism by which the bone cells control the effluxes of ions from the bone fluid (Neuman, 1977). So far, no single cause for the high glycolytic activity of tumours has been identified, although it has been claimed by Eigenbrodt and Glossmann (1980) that 'aerobic glycolysis' may be a prerequisite for the synthesis of 5-phosphoribose-1-pyrophosphate and of nucleic acids; this is particularly apparent in tumour cells which have an increased demand for precursors of nucleic acid

synthesis (Eigenbrodt and Glossmann, 1980).

The current view (Eigenbrodt and Glossmann, 1980) is that the inhibition of glycolysis by oxygen is due to the allosteric inhibition of phosphofructokinase by mitochondrial ATP from the Krebs' cycle (Krebs, 1972). Under sufficient oxygen supply normal cells adjust their pyruvate production to the level of acetyl-CoA consumption by the Krebs' cycle and their energy requirement. The inhibition by ATP of phosphofructokinase results in a decrease in the conversion rate of fructose 6-phosphate to fructose 1,6 diphosphate. Fructose 1,6 diphosphate is rapidly converted to pyruvate so that steady state levels of fructose 1,6 diphosphate are very low and not sufficient to overcome the ATP inhibition of phosphofructokinase. Glucose 6-phosphate accumulates as a result of this inhibition and blocks its own synthesis by hexokinase. In this way mitochondrial ATP production regulates the glycolytic sequence (Krebs, 1972). Citrate and Mg^{2+} also inhibit phosphofructokinase. Two kinds of activators of phosphofructokinase can be distinguished; enhancers which increase the activity of the enzyme in the absence of inhibitors and deinhibitors which counteract the effects of inhibitors. Passonneau and Lowry (1964) classified the inhibitors, enhancers and deinhibitors (Table VI.1).

Table VI.1 Factors which influence phosphofructokinase activity.

Inhibitors	Enhancers	Deinhibitors of ATP, citrate or Mg^{2+}
ATP	NH_4^+	Fructose diphosphate
Citrate	K^+	Cyclic 3'-5'-AMP
Mg^{2+}	Pi	5'-AMP
	5'-AMP	ADP
	Cyclic 3'-5'-AMP	Fructose 6-phosphate
	ADP	Pi
	Fructose diphosphate	

Under anaerobic conditions, mitochondrial ATP production from acetyl CoA is blocked. Thus ATP levels decrease; phosphofructokinase is de-inhibited; and fructose 1,6-diphosphatase is blocked by the increased AMP levels. The accumulation of fructose 1,6-diphosphate increases the phosphofructokinase activity. The fall in glucose 6-phosphate increases hexokinase activity. Therefore, under totally anaerobic conditions, glycolytic activity can be enhanced, with a concomitant increase in the oxygen-independent production of ATP by the Embden-Meyerhof pathway. However, the activity of glyceraldehyde 3-phosphate dehydrogenase (GAPD) generates NADH. Normally it may be that this is reoxidized to NAD^+, for example by the glycerophosphate-hydroxyacetone phosphate shuttle. However ultimately, this shuttle too is dependent on the presence of an adequate supply of oxygen, in the mitochondria, for the oxidation of the reducing equivalents of this shuttle. Consequently, under strictly anaerobic conditions, the NADH, generated by GAPD activity, is used to reduce pyruvate to lactic acid which is excreted from the cell.

To explain the high production of lactic acid in bone and cartilage, under normal aerobic conditions and oxidative metabolism by the Krebs' cycle, with a functioning mitochondrial electron-transport chain, the step by which pyruvate is oxidized to acetyl CoA may be crucial. The pyruvate dehydrogenase complex is fundamental in determining the fate of pyruvate produced by glycolysis (Fig. VI.10). The complex is

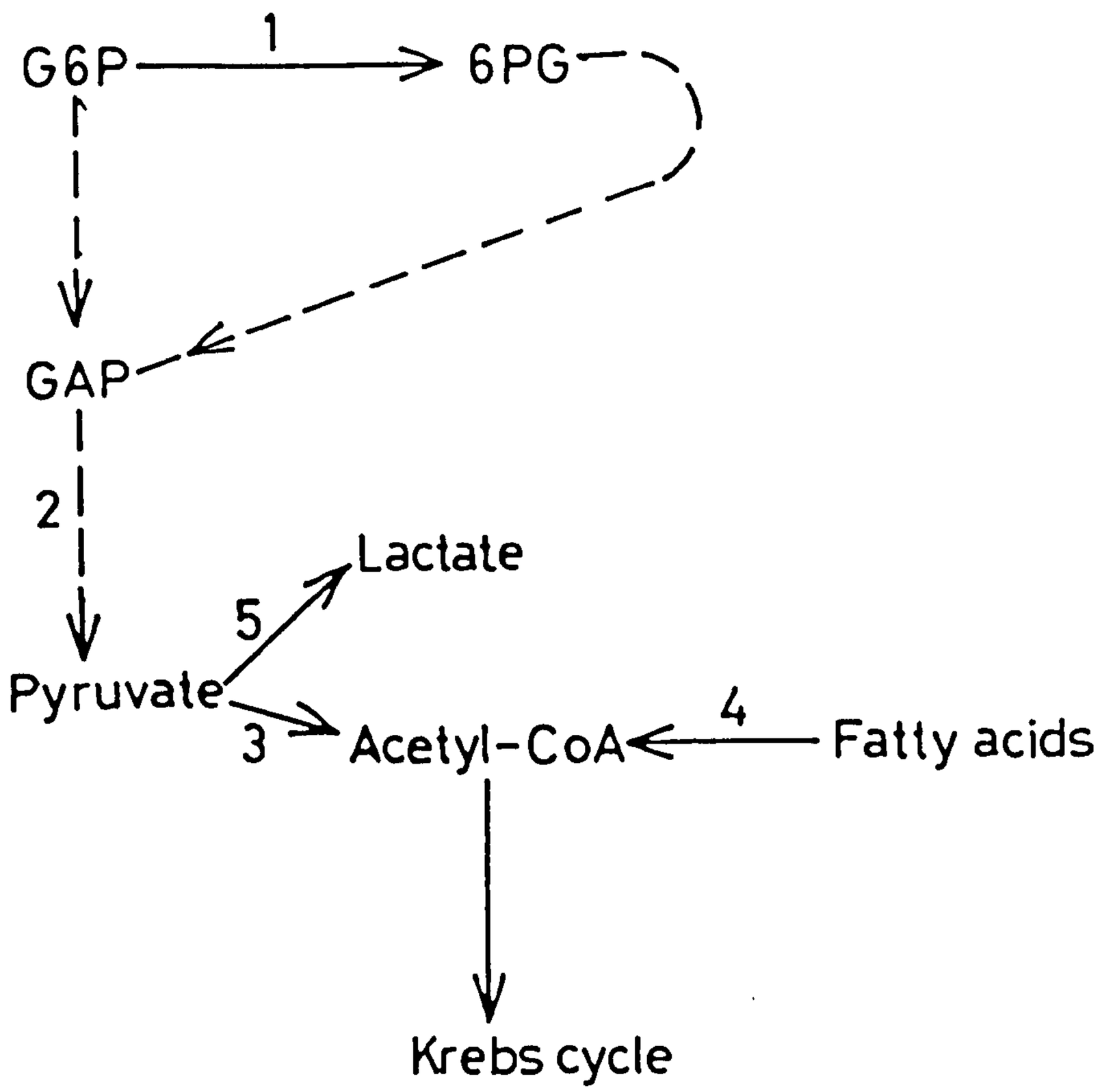

Fig. VI. lO Diagram of the oxidative metabolic pathways indicating the enzymes tested or discussed.

1 : glucose 6-phosphate dehydrogenase

2 : glyceraldehyde 3-phosphate dehydrogenase

3 : pyruvate dehydrogenase complex

4 : hydroxyacyl dehydrogenase

5 : lactate dehydrogenase

regulated by phosphorylation and dephosphrylation, by the enzymes pyruvate dehydrogenase kinase and pyruvate dehydrogenase phosphatase, respectively. The kinase catalyzes the ATP-dependent phosphorylation of one of the subunits of pyruvate dehydrogenase, a reaction which requires Mg^{2+}; this phosphorylation inactivates the enzyme. The inactive enzyme is reactivated by the phosphatase by hydrolytic removal of the inhibitory phosphate groups, again in the presence of Mg^{2+}.

The oxidative decarboxylation of pyruvate to acetyl CoA and Co, requires three different enzymes and five different co-enzymes organized into a multienzyme complex. The overall equation is:

Pyruvate + NAD^+ + CoA $\longrightarrow$ acetyl CoA + NADH + H^+ + CO_2

in the presence of thiamine pyrophosphate (TPP) and Mg^{2+}. The reactions are as follows:

1) Pyruvate + TPP ENZ (1) $\longrightarrow$ CO_2 + Hydroxyethyl-TPP ENZ (1)

   where ENZ (1) is pyruvate decarboxylase.

2) Hydroxyethyl-TPP ENZ (1) $\rightleftharpoons$ Acetoin + TPP ENZ (1)

3) Hydroxyethyl-TPP ENZ (1) + LIP (S.S) ENZ (2) $\rightleftharpoons$

   Acetyl-CoA + LIP (SH.SH) ENZ (2)

   where ENZ (2) is dihydrolipoate acetyltransferase and LIP (S.S) and LIP (SH.SH) are lipoate and acetylhydro-lipoate.

4) LIP (SH.S-acetyl) ENZ (2) + CoA $\rightleftharpoons$

   acetyl-CoA + LIP (SH.SH) ENZ (2)

   where LIP (SH.SH acetyl) is dihydrolipoate.

5) LIP (SH.SH) ENZ (2) + NAD^+ $\xrightleftharpoons{\text{ENZ (3)}}$ LIP (SS) ENZ (2) + NADH

where ENZ (3) is dihydrolypyl dehydrogenase (Lehninger, 1975; Kerby et al, 1975).

The activity of this complex is inhibited by the products of fatty acid oxidation, particularly by acetyl CoA (Kerby et al, 1976; Linn et al, 1969). Kerby et al (1975) came to the conclusion that increasing ratios of NADH /NAD^+ and of acetyl CoA / CoA favour phosphorylation and inactivation of pyruvate dehydrogenase. Kerby et al (1975) studied alloxan-diabetes where pyruvate oxidation is inhibited and postulated that the cause was an enhancement of fatty acid oxidation.

It therefore seemed appropriate to try to evaluate the oxidative metabolism of the various cellular components of bone and of cartilage to determine whether these tissues could oxidize fatty acids at such a rate, that the acetyl CoA, so produced, might become a factor in controlling the pyruvate dehydrogenase activity.

Materials and Methods

The materials and methods are identical to those in Part I together with the measurements of one oxidative enzyme of each of the major pathways in the same region of the growth plate of the metatarsals. The selected enzymes were as follows.

(1) Embden-Meyerhof pathway : glyceraldehyde 3-phosphate dehydrogenase (GAPD);

(2) Pentose-shunt: glucose 6-phosphate dehydrogenase (G6PD);

(3) Tricarboxylic acid cycle : succinate dehydrogenase (SDH);

(4) Lactate dehydrogenase (LDH);

(5) Fatty acid oxidation: hydroxyacyl dehydrogenase (HOAD) (as described in Part I).

For these reactions, the specific reactants were as follows:

Lactate dehydrogenase: sodium lactate, 60 mM; NAD^+, 2.5 mM.

Glucose 6-phosphate dehydrogenase: glucose 6-phosphate, disodium salt, 5mM; $NADP^+$, 3mM.

Glyceraldehyde 3-phosphate dehydrogenase: fructose 1-6 diphosphate, 5mM; aldolase, 10 units ml^{-1} NAD^+, 1.5 mM.

Succinate dehydrogenase: sodium succinate, 50 mM.

β-hydroxyacyl dehydrogenase: NAD^+ (2 mM); sodium nitroprusside (5 mM); menadione (3 mM) DL-S-β hydroxybutyryl-N-acetyl cysteamine (37 mM) or cysteamine (5 mM).

Except for the studies on succinate dehydrogenase, all the reaction-media contained 0.6% (10 mM) chloroform-purified neotetrazolium chloride (Serva) in a 30% (w/v) solution of polyvinyl alcohol (grade G04/140; Wacker Chemicals Ltd., Walton on Thames, Surrey, U.K.) in glycyl-glycine buffer (50 mM; pH 8.0).

For demonstrating the activity of succinate dehydrogenase, which is tightly bound within the mitochondria, a 0.1 M phosphate buffer, pH 7.8, was used. Except for the demonstration of hydroxy-acyl dehydrogenase activity, the media contained the intermediate hydrogen acceptor, phenazine methosulphate (0.7 mM) added to the medium just before use. All reactions were done at 37°C

in an atmosphere of nitrogen. The reactions were run for 45 minutes except for lactate dehydrogenase activity which was run for 10 minutes (the results being multiplied by 4.5 for comparison). Over these reaction times, the responses were linear with time.

Measurements. Again, measurements were as performed in Part I. The cell-types measured were again: chondrocytes in the resting, proliferating, and hypertrophic zones of the growth plate; and osteoblasts and osteocytes in the metaphysis.

To test the oxidative activity in a tissue that does not show "aerobic glycolysis", small pieces (3x3x3 mm) of the liver from three female Wistar rats (200 g) were chilled in hexane at -65 to 70°C and sectioned at 10 μm in a Bright's cryostat. The same reactions were done on the liver sections as done on the metatarsals.

The pentose-shunt involves the oxidation of glucose 6-phosphate, $NADP^+$ being the obligate co-factor. If the system is to remain an active cycle, there must be a feed-back into the normal glycolytic pathway, supplying either fructose 6-phosphate or glyceraldehyde 3-phosphate (Krebs and Kornberg, 1957). This feed-back is mediated by the enzymes, transketolase and transaldolase, and reflects the requirements of the cell for NADPH and ribose 5-phosphate. Thus the maximum activity of GAPD must be considered to be rate-limiting both for the pentose shunt and for the Embden-Meyerhof pathway. In fact, it reflects the maximum oxidation of

glucose 6-phosphate by either route.

In the Embden-Meyerhof pathway, the substrate-products of GAPD activity are finally converted to pyruvate. For this to be used by the Krebs' cycle, for the generation of ATP for the energy requirements of the cell, it is converted to acetate and linked to coenzyme A (CoA) to form acetyl-CoA. The oxidation of fatty acids yields acetyl-CoA directly. Thus the amount of activity of GAPD and HOAD is a measure of the total amount of acetyl-CoA available for the Krebs' cycle. SDH activity can be taken as the maximum Krebs' cycle activity of which the cell is capable (Lehninger, 1975). Thus the calculation of GAPD + HOAD activity minus SDH activity, gives a measure of whether there could be sufficient, or excessive amounts of acetyl-CoA produced in the cells, relative to the maximum amounts that could be dealt with by the Krebs' cycle.

Results and Discussion

Oxidative Activities in the Various Cell-types of the Bone and Cartilage

The results (Table VI.2) showed firstly, that under the conditions used, the hydroxyacyl dehydrogenase activity (HOAD) was equivalent to that of glyceraldehyde 3-phosphate dehydrogenase (GAPD); secondly the results showed that the succinate dehydrogenase activity was too small to accommodate the combined GAPD plus HOAD

Table VI. 2. Enzymatic activities (mean integrated extinction x 100 ± SEM) in various cell-types of the bone and cartilage of the growth-plate (values corrected to 45 min incubation) and in liver (10 min reaction).

*The control activities were measured either in the absence of substrate or, for HOAD activity, with cysteamine instead of the substrate. The different 'control' activities recorded for the two NAD-dependent enzymes are due to the different pH values at which these are done, in accordance with the different pH optima of the enzymes.

Enzyme	Osteocytes	Osteoblasts	Chondrocytes of:		
			Hypertropic zone	Proliferating zone	Resting zone
G6PD	12.0 ± 1.0	54.2 ± 2.6	29.4 ± 0.9	21.0 ± 0.9	13.4 ± 0.6
LDH	32.3 ± 1.0	63.2 ± 1.0	95.6 ± 1.0	81.9 ± 2.0	45.8 ± 1.0
GAPD	14.0 ± 1.0	24.2 ± 1.1	20.7 ± 1.3	11.6 ± 0.9	8.6 ± 2.9
HOAD	8.9 ± 1.9	19.6 ± 1.6	19.6 ± 2.6	14.2 ± 1.5	10.1 ± 3.2
SDH	13.0 ± 0.7	32.0 ± 2.0	9.0 ± 0.6	9.0 ± 0.5	6.0 ± 0.5
GADP+HOAD	22.9	43.8	40.3	25.8	18.7
(GADP+HOAD)-SDH	9.9	11.8	31.3	16.8	12.7

	G6PD	LDH	GAPD	HOAD	SDH	GAPD + HOAD	(GAPD + HOAD) - SDH
Activity (n = 3)	52 + 0.7	45 + 0.5	67 + 1.0	32 + 0.4	160 + 4.0	99	-61
Control*	(9 + 0.4)	(16 + 0.4)	(27 + 0.6)	(16 + 0.3)	(0)	-	-

activities; and thirdly, that there was a direct correlation ($r = 0.85$; $p = 0.02$) between the lactate dehydrogenase activities (LDH) and the value of (GAPD + HOAD) - SDH. The activities recorded when these reactions were done in the absence of the substrate (or with the 'control' substrate) were so low that they were not taken into account.

Oxidative Activities in Rat Liver

In the liver, the activities recorded using the reaction media without exogenous substrate were appreciable (Table VI.2). This probably reflects the considerable store of endogenous substrates in liver. However, whether or not these "control" values were taken into account, the combined activities recorded for glyceraldehyde 3-phosphate dehydrogenase and for hydroxyacyl dehydrogenase (GAPD + HOAD; Table VI.2) were far less than that recorded for succinate dehydrogenase activity, giving a negative value for (GAPD + HOAD) - SDH (Table VI.2).

General Conclusions

Thus these results may advance our understanding of the oxidative metabolism of bone in the following ways:

1. They indicate that fatty acid oxidation could play a significant part in the oxidative metabolism of bone-cells, even of established osteocytes which, until the development of the HOAD reaction, appeared inert,

metabolically. If, indeed, fatty acids are used, to an appreciable extent, as one of the 'energy-fuels' of bone, it will become of interest to investigate whether fatty, pathological changes of bone are related to altered oxidative metabolic activities.

2. They have suggested a different possible explanation of the phenomenon of 'aerobic glycolysis' that seems to pertain to bone, but which may have much wider implications. Thus it is postulated that lactic acid will be produced either when lack of oxygen causes blockade of the mitochondrial electron-transport chain as occurs under anaerobic conditions (and as discussed, above) or when the blockade occurs at the level of pyruvate dehydrogenase, as it is suggested might occur when the production of acetyl-CoA, by fatty acid oxidation, becomes disproportionately great.

CHAPTER VII

FRACTURE-HEALING IN THE SPRAGUE-DAWLEY RAT

Introduction

Shedden et al (1976) showed that the closed fracture of the metatarsals of one leg of the Wistar rat formed a useful, and remarkably reproducible, model for studying fracture-healing. Unfixed undecalcified sections from closed fractures of Wistar rat metatarsals were examined for histological change and for metabolic activity at various times after the fracture. The fracture of the metatarsal was produced by digital pressure. Histological changes were examined in sections stained with toluidine blue and quantitative cytochemistry was used for the study of the metabolic changes during the formation of the callus. As well as the study of the various cell types found in the callus, a detailed study was made of the histological and metabolic changes along the periosteum during the early development of the callus.

The two enzymes studied were glucose 6-phosphate dehydrogenase (G6PD) and alkaline phosphatase (Alk Phos). The first enzyme, G6PD, is the first and rate-limiting step in the pentose shunt which is important for supplying NADPH, to be used as reducing equivalents in many bio-synthetic reactions, and in producing ribose phosphate for nucleic acid synthesis. Coulton (1977), in an

investigation into the relation between the pentose shunt and the effect of a wound in the skin of a guinea pig, found that the greatest glucose 6-phosphate dehydrogenase activity preceded DNA synthesis, as would be expected if this pathway is involved with biosynthetic processes required for cell proliferation. The fracture provides a situation where both cellular proliferation and biosynthesis of more specialized components are very active. The second enzyme, Alk Phos, is classically used as an indicator of bone-activity. Since Robison (1923) found alkaline phosphatase associated with bone formation, many workers have concentrated on determining the role of this enzyme in bone metabolism. Although it is obviously important in the development and growth of bone, in the maintenance of mature bone, and is affected by metabolic bone diseases, the actual function of this enzyme in bone is still not known. Some of the theories put forward as to its function are discussed by Bourne (1972); and Anderson (1976).

These two enzymes, together with other relevant enzymes involved in bone metabolism are described in Chapter II. The cytochemical demonstration of the enzyme activities and their measurement are described in Chapter V and in the Appendix I.

<u>Reason for Studying Healing-fractures in the Sprague-Dawley Rat</u>

As outlined in Chapter III, over the last few years bone has been shown to contain the amino acid residue

γ -carboxyglutamic acid, in a small acidic protein that has been named osteocalcin (or bone Gla-protein). This comprises about 1% of the total bone-protein (Hauschka et al, 1975; Price et al, 1976a; Hauschka et al, 1978). The γ-carboxylation of this protein is dependent on the vitamin K_1-cycle (Stenflow and Suttie, 1977). There is considerable evidence that calcification of bone may involve this γ-carboxylation of glutamate residues, as is found in osteocalcin (Hauschka et al, 1975; Price et al, 1976a; Hauschka, 1978; Price et al, 1981a). It has been claimed that the anticoagulant, dicoumarol, inhibits the vitamin K-cycle by blocking the conversion of the vitamin-K epoxide back to the quinone (Whitlon et al, 1978). I therefore wanted to test the relevance of this cycle in ossification by feeding dicoumarol to rats in which a closed fracture of the metatarsal had been induced. However it was found that the Wistar rats, used by Shedden and colleagues, were too sensitive to dicoumarol: they died apparently from the anticoagulant effect. Sprague-Dawley rats were found to be more resistant to dicoumarol. Therefore before studying the effect of dicoumarol on fracture-healing, it was necessary to follow the fracture-healing process and the associated metabolic changes, in the Sprague-Dawley rat, making a direct comparison with the earlier work done on the Wistar rat by Shedden et al (1976) and Dunham et al (1977).

Materials and Methods

Sprague-Dawley rats (230-250 g) were anaesthetized with pentobarbitone sodium (usually 0.15 ml) given intraperitoneally. Closed fractures were imposed by digital pressure on two metatarsals of one hind-limb; the rats were allowed to revive and were killed at various times, up to six weeks later, by asphyxiation with nitrogen. The fractured bone, with its associated plantar muscle, was dissected free and immersed briefly in a 5% (w/v) solution of polyvinyl alcohol (G04/140). The bone was then chilled to -70°C in hexane (BDH 'low in aromatic hydrocarbons' grade, boiling range 67-70°C) and stored in dry tubes, at this temperature, for up to seven days. These methods have been fully described in Chapter VI.

Cytochemical Reactions. The sections were reacted in triplicate for G6PD activity and Alk Phos activity. Serial sections were stained with toluidine blue for histological study (Chayen et al, 1973). For G6PD activity the reaction-medium contained glucose 6-phosphate (5mM), $NADP^+$ (3mM), phenazine methosulphate (0.7mM) and 0.3% (5mM) purified neotetrazolium chloride in 0.05M glycyl glycine buffer, pH 8.0, containing 30% (w/v) of the G04/140 grade of polyvinyl alcohol. The reactions were done in an atmosphere of nitrogen and at 37°C. The medium for demonstrating alkaline phosphatase activity contained: α-naphthyl acid phosphate (Sigma; 2 mg), Fast blue RR (Sigma; 50 mg), with 0.2 ml of a 10% solution of magnesium chloride, in 50 ml of a 2% solution of sodium 5-diethylbarbiturate at a final pH of pH 9.2. This reaction was done in

Coplin jars at room temperature.

The coloured reaction-product of these cytochemical reactions was measured at discrete sites in the periosteum, and in histologically defined cell-types in the developing callus, by means of a Vickers M85 scanning and integrating microdensitometer, with a x40 objective, spot size 1 (equivalent to 0.4 μm in the plane of the specimen), with light corresponding to the absorption-maximum of the chromophore for the alkaline phosphatase reaction (580 nm) and to the isobestic point for the formazan from the dehydrogenase methods (585 nm). The reaction-times required to obtain ideal concentrations of the coloured reaction-product for measurement were 10 minutes for G6PD, and 3 minutes for alkaline phosphatase activity (multiplied by 10/3 to give a comparable value for a 10-minute reaction: Table VII.1).

Results

Histology

The sequence of events in the healing process of fractured metatarsals in the Sprague-Dawley rats, proved to be very reproducible and remarkably similar to that in the Wistar rat. However there were differences. The major difference was the time-scale, the fracture healing considerably faster in the Sprague-Dawley than in the Wistar rat. As in the Wistar rat, during the first few days after the fracture, a relatively undifferentiated callus comprised of few cells developed, surrounding the two fractured surfaces

(Fig. VII.1). Around 3 days the periosteum had considerably thickened and cells had apparently proliferated from it and migrated into the callus; the first indication of the formation of new bone was seen on the shaft of the bone at about 1.2mm -1.8 mm from the fracture-site (Fig. VII.2). This was much earlier than the appearance of new bone in the Wistar rat (around 5 days). By 5 days, the callus consisted of a large number of undifferentiated cell types (Fig. VII.3); it consisted of the fibroblastic, loose granulation tissue that grew out from the periosteum, and the compact cellular granulation tissue (spindle shaped and rounded cells) that, from their position in the callus, appeared to be the precursers of cartilage and bone. The callus had the standard fusiform shape, the dense ground-substance and cells completely surrounding the fracture. The first appearance of differentiation and the first cartilage was seen at about 5 days around the new bone forming on the side of the shaft. Toluidine blue is a useful stain for acidic mucopolysaccharides which it may stain metachromatically. Different regions of the matrix of the callus showed various shades of metachromasia. As the wedge of bone on the shaft enlarged,the perisoteum became elevated and extended into the callus.

By 8 days, a large external callus was present. In all cases, the callus on the dorsal side of the fracture was considerably larger than that on the plantar side.

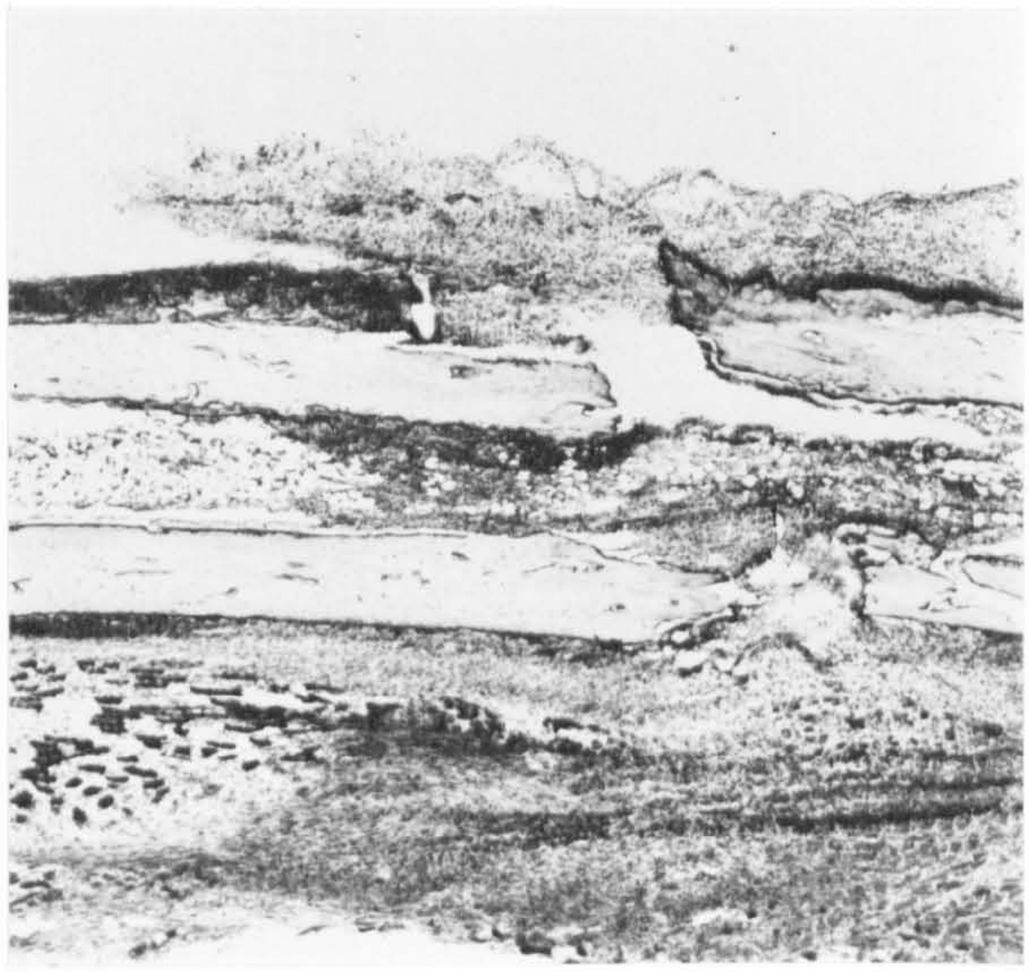

Fig. VII. 1 Cryostat section through the mid-plane of a fractured Sprague-Dawley rat metatarsal shaft, one day post-fracture. The fracture site is filled with haematoma and undifferentiated callus. Toluidine blue; X20

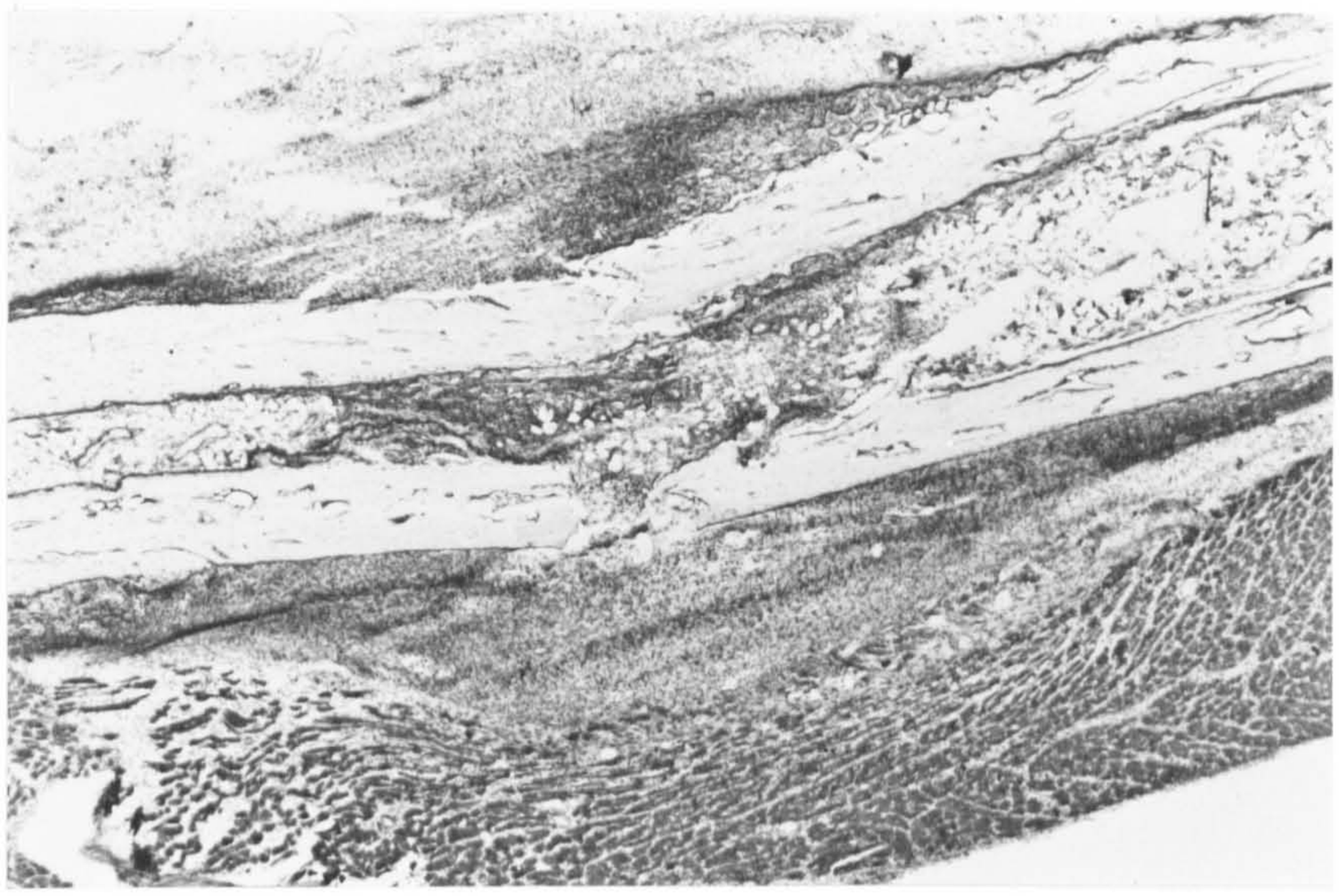

Fig. VII.2 Cryostat section of a three-day fracture showing more bone formation starting on the periosteal edge about 1mm from the fracture, seen on the dorsal surface distal to the fracture, and on the ventral surface (with the plantar muscle) proximal to it. Toluidine blue; X20.

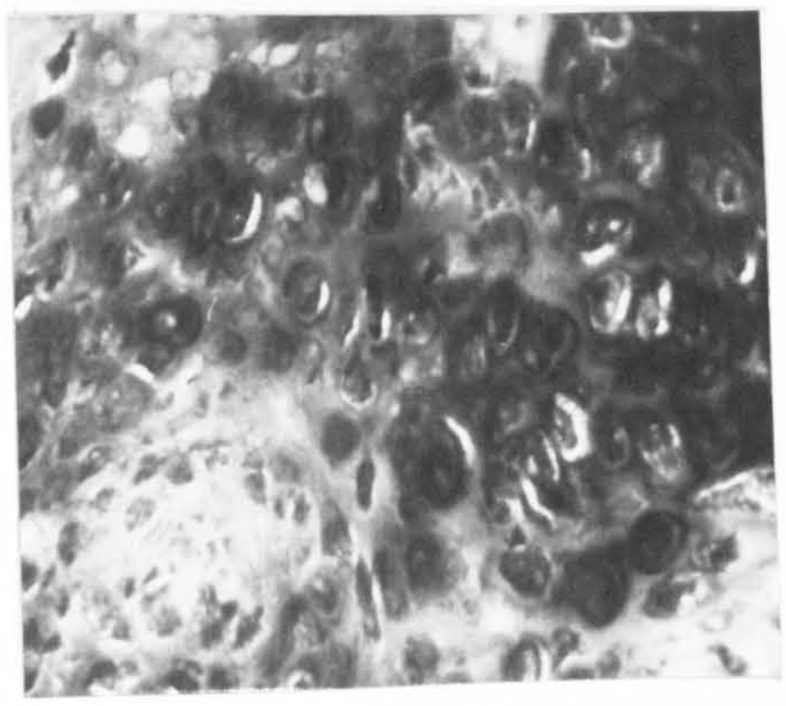

a

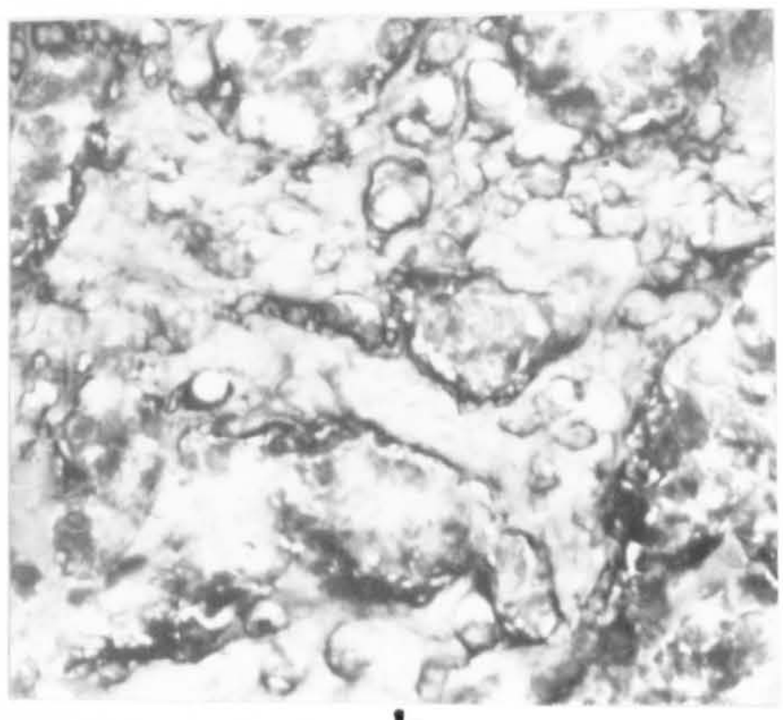

b

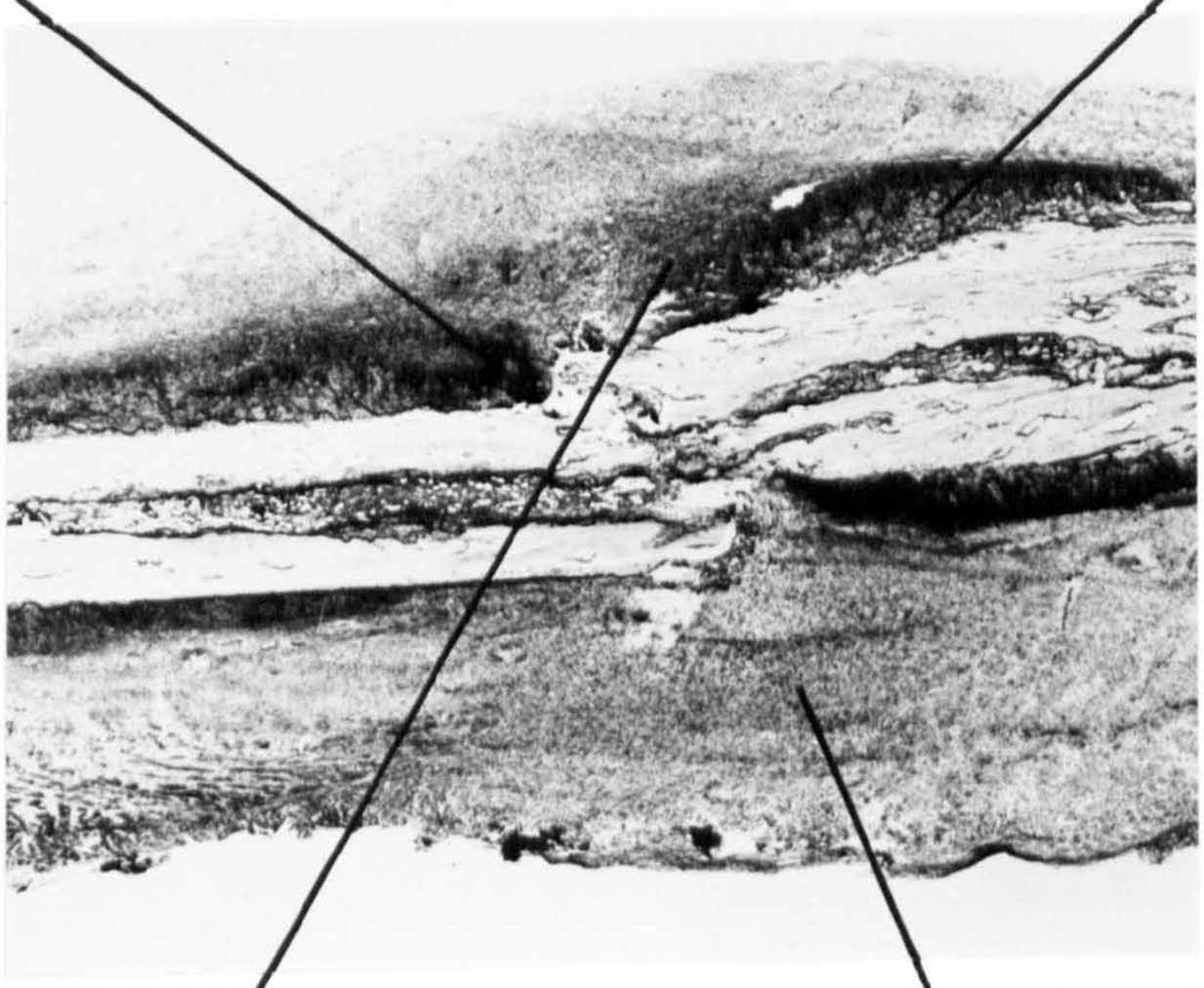

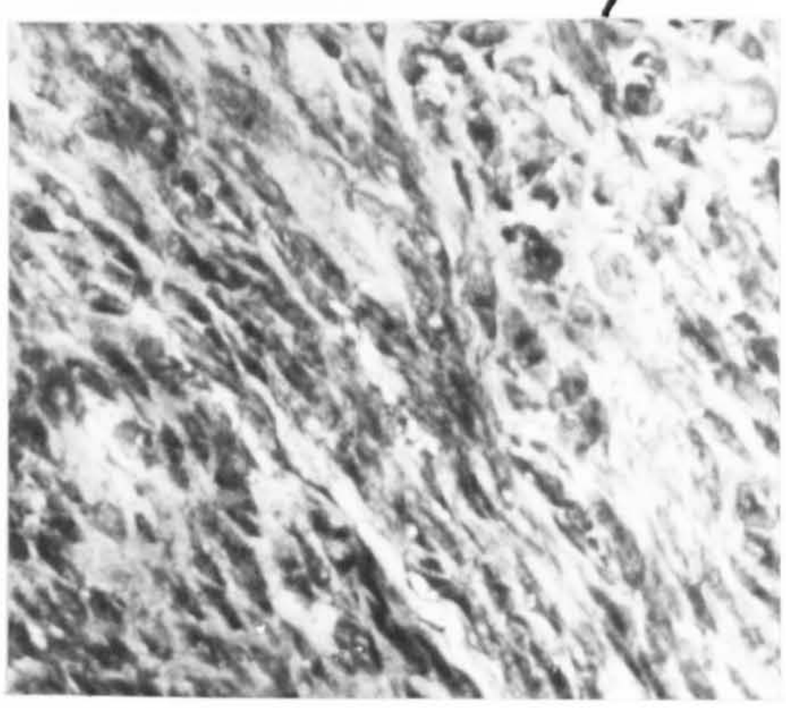

c

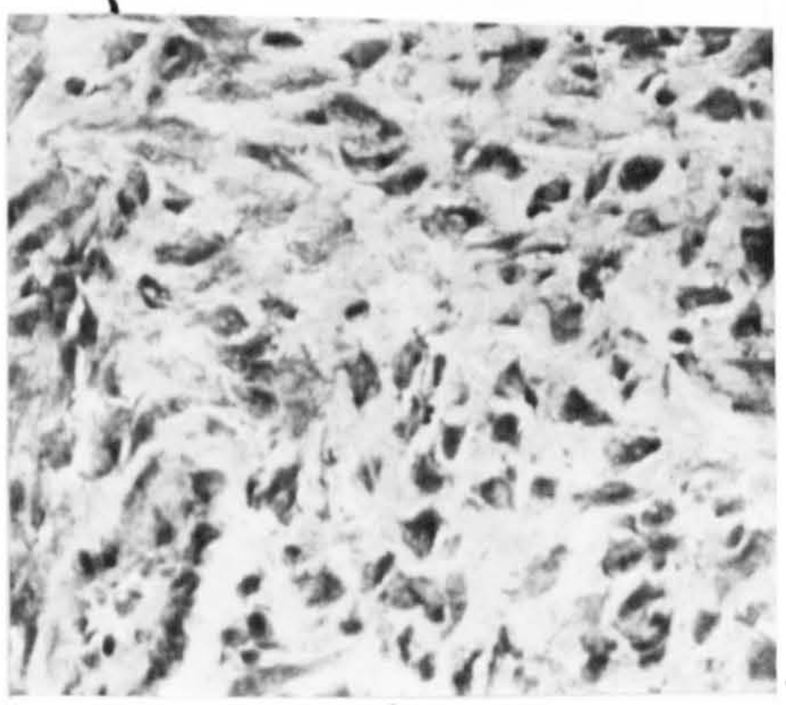

d

Fig. VII. 3 Cryostat section of a five-day fracture in which the callus is comprised of (a) cartilage forming as a cap on (b) new bone forming on the shaft distal to the fracture; (c) compact granulation tissue and (d) loose granulation tissue which still form the bulk of the callus. Toluidine blue: X12.

Together with the undifferentiated granulation tissue, there were large areas of cartilage, showing various degrees of proliferation, hypertrophy and calcificaion: all showed different shades of metachromasia; they surrounded the new bone on the shaft and extended into the callus. The gap between the two fragments was filled with undifferentiated granulation tissue (Fig. VII.4). In the Wistar rat the two fracture ends had overlapped up to this stage. This overlapping was not present in the Sprague-Dawley rat, the two fragments being closely aligned throughout.

Between 10 and 15 days the amount of new bone increased extensively, moving deeper into the callus (Fig. VII.5). Most of the metabolic studies involved in investigating the effects of dicoumarol were done on material of the 12 day post-fracture. The external callus gradually diminished in size and by 21 days there was generally very little external callus. The gap was filled with fibrocartilage-like material and cartilage (Fig. VII.6). The new bone on either fragment gradually replaced this material and by around 33 days, woven bone had almost completely united the two ends (Fig. VII.7). By 6 weeks the fracture was fully united, with extensive remodelling of the woven bone into adult bone (detected by the appearance of ordered collagen as seen by its birefringence under crossed polars).

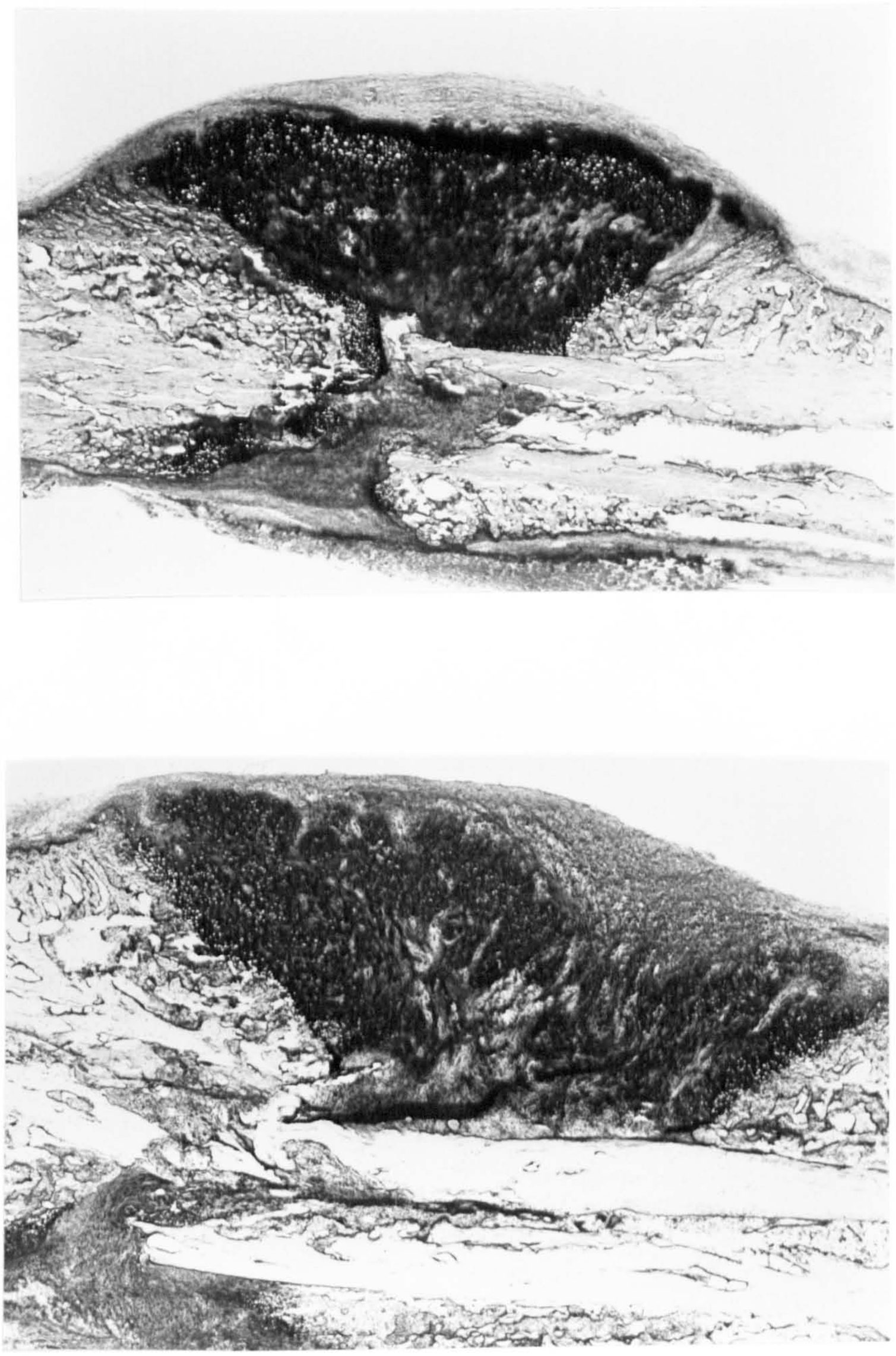

Fig. VII. 4 Two examples of sections of eight-day-old fractures to show the predominant callus on the dorsal side. The angulation of the fractures is minimal and there is no overlap. The gap between the fractured ends is still filled with undifferentiated callus. Toluidine blue: upper X15; lower X20.

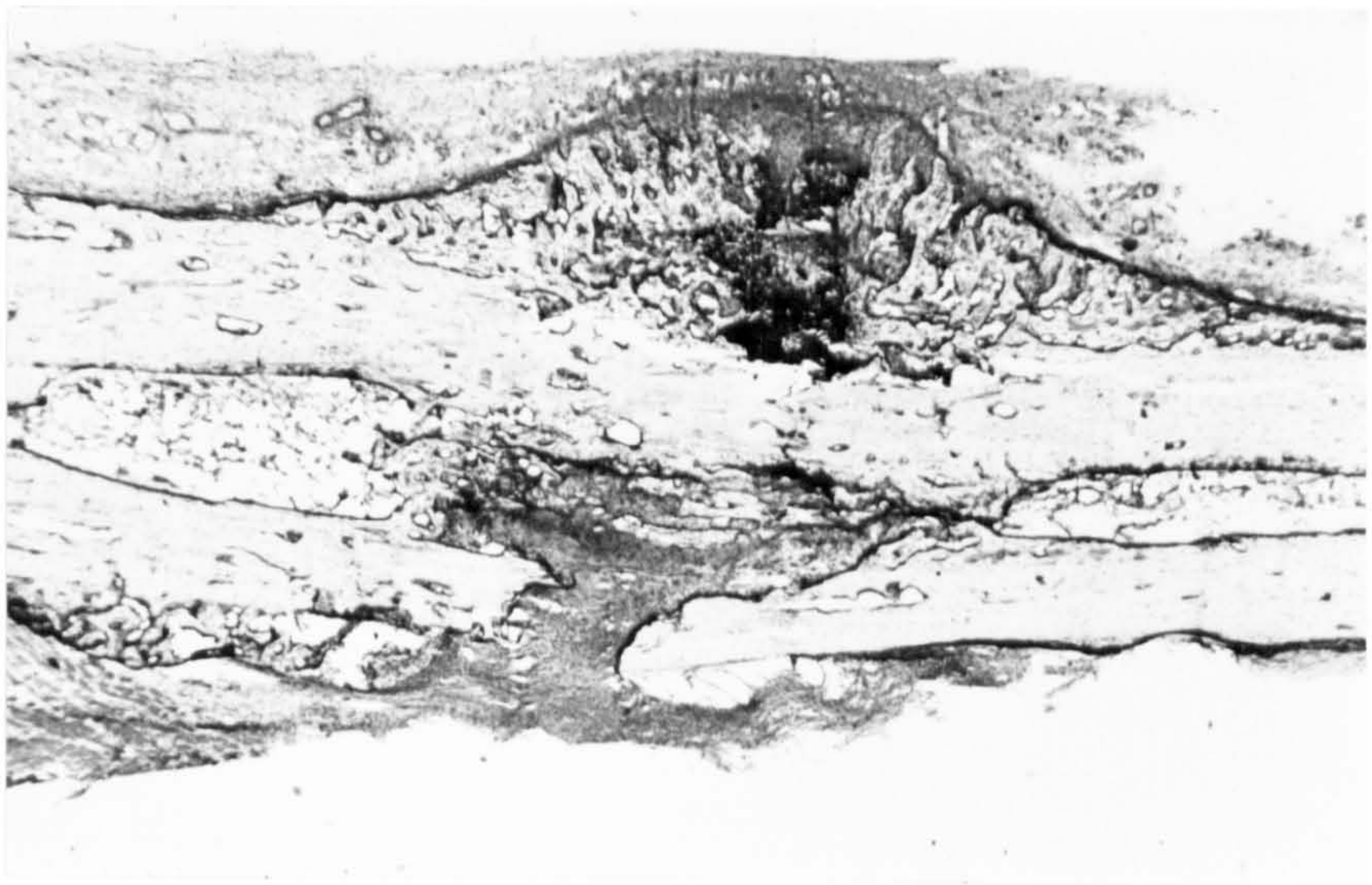

Fig. VII. 5 Cryostat section of a twelve-day callus in which external callus now consists almost entirely of new bone, separated at the fracture line by calcified and mature cartilage. Toluidine blue; X24.

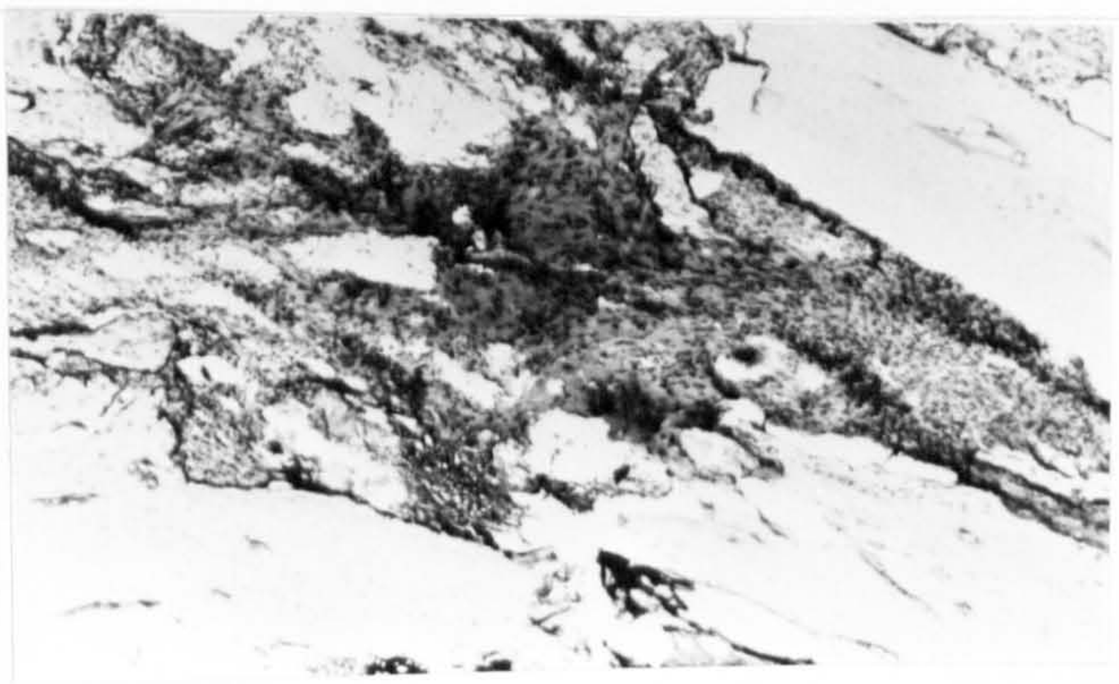

Fig. VII. 6 Before bony union, the fracture gap is filled with granulation tissue and fibro-cartilage.
Toluidine blue; X38.

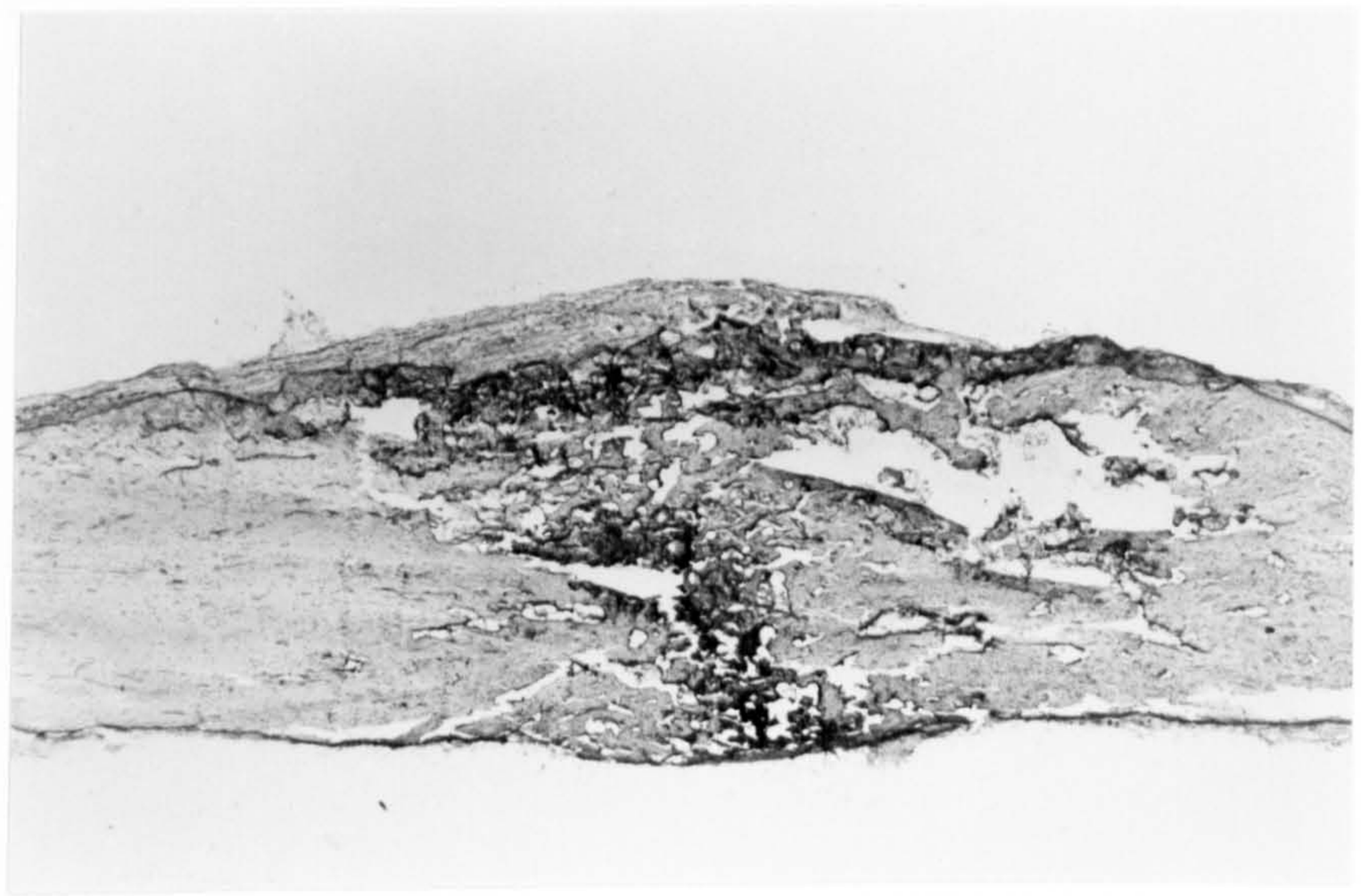

Fig. VII. 7 By six weeks post fracture, the fracture gap is closed by new bone. Toluidine blue; X15.

Cytochemistry

Glucose 6-phosphate dehydrogenase activity in the periosteum.

The G6PD activity in the fully differentiated periosteum of normal bone was unmeasurably low, in agreement with Sheddon and colleagues'(1976) work on the Wistar rat. The activity was measured in individual periosteal cells at measured distances from the fracture. In three rats, three days post-fracture, there was considerable activity close to the fracture reaching a mean extinction value of 22 units at 0.4 mm from the fracture; this was the region of very active proliferation where osteogenic cells and fibroblasts move outwards from the periosteum and into the callus. The activity rose to 27 units 1.2 mm from the fracture. This second peak corresponded to the site of the first formation of new bone seen on the side of the shaft of the bone 3 to 4 days after fracture (Fig. VII.8). This activity was observed to precede bone formation.

In the periosteum of the fractured bones from 15 rats taken 5 days after fracture, there were again two regions of elevated G6PD activity. However the precise location and value of these elevated activities varied from one rat to the next so that the overall mean values did not clearly show these variations (Fig. VII.9). The mean results showed considerable activity close to the fracture, reaching a mean extinction value

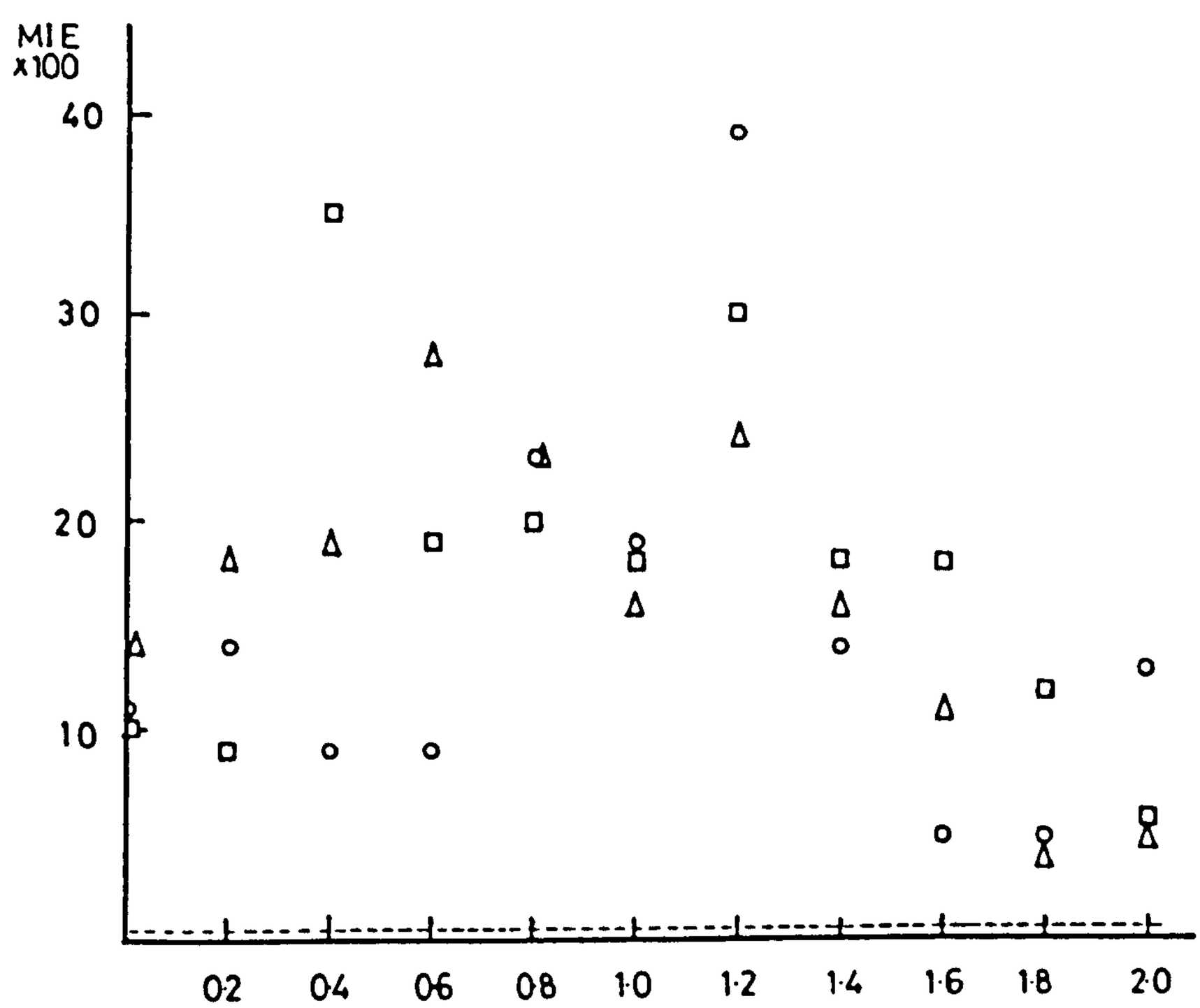

Fig. VII. 8 Glucose 6-phosphate dehydrogenase activity (G6PD; MIE x 100) in the periosteal cells measured (a) in a control metatarsal without fracture (dotted line) and (b) in each of three 3-day fractures from three different rats (circles, squares and triangles). In all the fractures, there is increased G6PD activity close to the fracture site and a second peak of activity 1.2mm away from it.

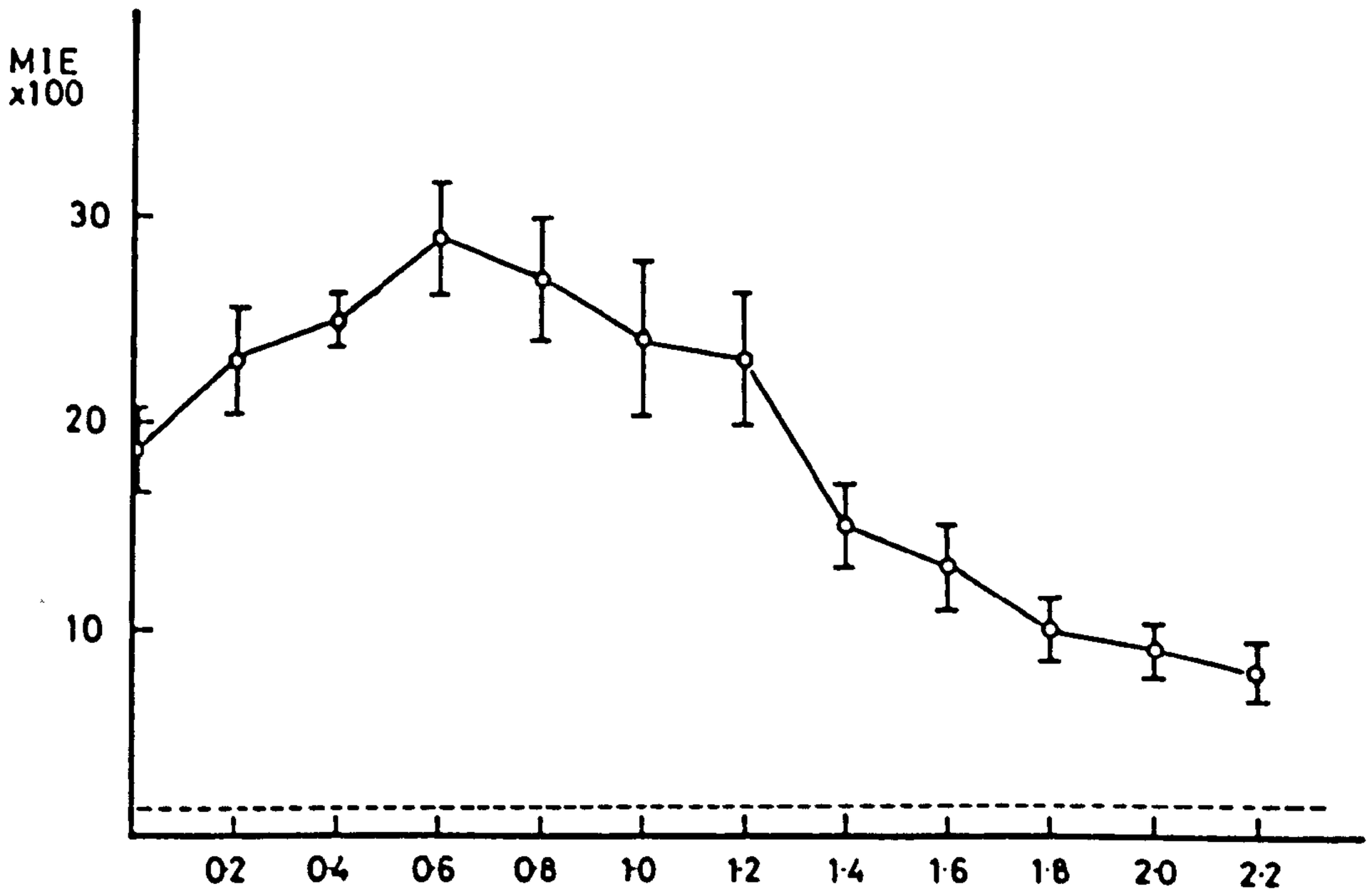

Fig. VII. 9 Combined results (mean ± SEM; n = 15) of glucose 6-phosphate dehydrogenase activity (MIE x 100) in the periosteum measured at set distances from the fracture site five days post-fracture. Because of small variations between rats, the precise location and magnitude of the second peak of activity (as seen in Fig. VII. 8 in three-day fractures) is obscured. The dotted line is the G6PD activity in the periosteum of control unfractured bone.

of 29 units at 0.6 mm from the fracture. The activity then dropped slowly to a mean value of 23 units at 1.2 mm from the fracture, and then fell rapidly thereafter (Fig. VII.9). In contrast, Fig. VII.10 represents G6PD activity along the periosteum from 1 rat. The second peak of activity occurred in the region of 1.2 to 1.8 mm from the fracture in all cases studied. This pattern of G6PD activity along the periosteum was similar to that found in the Wistar rat by Dunham and colleagues (1977). The appearance of the second peak of G6PD activity as early as 3 days post-fracture reflected the different time-scale in the Sprague-Dawley rats, compared to the Wistar rat.

The periosteum extended around the developing callus at about 5 days onwards and could be easily defined up to 12 days post-fracture. The G6PD activity was still high at 12 days post-fracture (20 units). The periosteum was difficult to define in the later fractures; however where it was definable, there was negligible G6PD activity. By around 33 days, when full union had occurred, there was no measurable activity present.

Alkaline Phosphatase Activity in the Periosteum

Three days after fracture there was low activity up to 0.8 mm from the fracture-site, becoming markedly elevated thereafter to values (around 57 units) exceeding those values (about 33 units) found uniformly throughout

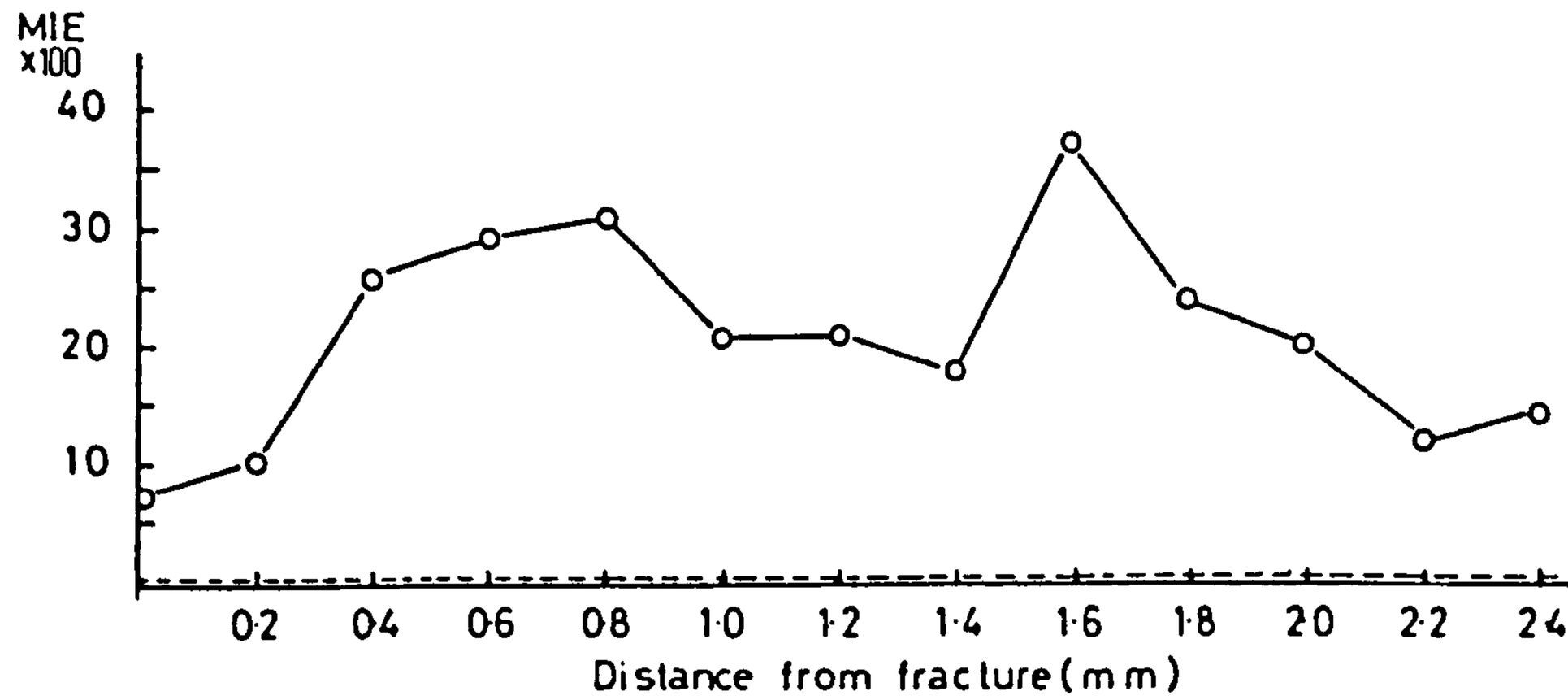

Fig. VII. 10 In contrast to the results shown in Fig. VII. 9, the two peaks of glucose 6-phosphate dehydrogenase activity (M.I.E. X 100) in periosteal cells of any one specimen are readily distinguished.

this region in intact metatarsal bones of this strain of rat (Fig. VII.11). This pattern was found in 14 rats five days after fracture (Fig. VII.12). These results were very similar to those found by Sheddon and colleagues (1976).

The alkaline phosphatase activity remained high in periosteal cells as the periosteum extended around the callus from 5 days onwards and up to complete union of the fracture, maintaining similar activities to that found in the intact metatarsals, i.e. 37 units, at 42 days post-fracture.

Enzyme Activity in the Cells of the Callus

Glucose 6-phosphate Dehydrogenase. G6PD activity was measured in 5 specified cell types in the callus: mature chondrocytes, chondrocytes in calcified cartilage, cellular granulation tissue, loose granulation tissue, and osteoblasts, 5 days (n=3), 8 days (n=3) and 12 days (n=10) post-fracture (Table VII.1). Measurements were also made 19 days, 33 days and 42 days post-fracture whenever it was possible to define the cell types (Table VII.1).

In the specimens taken 5, 8 and 12 days post-fracture, G6PD activity was moderately high in the undifferentiated cells of the loose granulation tissue that grew out from the periosteum. The increased activity was even greater in the more compact cellular granulation tissue; the activity increased from 28 units at 5 days post-fracture to 51 units 12 days post-fracture (Table VII.1).

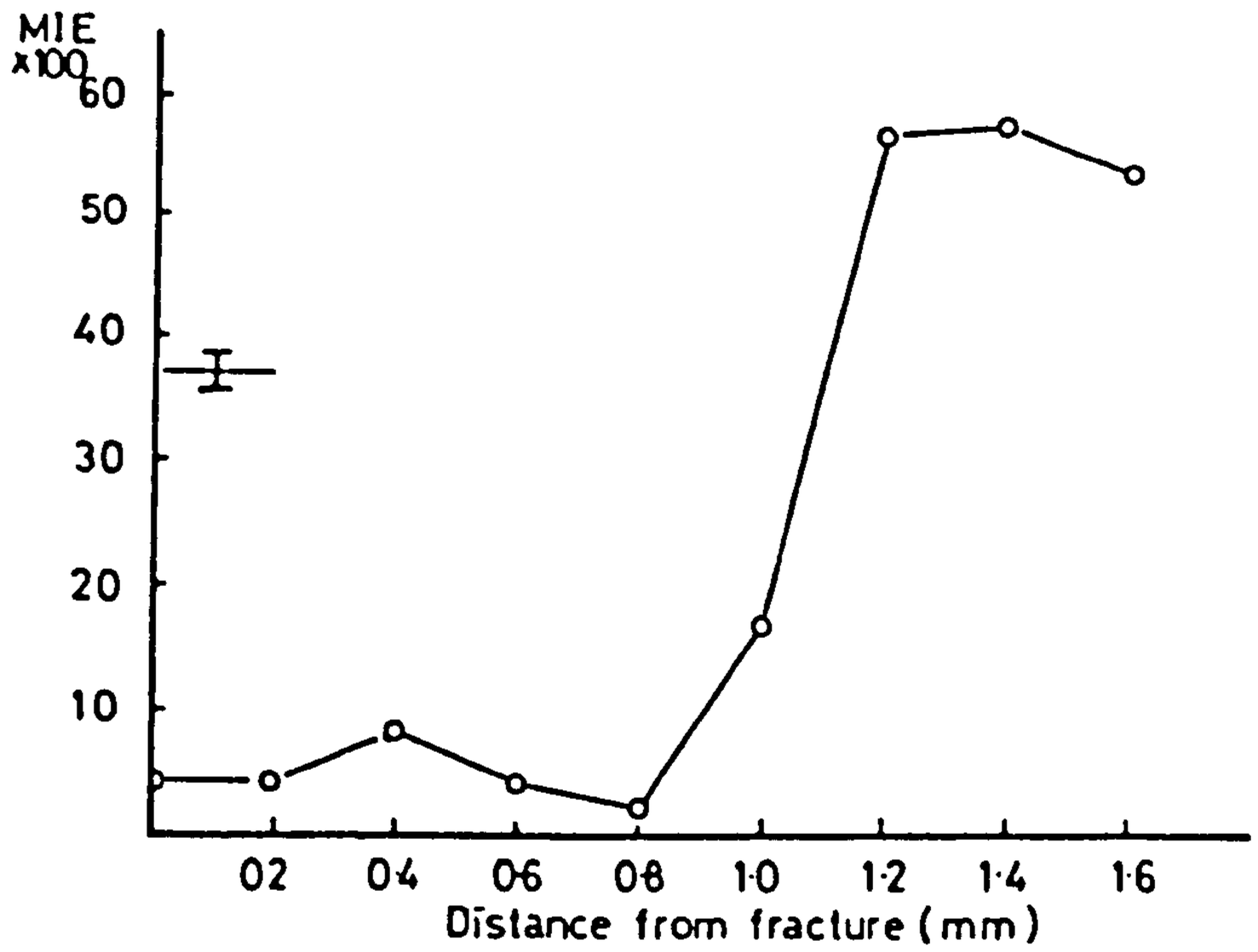

Fig. VII. 11 Alkaline phosphate activity (MIE X 100) of periosteal cells in a 3 day fracture. Up to 0.8mm from the fracture site, the activity is depressed below that of normal periosteal cells, shown by bars (mean ± SEM; n = 5 rats; left-hand side).

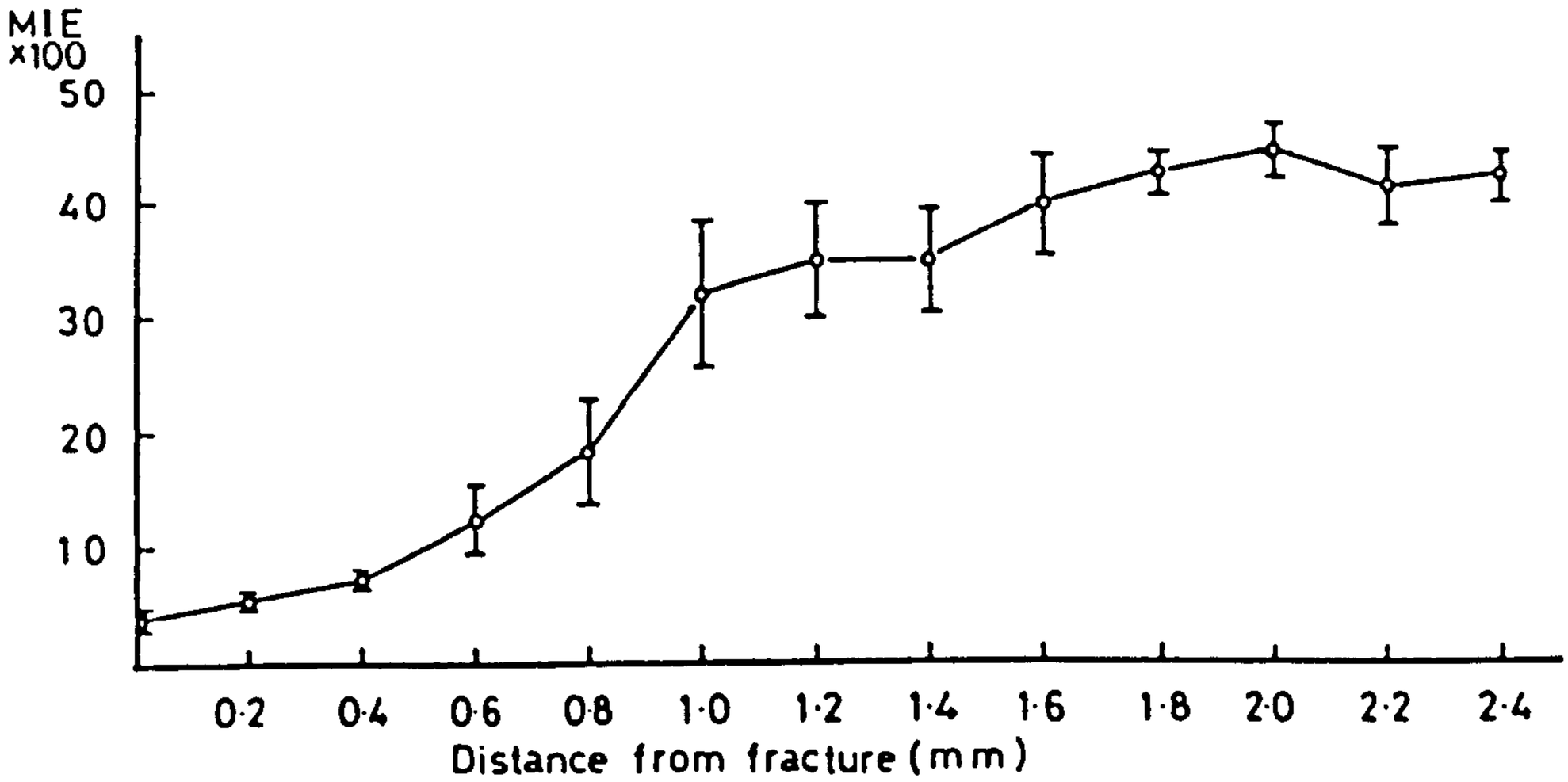

Fig. VII. 12 Combined results (M.I.E. x 100; mean ± SEM; n = 14) of alkaline phosphatase activity in the periosteum of five-day fractures; the depressed activity close to the fracture site is similar to that shown in Fig. VII. 11.

G6PD activity was also just as high in the mature chondrocytes. However the activity declined from 39 units, 5 days post-fracture, to 28 units, 12 days post-fracture. The activity further declined in the calcifying cartilage to a value of 11 units by 12 days post-fracture (Table VII.1).

The G6PD activity in the osteoblasts increased to a high level by the 12th day post-fracture; namely from 9 units at 5 days post-fracture to 37 units at 12 days post-fracture (Table VII.1). By 19 days post-fracture very little external callus remained, as described earlier, but when it was possible to define cell-types there was negligible G6PD activity in such chondrocytes as remained in the callus. However the activity remained high in the osteoblasts, even 33 days post-fracture when woven bone had completely united the two ends (22 units at 19 days and 13 units at 33 days: Table VII.1).

Alkaline Phosphatase in the Callus

Alkaline phosphatase activity was very low in the undifferentiated loose granulation tissue, being 2.3 units of MIE at 5 days, 13 units at 8 days and 3.3 units at 12 days post-fracture (Table VII.1). The activity was considerably higher in the cellular granulation tissue, giving values of 43 units at 5 days and rising to a fairly constant value (around 70 - 80 units) at 8 and 12 days post-fracture (Table VII.1).

Table VII. 1 The activity (mean integrated extinction x 100) of glucose 6-phosphate dehydrogenase (G6PD) and alkaline phosphatase (Alk. P) in five different cell types at different times during the maturation of the fracture callus.

Day after fracture	Enzyme	Osteoblasts	Chondrocytes Mature	Chondrocytes Calcified	Granulation tissue Cellular	Granulation tissue Loose
5*	G6PD	9 ± 7	39 ± 13	-	28 ± 5	16 ± 4
	AlkP	60 ± 13	53 ± 18	-	43 ± 9	2.3 ± 2
8*	G6PD	21 ± 8.4	41 ± 4.5	10 ± 3	38 ± 3.5	15
	AlkP	130 ± 6.6	103 ± 7	43 ± 6	83 ± 10	13 ± 3.3
12**	G6PD	37 ± 3.7	28 ± 2	11 ± 1.2	51 ± 6	18 ± 1.7
	AlkP	140 ± 7.3	107 ± 6.3	53 ± 8.3	70 ± 6.7	3 ± 2.2
19	G6PD	22	0	0	nm	nm
	AlkP	100	75	0	nm	0
33	G6PD	13	0	-	-	-
	AlkP	112	96	-	-	-
42***	G6PD	-	-	-	-	-
	AlkP	129	-	-	-	-

* n = 3 ; mean ± SD

** n = 10 ; mean ± S.E.M.

*** n = 2 ; mean value

Single values: one animal

nm = not measured

\- = no representative cells present

In the mature chondrocytes the activity was 53 units at 5 days post-fracture and rose to an appreciably high and constant value (around 103 - 107 units: Table VII.1) at 8 days and 12 days post-fracture. Calcification occurred at around 8 days post-fracture, and the alkaline phosphatase activity in the calcified chondrocytes decreased to about half that found in the mature chondrocytes (Table VII.1). The osteoblasts lining the trabeculae of the new bone showed the highest alkaline phosphatase activity, namely 60 units at 5 days post-fracture, rising to 130 units at 8 days and 140 units at 12 days post-fracture (Table VII.1).

Alkaline phosphatase remained extremely active in the later fractures, in the mature chondrocytes and osteoblasts. However by 42 days there was no detectable alkaline phosphatase activity in the adult bone formed from the remodelled woven bone.

Discussion

The closed fracture of the metatarsal of the Sprague-Dawley rat forms a useful and reproducible model for studying fracture-healing. It compares very closely, both histologically and metabolically, with the Wistar rat model, except for the faster time course in the Sprague-Dawley.

As found in work done by Sheddon and colleagues (1976, 1977.) , alkaline phosphatase appeared to be associated with calcification, and glucose 6-phosphate

dehydrogenase with cellular proliferation and ossification. Thus this model should prove useful in studying the effects of dicoumarol, a vitamin K_1 antagonist, on ossification (Chapter VIII).

CHAPTER VIII

EFFECTS ON FRACTURE-HEALING OF AN ANTAGONIST OF THE VITAMIN K-CYCLE

Introduction

A peptide that is relatively rich in γ-carboxy-glutamate residues (osteocalcin; bone Gla-protein) is an abundant non-collagenous protein of mammalian bone; its synthesis depends on the vitamin K-cycle (Hauschka et al, 1975). A detailed discussion of osteocalcin and of the vitamin K cycle and its possible role in calcification is given in Chapter III. Briefly, the production of the calcium-binding γ-carboxyglutamate residues is effected by a microsomal mixed-function oxidation-reduction in which vitamin K_1, or a similar naphthoquinone substituted at the 3-position (Olsen et al, 1978), is reduced by NAD(P)H (Stenflow and Suttie, 1977; Suttie et al, 1978). The reoxidation of the quinol is required for the process in which a proton is abstracted from the γ-methylene of a glutamate residue (Stenflo and Suttie, 1977); the resulting carbanion fixes carbon dioxide to form the γ-carboxyglutamate residue (Hauschka et al, 1978; Olsen et al, 1978; Fig. III.2)

The anticoagulant, dicoumarol (chemically related to Warfarin) antagonises the effect of vitamin K_1 in the vitamin K-cycle. Some evidence suggests

that dicoumarol blocks the reversible conversion of vitamin K to the vitamin K epoxide (Whilton et al, 1978). The work reported in this chapter was designed to investigate the effects of dicoumarol on ossification by feeding it to rats (Sprague-Dawley) in which a closed fracture of the metatarsal had been induced. A detailed metabolic and histological study was made in the periosteum and in the callus up to 6 weeks post-fracture, by which time the fracture was fully united in control rats (Chapter VII).

Previous studies on cellular metabolic activities in healing fractures in rats (Dunham et al, 1977 and Chapter VII) had shown that there was a marked increase in periosteal glucose 6-phosphate dehydrogenase (G6PD) activity at the site at which new bone was formed on the shaft. This activity preceded the first signs of new bone. The simple assumption would be that the NADPH, generated by this stimulated G6PD activity at this site, would be used in the vitamin K cycle for ossification.

Materials and Methods

Most of the materials and methods have been described in Chapter VII. Those rats that were treated with dicoumarol were given it in the drinking water as soon as they revived following the induction of the fracture. A standard dose was achieved by giving each rat, daily, 25 ml of drinking water containing 0.125 mg bis-hydroxy-coumarin (Sigma); once this had been drunk, the water

bottle was replenished with ordinary water. To obtain a "solution" of dicoumarol, 25 mg of dicoumarol were dissolved initially in 10 ml of 1M sodium hydroxide, with the pH decreased to pH 10 with 5 M HCl; this solution was diluted 1:500 with tap water, giving it a final pH of between 8 and 9. The control rats were given ordinary water only.

Clotting Times. The clotting time of normal rats was 2.0 minutes; in the dicoumarol-treated rats it became prolonged from day 4, to reach 7.5 minutes on day 10 and 9 minutes on day 12.

Cytochemical Reactions. Three enzymes were studied: glucose 6-phosphate dehydrogenase activity, alkaline phosphatase activity and hydroxyacyl-coenzyme A dehydrogenase activity. The procedures for demonstrating the first two enzymes are described in Chapter VII. For demonstrating hydroxyacyl-coenzyme A dehydrogenase activity (Chambers et al, 1982) the medium contained DL-S-β-hydroxybutyryl-N-acetyl cysteamine (Sigma; 37 mM, or 5 mM cysteamine, as control), NAD^+ (2mM), menadione (3mM), sodium nitroprusside (5mM) and 0.6% (10mM) of purified neotetrazolium chloride in a 0.05 M glycyl glycine buffer containing 30% of the polyvinyl alcohol with a final pH of 8.5. (Details are given in Chapter VI).

For histological examination, sections were selected that passed through approximately the mid-axis

of the endosteal space. To confirm that this gave a good representation of the various cellular components, one bone was sectioned serially from side to side, and the relative size of each component was ascertained at different levels. The image of the selected sections was thrown on to a screen; the enlarged image was traced on to tracing paper, and the areas of the selected tissue-components were measured by planimetry.

Histological Results

In all cases, the callus on the dorsal side of the fracture was considerably larger than that on the plantar side (Table VIII.1). This difference in size in the dorsal and plantar regions of the callus was found in both the control and the dicoumarol-treated fractures. However, up to 5 days post-fracture, the histological structure of the calluses did not appear to be appreciably influenced by the administration of dicoumarol to the drinking water except that, in the controls (even as early as 3 days post-fracture) there were signs of bone-formation that were never seen in the calluses of treated rats (Fig. VIII.1). In contrast, major changes were seen in the calluses in the later fractures (12 days onwards). All the planimetry measurements were made on specimens 12 days post-fracture (Table VIII.1). The total projected areas of the dorsal callus in the treated and control animals were very similar. However, the callus in the di-

Table VIII. 1 Total area and area of new bone formation (mean ± SEM) of dorsal and plantar callus in sections through the greatest diameter (midshaft) of fractured rat metatarsals 12 days post-fracture.

	Control (n=16)		Dicoumarol treated (n=13)	
	Dorsal	Plantar	Dorsal	Plantar
Area (mm^2 x 16)	29 ± 3.33	6 ± 1.02	25 ± 2.57	9 ± 1.71
New bone	15 ± 1.53	4 ± 0.77	10 ± 1.14*	3 ± 0.86
New bone %	56 ± 3.58*	45 ± 2.56*	39 ± 1.43	30 ± 1.71

*$p < 0.001$ as compared with dicoumarol treated: Student's t test.

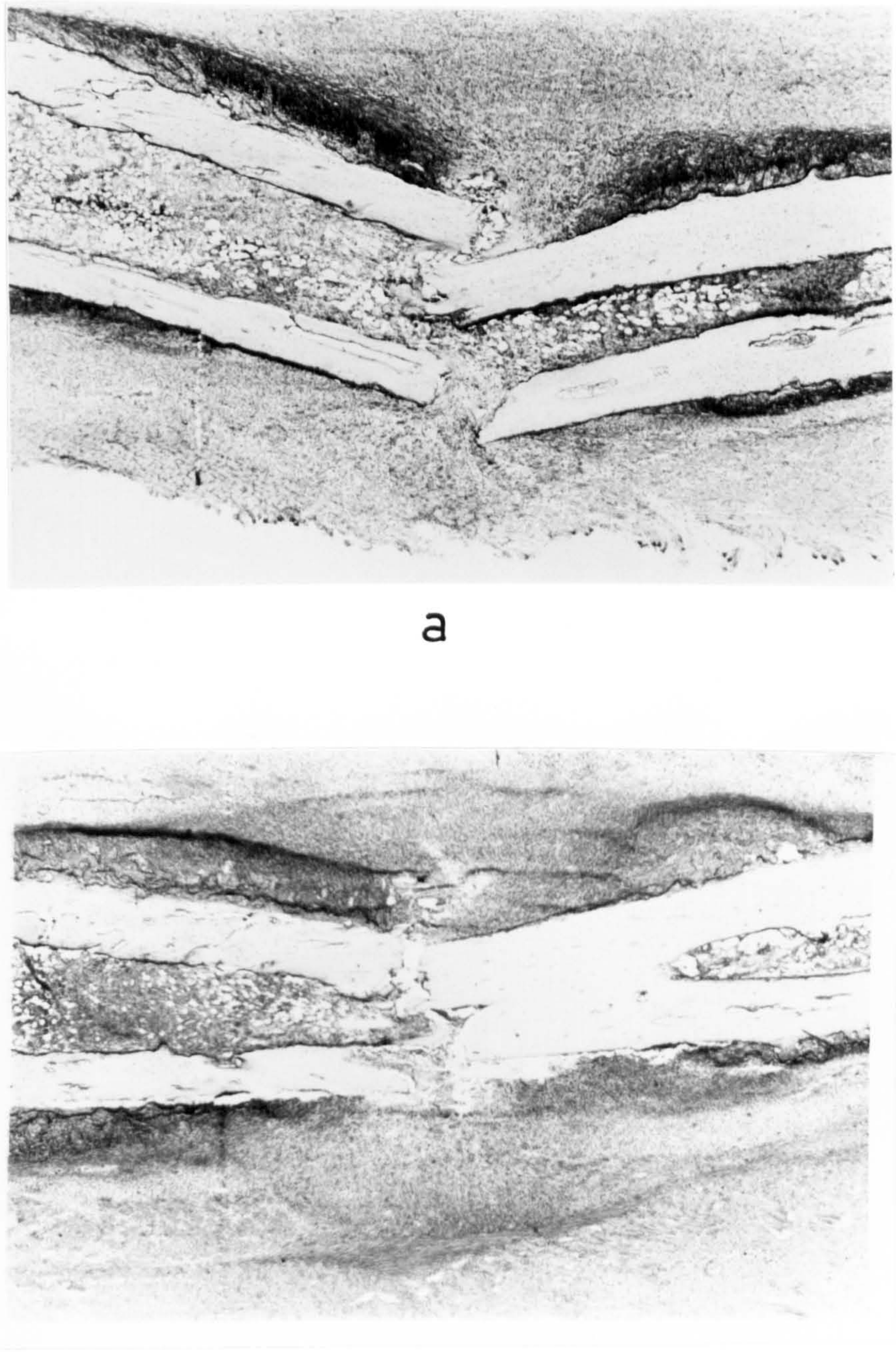

a

b

Fig. VIII. 1 Cryostat section of a five-day fracture in a rat treated with dicoumarol. The amount of new bone formed on the shaft (a) is much less than that seen in the control fractures (b) (and Fig. VII. 3) Toluidine blue; x 20

coumarol-treated rats appeared to be less advanced in terms of the degree of differentiation that it achieved (Fig. VIII.2). As a test of this suggestion, the area occupied by new bone was expressed as a percentage of the total area of the callus. When expressed in this way (Table VIII.1), in these specimens taken 12 days after fracture, the proportion of the callus occupied by new bone was significantly higher ($p < 0.001$) in the control rats (e.g. 56% ± 10; mean ± S.D.) than in those treated with dicoumarol (38% ± 6). In the controls, the centre of the callus around the fracture site (Fig. VIII.2) was occupied by fibrocartilage-like material, differentiating into mature cartilage further from the fracture. In the rats treated with dicoumarol, the region which should have contained fibrocartilage-like material contained effete, fibrous material with few cells. At 6 weeks, the fracture in the control rats was fully united, but union was still incomplete in those given dicoumarol (Fig. VIII.3).

Cytochemical Results

Glucose 6-phosphate Dehydrogenase Activity in the Periosteum.

The activity was measured in individual periosteal cells at measured distances (0.2 mm) from the fracture up to 2.2 mm away from the fracture site. Measurements were made 3 and 5 days post-fracture.

In 3 control rats, 3 days post-fracture, there was considerable activity close to the fracture, reaching

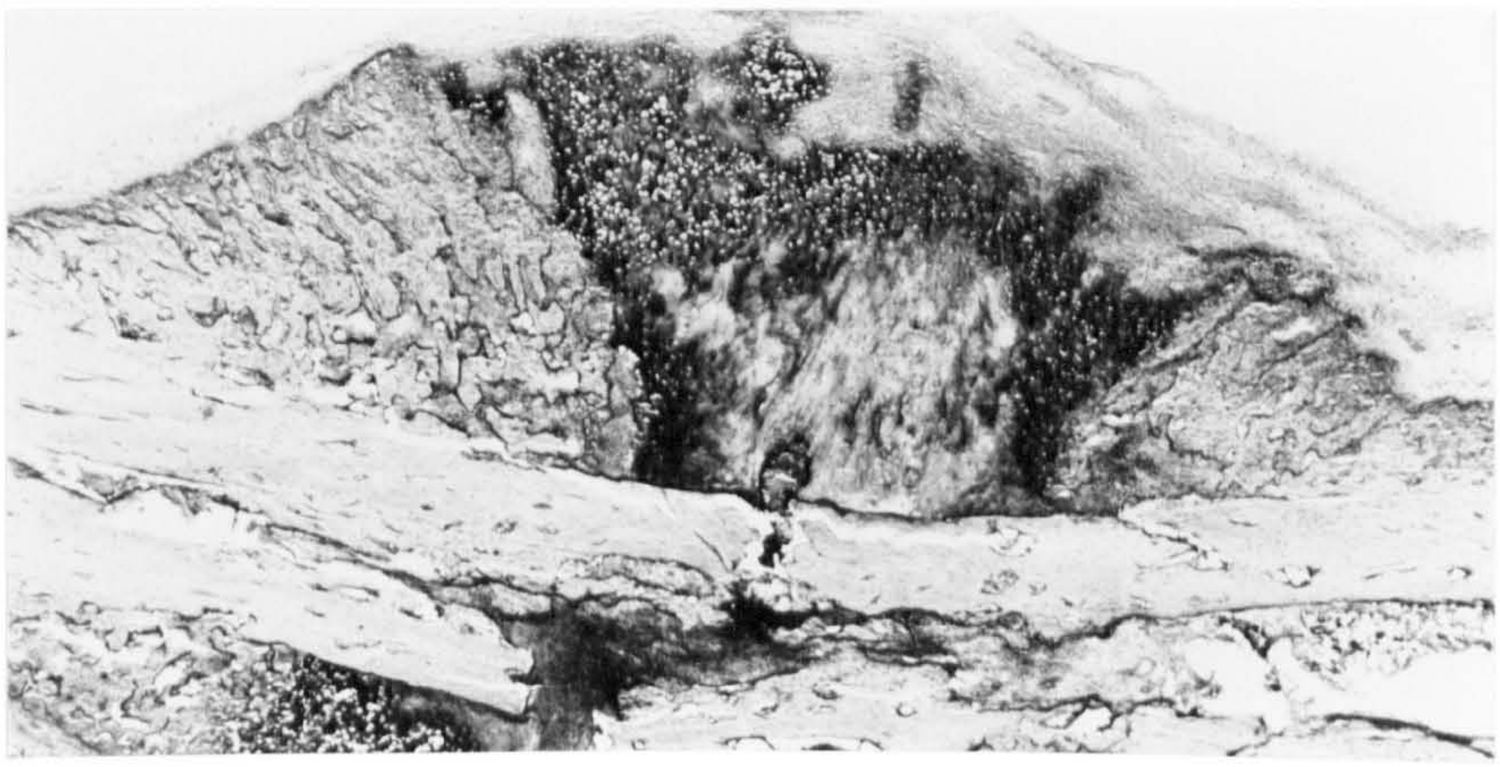

a

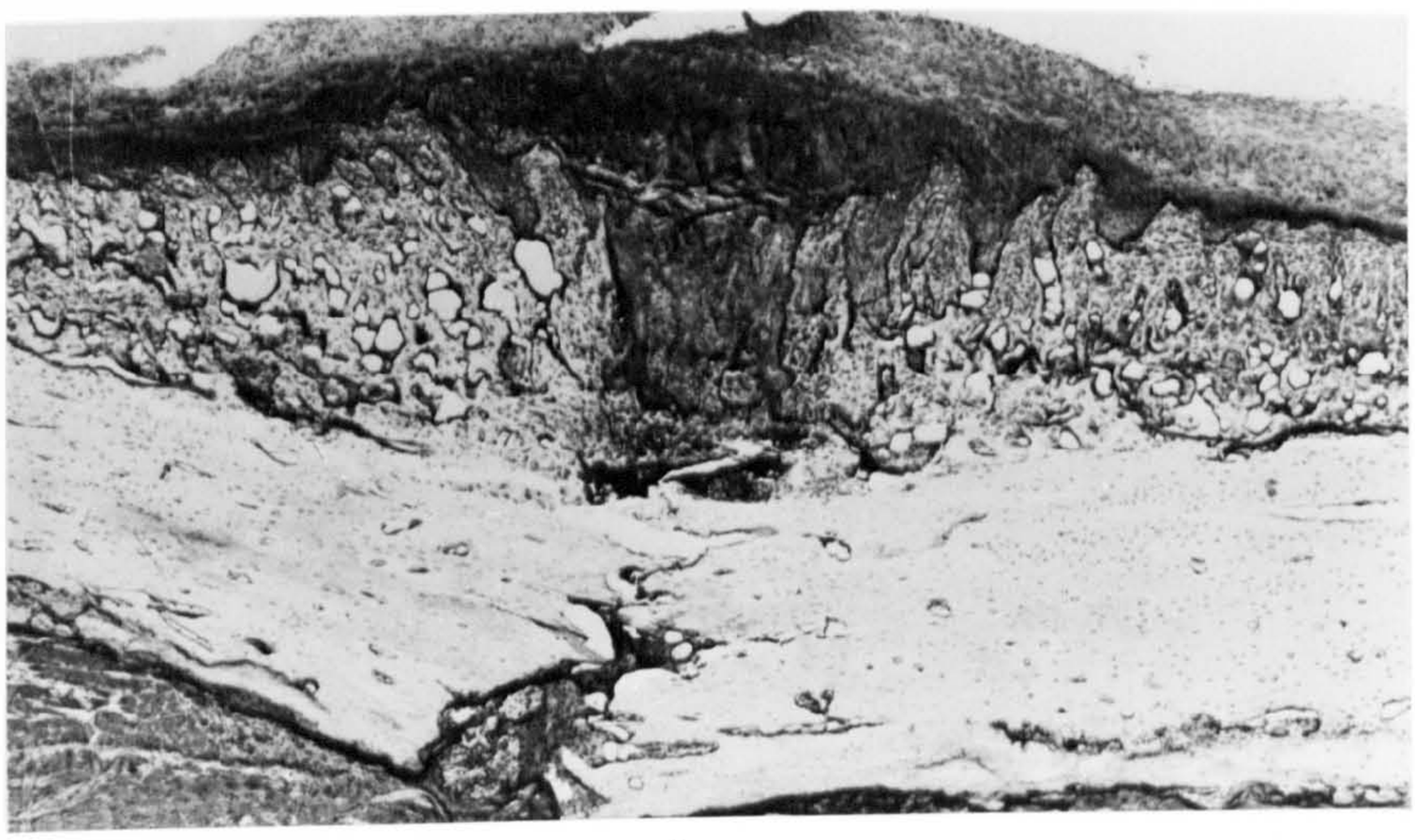

b

Fig. VIII. 2 The degree of differentiation in the callus formed at 12 days in a rat treated with dicoumarol (a) is less advanced than that seen at this time in the control rats (b).

Toluidine blue; X 20.

a

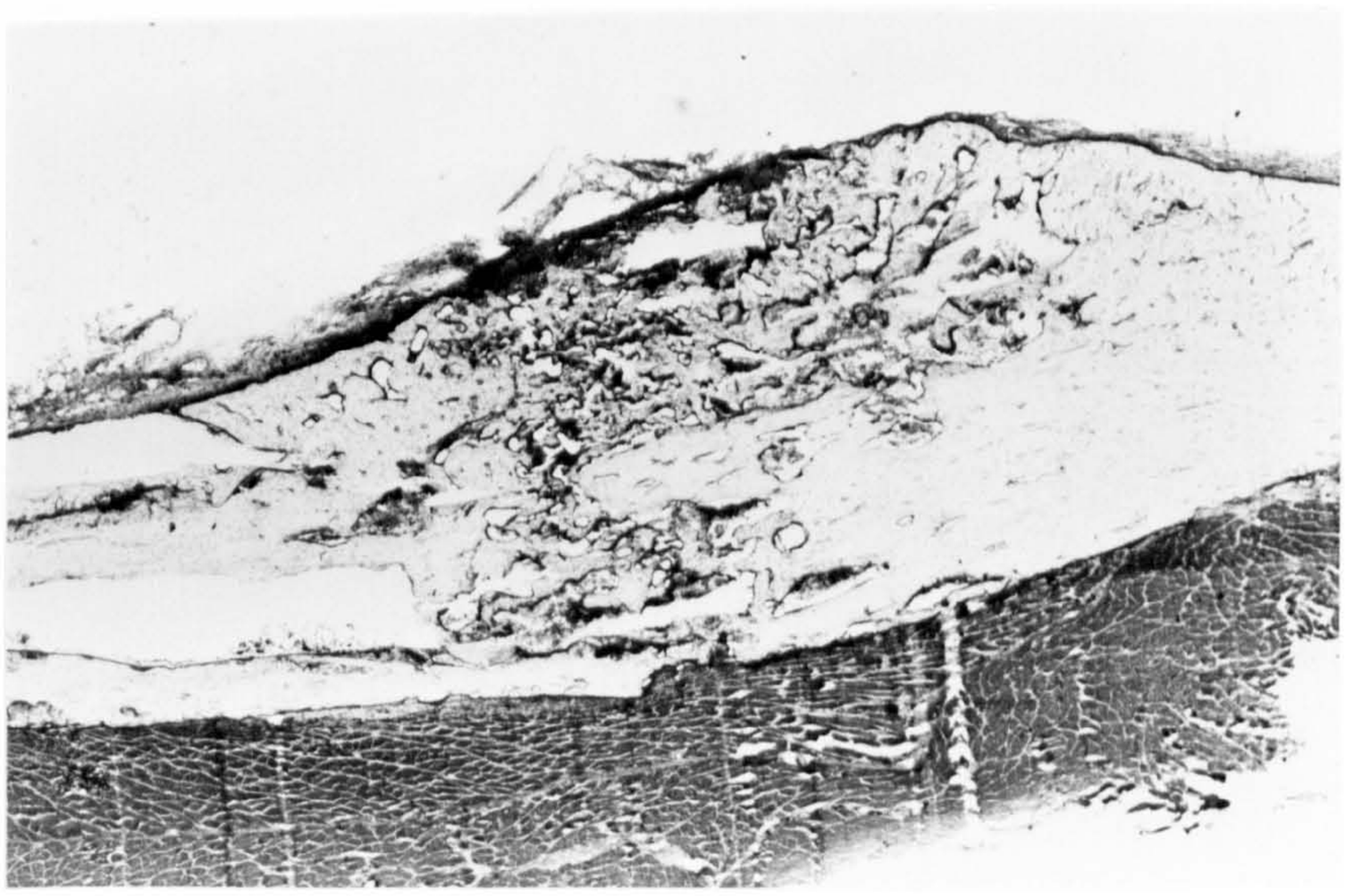

b

Fig. VIII. 3 At six weeks post fracture in a dicoumarol treated rat (a), union is still incomplete in that there is soft callus between the fracture ends whereas in control rats, union is complete (b).
Toluidine blue; X 24.

a mean extinction value of 22 units at 0.4 mm from the fracture, and rising to 27 units 1.2 mm from the fracture (Fig. VIII.4). In contrast, the G6PD activity in the dicoumarol-treated rats declined over this region of the perosteum (Fig. VIII.4). Each different symbol in Fig. VIII.4, closed and opened, represents a different animal.

In the periosteum of the fractured bones from 15 untreated and 14 dicoumarol-treated rats taken 5 days after fracture, the mean activity was depressed in the latter. This was found even though there were wide individual variations (Fig. VIII.5). The differences at 0, 0.2, and 0.4 mm from the fracture site were significant at the level of $p \leq 0.02$; at 0.6 mm the difference was significant at $p = 0.03$.

The precise location of the peaks of G6PD activity varied slightly in the different animals. Consequently, the mean results did not adequately represent the changes in activity either along the periosteum of any one animal, or the differences induced by dicoumarol treatment. In general, all the bones from the control rats, and most of the bones from the treated rats, showed two regions of elevated G6PD activity, an example of which is shown in Fig. VIII.6. The region closest to the fracture had relatively low activity, with higher activities over part or all of the first 0.8 mm from the fracture. Particularly in the controls, another peak of activity occurred in the region of 1.0 - 1.8 mm

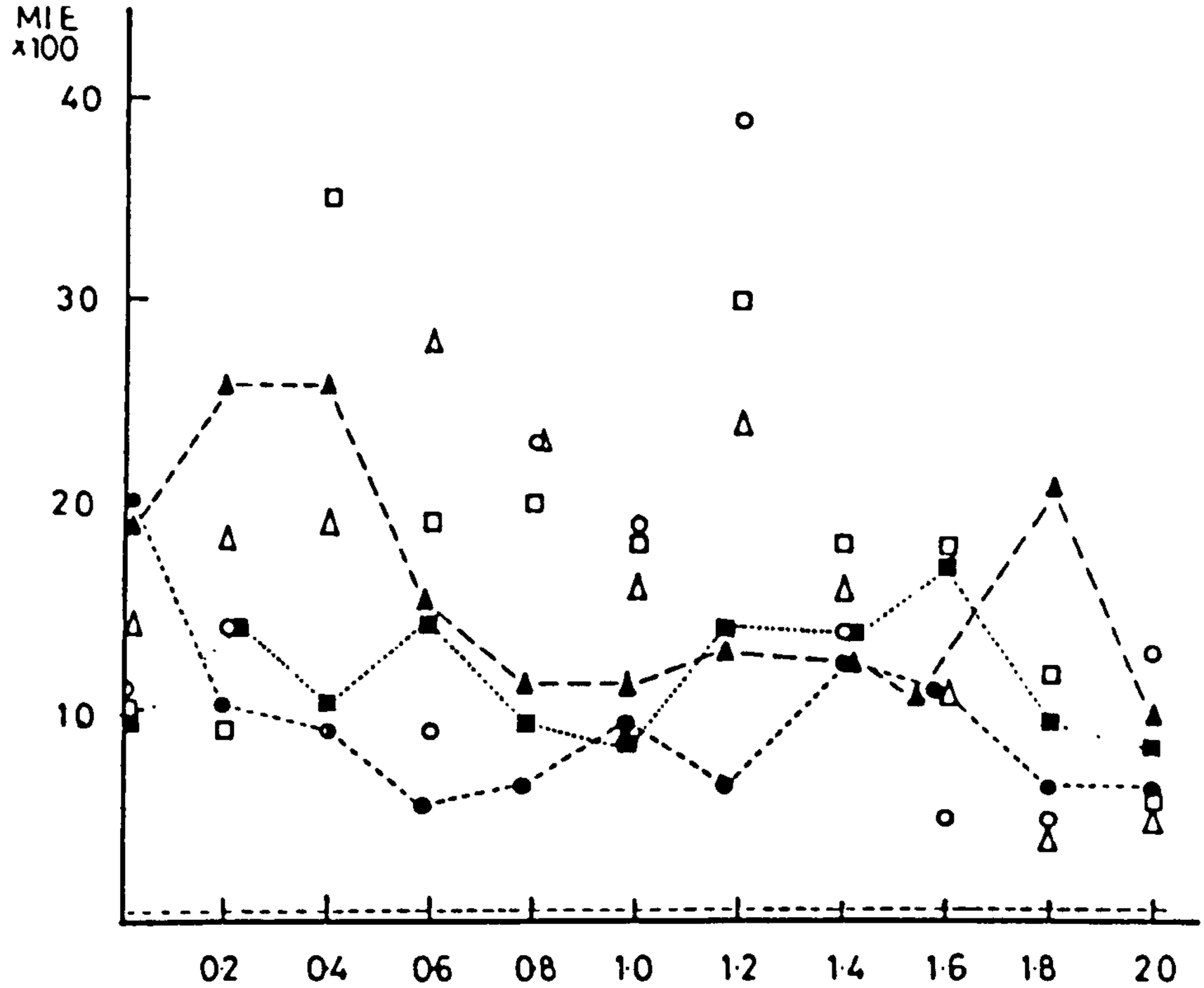

Fig. VIII. 4 Glucose 6-phosphate dehydrogenase activity (G6PD; M.I.E. x 100) in the periosteal cells of three-day old fractures. Each symbol represents a different animal; closed symbols: dicoumarol-treated rats; open symbols: control rats. In the dicoumarol-treated rats there is no peak of G6PD activity at the site where new bone formation begins (about 1.2mm away from the fracture). The dotted line just above the x-axis represents the activity in unfractured bone from either group.

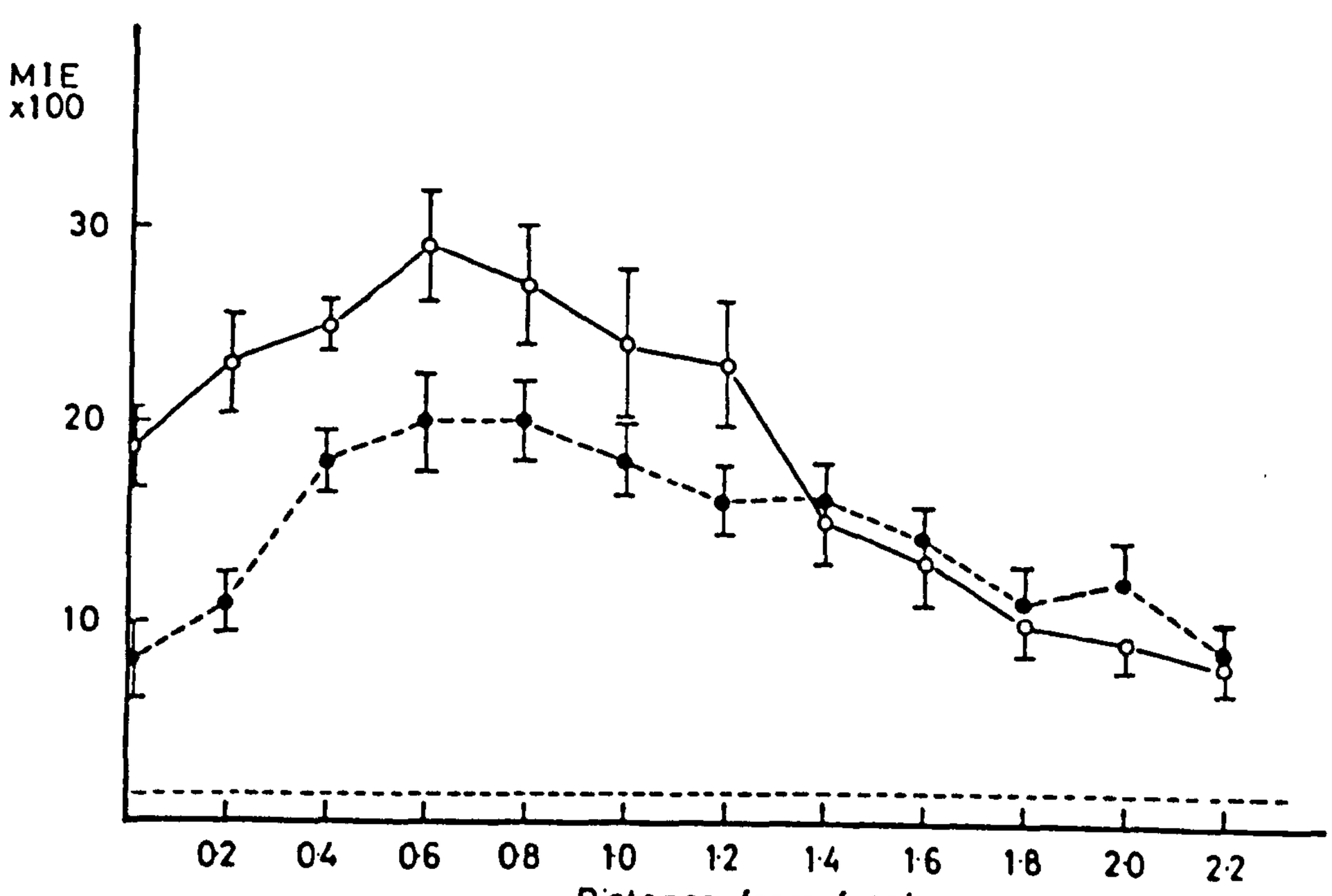

Fig. VIII. 5 Combined results of glucose 6-phosphate dehydrogenase activity (M.I.E. X 100 ± SEM) in the periosteal cells from 14 dicoumarol-treated rats (closed circles) and 15 control rats (open circles) 5 days after fracture. Up to 1.2 mm, the activity is less in the dicoumarol treated rats.

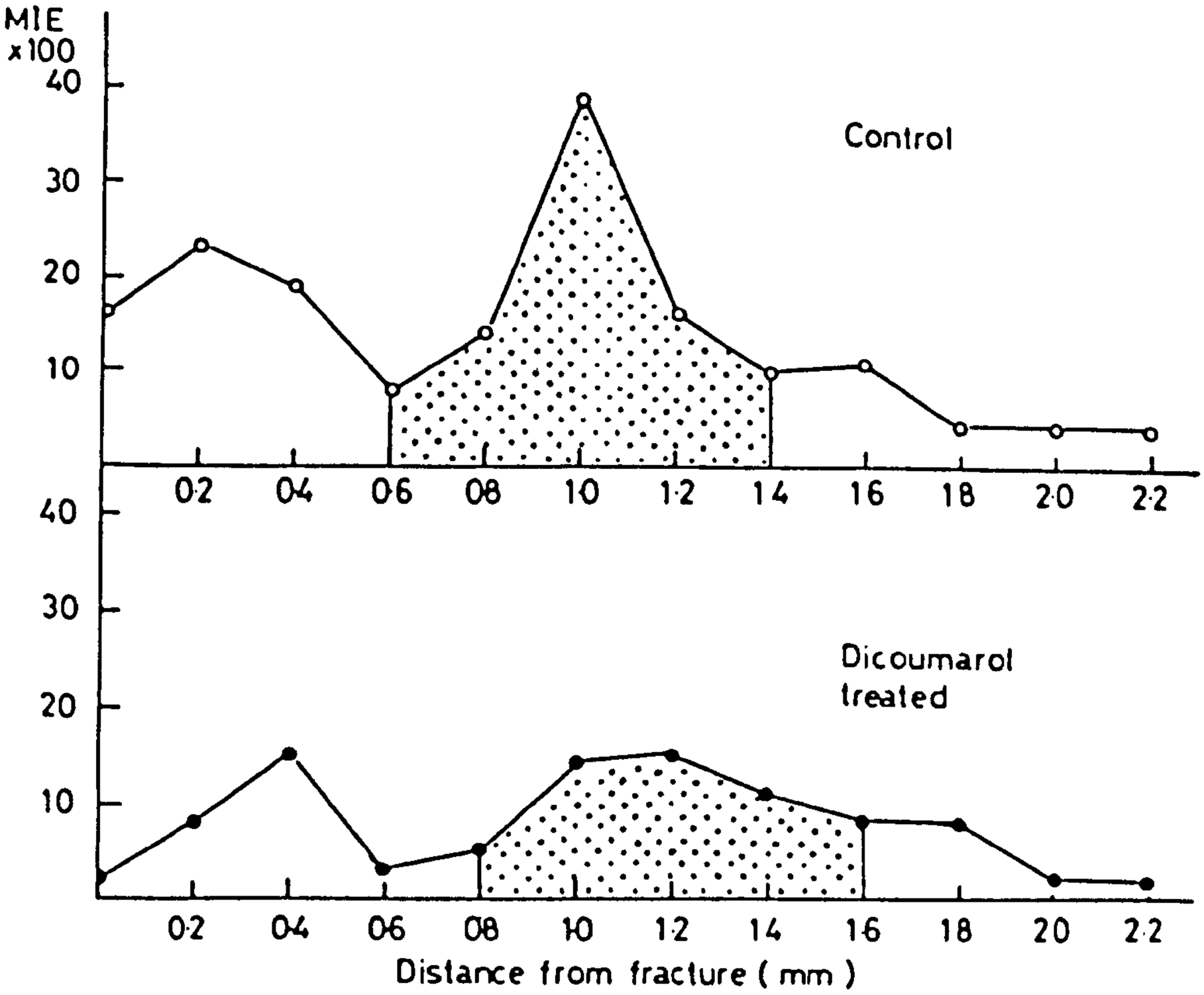

Fig. VIII. 6 Glucose 6-phosphate dehydrogenase activity (G6PD; M.I.E. x 100) in the periosteal cells of 5-day fractures in a control and a dicoumarol-treated rat. In both there are two peaks of G6PD activity but the exact height and location of the peaks varies between individuals so that the peaks cannot be distinguished when the results are combined. (Fig. VIII. 5) The vertical lines and shaded areas define the second peak.

from the fracture. The precise location of these elevated activities varied from one rat to the next. Thus the overall mean values (Fig. VIII.5) did not clearly show these variations. To express the first of these activities numerically, the activity in each section was plotted against the distance from the fracture, as in Fig. VIII.6, and the area under the graph up to the beginning of the second peak was measured by planimetry.

The results are shown in Table VIII.2. There was a barely significant depression of G6PD activity over this region of the periosteum in the dorsal callus of the rats treated with dicoumarol ($0.05 > p > 0.02$). A similar device was used to achieve a numerical representation of how the treatment influenced the second peak of activity in the region of 0.8 - 1.8 mm from the fracture. For this purpose, an increase from one measurement to the next (a distance of 0.2 mm) of more than 5 units of mean integrated extinction x100 (corresponding to 0.05 of absolute extinction) was defined as a "peak". The area of such peaks was marked on the graphs (as in Fig. VIII.6) and were measured by planimetry.

The results (Table VIII.2) showed that treatment with dicoumarol had markedly suppressed this second peak ($p < 0.001$).

Table VIII. 2 Glucose 6-phosphate dehydrogenase activity (mean ± SEM) in periosteal cells of fractured rat metatarsals 5 days post-fracture.

	Control (n = 15)	Dicoumarol (n = 15)
Area of first region of activity from the fracture	25 ± 2.8†	17.7 ± 1.7
Area of second peak* of activity	16 ± 2.7††	3 ± 0.98

*A peak was defined as a change in activity of greater than 5 units MIE x 100/0.2mm.

†0.05 >p>0.02 and †† p < 0.001 as compared with dicoumarol-treated rats: Student t test.

Alkaline Phosphatase Activity in the Periosteum.

In a control rat, 3 days after fracture, there was very low activity up to 0.8 mm from the fracture site, becoming markedly elevated thereafter to values exceeding those found uniformly throughout this region in intact metatarsal bones of this strain of rat (38 ± 0.8; mean ± SEM; n = 4 ; Fig. VIII.7). This loss of activity, close to the fracture site, was very much less marked in the dicoumarol-treated rats (Fig. VIII.7). This pattern was found in 14 control and 16 dicoumarol-treated rats 5 days after fracture (Fig. VIII.8). At all points in the periosteum, up to and including 0.6 mm from the fracture, the alkaline phosphatase activity was very significantly lower in the control rats than in those treated with dicoumarol ($P < 0.0004$); it was significantly lower also at 0.8 mm from the fracture ($P = 0.01$) but the activities thereafter were not significantly different.

HOAD Activity in the Periosteum. This enzymatic activity was measured in the periosteum from the fractures of 10 control rats and of 11 rats that had been treated with dicoumarol. Because inspection of the graphs of activity against distance for individual bones disclosed no obvious patterns, the results from all the specimens were plotted (Fig. VIII.9). There was no difference in activity as a consequence of treatment with dicoumarol.

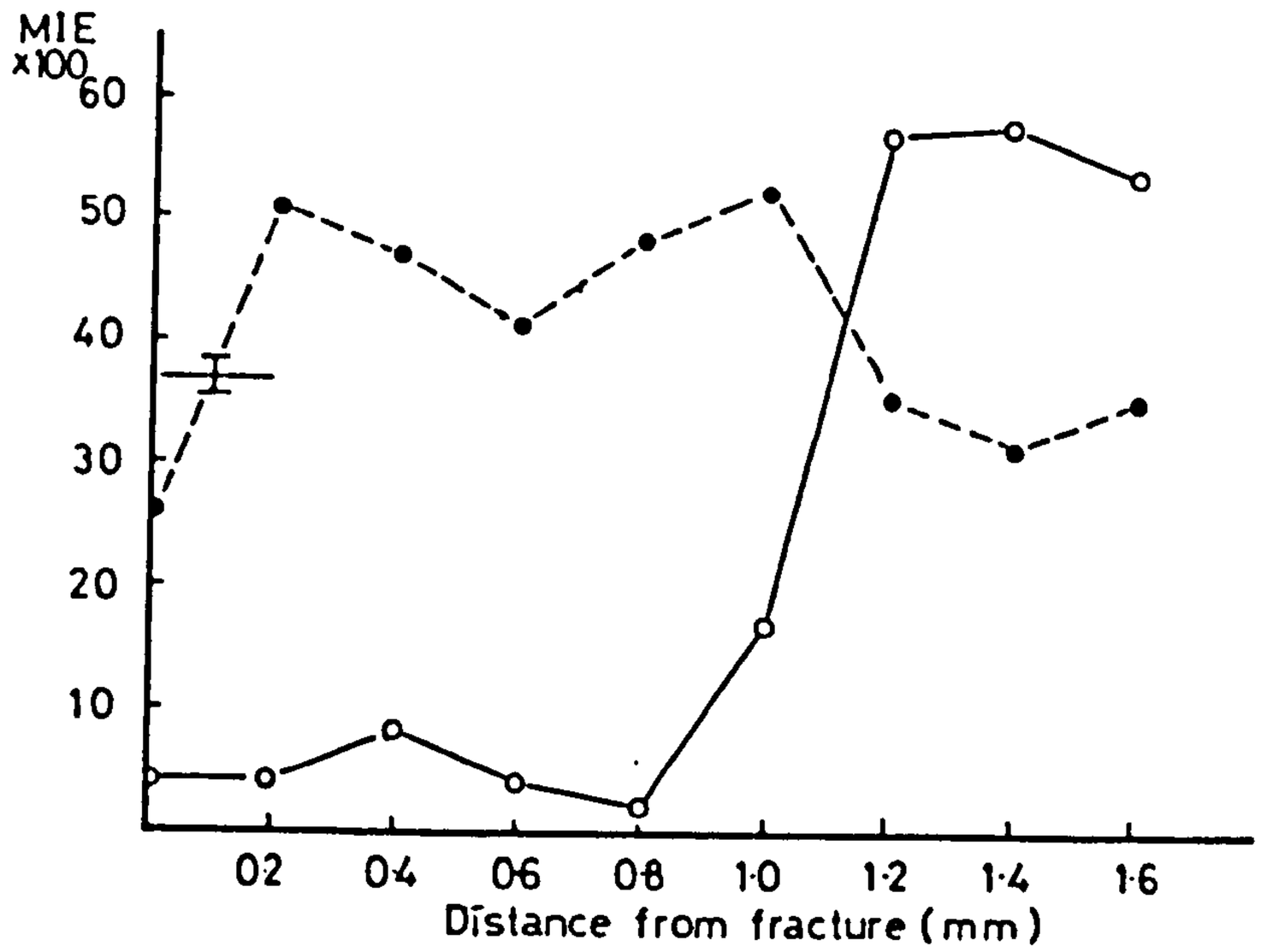

Fig. VIII. 7 Alkaline phosphatase activity (MIE x 100) in the periosteal cells of a control and a dicoumarol-treated rat, three days post-fracture. The characteristic depression of alkaline phosphatase activity close to the fracture is less marked in the dicoumarol-treated rat. The bars next to the y-axis indicate alkaline phosphatase activity in unfractured periosteum (mean ± SEM; n = 4 rats).

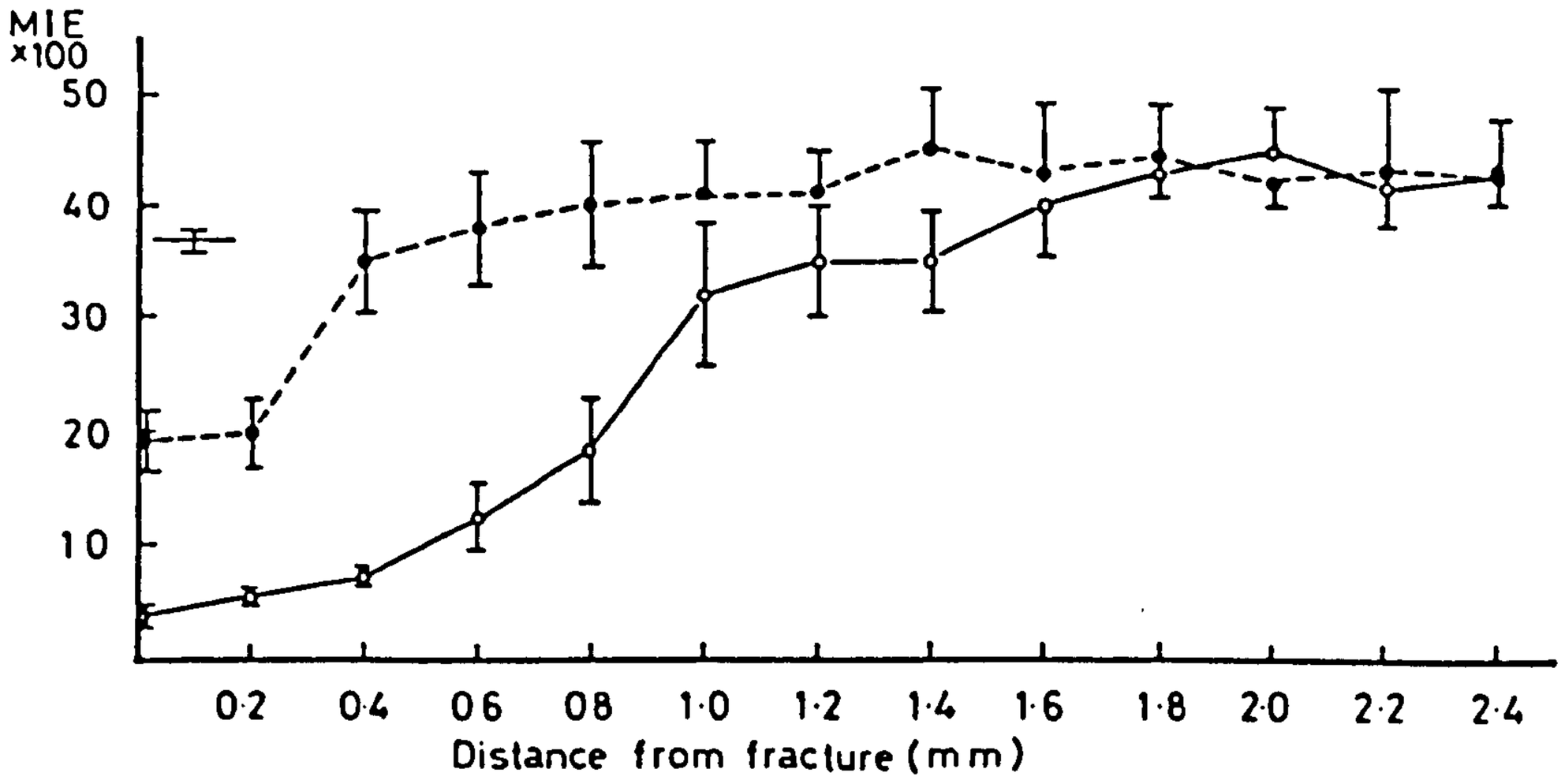

Fig. VIII. 8 Combined results (mean ± SEM) of alkaline phosphatase activity (MIE x 100) in the periosteal cells of 16 dicoumarol-treated rats (closed circles) and 14 control rats (open circles) five days after fracture. The activity close to the fracture in the dicoumarol-treated rats is less depressed and more approximates to the activity found in unfractured bone (bars close to the y-axis) than that of the control fractures.

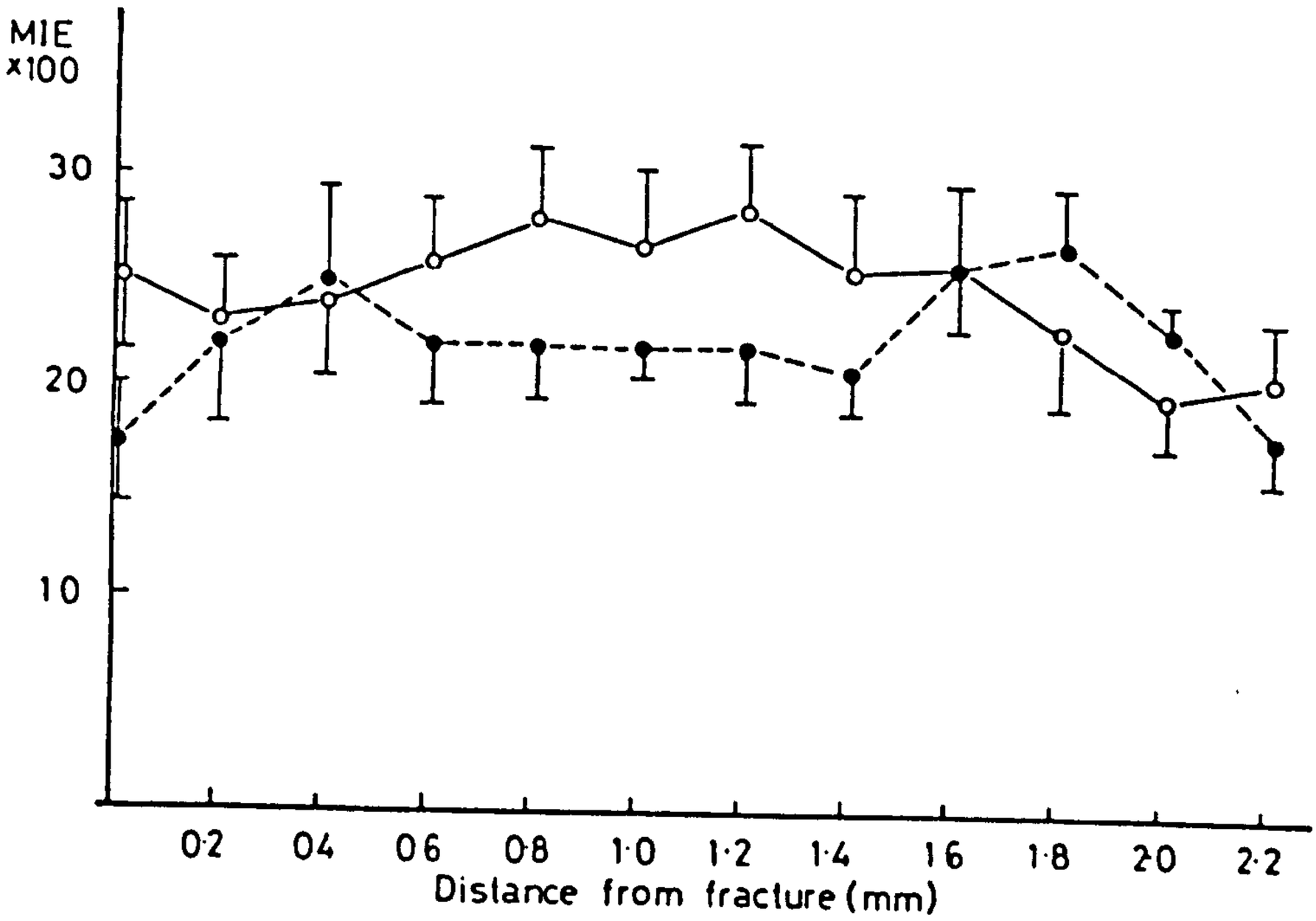

Fig. VIII. 9 Combined results of Hydroxyacyl dehydrogenase activity (M.I.E. x 100 ± SEM) in the periosteal cells of 11 dicoumarol-treated and 10 control rats, five days post-fracture. The activity in the two groups is relatively constant and similar.

Enzymatic Activity in the Cells of the Callus.

Most of the metabolic studies involved in investigating the effects of dicoumarol were done on material of the 12 day post-fracture, when the different cell types are easily defined. The enzyme activities were measured in 5 specified cell types in the callus; mature chondrocytes, chondrocytes in calcified cartilage, cellular granulation tissue, loose granulation tissue and osteoblasts (as described in Chapter VII). Measurements were made in earlier fractures (5 days and 8 days post-fracture) but it was difficult to define accurately the different cell types and there was also wide variation within each group. However the same pattern of results was observed as in the 12 day post-fractures. In the later fractures (19 days, 33 days and 42 days post-fracture) the control rats and dicoumarol-treated rats were at different stages of maturation. Therefore only the results from the 12 day post-fracture are shown (Table VIII.3).

Glucose 6-phosphate dehydrogenase activity was measured generally in 5 specified cell types in the callus of the fractures of 10 control, and 8 dicoumarol-treated rats, 12 days post-fracture. Only in the cells of the mature cartilage (Table VIII.3) was the activity in the dicoumarol-treated rats significantly lower ($p = 0.01$; $n = 19$) than in the controls. No differences were found in the activities of either alkaline phos-

Table VIII. 3 Enzyme activities (MIE x 100/10 min) on the various cell types of the callus 12 days post-fracture.

Cell Type		Enzyme: G6PD*	HOAD*	ALK PHOS*
Mature chondrocytes	Control:	28 ± 2	5.3 ± 0.5	107 ± 6.3
	Dicoumarol:	20 ± 2	5.5 ± 0.4	100 ± 8.3
Chondrocytes in calcified cartilage	Control:	11 ± 1.2	2.5 ± 0.2	53 ± 8.3
	Dicoumarol:	10 ± 1.0	3.0 ± 0.2	53 ± 6.0
Cellular granulation tissue	Control:	51 ± 6.0	7 ± 1.2	70 ± 6.7
	Dicoumarol:	32 ± 7.0	7 ± 1.0	73 ± 7.0
Loose granulation tissue	Control:	18 ± 1.7	3.0 ± 0.4	3.3 ± 2.2
	Dicoumarol:	14 ± 1.5	3.0 ± 0.3	3.3 ± 3.2
Osteoblasts	Control:	37 ± 3.7	9.0 ± 0.8	140 ± 7.3
	Dicoumarol:	20 ± 3.0	9.0 ± 0.9	123 ± 12

*
G6PD: glucose 6-phosphate dehydrogenase
HOAD: hydrozyacyl dehydrogenase
Alk.Phos:alkaline phosphatase

phatase or HOAD in any of these cell types 12 days post-fracture.

DISCUSSION

The histological results showed that the effect of dicoumarol treatment on fracture healing (Table VIII. 1) had no effect on the total size of callus that developed, but markedly delayed maturation so that at 12 days post-fracture, whereas 56% of the area of the callus of the controls was occupied by bone, only 38% was occupied by bone in the treated rats. Moreover, the latter showed large regions of cartilagenous material (Fig. VIII.2) and effete, fibrous material. These results are in accord with those of Stinchfield et al (1956), who found fibrous tissue and immature bone in the healing fractures of rabbits and a dog given dicoumarol at the rate of 2 mg/kg body weight each day. However the results reported here seem to be at variance with the results of Price and Williamson (1981) who detected no abnormality in the repair of fractures in rats fed with Warfarin. However, these workers studied young rats, in which the radius was fractured at 17 days of age. Because the amount of Warfarin given was apparently toxic, vitamin K_1 was also administered simultaneously. Thus the conditions were very different from those used in the present study. Also, evidence of repair was obtained radiologically and not histologically, thus allowing for the possibility that

an outer cuff of bone, overlying a region of unossified cartilage (as found in this study), could have confused the radiological evidence. In the literature there are further reports of delayed fracture healing in experimental animals after administration of derivatives of dicoumarol; this work has been reviewed by Hahnel et al (1976) and includes studies by Rokkanen and Slatis (1964), Blum (1964) and Knoth and Markgraf (1976). All seem to stress the anticoagulant properties of dicoumarol-like substances as opposed to their possible antagonism of the vitamin K_1 cycle.

Over the first 15 days after fracture of metatarsal bones, G6PD activity has been shown to be elevated in the region near the fracture and also in a region about 1.2 mm behind the fracture (Dunham et al, 1977, and Chapter VII). The first peak of activity was apparently associated with the proliferation required to form the callus, since this enzyme is the regulatory enzyme of the pentose shunt which is required for growth (Krebs and Eggleston, 1974). The second peak of activity was seen to be associated with the region at which bone first formed on the shaft of the fractured bone (Dunham et al, 1977 and Chapter VII). The biochemical function of the second peak of G6PD may be related to the fact that this enzymatic activity is a major source of cytosolic NADPH which may be used in the vitamin K_1 cycle (Suttie et al, 1978).

The results in the present study indicated that treatment with dicoumarol only slightly depressed G6PD activity in the first region of the periosteum (Table VIII.2), but virtually obliterated the second peak. There was also depressed G6PD activity in the cells of the mature cartilage (Table VIII.3). Thus, not only could it be acting as an antagonist of the vitamin K cycle, blocking the conversion of the epoxide to the naphthoquinone, but it also depressed the amount of reducing equivalents, from NADPH, available for the cycle at these points of ossification.

This action of dicoumarol was not a universal effect in that it had no influence on the G6PD activity of the other cells of the callus (and therefore on the proliferative capacity of the callus or its ultimate size); nor did it influence fatty acid oxidation, as shown by the hydroxyacyl dehydrogenase activity (Table VIII.3). Furthermore, it enhanced periosteal alkaline phosphatase activity(Fig. VIII.8) and left that of the various cells of the callus unaltered (Table VIII.3). Thus it would seem, from the histological results, that dicoumarol treatment retarded the ossification of the callus. This is consistent with it having an antagonistic effect against vitamin K_1 in the vitamin K cycle. In addition, dicoumarol decreased the amount of reducing equivalents for this cycle selectively at points at which ossification should have occurred.

CHAPTER IX

THE EFFECT OF VITAMIN B_6 DEFICIENCY ON FRACTURE HEALING

Introduction

Interest in G6PD Activity

Studies on the cellular metabolic activities in early healing fractures in rats showed a striking increase in periosteal glucose 6-phosphate dehydrogenase (G6PD) activity, at the fracture-site (associated with cell growth in the callus) and at the site at which new bone forms on the shaft (Dunham et al, 1977; Dodds et al, 1984). G6PD is the first and rate-limiting step in the pentose shunt and is important for supplying NADPH, to be used in many reductive biosynthetic reactions, and in producing ribose phosphate for nucleic acid synthesis. Thus the fracture involves both active proliferation and biosynthesis. The increased periosteal G6PD activity at the site at which new bone forms on the shaft precedes the first signs of new bone. As described in Chapter VIII it may also be that the NADPH, generated by this stimulated G6PD activity, would be used in the vitamin K_1 cycle for ossification.

It was therefore of interest to investigate the chemical mediator of G6PD activation. Investigations into the various forms of G6PD have shown that it can

aggregate to an active form, or dissociate into inactive units and that NADP by binding to the enzyme at a non-catalytic site can hold the enzyme in the active state (as reviewed by Bonsignore and de Flora, 1972; Chayen and Bitensky, 1982). This allows for a rapid response to stimuli in that the cell would not necessarily have to synthesize more enzyme during rapid changes in activation (Chayen and Bitensky, 1982). In the liver, the active form of G6PD is a tetramer which can be dissociated into two active dimeric units. The enzyme can be further dissociated into inactive monomers if it is incubated in the presence of free fatty acids. NADP specifically antagonizes the inactivating effect exerted by fatty acids (Bonsignore and de Flora, 1972).

Inhibitory Effects of Fatty Acid-CoA on Isolated G6PD

It has also been demonstrated that long chain fatty acyl-CoA thioesters, such as palmitoyl-CoA inhibit yeast and liver G6PD activity in vitro (Taketa and Pogell, 1966). However the physiological significance of this finding was excluded (Taketa and Pogell, 1966) on the basis of a complete lack of specificity, in that palmitoyl-CoA also inhibited several other enzymes. Taketa and Pogell (1966) suggested that the detergent-like properties of the long chain acyl-CoA esters produce conformational changes in the various enzymes studied, that may or may not alter the enzyme activity. It may be remarked that all these studies were done on isolated enzymes in solution.

Mita and Yasamasu (1979, 1983) demonstrated that the polyamines spermine and spermidine, but not putrescine, released the inhibitory effects of palmitoyl-CoA on yeast and bovine adrenal G6PD activity, in vitro. Polyamines and their metabolism are discussed in detail in Chapter IV. Despite the fact that the precise function of polyamines has not been resolved, it is generally accepted that they play an important role in the growth and differentiation of most cell types.

In the study by Mita and Yasumasu (1978) on isolated G6PD, spermine enhanced G6PD activity, whereas spermidine and putrescine had no activating effect. However, they concluded that the reversal effects of polyamines on the inhibition of G6PD by palmitoyl-CoA was not a result of the activation of the enzyme (Mita and Yasumasu, 1978). These authors postulated that the positively charged polyamines neutralize the negative charge of the palmitoyl-CoA, and this is supported by the fact that a polyamine with a large number of amino groups was more effective on the palmitoyl-CoA inhibition. They also showed that substitution of the terminal amino groups in polyamines by carboxyl or hydroxyl groups reduced the reversal effects. Finally Mita and Yasumasu reported that polyamines are able to bind to palmitoyl CoA.

Possible Linkage Between G6PD Activity and Putrescine

As has been discussed (above), the activity of G6PD can be markedly changed, rapidly, by NADP added to the enzyme but at non-catalytic sites. Several studies have been made in this Laboratory on possible mediators that can affect this activity in life. One possibility was that, in life, a polyamine might take the place of $NADP^+$ at non-catalytic sites. In studies on smooth muscle (Naomi Chayen, 1984) it was shown that 5-hydroxytryptamine (e.g. at 10^{-4}M or 10^{-5}M) caused an increase in G6PD activity within 1 minute of its application to strips of rat gastric fundus muscle, and that this increase was related to an influx of extracellular calcium. Quantitatively similar changes were produced by putrescine. It therefore seemed possible that the 5-hydroxytryptamine was activating ODC; preliminary investigations with the new cytochemical method for measuring ODC activity (Dodds and Chayen, 1984) supported this view. It therefore seemed reasonable to examine whether the increased periosteal G6PD activity, observed early in fracture-healing (Chapter VII) could be inhibited by inhibiting ODC activity, or by decreasing tissue-levels of polyamines, and whether such inhibition altered the course of fracture-healing.

Inhibition of Polyamine Synthesis

The rate-limiting steps of polyamine synthesis in mammalian tissues are catalysed by two decarboxylases (i) ornithine decarboxylase (ODC), which shows an absolute

requirement for pyridoxal phosphate, and (ii) putrescine-activated S-adenosyl methionine decarboxylase (SAMD) (Raina and Janne, 1975). Exceptionally, SAMD has no requirement for pyridoxal phosphate (Eloranta et al, 1976; Pegg, 1976). Eloranta et al (1976) and Pegg (1976) studied the effects of pyridoxine (vitamin B_6) deficiency on these two decarboylases and on the concentraion of the polyamines putrescine, spermidine and spermine, in various tissues in the rat. Briefly, 40g rats (male/female Wistar) fed a pyridoxine-deficient diet for 3-6 weeks had a lower concentration of putrescine and spermidine in their tissues than the appropriate controls; spermine levels remained fairly constant. Thus this may indicate that the effective ornithine decarboxylase activity in vivo was decreased due to the decreased amounts of the cofactor. In the study by Pegg (1976) ODC activity was decreased by B_6 deficiency when assayed in tissue extracts without pyridoxal phosphate being present, and increased when the cofactor was present in the assay-system. Pegg (1976) suggested that the cell may try to compensate for the decreased activity of ODC in pyridoxal phosphate-deficiency by increasing the concentration of the enzyme. SAMD was not decreased in the tissues from the B_6 deficient rats.

The conclusions from the studies by Eloranta et al (1976) and Pegg (1976) were that pyridoxal phosphate is not a cofactor for SAMD, and that although the concentrations of putrescine and spermidine were decreased in B_6-deficient rats, the ODC and SAMD activities, measured

under optimal conditions in vitro, in no way correlated with the concentration of polyamines in vivo. Nevertheless, pyridoxine deficiency seemed to be a useful tool in studying the metabolic effects associated with fracture-healing in the rat, especially the stimulation of periosteal glucose 6-phosphate dehydrogenase, discused at the beginning of this chapter. Consequently, a detailed metabolic and histological study has been made of the effects of vitamin B_6-deficiency in the fracture-healing response in male Wistar rats.

Materials and Methods

Most of the materials and methods have been described in Chapter VII. Male Wistar rats weighing 40 - 60 g were divided into two groups, one fed on a pyridoxine deficient diet (25g/daily: see appendix III) for 24 days before induction of the fracture, the other control group receiving the same diet supplemented with pyridoxine. The diet in both groups was changed daily, and care was taken to avoid contamination of the food by the excreta of the rats. After fractures were imposed by digital pressure on two metatarsals on one hind limb, the rats were retained on their respective diets. At various times after fracture, up to 9 weeks, the rats were killed and the bones removed and chilled (as described in Chapter VII).

Body Weights of Rats

The weights of the B_6 deficient and control rats were recorded at set times after fracture. Up to 54 days

on the diet there was no significant difference in the weights. By the 80th day the control rats weighed an average of 346 g whereas the B_6 deficient rats weighed 316 g.

Cytochemical Reactions: The bones were sectioned (10 μm) on a Jung 1130 rotary microtome set in a Bright's cryostat (Johnstone et al, 1972; Johnstone, 1979; and discussed in Chapter V). Six enzymes were studied: glucose 6-phosphate dehydrogenase (G6PD) activity; glyceraldehyde 3-phosphate dehydrogenase (GAPD) activity; succinate dehydrogenase (SDH) activity; lactate dehydrogenase (LDH) activity; hydroxyacyl dehydrogenase (HOAD) activity; and alkaline phosphatase (Alk Phos) activity. Corrections had to be made for the time of reaction. The procedures for demonstrating these enzyme activities are described in Chapters VI and VII. The cytochemical reactions were measured at discrete sites in the periosteum, and in histologically defined cell types in the developing callus. The coloured reaction product of these cytochemical reactions was measured by means of a Vickers M85 scanning and integrating microdensitometer, with a x40 objective, spot size 1 (equivalent to 0.4 μm in the plane of the specimen) as described in Chapters VI and VII.

Serial sections were stained with toluidine blue for histological study (Chayen et al, 1973). At 12 days post-fracture the image of selected sections was

thrown on to a screen, and the enlarged image traced. The areas of the selected tissue-components were measured by planimetry (as described in Chapter VIII).

Histological Results

A detailed histological study is still in progress and further experiments are under way, so only a brief discussion of the results will be given.

As described in Chapter VII, the sequence of events in the healing process of fractured metatarsals in the Wistar rat differs in many ways from that of the Sprague-Dawley. In general, the resulting fractures are very angulated in the Wistar rat. The callus on the dorsal side of the fracture was in most cases larger than the plantar side, but not to the same extent as that found in the Sprague-Dawley rats (as described in Chapter VII). The Wistar rats in this study were very young at the time that their bones were fractured (e.g. 180 g instead of 250 g as in the study of Shedden et al, 1976); it was therefore not surprising that the fractures in the control animals healed rapidly, being fully united in all 8 specimens studied between 26 and 30 days post-fracture. In contrast in the B_6 deficient rats union was delayed so that in all 8 rats studied, there was still an extensive callus 26 days post-fracture; by 9 weeks, all the fractures were united.

This delay in union was reflected by many, quite bizarre, changes earlier in fracture healing. In the

fractures in the B_6-deficient rats, up to 5 days post-fracture, although there was considerable proliferation and thickening of the periosteum, much of the tissue surrounding the fracture ends was acellular, except for sparse inflammatory cells and macrophages (Fig. IX.1).. There was extensive invasion of the periosteum into the old bone, all along the shaft, but predominantly at the metaphyseal end (Fig. IX.2). Occasionally, even as early as two days post-fracture, it was noted that what appeared to be thickened periosteum was, in fact, 'altered' old bone (as seen under crossed polars: Fig. IX.3), containing some undefinable cell-like material.

At all the times investigated, the metaphyseal trabeculae in the B_6-deficient group were strikingly narrowed (Fig. IX.4). Further from the metaphysis, this narrowing became accentuated so that the solid bone was converted into small, isolated fragments of what seemed to be trabeculae surrounded by bone marrow (Fig. IX.5). Since trabecular bone, in its normal sense, does not occur normally in rat metatarsals, this effect has never been seen previously in this laboratory.

Complex changes also occurred in the main shaft. In the B_6-deficient rats, and beginning predominantly but not exclusively close to the metaphyseal end, from 5 days onwards there was partial replacement of cortical bone by woven bone. This seemed to occur in areas which, earlier, had the appearance of 'altered' bone. This woven

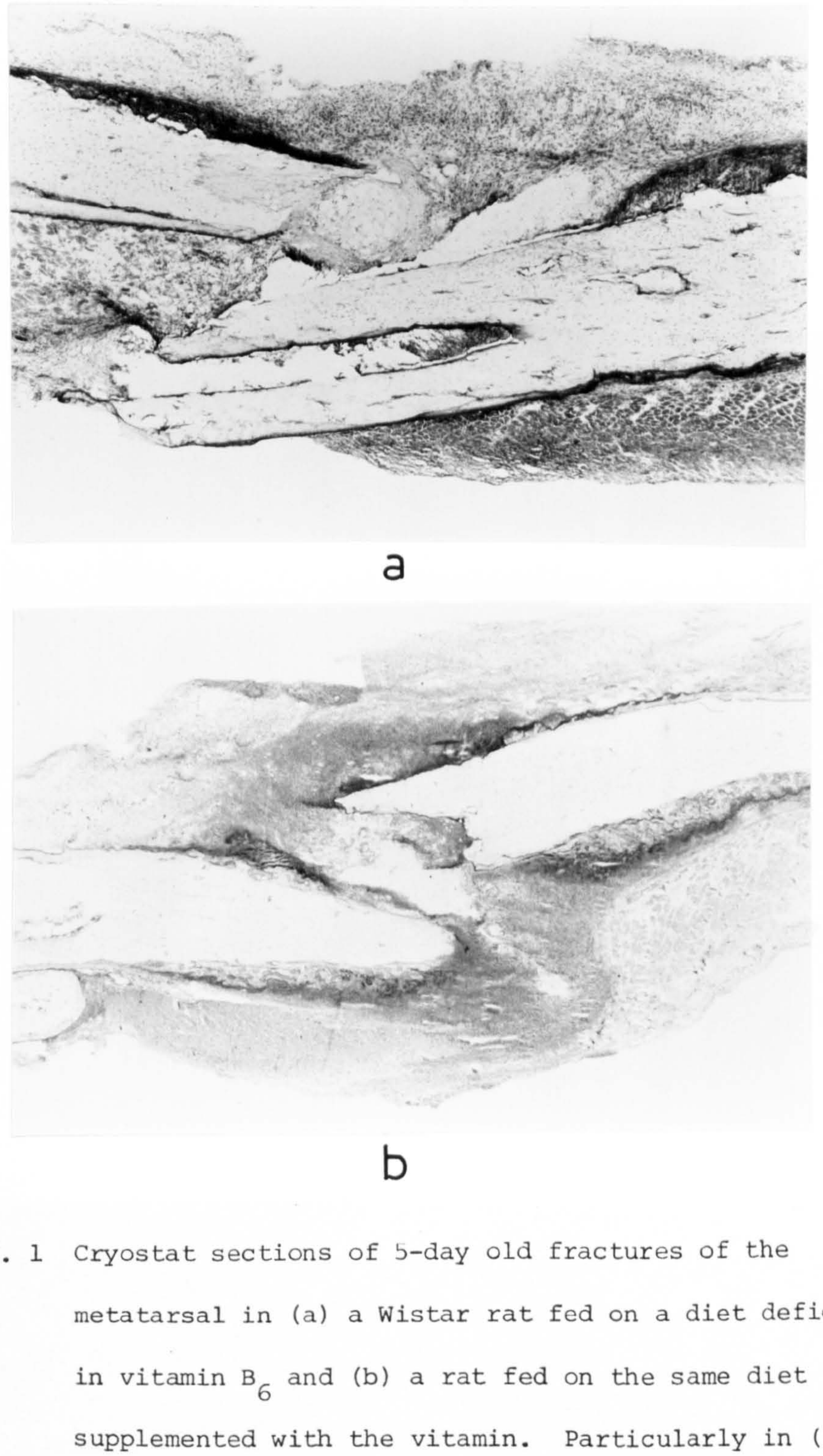

a

b

Fig. IX. 1 Cryostat sections of 5-day old fractures of the metatarsal in (a) a Wistar rat fed on a diet deficient in vitamin B_6 and (b) a rat fed on the same diet supplemented with the vitamin. Particularly in (a) the overlap at the fracture-site that occurs with this fracture in this strain of rat, is noticeable. Despite periosteal thickening, the soft callus surrounding the fracture ends is larger, more obviously cellular and more advanced in (b) than in the vitamin B_6 deficient animal (a).

Toluidine blue; (a) X 24; (b) X 15.

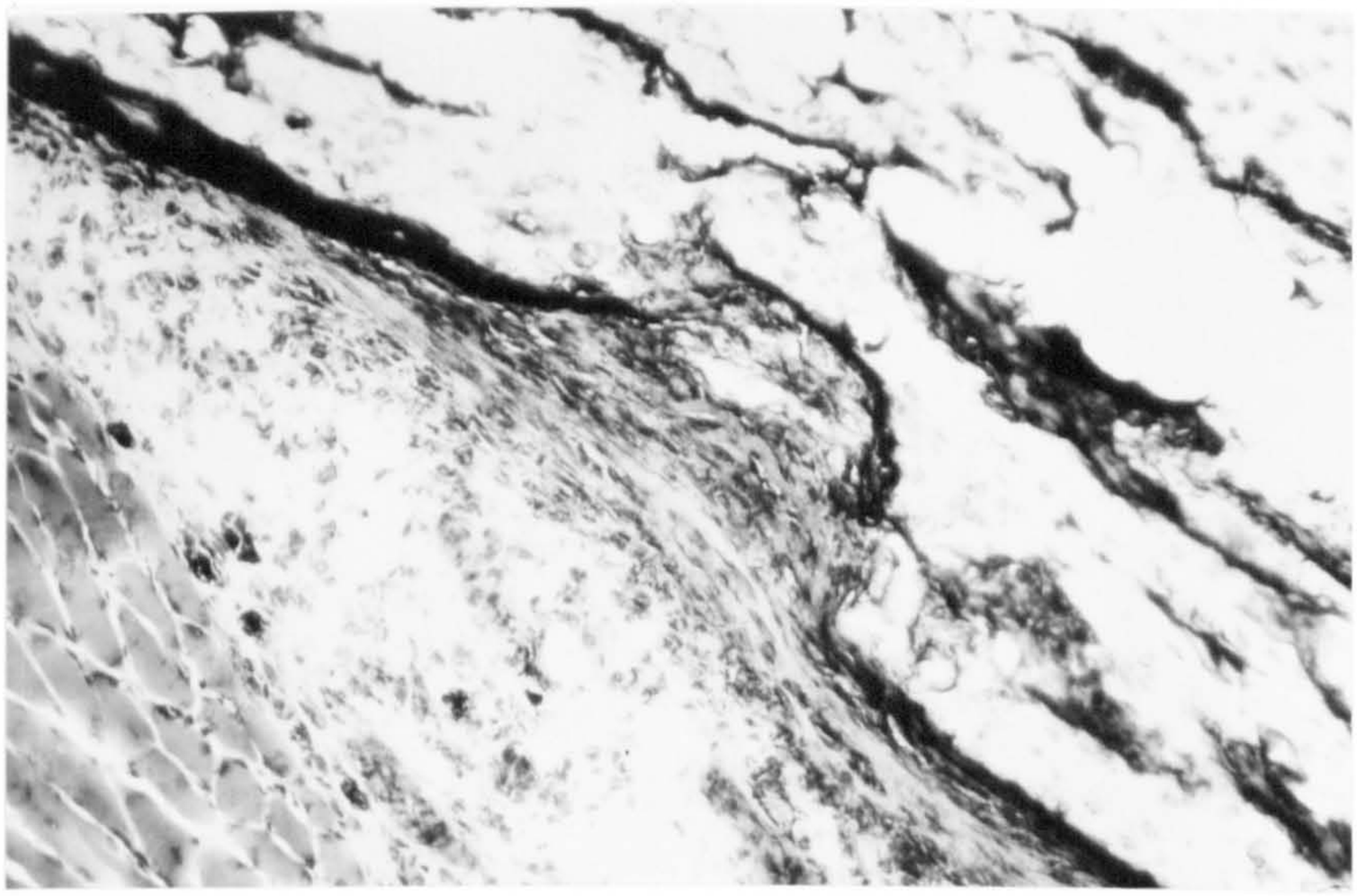

Fig. IX. 2 Cryostat section of metaphyseal end of a 5-day old fractured metatarsal in a vitamin B_6 deficient rat. There is invasion of the shaft of the bone by proliferating periosteum seen as an irregular edge to the shaft, particularly on the upper surface.

Toluidine blue; X38.

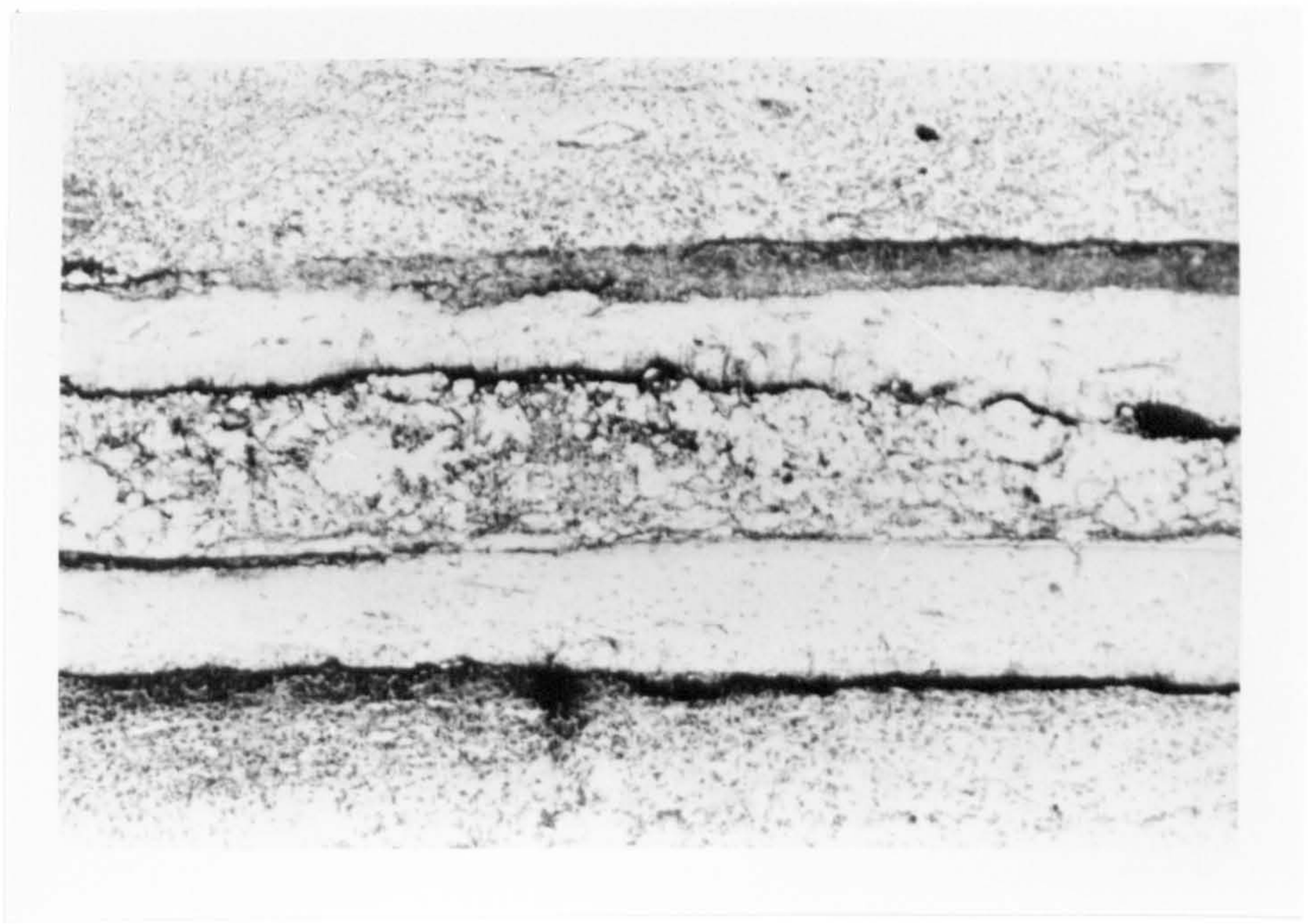

Fig. IX. 3 Cryostat section of the shaft close to the fracture of a 2 day old metatarsal fracture in a vitamin B_6 deficient rat. On the dorsal surface the shaft is invaded by what appears to be thickened periosteum. This material represents 'altered' bone.

Toluidine blue; X38

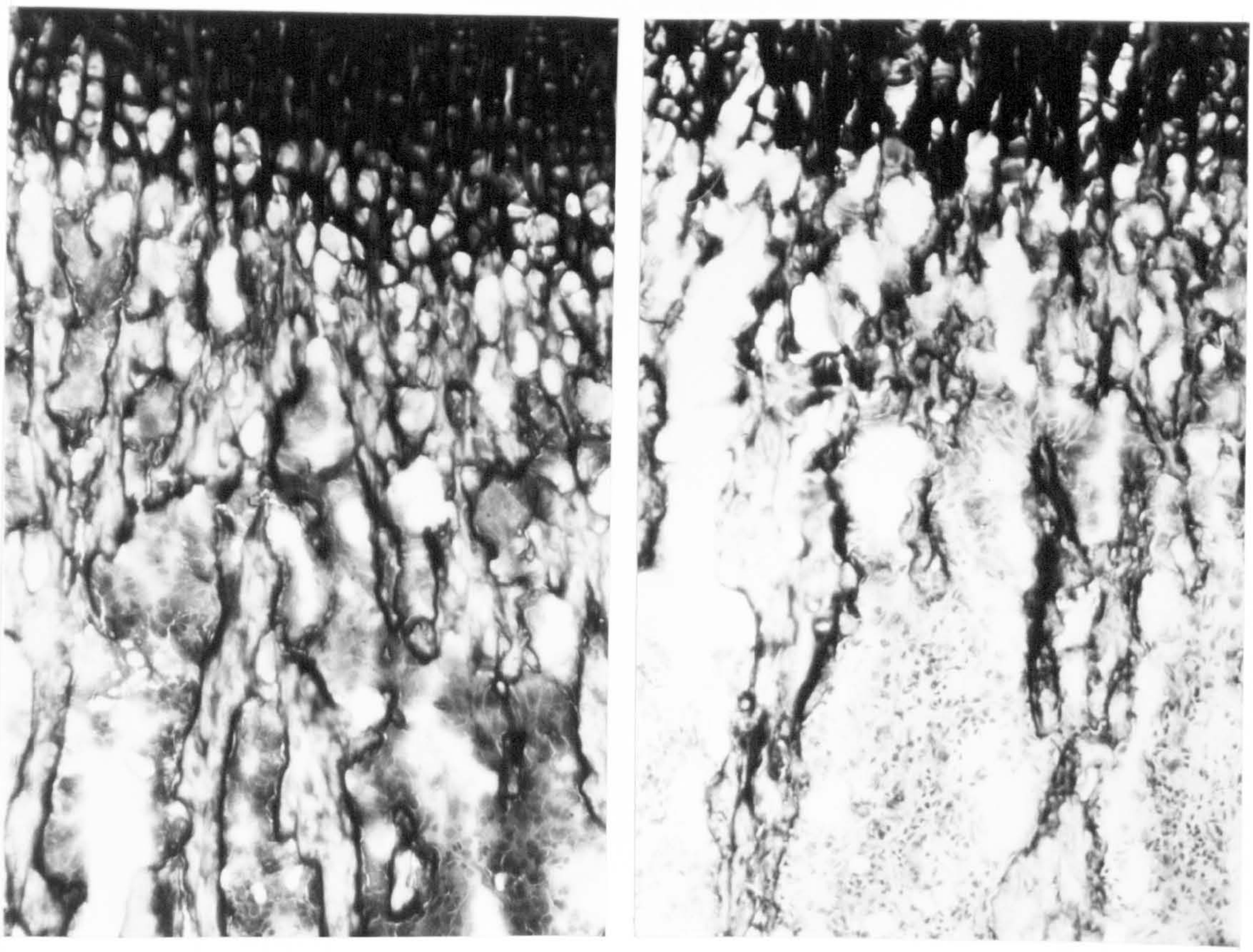

control b_6-deficient

Fig. IX. 4 Comparison of the metaphyseal end of the metatarsal from vitamin B_6 deficient rat and a rat fed on the supplemented diet. The bone trabeculae are narrowed and distorted in the B_6 deficient metaphysis.

Toluidine blue; X220.

Fig. IX. 5 In the metaphyseal end of the metatarsal shaft of a 5 day old fracture in a vitamin B_6 deficient rat, the bone is split up into small isolated fragments surrounded by bone marrow.

Toluidine blue: X 38

bone within the shaft apparently merged with the newly formed woven bone on the outside of the shaft as a normal consequence of fracture (Fig. IX.6). This gave an exaggerated impression of the content of new bone formation. There was also a striking increase in the size of the vascular spaces, many of which appeared to be lined with osteoid and some of which were lined by cells which, in some instances, resembled osteoclasts whereas in others they had the appearance of osteoblasts (Fig. IX.7).

At 8 - 12 days post-fracture, the shaft in the bone in the B_6-deficient rats was virtually replaced by large lacy spaces so that the bone was fragmented into small regions resembling trabecular bone (Fig. IX.8). The replacement occurred both from the periosteum and endosteum.

Analysis of 12-day Fracture

Attention has been concentrated on the 12 day callus in rats fed with the B_6-deficient diet, or with the same diet supplemented with vitamin B_6. The images of the fractures in eight control and nine B_6-deficient specimens were projected through a photographic enlarger to attempt to quantify the areas occupied by such components as could be measured.

The callus in the B_6-deficient rats often appeared to be flattened. Thus the mean ($\pm$ SD) width and length of the dorsal callus in 8 control rats was 2.0 cm $\pm$ 0.4 and 8.6 cm $\pm$ 1.1 respectively whereas that of 9 B_6-deficient rats was 1.3 cm $\pm$ 0.4 ($p < 0.001$) and 8.6 cm $\pm$ 0.8

Fig IX. 6 Cryostat section of the shaft of a 8 day old fracture in a vitamin B_6 deficient rat. The shaft is extensively replaced by woven bone which merges with the woven bone on the outer side of the shaft.

Toluidine blue; X 30.

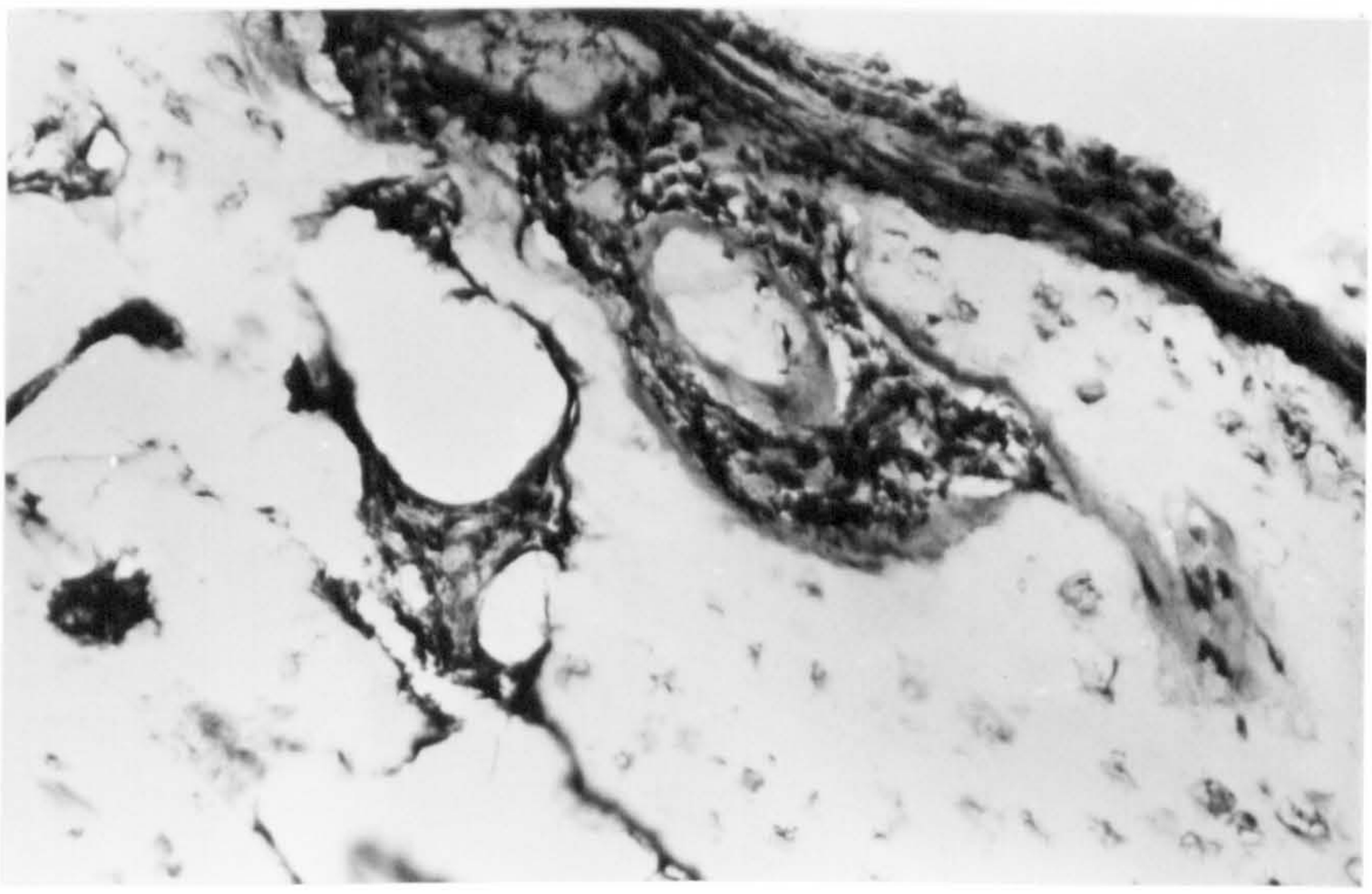

Fig. IX. 7 Cryostat section of the shaft of a 5 day old fracture in a vitamin B_6 deficient rat. The vascular spaces are enlarged and many are lined with osteoid; some are lined by flattened cells while in others the cells appear multinucleate.

Toluidine blue; X220.

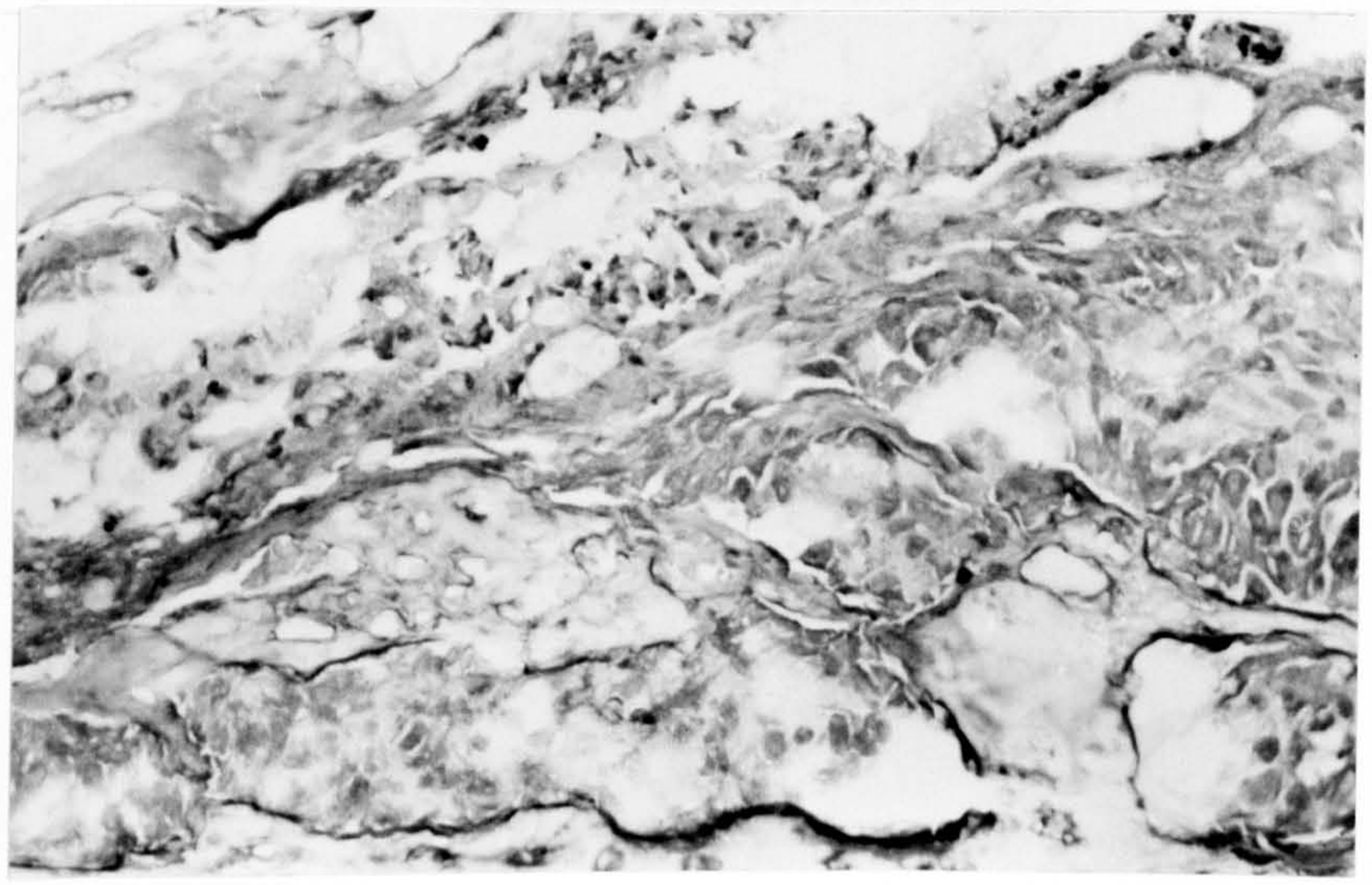

Fig. IX. 8 Cryostat section of the shaft of a 5 day old fracture in a vitamin B_6 deficient rat. The bone appears fragmented into small pieces surrounded by interlacing spaces. Toluidine blue; X 220.

respectively. The plantar callus showed the same pattern. The total width of the callus (including shaft) was 3.7 cm ± 0.6 in 8 control rats and 2.7 cm ± 0.5 in 9 B_6-deficient rats (Table IX.1). There were also diminished areas of calcifying cartilage (Fig. IX.9). In the controls, there were clearly defined areas of dense granulation tissue, cartilage and calcifying cartilage, very much as described in Chapter VII for both Sprague-Dawley and Wistar rats fed on a normal pellet diet. In contrast, the callus in the B_6-deficient rats still contained very undifferentiated cells and often had large areas which were largely acellular.

The width of the shaft, measured from the endosteum to the periosteum (inclusive) confirmed the impression that, in the B_6-deficient rats, the shaft was being eroded and replaced by woven bone. Thus the mean (± SD) thickness (as defined above) in 5 B_6-deficient animals (46 measurements) was 0.31 cm ± 0.9 whereas that of five control animals (44 measurements) was 0.37 cm ± 1.3 ($0.05 > p > 0.02$) (Table IX.1). As shown in Table IX.2 (also Fig. IX.10) the size of the total callus in the B_6-deficient rats was smaller than in the controls ($0.05 > p > 0.02$). Initial measurements showed that although there was less new bone ($p = 0.05$) formed in the B_6-deficient rats (Fig. IX.11) the proportion of callus occupied by new bone was the same (41%) in both groups. However, this apparent discrepancy is almost

Table IX. 1. Analysis of the 12 day Fracture.

Length of metotarsals (mm)

(mean ± SEM)

Control	B_6 - deficient
14.7 ± 0.11	14.6 ± 0.32

Length (L) and Maximum Width (W) of Callus (mm)

Control			B_6 - deficient		
Dorsal		Plantar	Dorsal		Plantar
8.6 ± 0.4	L	7.6 ± 0.59	8.6 ± 0.28	L	6.9 ± 0.5
and					
2 ± 0.15***	W	1.1 ± 0.38	1.3 ± 0.14	W	0.76 ± 0.06

Totol maximum width of collus (mm)

Control	B_6 - deficient
3.7 ± 0.2***	2.7 ± 0.17

***
p < 0.002

Controls: n = 8; B_6 - deficient : n = 9

All results : mean ± SEM

Thickness of shaft

Control	B_6 - deficient
(n = 46)	(n = 45)
0.37 ± 0.019*	0.31 ± 0.013

*p < 0.02

Table IX. 2. Measurements of the area of the callus and the area occupied by new bone in 12 day old fractures of the metatarsals from vitamin B_6 deficient and supplemented rats.

	n = 8 Control	n = 9 B_6- deficient
Total area of callus (mm^2 : mean ± SEM)	21 ± 2.2*	1 5 ± 1.67
Area of New Bone (mm^2 : mean ± SEM)	8.6 ± 1.09**	6.2 ± 0.6

* $p < 0.05$

** $p < 0.02$

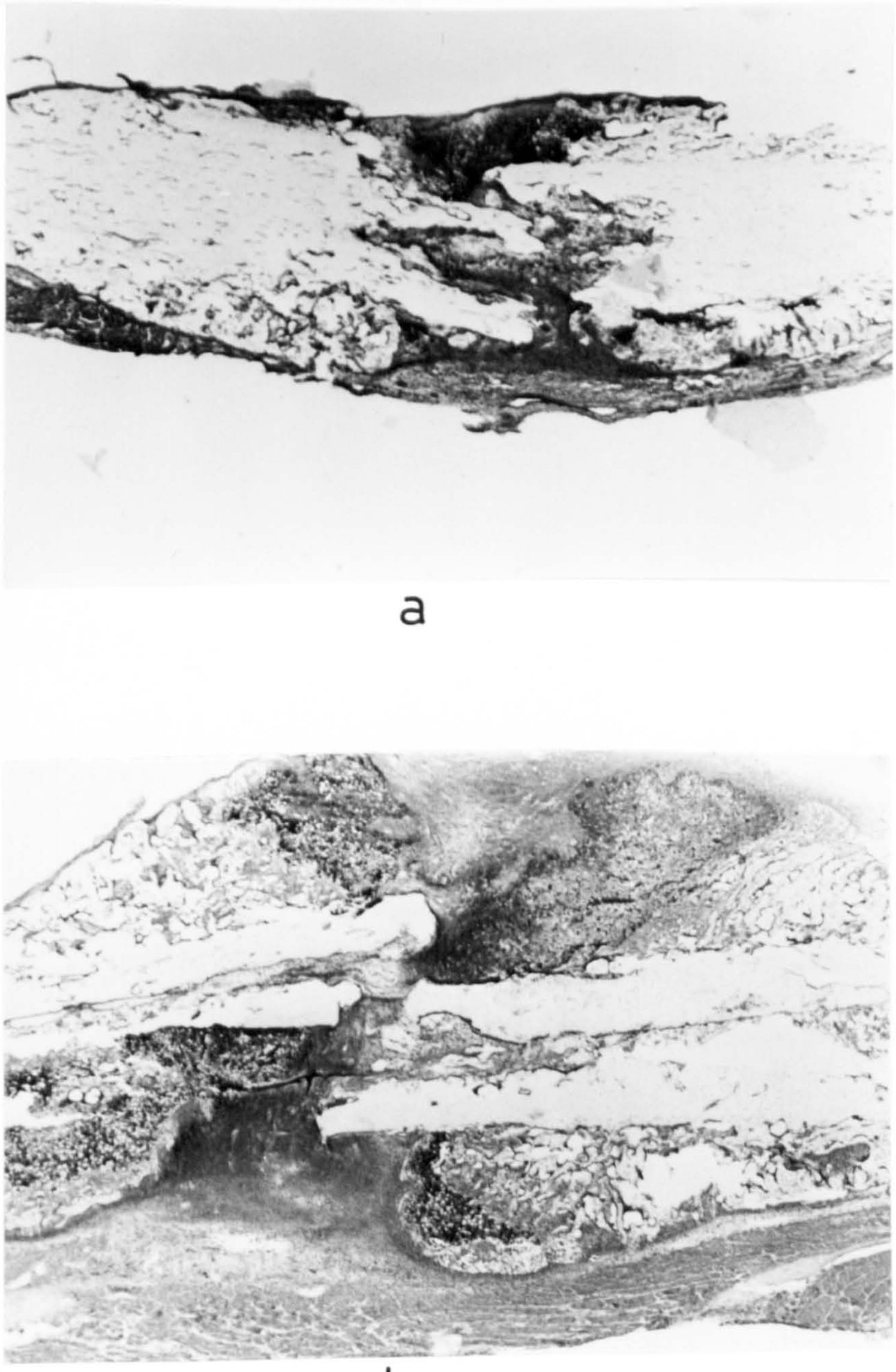

a

b

Fig. IX. 9 Cryostat sections through the mid-shaft of the fractured metatarsal, 12 days post-fracture in (a) a rat deficient in vitamin B_6 and (b) a rat supplemented with the vitamin. The callus in the vitamin B_6 deficient animal is flattened and less well differentiated; the area of calcifying cartilage is diminished.

Toluidine blue, X 20.

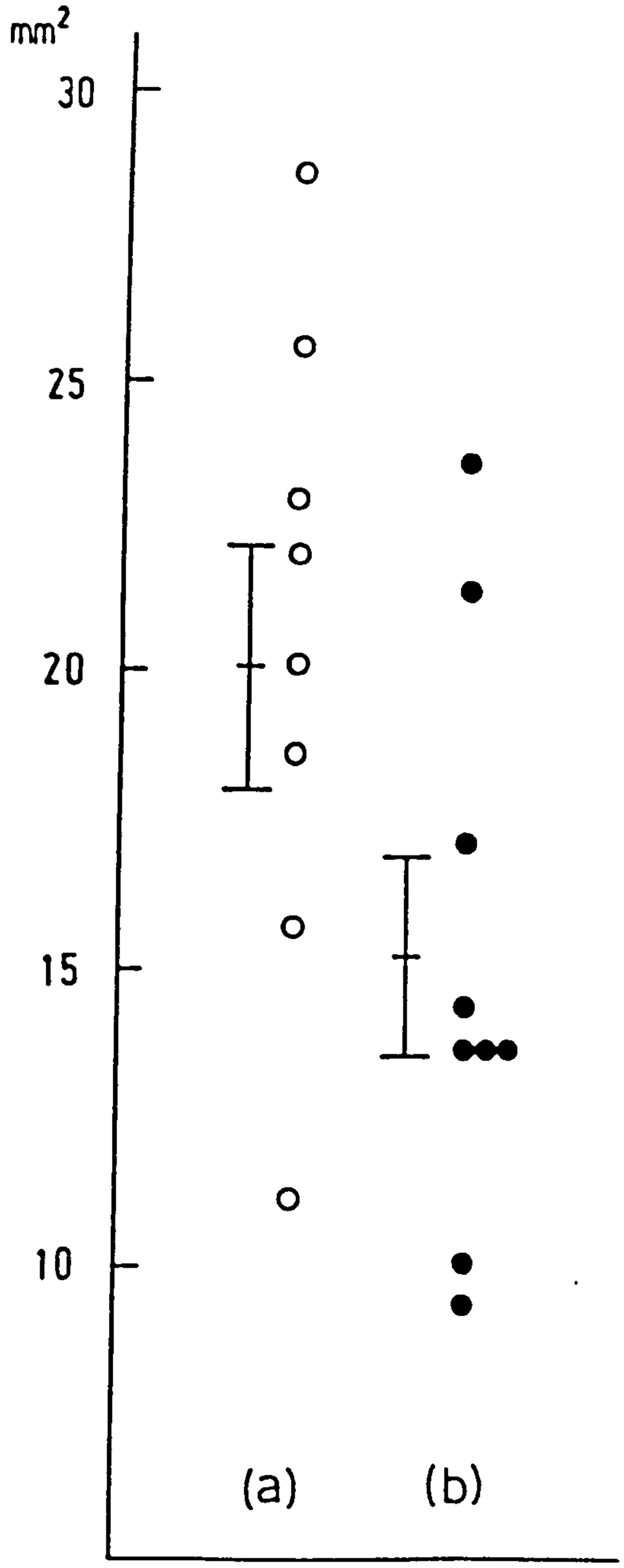

Fig. IX. 10 Scattergram of the total area (mm^2) of the callus in sections through the mid-line of the shaft of 12-day fractured metatarsals (a) in 8 control rats fed with a supplemented diet and (b) in 9 vitamin B_6 deficient rats.

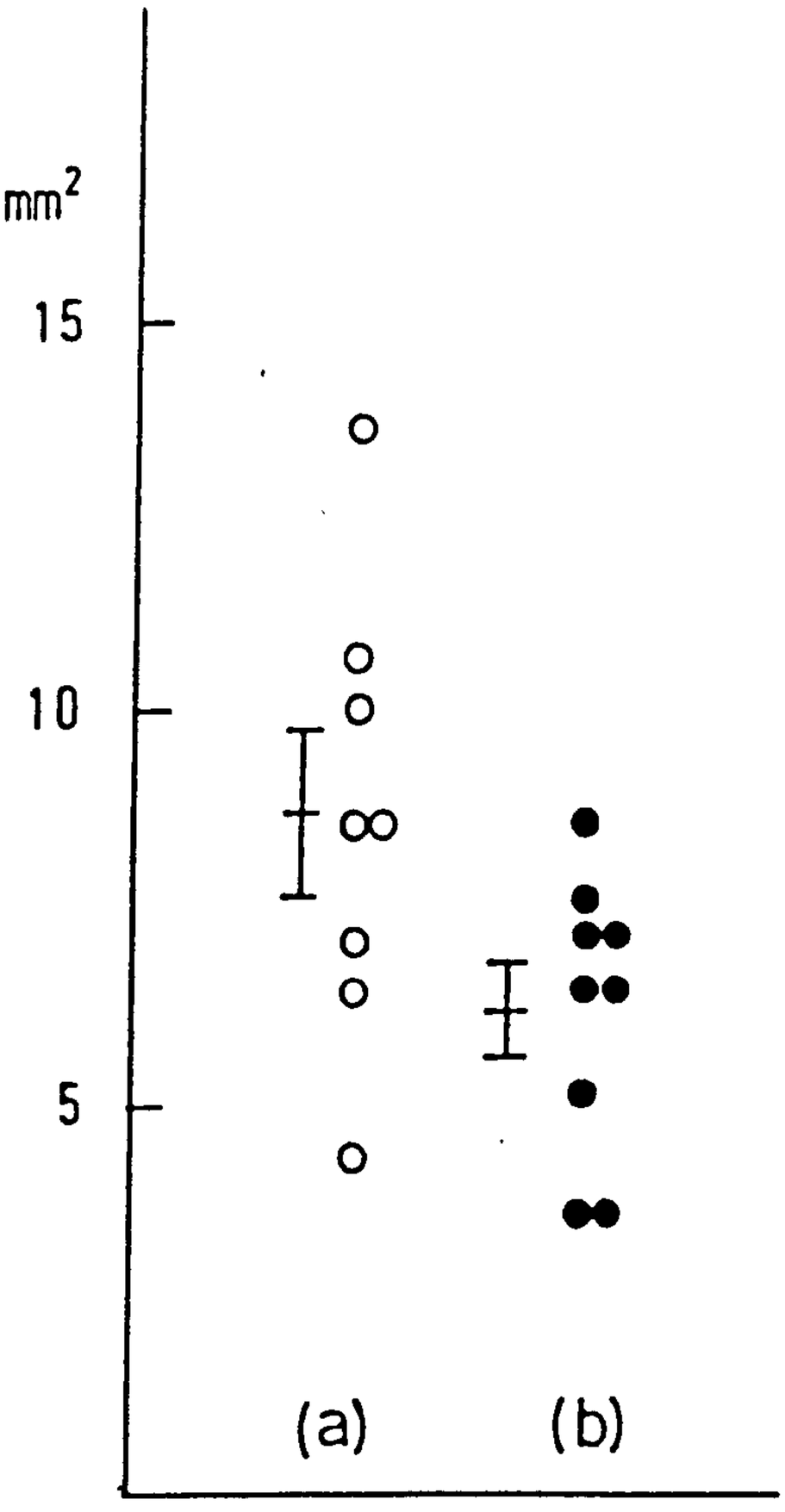

Fig. IX. 11 Scattergram of the area of the fracture callus occupied by new bone in 12-day fractured metatarsals (a) in 8 control rats fed with a supplemented diet and (b) in 9 vitamin B_6 deficient rats.

certainly due to over-estimating the area occupied by new bone in the B_6-deficient rats by including some of the remodelled old shaft within this estimate, and within the estimate of the size of the callus.

Cytochemical Results

Glucose 6-phosphate Dehydrogenase Activity in the Periosteum. The activity was measured in individual periosteal cells at set distances (0.2 mm) from the fracture site up to 2.6 mm from the fracture site, 3 and 5 days post-fracture. G6PD activity was negligible in periosteal cells from unfractured metatarsals.

No obvious differences were observed between 3 control rats, and 2 B_6-deficient rats, 3 days post-fracture (Fig. IX.12). However larger numbers of rats will have to be examined. There was considerable activity close to the fracture site, values ranging from 14 to 20 units of mean extinction in both groups up to 0.4 mm away from the fracture site. In two control rats there was a peak of G6PD activity 1 mm away from the fracture site; in the two B_6-deficient specimens and in one control the periosteal activity declined in the region after 0.4 mm.

In the periosteum of the fractured bones from 3 control and 5 B_6-deficient rats taken 5 days after fracture, there was no difference in activity between the two groups close to the fracture-site, values reaching as high as

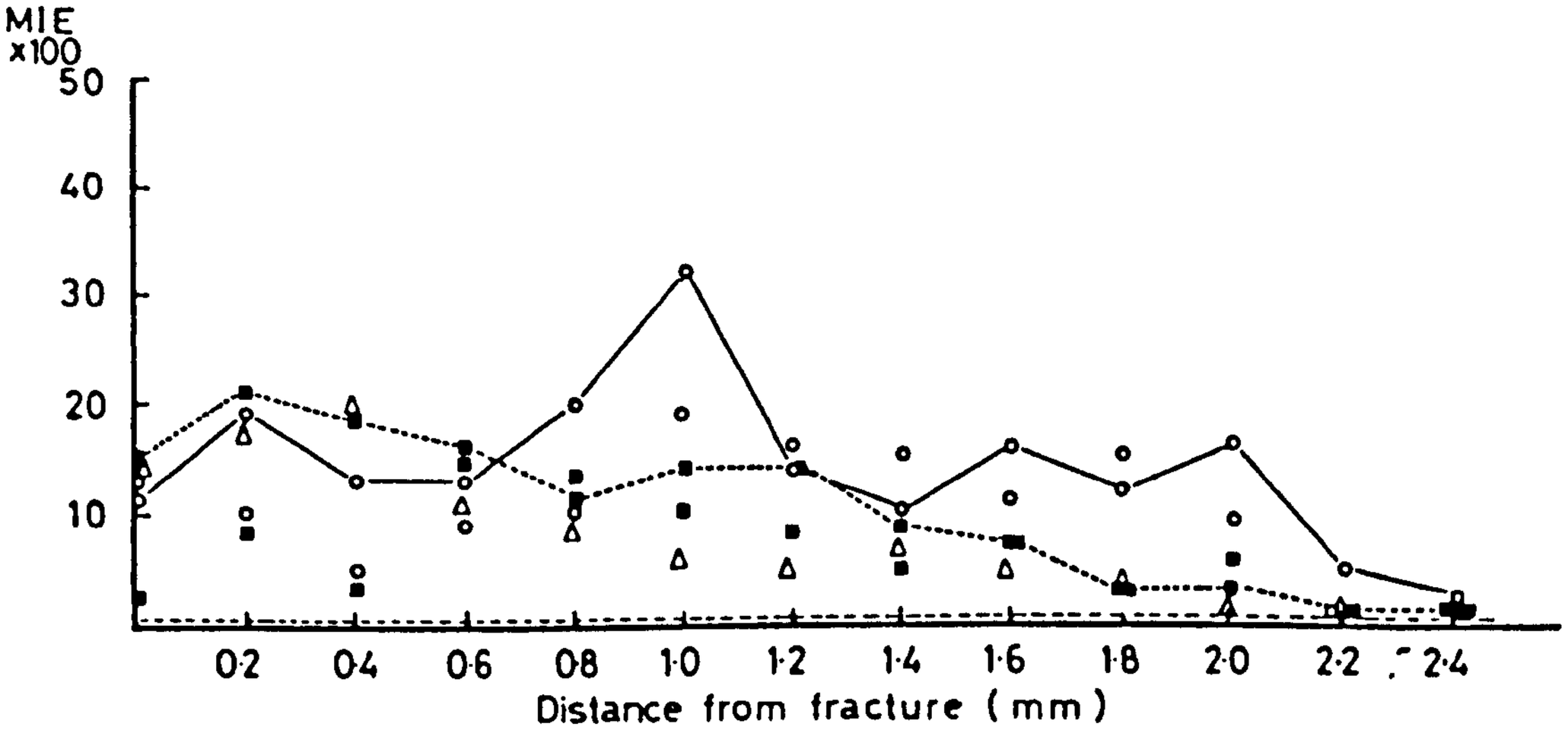

Fig. IX. 12 Glucose 6-phosphate dehydrogenase activity (MIE x 100) in the periosteal cells of 3 day-old fractures. Each symbol represents a different rat; open symbols: control rats fed with the supplemented diet; closed symbols: vitamin B_6 deficient rats. The dotted line close to the x-axis represents this activity in the periosteum in unfractured bone.

40 units of mean extinction in both groups. In contrast, whereas there was a large second peak of G6PD activity in the control rats, 1.4 to 1.6 mm away from the fracture site, (as fully described by Dunham et al, 1977, and in the Introduction to the present Chapter), the activity declined over this region of the periosteum in the B_6-deficient rats (Fig. IX.13). The peaks of activity ranged from 56 to 80 units of mean extinction in the control rats, and between 15 and 37 units of mean extinction in the B_6-deficient rats.

Alkaline Phosphatase Activity in the Periosteum.

In 3 control rats, and 2 B_6-deficient rats, 3 days after fracture, there was low Alk Phos activity up to 0.6 mm from the fracture site (Fig. IX.14). The activity thereafter became more elevated in both groups. In the control rats this activity exceeded those values found uniformly in the periosteum of intact metatarsal bones of this strain of rat (29 ± 3.8; mean ± SEM; n=3). This increase in Alk Phos was much less marked in the B_6-deficient rats: mean value of 29 units of mean extinction compared to a mean value of 38 units of mean extinction in the control rats. However as stated previously, a larger number of rats will be required to establish this finding.

The same general pattern was found 5 days post-fracture in 3 control rats and 5 B_6-deficient rats (Fig. IX.15). However there was no difference in activity

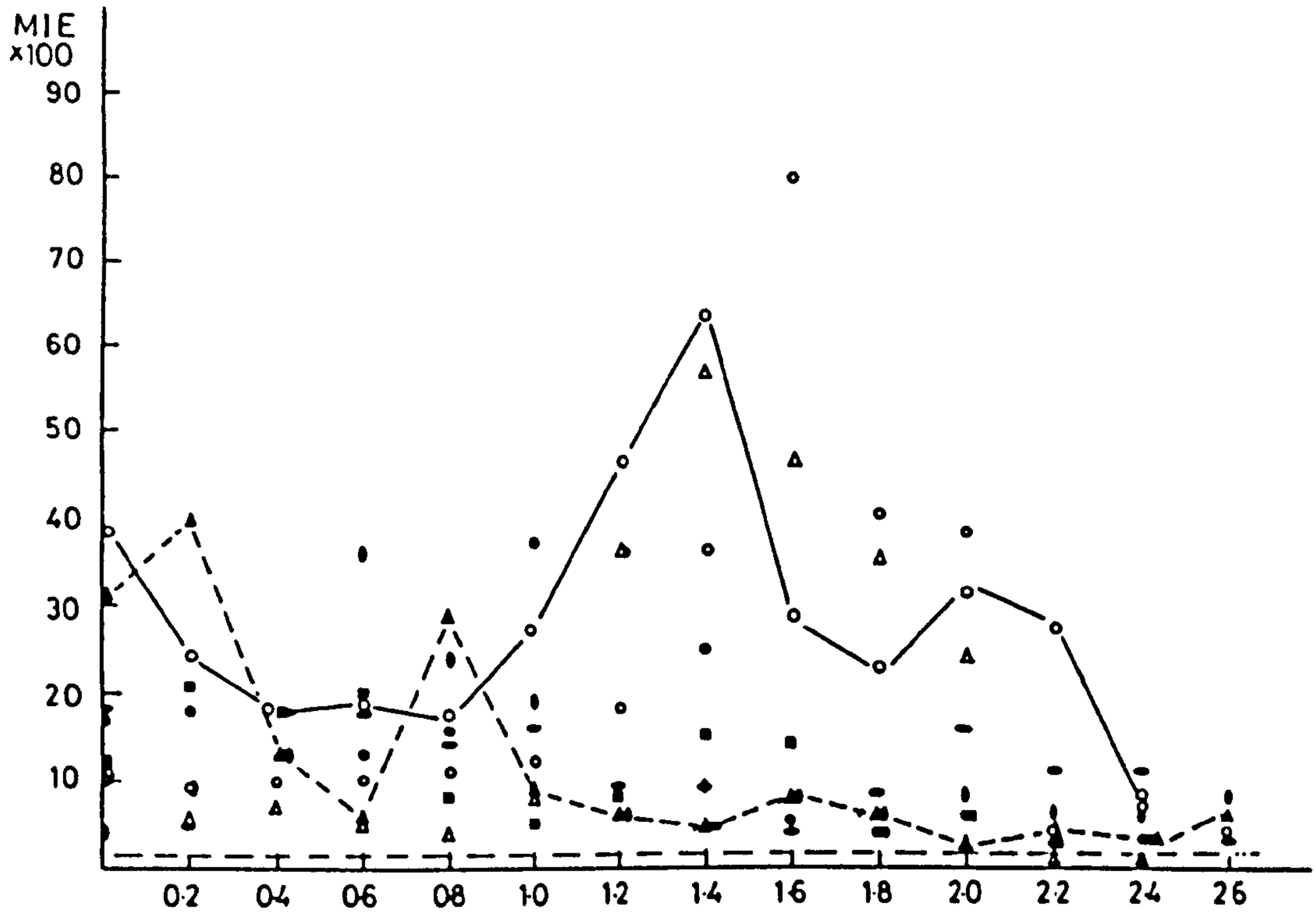

Fig. IX. 13 Glucose 6-phosphate dehydrogenase activiey (MIE x 100) in the periosteal cells of 5 day-old fractures. Each symbol represents measurements made in a different rat; open symbols: control rats fed with the supplemented diet; closed symbols: vitamin B_6 deficient rats. The high activity, in the periosteum about 1.5mm distal to the fracture, that is evident in the control rats, is not present in the 5 vitamin B_6 deficient rats. The dotted line just above the x-axis represents the activity in the periosteum of normal bone.

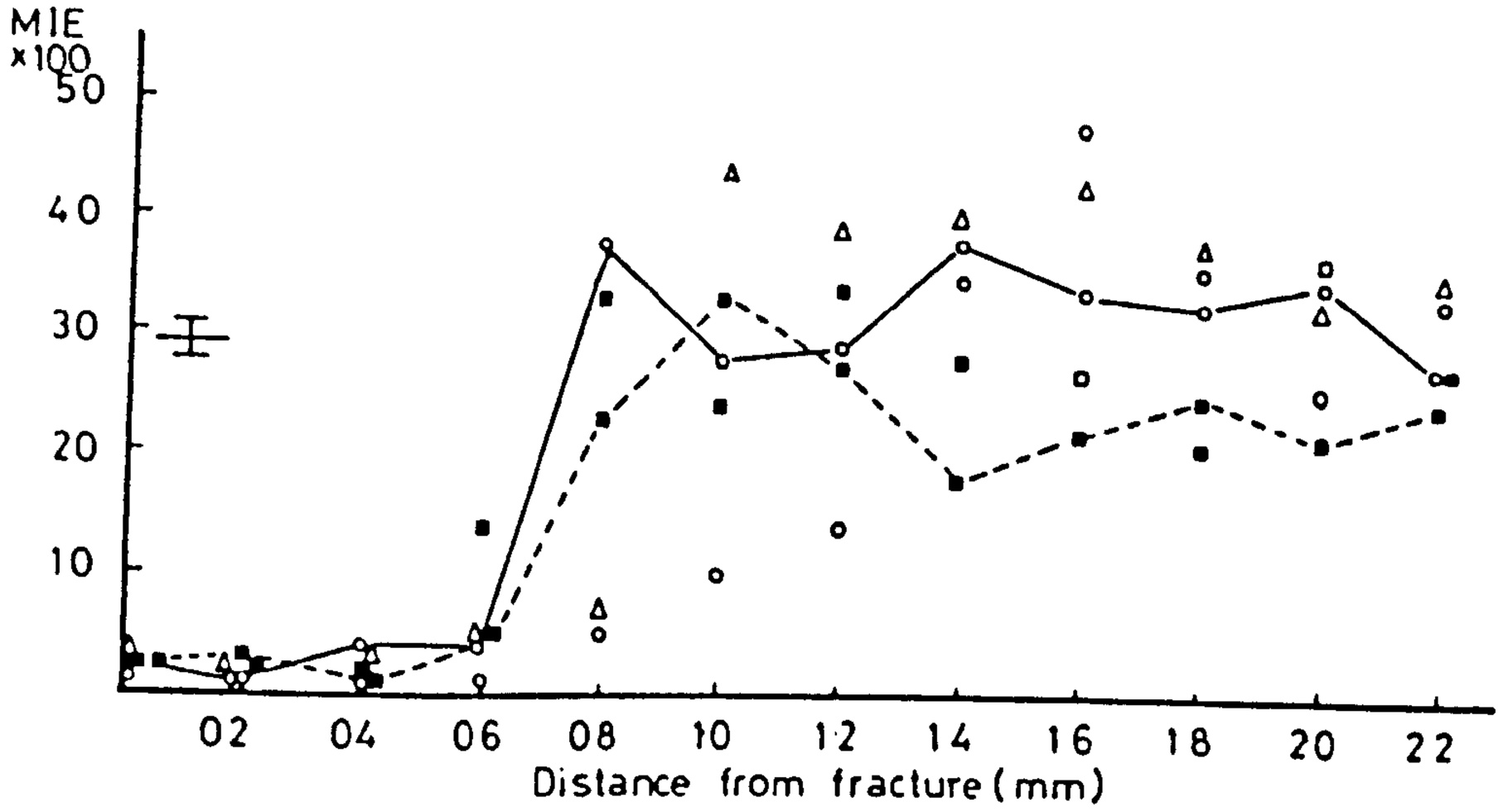

Fig. IX. 14 Alkaline phosphatase activity (MIE x 100) in the periosteal cells in 3 day old fractures of three control rats (open symbols) and two vitamin B_6 deficient rats (closed symbols). The bars near the y-axis represent the mean (± SEM) activity in the periosteum from unfractured metatarsal.

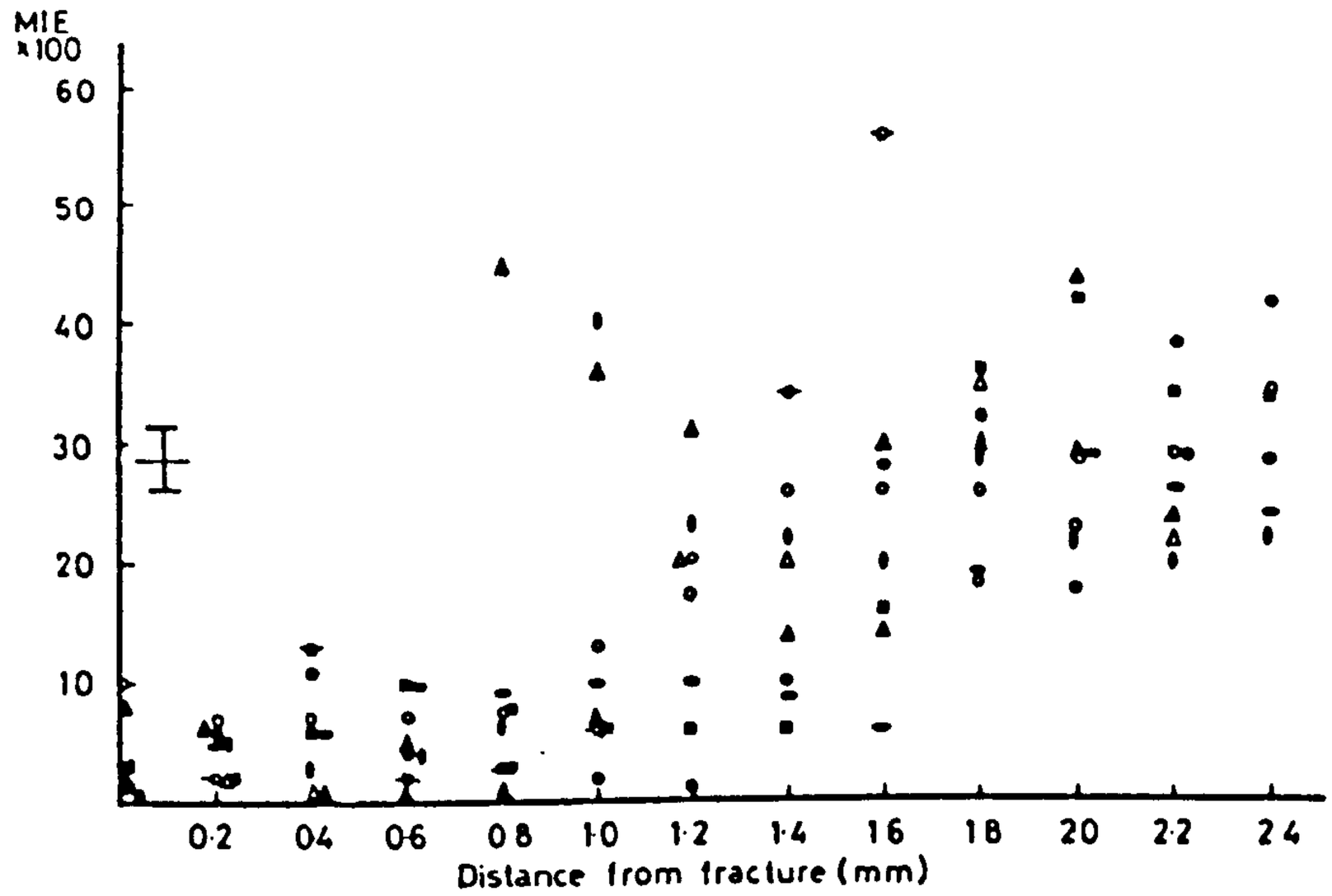

Fig. IX. 15 Alkaline phosphatase activity (MIE x 100) in the periosteal cells in 5-day old fractures in 3 control rats fed with the supplemented diet (open symbols) and 5 vitamin B_6 deficient rats (closed symbols). The bars near the y-axis represent the mean (± SEM) activity of the periosteum in unfractured metatarsals.

after 0.6 mm and onwards in these rats (mean value of 28 units of mean extinction in the control rats and 30 units of mean extinction in the B_6-deficient rats).

HOAD Activity in the Periosteum. HOAD activity was measured in the periosteum from the fractures of 3 control rats and of 2 B_6-deficient rats 3 days after fracture, and in 3 control and 5 B_6-deficient rats 5 days after fracture. In both cases there was no difference in activity as a consequence of B_6-deficiency (Fig. IX.16, 17).

Enzymatic Activity in the Cells of the Callus

Metabolic studies on the cells of the callus were done on material of the 12 day post-fracture. As explained in Chapters VI and VIII the different cell-types are easily defined in this mature callus. The enzyme activities were measured in 5 specified cell-types of the callus from 8 control and 9 B_6-deficient rats: mature chondrocytes; chondrocytes in calcified cartilage; cellular granulation tissue; loose granulation tissue; and osteoblasts (as described in Chapter VII). The results for all the enzyme activities are shown in Table IX.3. In all cell-types, except the chondrocytes in the calcified cartilage, G6PD activity was significantly decreased in the B_6-deficient rats. Either no, or relatively small differences were found in the activities of LDH, GAPD, HOAD, SDH or Alk Phos activities, in any of these cell-types 12 days after fracture. It was of interest to note that, whereas G6PD activity was 33%

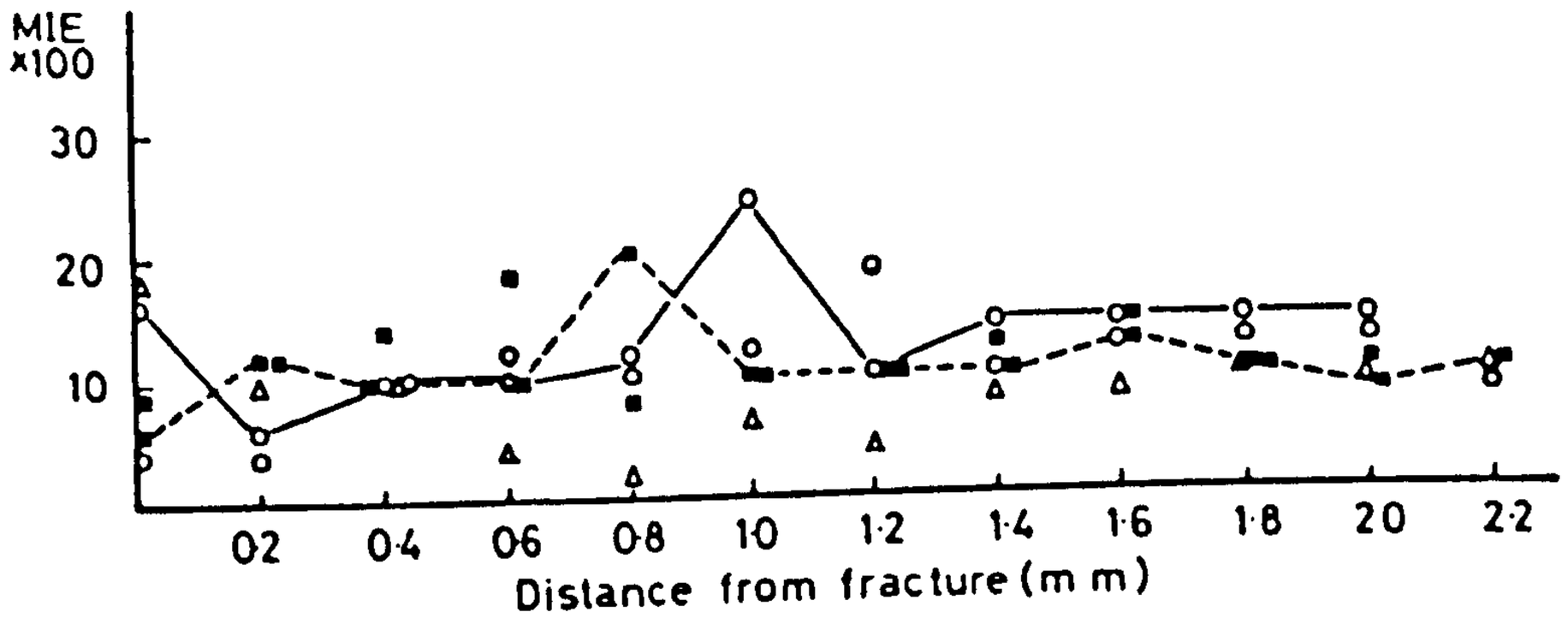

Fig. IX. 16 Hydroxyacyl dehydrogenase activity (MIE x 100) in the periosteum of 3 day old fractures in 2 vitamin B_6 deficient rats (closed symbols) and 3 control rats fed with the supplemented diet.

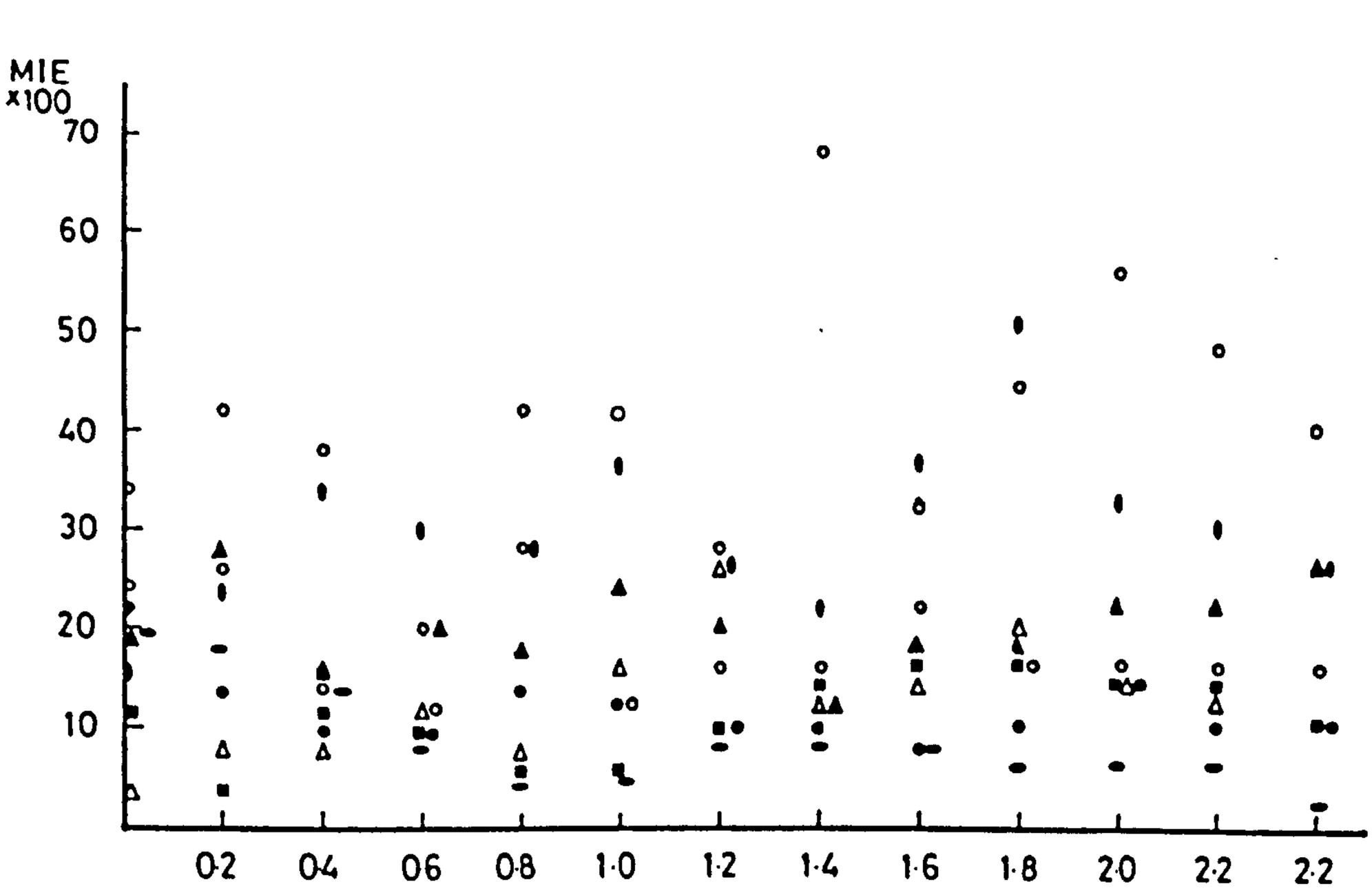

Fig. IX. 17 Hydroxyacyl dehydrogenase activity (MIE x 100) in the periosteum of 5-day old fractures in 5 vitamin B_6 deficient rats (closed symbols) and 3 control rats fed with the supplemented diet (open symbols).

Table IX. 3 The activity (mean integrated extinction x 100) of various enzymes in different cell types in the callus of 12 day old fractures of the metatarsals from vitamin B_6 deficient (b_6d) and supplemented (c) rats. (Values corrected to 20 min incubation; mean ± SEM).

ENZYME ACTIVITIES IN VARIOUS CELL TYPES OF
12 - day fracture callus

Enzyme	Osteoblasts	Chondrocytes		Granulation tissue	
		Mature	Calcifying	Loose	Cellular
G6PD[1] c	45 ± 2.8***	56 ± 3.2***	14 ± 1	22 ± 2**	80 ± 6.6***
b_6d	31 ± 2.6	27 ± 2.5	11 ± 0.7	15 ± 1.4	47 ± 3.5
LDH[1] c	50 ± 3.2	106 ± 3.2***	32 ± 1.6	32 ± 2.2	69 ± 6.6
b_6d	47 ± 1.96	71 ± 3.6	25 ± 1.4	30 ± 1.4	53 ± 3.4
GAPD[1] c	11 ± 2	22 ± 1.8	6 ± 0.5	3 ± 0.8	39 ± 10
b_6d	10 ± 1	22 ± 2.0	7 ± 0.3	9 ± 0.3	34 ± 6
HGAD[1] c	14 ± 0.5	10 ± 0.75	5 ± 0.39	5 ± 0.5	9 ± 1.4
b_6d	15 ± 0.8	11 ± 1.1	4 ± 0.19	5 ± 0.39	9 ± 1.2
SDH[2] c	22 ± 1.0	~0	~0	5 ± 0.25	10 ± 0.5
b_6d	22 ± 2.2	~0	~0	6 ± 0.8	14 ± 1.2
Alk.Phos.[1] c	166 ± 25.5	173 ± 10.5	68 ± 9.5	24 ± 4	99 ± 4.5
b_6d	189 ± 14	169 ± 11	73 ± 8.5	33 ± 4	98 ± 6.5

1. Control n = 8; B_6 def n = 9
2. Control n = 4; B_6 def n = 5

* $p < 0.02$

** $p < 0.01$

*** $p < 0.001$

lower in the osteoblasts and 52% lower in the mature chondrocytes, it was less decreased in the loose granulation tissue (30% decrease), and in the cellular granulation tissue (39% decrease).

Discussion

As has been shown in this thesis (Chapters VI, VII) and in previous studies (Dunham et al, 1977), one of the remarkable biochemical responses to fracture is the striking elevation of periosteal G6PD activity. It was suggested that this activity plays a major role both in the periosteal proliferation to form the callus and in the process of new bone formation. This increase in G6PD activity is therefore so fundamental to the process of fracture healing that it seemed important to try to define the mechanism by which it is brought about. One possibility was that it is stimulated by the formation of putrescine from ornithine decarboxylase (ODC) activity. This activity is readily stimulated by many hormones acting on their target cells (Bachrach, 1980) and it was not inconceivable that the trauma of fracture might act similarly. ODC activity depends on pyridoxal phosphate (vitamin B_6), and it has been shown (Eloranta et al, 1976; Pegg, 1976) that young rats can be made deficient in polyamines if fed on a particular diet. Consequently it seemed possible to test whether the stimulation of G6PD, in fracture-healing, could be modified by depleting the rats of

vitamin B_6.

The results of these studies were in conformity with the view that ODC activity might regulate G6PD activity. Thus of all the enzymes tested only G6PD activity was markedly decreased in the B_6-deficient callus (Table IX.3). For example, the HOAD activity was totally unaffected. It was of interest that the decreased G6PD activity was most marked in bone-forming regions of the periosteum (Figs. IX.12, 13) and in the osteoblasts and mature chondrocytes of the callus (Table IX.3). Thus although there was significant decrease in G6PD activity available for proliferation, there was even less available for the formation of new bone.

Thus although it is appreciated that deficiency of vitamin B_6 can influence many enzymes, these results support the suggestion that this deficiency would be reflected in decreased G6PD activity.

The decreased G6PD activity, for proliferation and for bone-formation, was also reflected in the histological changes found in the B_6-deficient fractures. These included a flattened callus of diminished width and a decrease in the area occupied by new bone. What was totally unexpected were the bizarre histological changes found in the shaft of the bone and which, as discussed above, led to an under-estimate of the size of callus and extent of new bone. These changes were remarkably similar to the appearance found in human osteoporosis.

This requires much more investigation: if they are fully substantiated they would indicate that here we may have a much needed animal model of osteoporosis. The results suggest that the deficiency of vitamin B_6 may have lead to an uncoupling of the normal turnover of bone, with decreased anabolic activity (possibly related to G6PD activity). However, this is for the future.

CHAPTER X

CHANGES IN CRYSTAL SIZE AND ORIENTATION OF GLYCOSAMINOGLYCANS AT THE FRACTURE SITE IN FRACTURED NECKS OF FEMUR.

Introduction

The aim of this study was to try to elucidate the increased susceptibility of the neck of femur to fracture. The incidence of this condition rises exponentially after the age of 50 years (Knowelden et al, 1964) and the fractures are usually the result of only relatively minor trauma. An estimated 40,000 such fractures occur in the United Kingdom each year (Lewis, 1981) and represent, therefore, a significant social and medical problem in terms of treatment and rehabilitation (Lewinnek et al, 1980). The rate of fracture of the femur rises with age, generally more steeply in women than in men(Alffram, 1964; Knowelden et al, 1964 Fig. X.1).

It is apparent from the reported studies on the aetiology of fractures of the femoral neck that there is no single cause of the fracture but rather it is associated with a combination of factors such as age, sex, nature and type of fall, and changes in bone fragility (Elsasser et al, 1980; Cook et al, 1982).

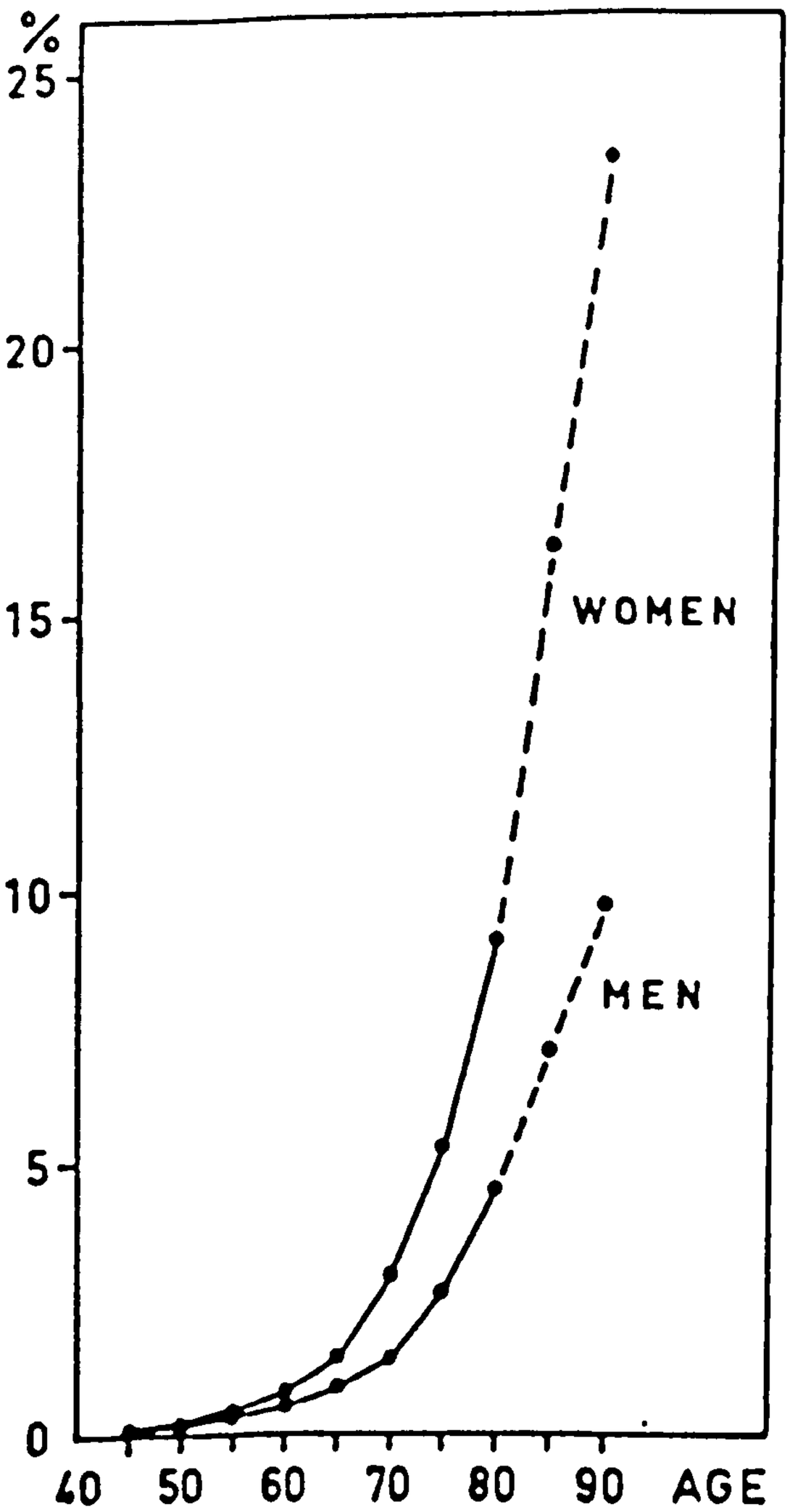

Fig. X. 1 Cumulative incidence of fracture of the neck of femur with age.

(from Alffram, 1964)

The structural changes that occur in the femoral neck prior to fracture are not understood. They may be a result of several sequential or concurrent changes such as osteoporosis or osteomalacia, or in the tensile strength of the bone matrix (Wall et al, 1979; Cook et al, 1982). Cook et al (1982) found that osteoporosis is of major importance in the aetiology of fractured neck of femur. However there was a trend towards an inverse relationship between osteoporosis and osteomalacia in that patients who suffer these fractures and who do not have osteoporosis seem more likely to have osteomalacia. Wall et al (1979) showed that both the density and the intrinsic strength of bone increase up to about the fourth decade of life and then decrease with age. However the decrease in tensile strength of bone with age progresses at a greater rate than the decrease in bone density. This fact indicated that a change in structure of the bone or in the interaction between the organic matrix and the mineral phase could explain the increased liability of the femoral neck to fracture. Changes in the mechanical properties of machined pieces of the femoral shaft, from such fractures, compared with similar pieces prepared from normal subjects, have been found (Dickenson et al, 1981). The bone specimens tested under tension from patients who had femoral neck fractures had less stiffness and strength compared with normal bone and these changes were correlated with the degree of osteoporosis.

These bones also had considerably reduced energy absorption before failure and this was not related to changes in mineral content of the bone or to the degree of osteoporosis. Thus this bone has a much greater tendency to fracture during the sudden stress of a fall when the work done on the bone is too great to be elastically absorbed.

The three-dimensional structure of bone, especially the morphology of bone mineral, has been studied with techniques such as polarised light microscopy (von Ebner, 1894; von Schmidt, 1938), x-ray diffraction (Carlstrom, 1955; Engström, 1972; Chatterji et al, 1981), electron-microscopy (Robinson, 1952; Bernard, 1969; Bocciarelli, 1970; Voegel and Frank, 1977) and scanning electron microscopy (Jackson et al, 1978). There is some disagreement as to the shape of the apatite crystals (needle-like or plate-like crystals) and of the orientation of the crystallite c-axis with regard to the long axis of the collagen fibre (parallel or perpendicular). There is however good agreement that the apatite crystals must be small in size (50 nanometres or less in the long axis). Chatterji et al (1981), using x-ray diffraction techniques, measured the orientation and size of crystals in human femoral cortical bone taken from subjects within the ages of 13 to 97 years. After the age of 60, there was a marked change in the distribution of crystallites so that older bones had a greater proportion of large crystallites (over 600 nm).

They showed that ultimate tensile strength and mineral particle size correlated closely with respect to age. They discussed the fundamental basis for this correlation: The bond between apatite and collagen matrix is strong (Swanson, 1971 as cited by Chatterji et al, 1981), so that with a decreasing percentage of small particles, the specific surface area available for bonding decreases and so decreases the tensile strength of bone. This would occur irrespective of bone density.

In the present study, quantitative polarised light microscopy has been used to identify changes in the microstructure of some of the components of bone at the site of fracture that could explain the increased fragility of the bone in these patients.

Materials and Methods

The femoral heads were obtained from Northwick Park Hospital over an eleven month period, from patients undergoing total hip replacement for severe osteoarthritis or Thompson replacement for subcapital femoral neck fractures; others were obtained at necropsy from patients whose death was not related to any bone disease.

Small blocks of trabecular bone (about 2 x 1 x 3 cm) were sawn from the femoral head to include the fracture site or from an equivalent position at the epiphysial region of the osteoarthritic and cadaveric bones (Fig.X.2). Pieces of bone were also collected at operation from three patients who had suffered traumatic

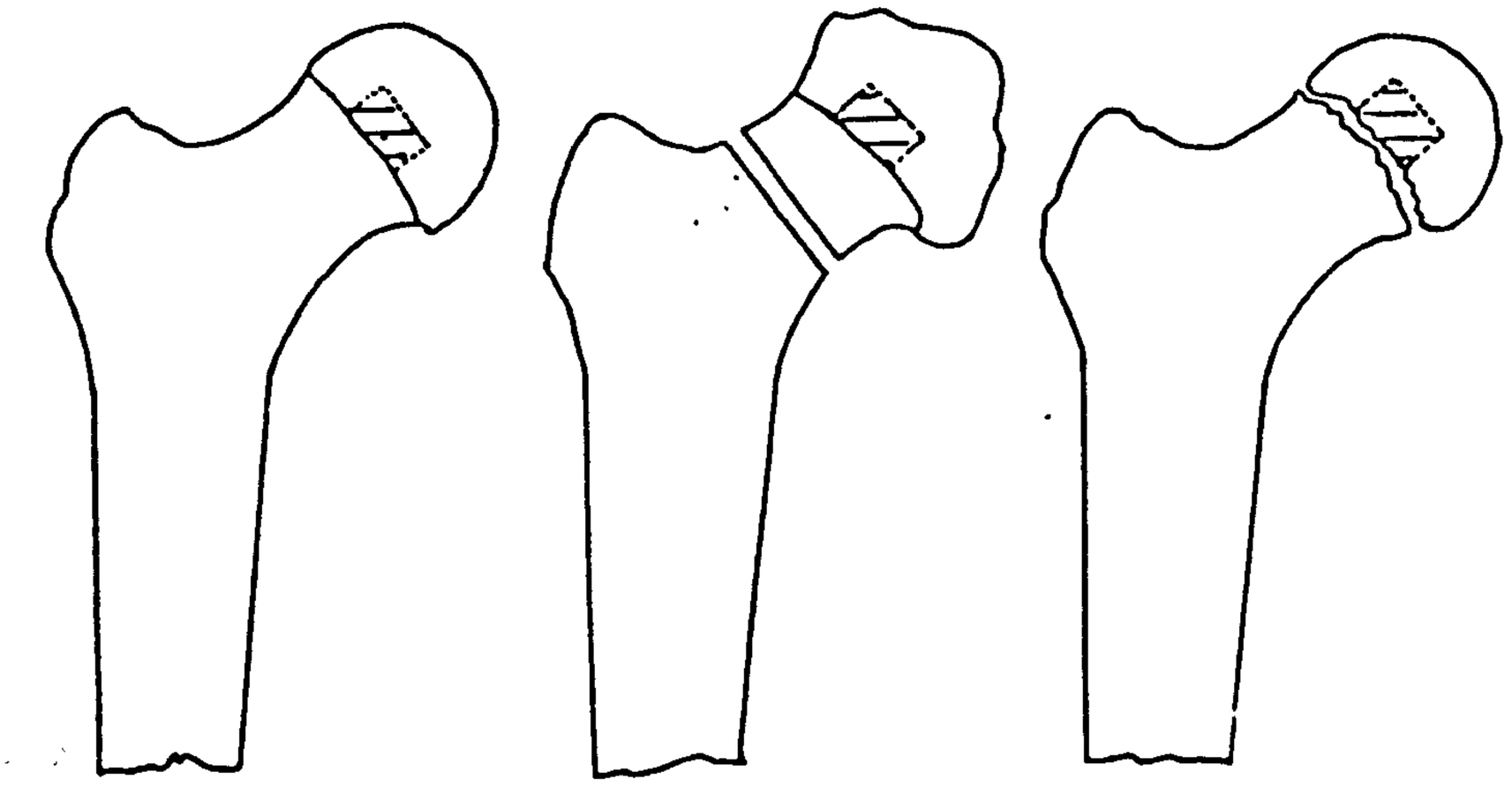

Fig. X. 2 Diagrammatic representation of the femoral head and neck to show the site of sampling.

fractures of the tibial or femoral shaft or the neck of humerus. The small blocks were immersed in 5% (w/v) polyvinyl alcohol (G04/140 Polyviol; Wacker Chemicals) before being chilled to -70° C in n-hexane. Cryostat sections (10 microns thick) of the unfixed, undemineralised bone were prepared as described in Chapter V. These sections were cut from the blocks orientated in such a way that one side of the section was at the fracture surface or the equivalent surface from the osteoarthritic or cadaveric specimens. All sections were dried overnight at 37° C.

Crystal Study. For the study on crystals, 19 osteoarthritic samples (7 male, and 12 female; mean age and standard deviation, 67.6 ± 11.5 years), 16 cadaveric samples (5 male, 11 female; mean age and standard deviation, 73.7 ± 8.2 years) and 21 samples of fractured necks of femur (1 male; mean age and standard deviation 76.7 ± 12.6 years) and 3 samples of traumatic fracture were investigated (Table X.1).

Birefringence Study. For the study on the birefringence of collagen and of the glycosaminoglycans (GAGs), the number of specimens and the ages of the subjects were 8 osteoarthritic (62.1 ± 14.7 years), 8 cadaveric samples (72.3 ± 5.1 years) and 11 samples of fractured necks of femur (80.4 ± 12.0 years) (Table X .2).

The sections were then inspected, under crossed polars, either unstained or after staining with Alcian

Table X. 1 Crystal study : age and sex of patients.

	Osteoarthritic	Cadaveric	Fractured neck of femur
No. studied	19	16	21
sex	7M : 12F	5M : 11F	1M : 20F
age mean ± SD	67.6 ± 11.5	73.7 ± 8.2	76.7 ± 12.6

Table X. 2 Collagen and GAG birefringence : age of patients.

	Osteoarthritic	Cadaveric	Fractured neck of femur
No. studied	8	8	11
Age mean ± SD	62.1 ± 14.7	72.3 ± 5.1	80.4 ± 12

blue, by the critical electrolyte concentration method of Scott and Dorling (1965) as described by Chayen, Bitensky and Butcher (1973) (see later).

All the microscopic exainations and birefringence measurements were done using a Brace-Köhler λ/30 compensator on a Zeiss universal microscope equipped with a range of polarising objectives (16X, 0.32 NA; 40X, 0.85 NA; 63X, 0.9 NA).

Polarised Light Microscopy

Polarised light microscopy is used for the detection and measurement of matter that has crystalline or crystalline-like properties. Light has electro-magnetic properties and is therefore influenced by the electromagnetic properties of the material through which it passes. Thus all matter will retard light to a greater or lesser extent.. The degree of retardation is given by the term 'refractive index' (RI):

$$RI = \frac{\text{velocity of light in air}}{\text{velocity of light in the material}}$$

In general, crystals, and crystal-like material, have three optical axes, corresponding to the length, breadth and depth of the material. For non-crystalline, or isotropic, material, the refractive index along all three axes is the same. In contrast, the RI along the length of most crystalline-like, or anisotropic,

material is different from that along one or other (or both) of the other axes. Such anisotropic material shows the property of birefringence, which is defined as the difference between the refractive index measured with light parallel to the long axis ($n_{||}$) and with light vibrating perpendicular to the long axis ($n_{\perp}$) - that is $n_{||} - n_{\perp}$. The polarising microscope actually measures the optical path difference in our material, that is the interaction of both refractive indices that causes a change in the velocity of the light. This is influenced by the thickness of the specimen. Thus

$$\frac{\text{optical path difference}}{\text{thickness}} = \text{birefringence}$$

Consequently a thicker crystal appears brighter than a thinner crystal of the same material.

The Mechanism. The theory of polarised light microscopy is very complex but can be explained very simply by the use of vectors (Fig. X.3).

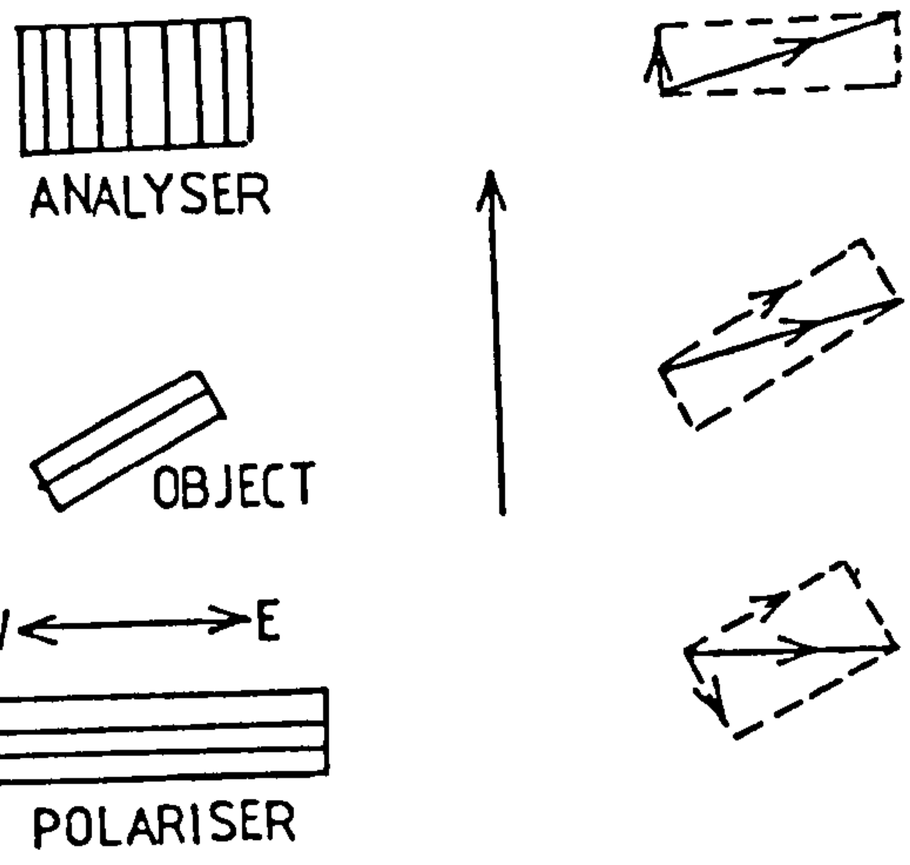

Fig. X. 3 Diagrammatic representation of the theory of polarized light microscopy. (from Chayen, 1983)

The polariser is situated below the condenser and can be rotated to give plane-polarised light vibrating solely in the east - west (E - W) direction. Consequently it has vectors in the 45° positions. It has no vectors in the N - S direction and thus will not pass the rotatable analyser, set to the N - S position. The analyser is set between the objective and the eyepiece. The analyser is apolar and transmits light that vibrates in one direction only. Positioned in the N - S position the field will appear black.

When a birefringent object, in which light vibrates more rapidly (or more slowly) along its long axis than its short axis, is placed in the field in a 45° position it will be maximally bright. This is because one of the 45° vectors of the E - W light will be moving along this long (fast) axis, the other 45° vector being retarded.

The vibration of the resultant light will be turned towards the N - S axis, the object having turned the plane of polarisation. This resultant vibration now has a vector that is in the N - S position and will pass through the analyser (set to N - S position). The object will appear bright with the background remaining black.

The theory of polarised light microscopy involves the interference between the two vectors of the light which, moving slightly out of phase with one another, will give the resultant light.

Types of Birefringence. There are two main types of birefringence.

1. Crystalline (intrinsic). This is determined by the chemical structure of the material.

2. Form (textural). Structures such as collagen fibres which contain orientated elongated submicroscopic particles show form birefringence.

Crystalline birefringence depends directly on the electromagnetic characteristics of the material and thus is not dependent on the refractive index of the mounting medium. Form birefringence depends on the different velocity of light in the array of particles (or fibrils) and the velocity in the material in which they are mounted.

Measurement of Birefringence

This subject has been fully reviewed by Hartshorne and Stuart (1970). In practice, since the measurement of birefringence requires that the thickness of the object has been determined (see above), it is preferable to record the optical path difference (opd). This can be measured accurately by the use of various compensators. In the present study, a Brace-Köhler λ /30 rotatable compensator has been used with a Zeiss universal microscope (Fig. X.4). It is inserted at the 45° position, above the objective and below the analyser; it is rotated, about its own axis, until the retardation imposed by it compensates for the retardation caused by the birefringent object. For

Fig. X. 4 A. Zeiss Brace-Köhler λ/30 compensator.

precision, it is advisable to use monochromatic light.

Procedure. The polariser and analyser are crossed and the compensator is set to extinction (that is, with its vibration directions parallel to those of the polariser and analyser). The crystal or fibre(s) is turned into either of its 45° positions. The compensator is then rotated until extinction is obtained. Birefringence is expressed as nanometres of optical path difference (R_{obj}) after conversion of the angle of rotation of the compensator (ψ) according to the equation

$$R_{obj} = R_{comp} \sin 2 \psi_{comp}$$

where R_{comp} is the optical path difference imposed by the compensator (Chayen and Denby, 1968).

Orientation of GAGs and Related Compounds

Collagen fibres naturally show form birefringence. In contrast, the other major organic component of bone-matrix, namely GAGs, cannot be detected by polarised light microscopy. This may be due to various causes. They may be totally unorganized, so that they would show no overall birefringence even if they were capable of showing form-birefringence; or their form-birefringence could be so low that, even if they were highly oriented, they would be undetectable. Yet it is of some importance to know if they are oriented in normal bone, and if that orientation were to become altered in pathological conditions.

To examine this question in detail, we have developed a procedure involving 'induced birefringence', along the lines indicated by Modis (1974). In this procedure we stain the bone with a planar dye, Alcian blue, which is highly birefringent either in the dry, semi-crystalline state, or when caused to become oriented, namely when a solution is drawn out into thin lines and allowed to dry. I found that the GAGs of normal bone-matrix, stained with this dye, showed strong birefringence (hence the term 'induced birefringence'). The staining was done by the critical electrolytic method of Scott and Dorling (1965), as described by Chayen et al (1973).

Alcian Blue Staining: concept of the critical electrolyte concentration. The theory states that the intense negatively charged field of a polyanion attracts positively charged coloured dyes, such as Alcian blue, producing a coloured bound stain. Addition of an uncoloured cation leads to competition between the dye and the electrolyte. Although all the glycosamino-glycans are negatively charged and bind Alcian blue, they vary in their ability to compete with increasing concentrations of magnesium ions (magnesium chloride).

Ten micron sections were stained with an 0.05% solution of Alcian blue in 0.25M sodium acetate buffer at pH 5.8. To this solution was added magnesium chloride at the appropriate molarity:

0.025M to stain all GAGs and acidic moieties that remain ionized at this pH

0.5M to stain only chondroitin sulphate and keratan sulphate (and suppresses sialic acid residues).

The use, therefore, of the potential birefringent properties of Alcian blue allows the study of the orientation of glycosaminoglycans on sections of bone.

Demonstration of Crystals. Sections were inspected either dry or in benzaldehyde (R.I. 1.544) under crossed polars. Crystals were examined to determine their sign of birefringence, extinction angles, general habit and refractive index.

Sign of birefringence. This defines whether the optically slow axis is along the long or short geometric axis of the crystal. This is determined by orientating the crystal along its long axis at the 45° position that intersects the N-E angle. The crystal will appear maximally bright on a black background. A quartz-red plate is then inserted into the slot in the microscope tube. The quartz red plate is cut in such a way that the vectors (or rays) interfere with one another to give first order red light in Newton's scale. The field now appears red. Then if the slow axis of the retardation plate is parallel to the slow axis of the crystal, and since

$R_{total} = R_{plate} + R_{specimen}$, the crystal will appear blue (increased resultant interference wavelength).

Such a crystal is called a positive crystal. If the slow axis of the plate is parallel to the fast axis of the crystal then

$$R_{total} = R_{plate} - R_{specimen}$$

and the crystal will appear yellow on a red background (decreased resultant interference wavelength). Such a crystal is called a negative crystal. (R_{total} etc. refers to the retardation of the plate or specimen).

Extinction angle. Crystals that appear blackest when set to the N-S or E-W position (but bright at intermediate positions) show straight extinction. Some crystals do not become darkest at exactly the N-S position, but at some angle to this direction. This may be related to whether the three axes of the unit crystal are at right angles or not. The extinction angle is very useful in defining the crystalline material, e.g. crystals of apatite show straight extinction.

Refractive index. The refractive index of crystals was determined by the method described by Watts et al (1971). Briefly, crystals were chosen and individually orientated to the position that made them maximally bright: the microscope stage was locked and the amount of birefringence (actually, optical path difference) was measusred by Brace-Köhler compensation as described earlier. The measurement of birefringence was repeated with the section mounted in media of differing refractive

index, keeping the chosen crystal in the centre of the field. The refractive indices of the fluids were then plotted against their retardation values. The refractive index which gave the lowest birefringence was taken as the refractive index of the crystal.

Results

Appearance of sections under crossed polars. All sections from all 35 osteoarthritic or cadaveric specimens, mounted either in air or in benzaldehyde (RI = 1.545), showed highly birefringent lamellae of collagen. Haversian systems were often in the plane of the section. Between these arrays of collagen, the section appeared to be as black as the background. This indicated an apparent lack of suitably orientated birefringent material in between the circular or linear arrays of collagen (Fig. X.5 and 6). Such sections, which were fully mineralised, were indistinguishable from sections of bone that has been chemicaly fixed, decalcified, embedded in paraffin and sectioned in a routine histological laboratory. An exactly similar image was obtained when the sections of undemineralised bone were treated with EDTA (0.1M) at pH 7 for 16 hours to remove the mineral component. These results implied that the crystals of mineral, in the undecalcified sections, were too small, and too disorientated, to be detected in this microscopic system.

Fig. X. 5 An example of a cryostat section of fresh human undemineralized bone from the femoral epiphysis viewed under crossed polars showing the Haversian arrays of collagen. The spaces in between the birefringent collagen bundles show no birefringent material and appear black. X 220.

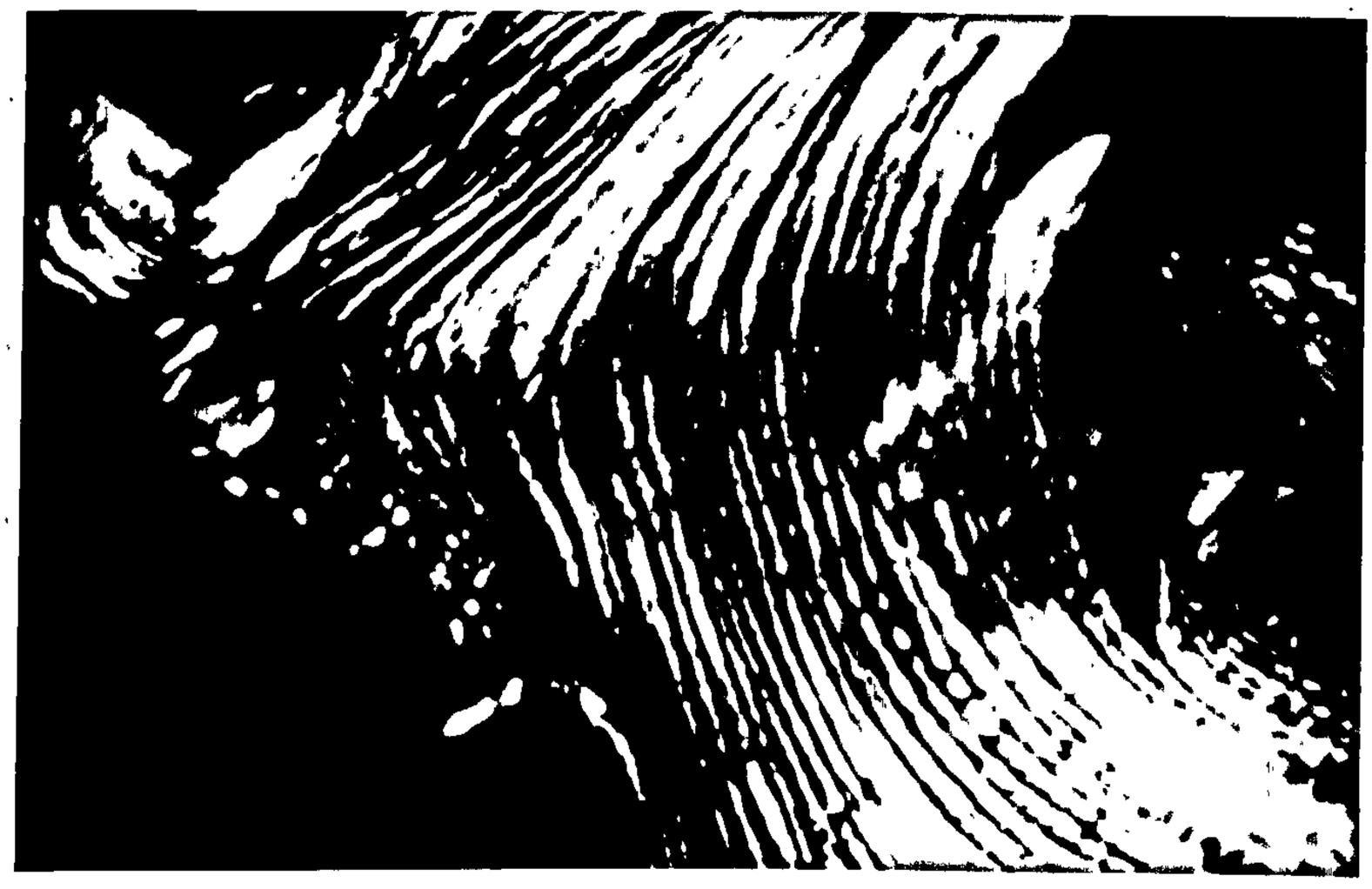

Fig. X. 6 A section of trabecular fragment from a human femoral epiphyseal region viewed under crossed polars. As in Fig. X. 5, the spaces between the bright birefringent linear arrays of collagen appear black. X 220.

In marked contrast, in all 21 samples of fractured necks of femur, discrete crystalline material was found, particularly close to the site of fracture, in between the collagen lamellae (Figs. X.7 and 8). The incidence of crystals apparently decreased with distance (up to 3 cm) from the site of fracture.

Characteristics of the crystals. These crystals showed true crystalline birefringence in that their birefringence was relatively unaffected by the refractive index of the medium in which the sections were mounted. They showed straight extinction, positive birefringence and appeared to be hexagonal (Figs. X.7 and 8). Although many of the crystals were small, about 0.5 μm long, many were 2.5 by 0.5 μm. The optical path difference through these large crystals was only 19 nm; if the thickness of these crystals is taken to be 0.5 μm, this indicates a birefringence of 3.8×10^{-2}. The refractive index was greater than 1.545 (the RI of benzaldehyde). Thus in all features, these crystals corresponded to crystals of apatite.

Birefringence of collagen and of GAGs. Untreated sections were examined by polarised light microscopy. The optical path difference measured in the collagen lamellae was the same in all three types of specimen (Table X.3 and Fig. X.9).

Sections stained with Alcian blue, in the presence of either 0.025M or 0.5M magnesium chloride, (Fig. X 10 (a) and 11 (a)) were examined by polarised light microscopy. They showed blue birefringent matter

Fig. X 7 and 8

Low and high power photomicrographs of a section from the sub-capital fracture site of a human femur. In contrast to Figs. 5 and 6, scattered between the bright birefringent collagen bundles are bright birefringent crystals. Fig. 7 X 220; Fig. 8 x 343

Table X. 3 Birefringence (optical path difference) of collagen and sections of bone stained with Alcian blue, measured in nanometres of retardation (mean ± SEM).

Treatment	Osteo-arthritic ($n=8$)	Cadaveric ($n=8$)	Fractured neck of femur ($n=11$)	Traumatic fractures ($n=2$ or 3)
Unstained collagen	17.4 ± 0.5	17.2 ± 0.6	16.7 ± 0.2	14.7, 16.9
Alcian blue + 0.025M-$MgCl_2$	20.3 ± 0.4	20.2 ± 0.3	11.2 ± 0.4*	19.1, 21.0
Alcian blue + 0.5M-$MgCl_2$	15.2 ± 0.6	15.8 ± 0.6	7.8 ± 0.5*	17.3, 15.8, 15.1

*Significantly different ($P<0.001$) from osteoarthritic and cadaveri. groups; Student's t-test

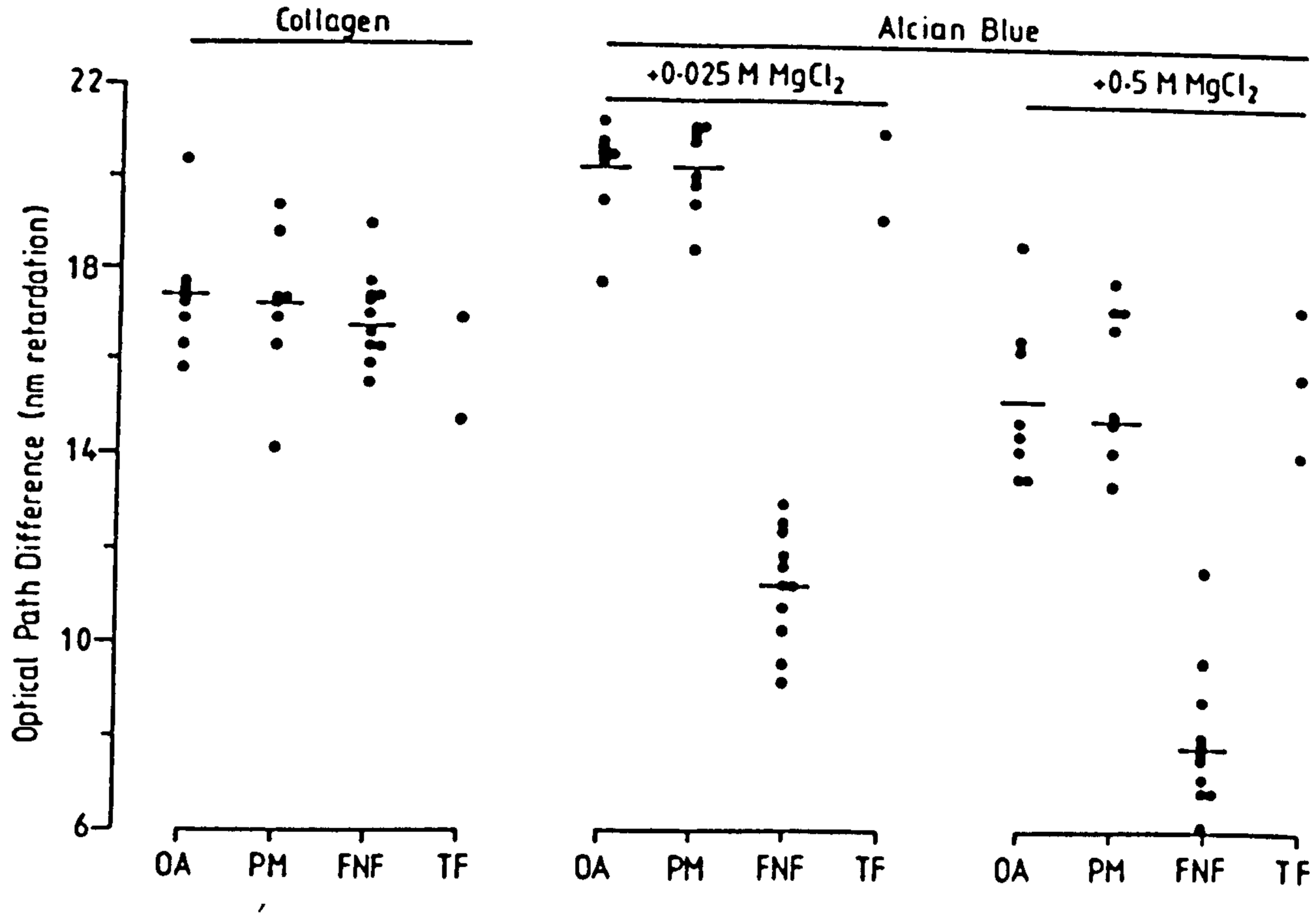

Fig. X. 9 Scattergram of the values of optical path difference (opd) measured in unstained sections (collagen) and sections stained with Alcian blue in the presence of either 0.025M or 0.5M $MgCl_2$ of samples of human femoral epiphyseal region taken from osteoarthritis (OA), cadaveric (PM), and subcapital fractures (FNF). Three examples of traumatic fractures are also shown. The horizontal bars indicate the mean for each group.

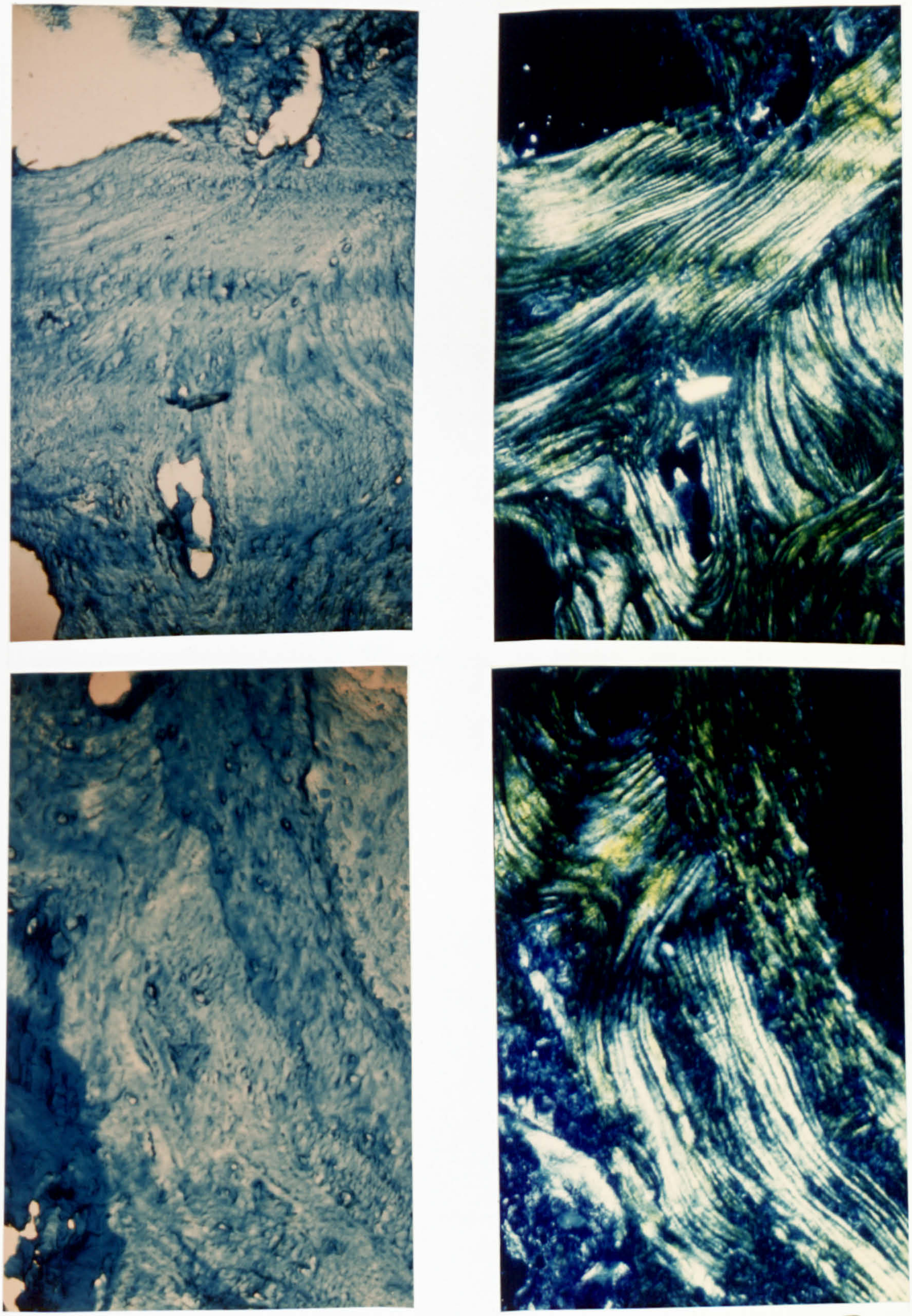

A B

Fig. X. 10 and 11

Two examples of sections of samples of the human femoral epiphyseal region stained with Alcian blue viewed (a) by ordinary light microscopy and (b) under crossed polars. The blue 'induced' birefringence is superimposed on the

apparently coincident with the collagen lamellae, which largely obscured the white birefringence of the collagen lamellae (Fig. X.10 (b) and 11 (b)). The optical path difference induced by this blue birefringence in sections of osteoarthritic and cadaveric samples, stained by Alcian blue in the presence of 0.025M $MgCl_2$ was identical. However it was markedly depressed in sections from the fractured necks of femur (Table X.3): it was least when close to the site of fracture and rose to high values up to 15 mm from the fracture (Fig. X.12), although even at this distance from the fracture, the values were well below normal levels. However, it may be noted that the induced birefringence was considerably greater than the natural birefringence of the collagen.

The higher concentration of magnesium chloride (0.5 M) decreased the amount of Alcian blue birefringence but essentially similar results were observed (Table X .3; Figs.X .9, 11 and 12).

Content of GAGs. In a few sections, the amount of Alcian blue stain present was measured by direct photometry in the same regions as had been selected for birefringence measurements. The results are shown in Fig. X .13. They show that the content of GAGs through the thickness of the section was equivalent in all three types of specimen even though the amount of birefringence in the individual lamellae in sections

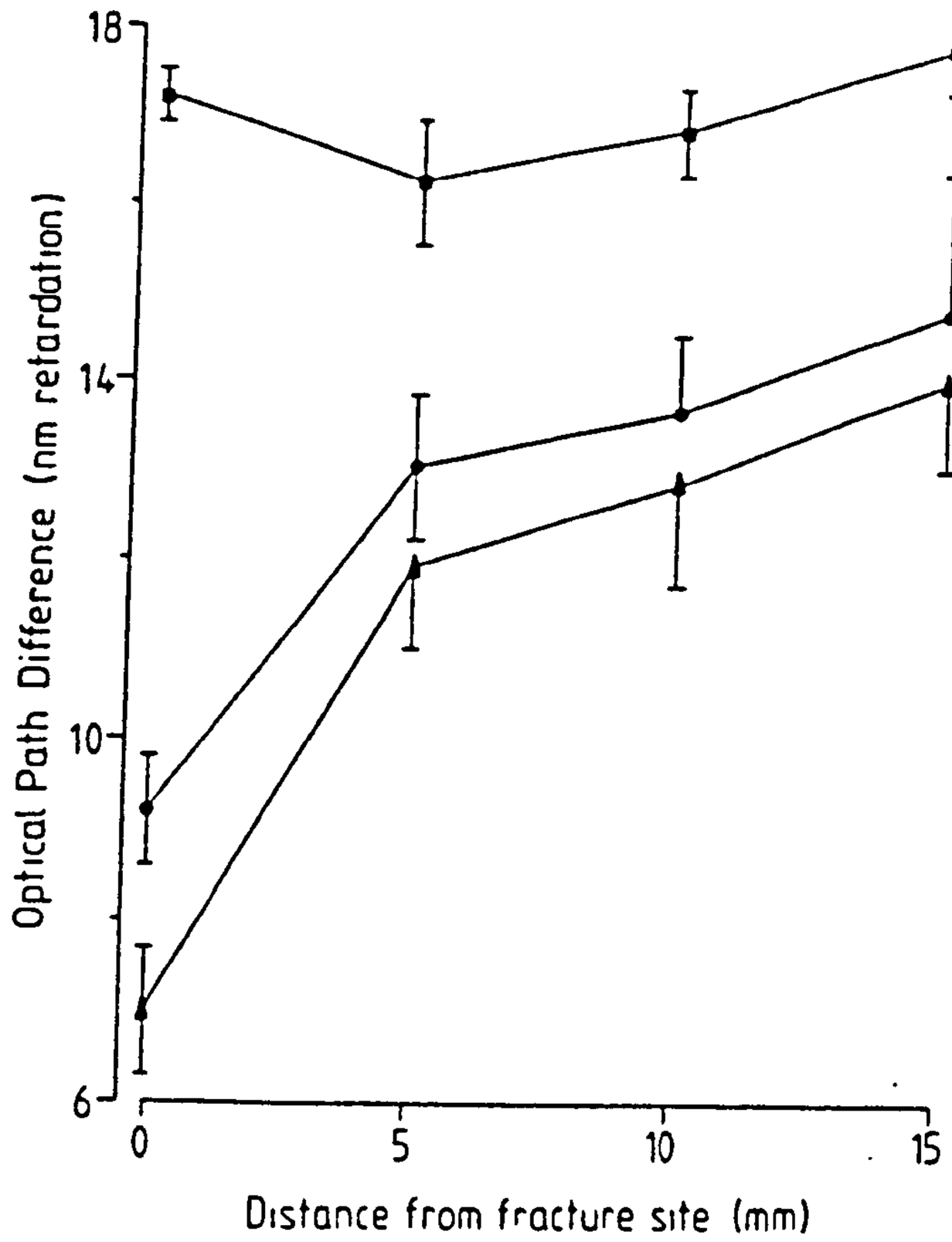

Fig. X. 12 The mean optical path difference measured in sections from five different cases of subcapital femoral fracture (mean ± SEM) with distance from the fracture site. The collagen birefringence (squares) in unstained sections remains constant whereas the 'induced' Alcian blue birefringence (low $MgCl_2$: circles; high $MgCl_2$: triangles) increases with distance from the fracture site but does not reach normal values.

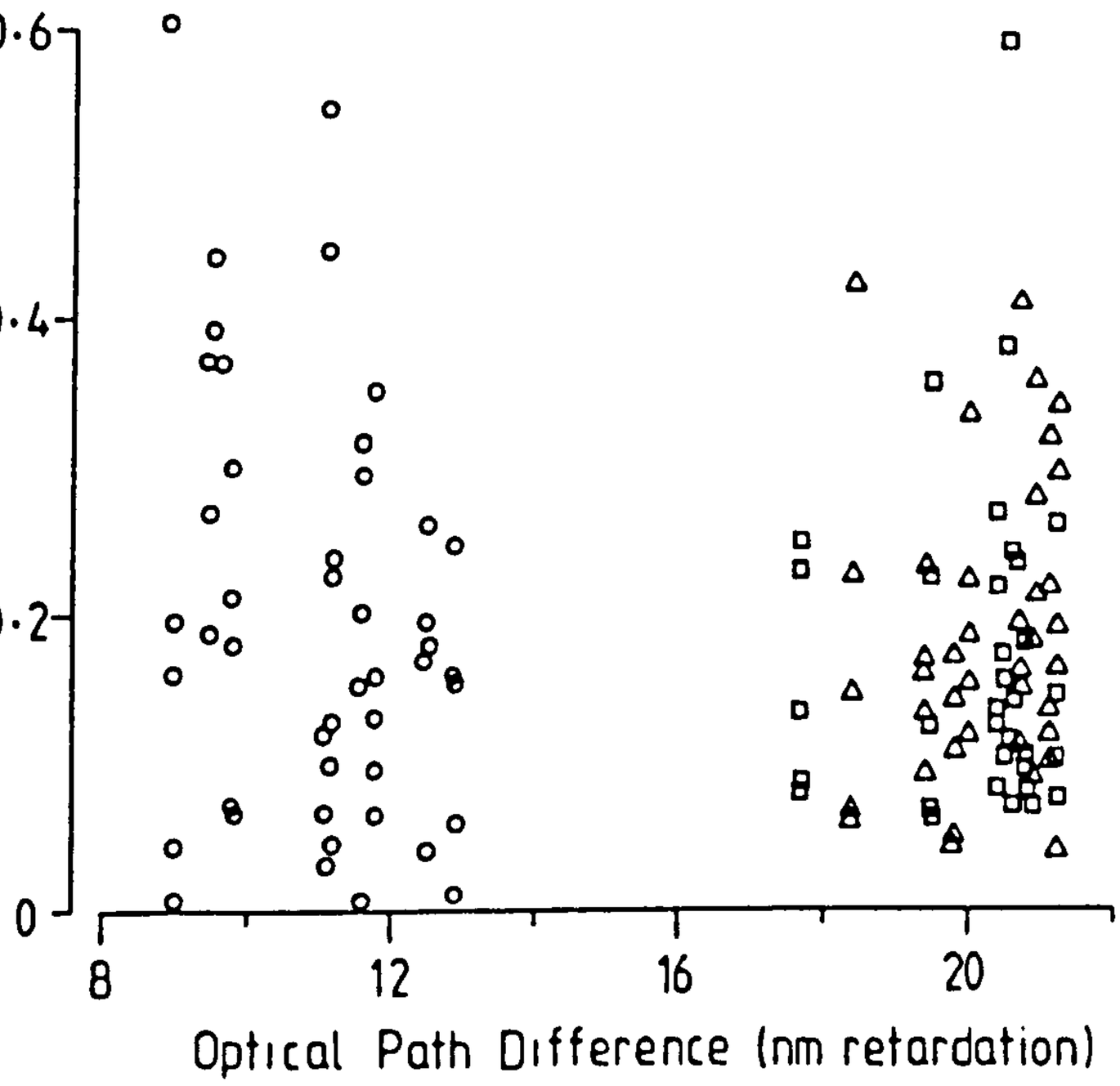

Fig. X. 13 The optical path difference (opd), measured under crossed polars, plotted against the absorption produced by the Alcian blue stain (concentration) in the same region of the same sections of samples of (a) sub-capital fractures (circles) and the equivalent epiphyseal region from (b) cadaveric (triangles) and (c) osteoarthritic (squares) femoral heads. The amount of Alcian blue staining in all three groups is similar but the induced opd is depressed only in the fracture group.

from the fractured necks of femur was decreased by about 45%.

Results from traumatic fractures. No crystals were found in several serial sections taken from these fractures. The optical path difference measured in the native collagen and the Alcian blue birefringence in sections stained at both concentrations of magnesium chloride agreed closely with the values found in the non-fractured specimens (Table X.3 and Fig. X.9).

Reproducibility of measurements of birefringence.

On six occasions, the birefringence (optical path difference) was measured 5 times by myself and by Dr. N. Kent. The overall coefficient of variance was 9.5%.

Discussion

Dickenson et al (1981) investigated the relationship between applied tensile load and resultant strain in normal and osteoporotic bone; they showed that the elastic component (presumably related to the collagen) was virtually identical in both. However they showed that osteoporotic bone will break at lower load than normal bone, and this is probably related to the properties of the mineral component. The results from the present study are in agreement with those of Dickenson et al (1981). The degree of orientation of the collagen lamallae was the same in the specimens of fractured

neck of femur as in the osteoarthritic and cadaveric samples. The mineral phase was found to be different in that, close to the site of fracture, some of the mineral phase occured in the form of crystals of the size that could readily be resolved by normal, polarised light microscopy. The crystals observed in sections from fractured necks of femur were not seen in the few traumatic fractures that were available for study.

This last point shows that the crystals seen in fractured necks of femur were unlikely to be due simply to the fracture process.

The use of the potential birefringent properties of Alcian blue allowed studies to be made on the orientation of glycosaminoglycans (GAGs). As defined by Scott and Dorling (1965) and described by Chayen et al (1973) Alcian blue in the presence of 0.025M $MgCl_2$ will stain all GAGs and other acidic molecules, such as hyaluronic acid and acidic proteins. These acidic molecules may not be birefringent, even when orientated; however, when Alcian blue becomes bound to such orientated molecules, the complex with the dye does exhibit birefringence (Modis, 1974). Alcian blue in the presence of 0.5M $MgCl_2$ will only bind to highly sulphated, long-chain moieties, mainly chondroitin and keratan sulphates (Scott and Dorling, 1965; Scott, 1973). Thus it is possible to distinguish between the orientation of acidic, long-chain molecules generally and that of chondroitin and keratan sulphates..

The total content of GAGs was the same in all samples tested in this study. However, the degree of orientation of all long-chain acidic molecules (stained in the presence of 0.025M $MgCl_2$) and of the chondroitin and keratan sulphate-like moieties, was found to be about 45% less in the bone from the fractured necks of femur than in the osteoarthritic or cadaveric specimens. This decreased orientation was largest close to the site of fracture and tended towards more normal values further from the fracture. However even 15 mm from the site of fracture the birefringence was somewhat abnormal (Fig. X.12). This effect was unlikely to be the result of fracture since the orientation of Alcian blue-stained material in the lamellae of traumatic fractures was the same as in the "control" specimens (Table X.3 and Fig. X.9).

This study showed that close to the fracture site, relatively large crystals exist, that have the optical properties of apatite. This was seen in all 21 cases of fractured necks of femur and in none of the 35 other "control" specimens or in the three traumatic fractures. This finding was in keeping with the observations of Wall et al (1979) and Chatterji et al (1981), that, with advancing age, some microstructural change occurs in bone and that the density of the bone is not the sole determining factor in its resistance to fracture. The development of crystals, of the size found in the present study,

would be in keeping with a microstructural change that could predispose the bone to fracture. The presence of such crystals in otherwise microcrystalline metals can be a source of structural failure or fracture (Forsyth, 1969; Engel and Klingele, 1981).

The finding that the orientation of ordered components of the non-collagenous ground substance was also decreased in the fractured necks of femur could indicate a cause for the development of such anomalously large crystals of apatite in the microcrystalline mineral phase. This arises from the fact that the crystallisation of apatite can be modulated by GAGs (Boskey, 1981). The fact that these changes, and the appearance of crystals, occur only at a specific locus may be related to the fact that this region is the site of greatest shear. It is certainly the site of greatest tension, as shown by Singh et al (1970).

CHAPTER XI

DEVELOPMENT OF A METHOD FOR MEASUREMENT OF SODIUM POTASSIUM ATPase

Introduction

Relation of G6PD and Na^+-K^+-ATPase

Much of the work in this thesis has been concerned with changes in glucose 6-phosphate dehydrogenase (G6PD) activity. It has been suggested that this activity is central to cellular activity, particularly in fracture-healing, both because it controls pentose-shunt activity (and therefore the production of ribose sugars) and because it is a major source of cytosolic NADPH. The latter is implicated in many cellular physiological functions, some of which have been discussed earlier. However there is also evidence (Dikstein, 1971) that there may be a relationship between G6PD activity, or the generation of NADPH, and the activity of sodium-potassium-dependent adenosine triphosphatase (Na^+-K^+-ATPase). Because this enzymatic activity is vital to the life of cells, and may play a major role in cellular oedema, as in fracture-healing, it was considered necessary to investigate this enzymatic activity.

Background to Na^+-K^+-ATPase

As reviewed by Baker (1972) the energy-requiring cellular process of active transport of sodium and

potassium plays a major role in the maintenance of cell volume; in absorption processes in kidney and intestine; and in the propagation of action-potentials in excitable and contractile tissue. The active transport of sugars and amino acids is also possibly dependent on the distribution of sodium and potassium ions (Hokin and Dahl, 1972; Katz et al, 1979). The energy dependent intracellular control of sodium and potassium ions apparently depends on sodium-potassium-ATPase activity as a "pump" (Baker, 1972). The important feature of this pump is that ATP appears to be the energy source for this transport. It is now established that the sodium-potassium dependent, magnesium - stimulated adenosine triphosphatase ($Na^+ - K^+ - ATPase$) of cell plasma membranes provides the catalytic machinery for the coupling of the energy released by the hydrolysis of ATP allowing the exchange of Na^+ for K^+ across plasmalemmal surfaces against their respective concentration gradients (Pérez-González de la Manna et al, 1980).

Because of the critical importance of this ATPase in cellular physiology, several workers have sought a cytochemical procedure for demonstrating its activity. A great deal of this work has been done on the kidney. This is an ideal test material for the following reasons:

(i) The $Na^+ - K^+ - ATPase$ activity, measured biochemically, is high in the renal cortex;

(ii) The relative activities of this enzyme, in different regions of the nephron, have been investigated in detail

by microdissection studies with radio-labelled ATP; and (iii) The activity of the enzyme is likely to be under hormonal control (as will be discussed later), so that changes in the activity (in different regions of the nephron) induced by physiological conditions or hormonal influence should be reflected by changes measured cytochemically.

One of the major problems of the earlier cytochemical methods for demonstrating $Na^+ - K^+$ -ATPase activity was the inability to demonstrate activity in proximal tubules, in which this enzymatic activity appears to fulfil major physiological functions, namely the transport of glucose and of calcium (Kinne et al, 1978). This disadvantage, along with many others, in the earlier methods will be discussed briefly.

Earlier Histochemistry of the Enzyme.

The initial attempts to localize $Na^+ - K^+$-ATPase cytochemically centred about the Wachstein and Meisel (1957) techniques. The methods employed lead ions to trap the phosphate liberated by the ATPase activity. However these methods fell into disrepute because the lead ions themselves caused a non-enzymic hydrolysis of the ATP that was used as substrate, and also because free lead ions strongly inhibit $Na^+ - K^+$ -ATPase activity (as reviewed by Ernst and Hootman, 1981; Ernst, 1972(a); Beeuwkes and Rosen, 1975, 1980). Moreover, ouabain,

the specific inhibitor of $Na^+ - K^+$ - ATPase, had no effect on the activity. Omission of Na^+ or K^+ had little effect either (Novikoff, 1961; Farquhar and Palade, 1966; Tormey, 1966).

In an attempt to overcome these problems, Ernst (1972 (a), (b)) introduced the use of the substrate p-nitrophenyl phosphate (PNPP) for demonstrating the ouabain sensitive, potassium-dependent phosphatase activity which is now believed to function as part of the $Na^+ - K^+$ - ATPase activity (Ernst, 1972 (a); Hokin and Dahl, 1972). Hydrolysis of the phosphate bond of p-nitrophenylphosphate (PNPP) yields inorganic phosphate which can be precipitated by heavy metal capture ions. Strontium was used as the trapping agent because its inhibitory effect on activity was less than that of lead at equivalent concentrations However this still left an unsatisfactory degree of inhibition and left untouched the related problem of the requirement of an alkaline pH for efficient precipitation of the phosphate. This alkaline pH is sub-optimal for enzymatic activity(Ernst, 1972 (a)). Furthermore, PNPP is readily hydrolysed by alkaline phosphatase at pH values above 8. Thus for most tissues it becomes essential to add a sufficient concentration of an appropriate inhibitor of alkaline phosphatase activity to the reaction medium if the reaction for K^+NPPase activity is to be valid. However it is fortunate that alkaline phosphatase and K^+-PNPPase activities are localized in different plasmalemmal surfaces in the kidney cortical tubules. This method has apparently been found to be unsatisfactory

so that Guth and Albers (1974) modified it in two ways: first, by adding dimethyl sulphoxide to the medium, which at 30% concentration, changes the optimal pH to 9.0 (Beeuwkes and Rosen, 1980), and inhibits alkaline phosphatase activity(Ernst et al, 1980); and secondly, by leaving out the strontium, relying on the phosphate being captured by the magnesium and potassium ions endogenous to the tissue (Beeuwkes and Rosen, 1975; Ernst et al, 1980). The precipitated phosphate was converted to cobalt phosphate, by immersion in a solution of cobalt chloride, and thence to cobalt sulphide.

So, although the phosphates of both potassium and magnesium are appreciably soluble, and although this method depends on the presence of sufficient concentrations of these ions in the tissue, it is hoped that phosphate, hydrolysed during the reaction, remains within reactive cells without the need of a heavy metal capture-ion. This method was used by Beeuwkes and Rosen (1975, 1980) who used electron-probe analysis to quantify the reaction-products. In the kidney, Beeuwkes and Rosen (1975) showed highest activity in the thick ascending limbs of the loop of Henle, and in the distal convoluted tubules. They reported no PNPPase activity in the proximal tubules, even though the ATPase activity, recorded in these tubules by the microchemical, micro-dissection studies of Schmidt and Dubach (1969), of Schmidt et al (1974) and of Katz et al (1979) showed that the activity in these tubules was one third that

of the distal tubules. Beeuwkes and Rosen (1975) concluded that their inability to record activity in proximal tubules might have been due to the relative insensitivity of their method. Morphological preservation is poor in this method and the nature of the phosphate precipitation process precludes subcellular definition of the distribution of the reaction product (Ernst and Hootman, 1981).

Mayahara et al (1980) presented a modification of the PNPPase procedure. Lead citrate was substituted for strontium as the trapping agent. A study by Mayahara and Ogawa (1980), using this method, demonstrated K^+-dependent activity in the rat kidney that paralleled the distribution obtained with the original method, as used by Firth (1974) and by Ernst (1975). The advantage of this technique is that it is methodologically simple.

Thus until recently, this important enzyme, $Na^+ - K^+ -$ ATPase, has been examined cytochemically only by an indirect method that has a number of disadvantages. Most importantly, as far as studies on the kidney are concerned, the methods described do not demonstrate activity in proximal tubules. Yet, the Na^+-$K^+ -$ ATPase activity in the proximal tubules may be about half that found in the strongly active distal tubules (Katz et al, 1979). Secondly, although there seems little doubt that the K^+-dependent phosphatase, demonstrable by the PNPP-method, is associated with

the Na^+-K^+-ATPase, there are several discrepancies, as reviewed by Hokin and Dahl (1972). It is of interest, for instance, that differences between Na^+-K^+-ATPase and PNPPase in sensitivities to certain ions and inhibitors become less significant when the phosphatase assay conditions are made similar to the usual assay conditions for the Na^+-K^+-ATPase i.e.assayed in presence of Na^+ and ATP (Yoshida et al, 1969).

It would therefore be preferable to have a cytochemical procedure that can demonstrate Na^+- K^+-ATPase activity directly by its response to its normal substrate (ATP) and in relation to the ions that are known to influence such activity. The method should be significantly inhibited by ouabain or other cardiac glycosides that are established inhibitors of Na^+- K^+-ATPase activity.

The original, direct method of Washstein and Meisel (1957) failed because lead ions hydrolyse ATP in solution and inhibit the enzyme. Furthermore few, if any, lead salts are readily soluble at the pH at which the reaction should be done for maximum Na^+- K^+-ATPase activity. It was therefore decided to complex the lead with weak acid moieties which should sequester the lead from the ATP and from the active site of the enzyme, but which would be displaced by the electrochemically more active phosphate ions when these were liberated by the action of the ATPase on ATP. Consequently, a mixture of lead salts was prepared (by Mr. G.T.B. Frost, of Sigma, London) which, when dissolved in water with the addition of a dilute solution of ammonia, would give a buffered solution of lead ammonium citrate acetate.

This lead ammonium citrate acetate material contained approximately 10% lead in a bound form; it is readily soluble at pH values from 7 to 8; and it does not hydrolyse solutions of ATP although it forms a rapid and dense precipitation when free phosphate is present. This chapter records the use of lead ammonium citrate, as a capture reagent in a method for Na^+- K^+-ATPase activity.

Development of the Method

In the development of a cytochemical method for assaying magnesium-activated Na^+- K^+- ATPase activity in the kidney the following technique was used.

Segments (about 5 x 5 x 3 mm) were cut from the kidneys of Wistar rats (of either sex) or of guinea-pigs (Hartley strain, either sex) that had been killed by asphyxiation in nitrogen and chilled to -70° C in n-hexane (BDH; free from aromatic hydrocarbons, boiling range 67 - 70° C). The tissue was stored in cold tubes, at -70° C and used within 2 days because the activity alters markedly after this time, as assessed biochemically (Perez-Gonzalez de la Manna et al, 1980). The tissue was sectioned at 10 µm (Chapter V) and picked off the knife on to glass slides. To economize on the relatively costly components of the reaction-medium, the reactions were done by placing a small Perspex ring around each section and pouring the medium into the ring (Chayen et al, 1973).

The method for assaying the Na^+-K^+- ATPase activity was derived from the biochemical procedure

of Schwartz et al (1971). The reaction medium contained the substrate ATP (disodium adenosine 5' triphosphate), sodium chloride, potassium chloride, magnesium chloride and lead ammonium citrate acetate. Despite the fact Na^+- K^+-ATPase is a membrane-bound enzyme, no activity was found unless a stabilizer was used in the reaction medium: in this case a 40% solution of Polypep 5115 in the reaction medium gave optimum results. To overcome the lower diffusibility in this viscous polypeptide medium, all the reactants were used at four times the concentrations used by Schwartz et al (1971). The 40% solution of Polypep was prepared in 0.2M Tris buffer at pH 7.4 containing sodium acetate (1 mM for sections of rat kidney and 2 mM for the more delicate guinea pig tissue). Then the following concentrations of reactants were dissolved sequentially in this medium : sodium chloride (24 mg/ml; 410 mM), magnesium chloride (4 mg/ml; 20 mM), potassium chloride (2.8 mg/ml; 37.5 mM). The lead ammonium citrate acetate complex (Sigma) was dissolved, with constant shaking, in the smallest volume of dilute ammonia (5 drops of 0.88 ammonia per ml) to give a final concentration of 32 mg/ml. The final pH used initially was 7.5 adjusted by the addition of either of a mixture of sodium and potassium hydroxides (10: 1 on a molar basis; 2.5 mM) or of 0.1 M hydrochloric acid.

The first experiment was to use different concentrations of ATP based on four times the concentration used by Schwartz et al (1971), to obtain the optimum

concentration for this reaction. It was also essential to show that the reaction was ouabain-sensitive. Serial sections were treated with the same medium containing 0.4 mM (0.3 mg/ml) ouabain (ouabain octahydrate; Sigma). The different concentrations of ATP used were 0, 5, 10, 15, 20 mg/ml. The reaction was done at 37° C and it was found that a time of 15 minutes was required to give sufficient reaction-product for accurate quantification. The sections are then rinsed in Coplin jars, in several changes of 0.2 M Tris buffer, pH 7.4, at 37° C to remove all the Polypep. They were then immersed, at room temperature, in water that had been saturated with hydrogen sulphide (1 - 2 min). They were then rinsed several times in distilled water and allowed to dry. They were mounted in the Z5 medium that is based on polyvinyl alcohol (Zaman and Chayen, 1981).

The reaction-product is assumably lead sulphide and was measured by means of a Vickers M85 microdensitometer, with a x40 objective, at 585 nm (since this gave best discrimination from the background), and with a flying-spot of 0.4 μm diameter in the plane of the section. The size of the mask allowed measurement of the reaction-product in one cell. By suitable calibration (Chayen 1978 (a), (b); Bitensky, 1980) the microdensitometric readings were expressed as the mean ± SEM of the integrated extinction. In general, duplicate sections were measured, with 10 or 20 cells from different regions of the nephron being measured in each section. L-p-

bromotetramisole oxalate (Aldrich; 0.4 mM) was included in both reaction mediums i.e. with and without ouabain, to prevent interference by alkaline phosphatase activity. The reaction-product was found on the contralumenal boundary of the tubule cells and was decreased when ouabain was included in the reaction-medium.

Optimal concentration of ATP. This was examined in the thick ascending limbs (TAL) of the loop of Henle. With the full reaction-medium, the optimal concentration for total activity was 10 mg/ml (Fig. XI.1). The activity of the ouabain-insensitive activity was increased by 5 mg/ml but was unchanged by higher concentrations. Subtraction of the results for these two activities gave the activity of the ouabain-sensitive ATPase, i.e. the Na^+- K^+-ATPase. Such subtraction indicated that the optimal concentration of ATP for this enzyme was 10mg/ml (17 mM). Conditions for optimal pH are shown in Fig. XI

Specificity. Very low activity was found when ATP was replced, at approximately equimolar concentrations (10 mg/ml), by either adenosine diphosphate or tri-sodium guanosine 5'-triphosphate (Fig. XI.3). When the sodium and potassium chloride were excluded from the reaction-medium, the total activity and the ouabain-sensitive activity were depressed, with the ouabain-insensitive activity being unaffected. It is probable that the residual ouabain-sensitive activity was due to the sodium/potassium hydroxide used to establish the final pH, and to endogenous ions within the section. The addition of L-p-bromotetramisole oxalate (0.4 mM;

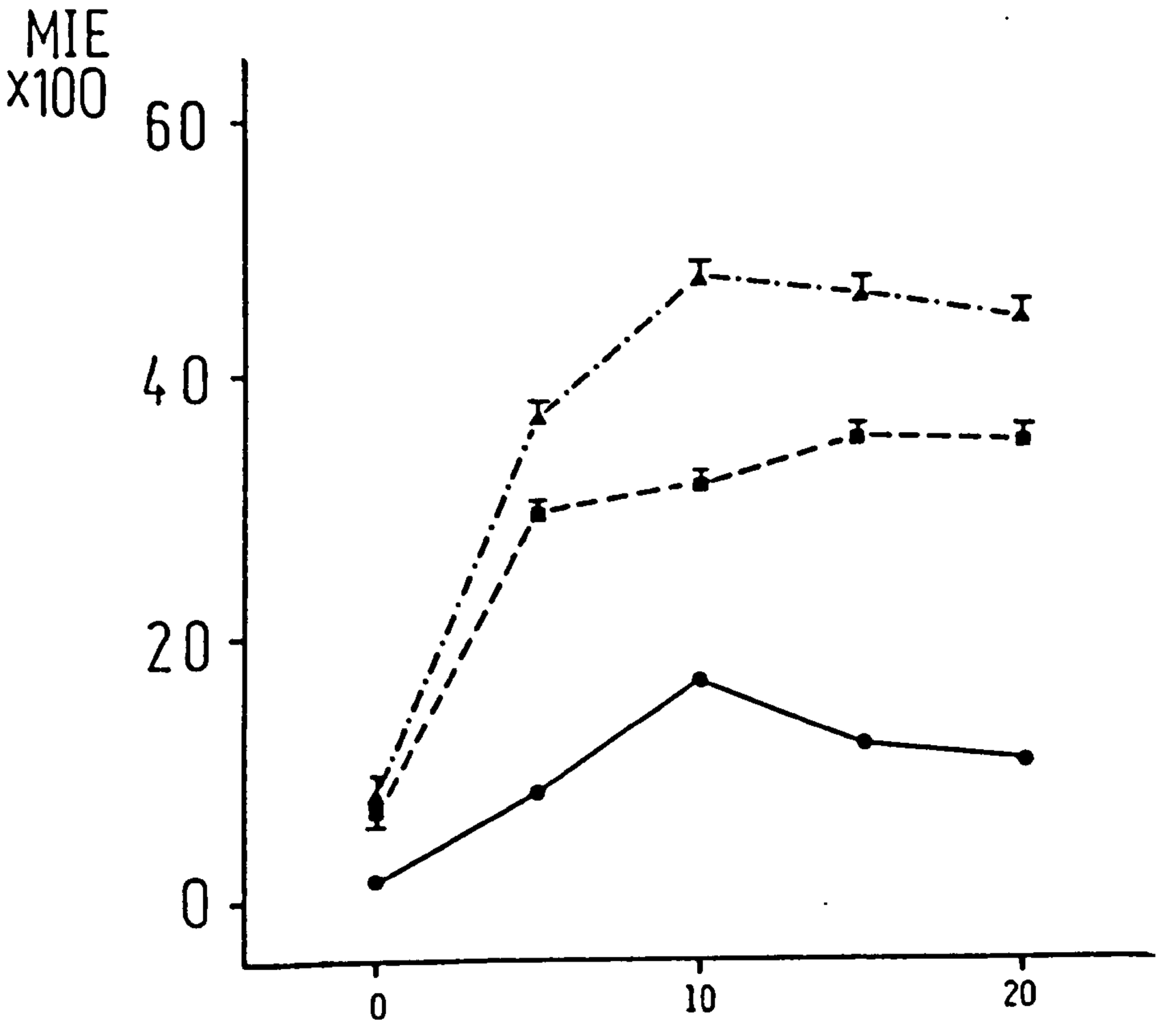

Fig. X1. 1 The effect of increasing concentrations of ATP on the activity of (MIE x 100; mean ± SEM) of total ATPase (triangles) and ATPase in the presence of ouabain (squares) measured in the cells of the thick ascending limb of the loop of Henlé (TAL). The Na^+-K^+-ATPase activity (calculated by subtraction) is shown by the solid line.

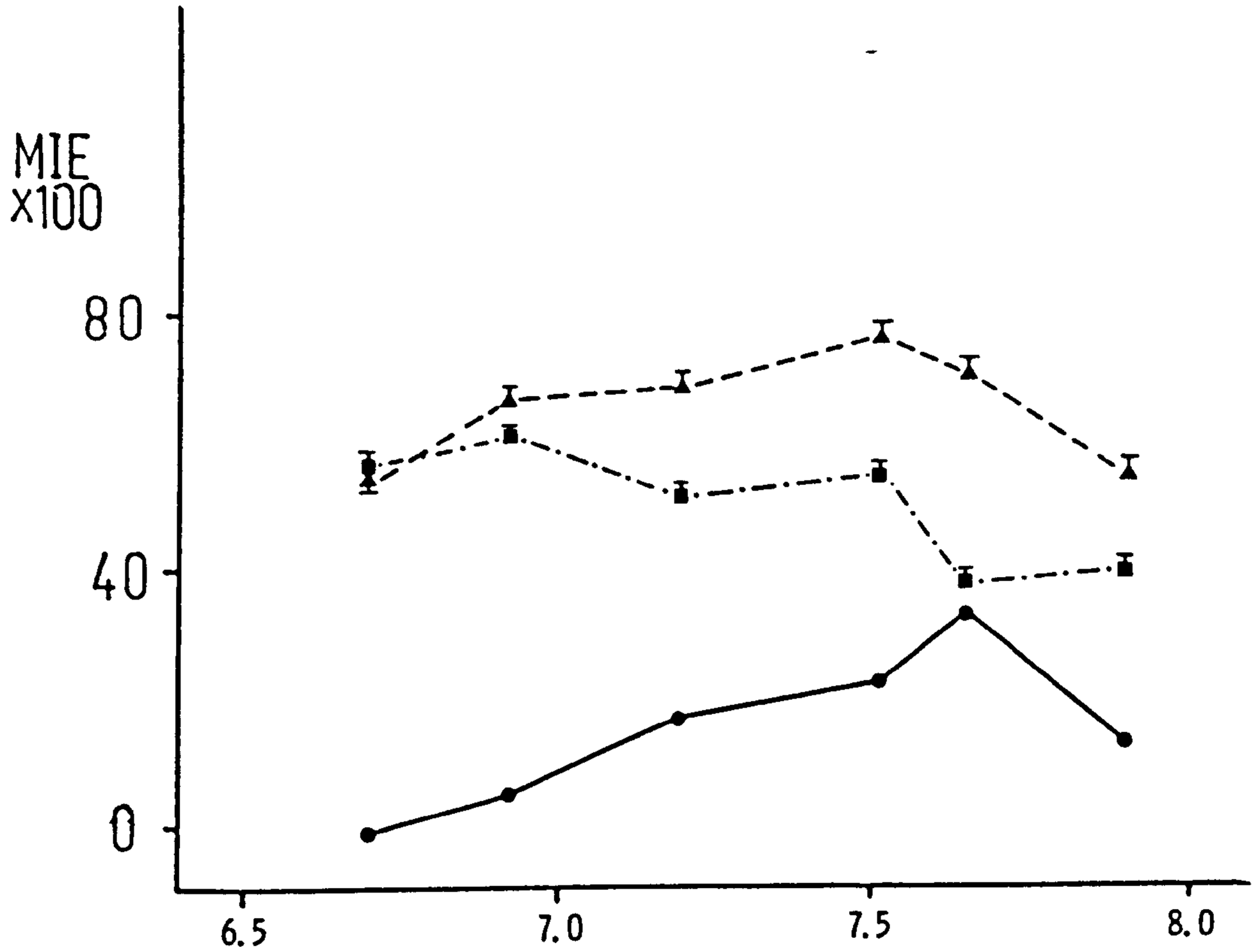

Fig. XI. 2 The effect of pH on the activity (MIE x 100; mean ± SEM) of total (triangles) and ouabain-insensitive (squares) ATPase activity in TAL; Na^+-K^+-ATPase activity is shown by the solid line.

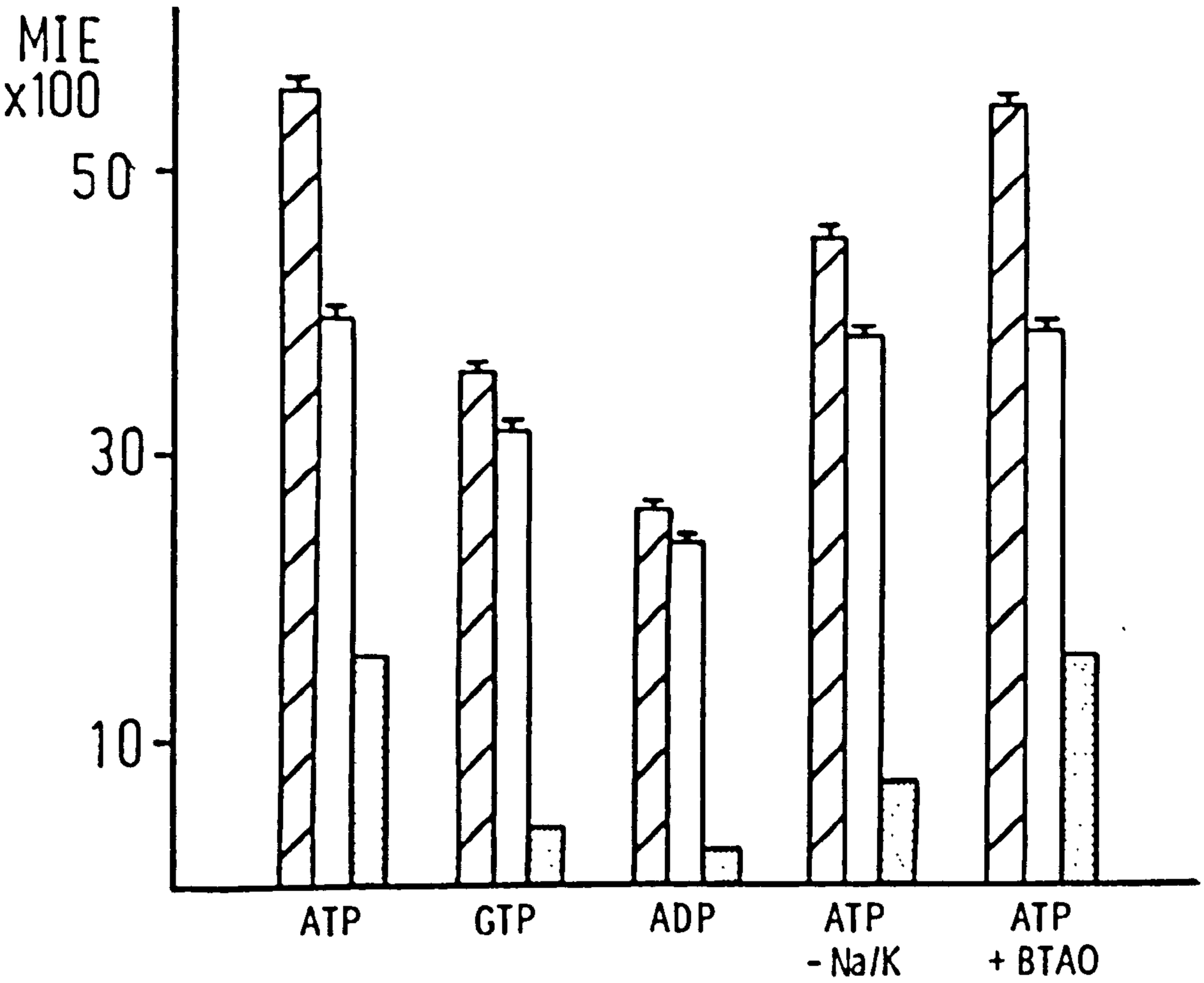

Fig. XI. 3 Histograms of the activity MIE x 100; mean ± SEM) in TAL of total (hatched columns), ouabain - insensitive (open-columns) and Na^+-K^+-ATPase activity in the presence of adenosine triphosphate (ATP); guanosine triphosphate (GTP); adenosine diphosphate (ADP); ATP without added Na^+ or K^+; and ATP but in the presence of bromotetramizole.

0.15 mg/ml), to inhibit alkaline phosphatase, did not affect the measured Na^+- K^+- ATPase activities in this region of the nephron.

Linearity of response. The activities, in the same region of the nephron, measured in serial sections, were linear with thickness of the sections from 5 - 20 µm (Fig. XI.4) and with time, for at least 20 minutes.

Activities in other regions of the nephron. As discussed previously, earlier methods did not demonstrate Na^+- K^+- ATPase activity in proximal tubules. Using this new technique, in both the rat and the guinea pig, total and ouabain-sensitive Na^+- K^+-ATPase activity was found on the contra-lumenal boundary of the cells of proximal convoluted tubules (characterized by the lumenal alkaline phosphatase activity). Activity was also found on the contra-lumenal boundary of the cells of the distal convoluted tubules and in the cells of tubules that were grouped in clusters at the cortico-medullary boundary and extended into the medulla (Fig. XI.5) Following Beeuwkes and Rosen (1975), these last tubules were taken to be the thick ascending limbs (TAL) of the loop of Henle.

Comparison of results with other assays. Measurements were made of the total and the ouabain-sensitive Na^+- K^+- ATPase activities, at various times, in cells in these three regions, in seven guinea-pigs (part of this work was done by J. Pitchfork). The total activity (15 minutes reaction time; mean integrated extinction x100; mean ±SEM)

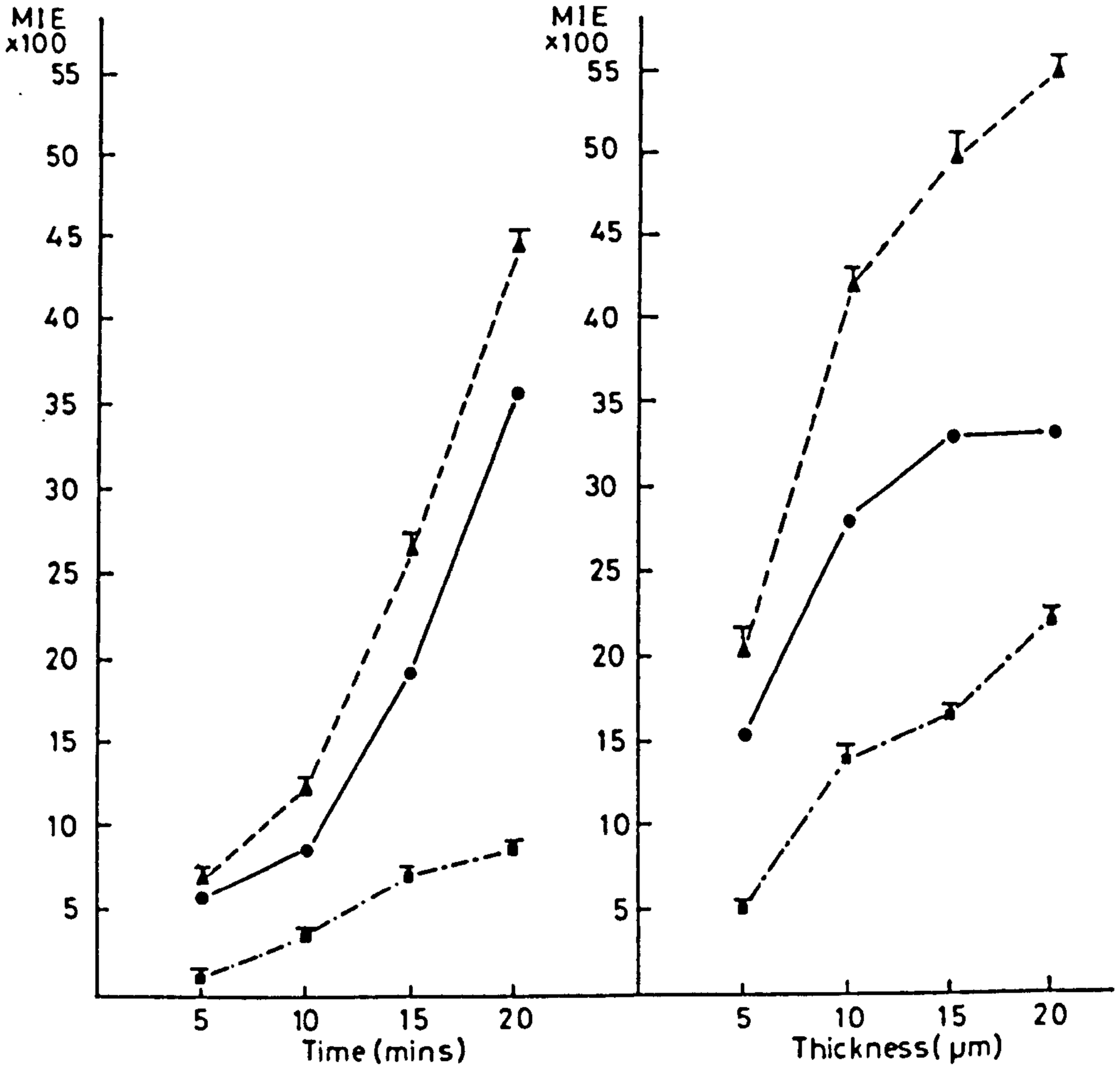

Fig. XI. 4 The effect of time or thickness on the activity (MIE X 100; mean ± SEM) in TAL of total (triangles) and ouabain-insensitive (squares) ATPase activity; Na^+-K^+-ATPase activity is indicated by the solid line.

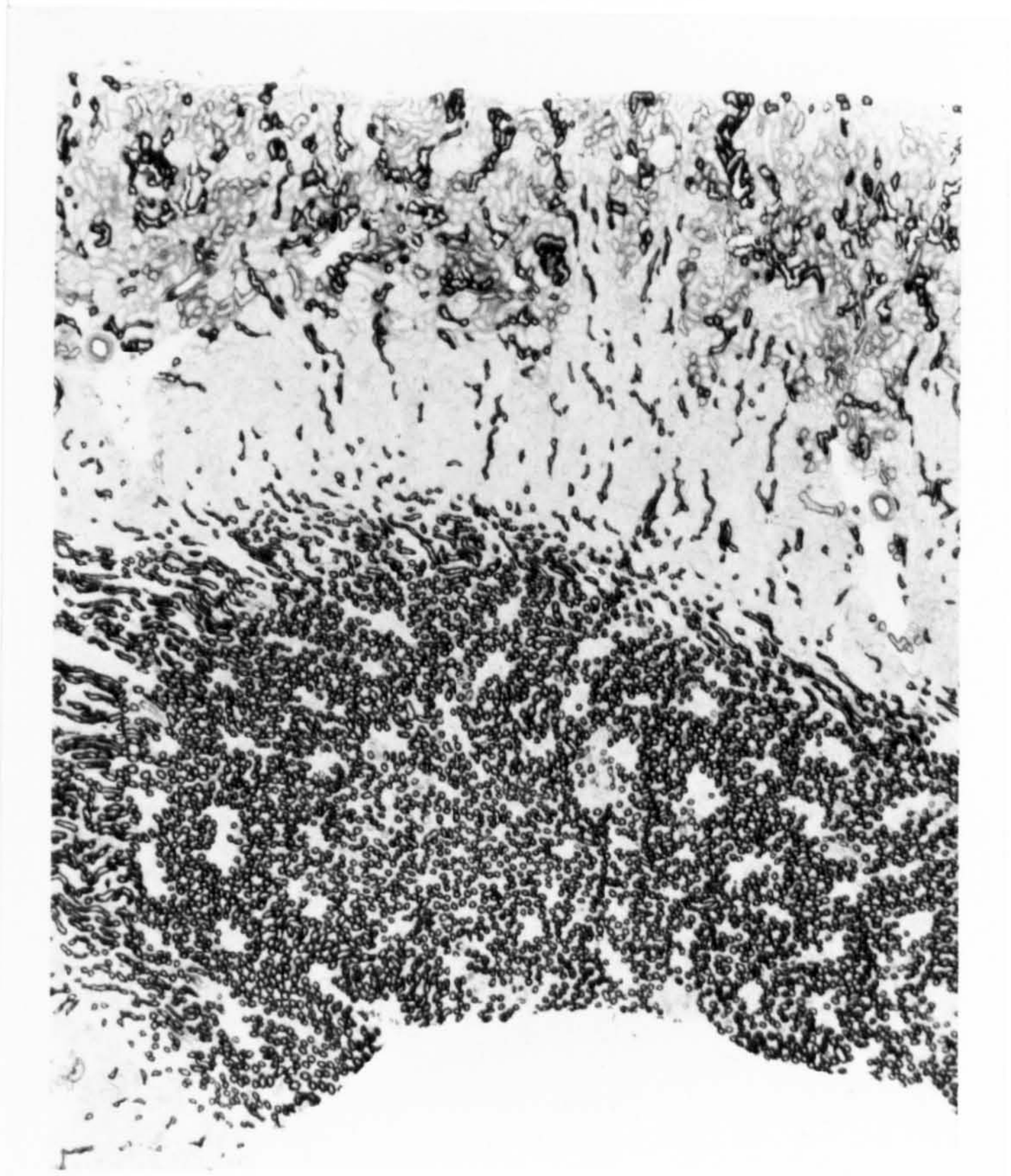

Fig. XI. 5 Photomicrograph of total ATPase activity in a cryostat section of rat kidney showing strong activity in small clusters of distal convoluted tubules in the cortex and moderately strong activity in the tubules at the cortico-medullary junction (TAL) X 21.

in the proximal convoluted tubules was 12.4 ± 1.1. In the distal convoluted tubules and in the TAL, the total activity was 29.5 ± 4.2 and 33.8 ± 2.8 respectively (Table XI.1). The ouabain-insensitive activity, measured in duplicate sections that were reacted with the same reaction medium with added ouabain, gave activities of : proximal convoluted tubules 7.5 ± 1.2; distal convoluted tubules 13.2 ± 2.7 ; and TAL 15.9 ± 2.3. The percentage of the total activity that was represented by the ouabain-sensitive Na^+- K^+- ATPase was then calculated. The activities were 41%, 58% and 54% respectively.

To compare this study with that done by Katz et al (1979), the concentration of ouabain was increased from 0.4 mM to 1 mM. The results for total activity (mean integrated extinction x100; mean ± SEM), in the presence of bromotetramizole were as follows: proximal convoluted tubules, 9.2 ± 1.2; distal convoluted tubules 25.4 ± 2.8; and TAL 16.9 ± 2.2. The percentage of the total activity that was due to ouabain-sensitive Na^+- K^+- ATPase activity was calculated as 38%, 60% and 64% (Table XI.1) in the proximal convoluted tubules, the distal convoluted tubules and in the TAL respectively.

Background problems. In all these studies using this method for assaying Na^+- K^+- ATPase there was always a strong background colouration on the section. Under the microscope this background colouration appeared to sit above the section, making the measurement, at times, very difficult. It was envisaged that the "fuzz"

Table XI. 1. The activity (mean integrated extinction) of total ATPase, ouabain-insensitive and -sensitive ATPase in three regions of the guinea-pig and rat nephron.

	Total	Ouabain insensitive	Ouabain sensitive	%
Prox	12.4 ± 1.06	7.5 ± 1.18	4.9 ± 0.59	41% ± 5.8
Dist	29.46 ± 4.24	13.15 ± 2.65	16.3 ± 2.49	58% ± 5.9
T.A.L.	33.8 ± 2.8	15.94 ± 2.28	17.9 ± 1.79	34% ± 4.8

n = 7 guinea pigs : [ouabain] 0.4mM

Prox	9.2 ± 1.2	5.7	3.5	38%
Dist	25.4 ± 2.8	10.16	15.24	60%
T.A.L.	16.9 ± 2.2	6.08	10.82	64%

n = 1 rat : [ouabain] 1mM

might have been due to deleterious effects produced by the last three stages of the reaction, namely (i) the rinse in 0.2M Tris buffer at pH 7.4 used to remove the reaction-medium; (ii) the immersion in distilled water that had been saturated with H_2S to blacken the lead deposit; and (iii) the final rinse in distilled water. Many variants of these were tested (Fig. XI.6) but all were unsuccessful. Consequently attention was focussed on the earlier stages of the procedure and it was realized that the "background" colouration might be caused by free phosphates that were being retained in, or close to, the sections by the stabilizer. Thus the next step was to rinse the sections before actually pouring the reaction medium onto the section. A 40% solution of Polypep 5115 containing 1 mM potassium acetate in 0.2 M Tris buffer at pH 7.4, was poured onto each section (potassium phosphate being very soluble). This medium was sucked-off after 5 minutes. A little of the full reaction-medium was added to each section, and then sucked off again to ensure adequate replacement of the initial Polypep medium. Then the full reaction-medium was added. After the reaction, the sections were immersed in distilled water saturated with H_2S and the final rinse was done with distilled water. This pre-rinse in Polypep proved very successful and is now done routinely. The background colouration was almost completely removed and the artifact that was observed i.e. the colouration sitting above the section disappeared. The relative activities were

unaltered by the rinsing procedure.

Discussion

The enzymes which hydrolyze ATP are of considerable importance in normal cell-function. These include the mitochondrial ATPases, myosin ATPase activity of muscle, and the various ATPases of the cell surface. Initially it might have been hoped that the procedure of Wachstein and Meisel (1957) could have been used to demonstrate all these enzymes. However, the free lead ions used in this method inhibited the enzymes and hydrolyzed, non-enzymatically, the ATP used as substrate. A huge controversy grew up over the validity of the procedure (as reviewed by Ernst, 1972a; Ernst et al,1980). As regards the Na^+- K^+-ATPase activity that is associated with cell membranes, and to avoid the disputed arguments over the validity of the use of lead ions as trapping agents, Ernst (1972a,b) and Guth and Albers (1974) turned to methods for demonstrating the K^+-dependent phosphatase activity. This is related to Na^+- K^+-ATPase activity in that the hydrolysis of ATP by the Na^+- K^+-ATPase is believed to proceed in at least two steps involving a sodium-dependent phosphorylation (Hokin and Dahl, 1972). However, there is considerable evidence that the K^+-dependent phosphatase, responsible for the phosphorylation, is not specific to the phosphorylated intermediate but can act on a variety of phosphate esters (as reviewed by Ernst, 1972a). Beeuwkes and Rosen (1975, 1980) used a modified form

of Ernst's (1972a,b) paranitrophenyl phosphate (PNPP) method ; following Guth and Albers (1974) they relied on the rather inefficient (Ernst et al, 1980) capture of the liberated phosphate by magnesium and potassium ions. They did, however, show clear differences in activities in the various parts of the nephron, both by visual inspection and by the use of electron probe analysis to quantify the amount of reaction-product produced in each region. They found high activities in the distal convoluted tubules and in tubules which they considered to be the thick ascending limbs (TAL) of the loop of Henle. These activities were in agreement with microchemical results done after microdissection of the nephron (e.g. Schmidt and Dubach, 1969).

The disadvantages of the PNPP method were: (i) it was indirect, measuring the K^+-dependent phosphatase activity that was generally, but not necessarily, related to the Na^+- K^+-ATPase activity; it was of concern that the K^+-dependent phosphatase was not specific for the phosphorylated intermediate generated by Na^+- K^+-ATPase activity; (ii) it did not demonstrate the Na^+- K^+-ATPase activity that was known, from biochemical studies, to be present in the proximal convoluted tubules; thus it was unlikely to be of value in the study of less active ATPases in cells in which this activity was not as great as it is in the distal convoluted tubules and TAL.

The new method has reverted back to the Wachstein and Meisel method but has overcome its deficiencies by

ensuring that there are no free lead ions in the reaction-medium. In the lead ammonium citrate/acetate complex, the lead is hidden (and so made soluble in neutral and alkaline solutions) by ammonium citrate. Thus when it is added to a solution of ATP, the solution remains crystal-clear. However free phosphate, generated by enzymatic hydrolysis, successfully competes with the ammonium citrate moieties and precipitates lead phosphate, which can be converted to the brown-black lead sulphide. With this trapping agent, the enzymatic activity was linear with thickness (amount of enzyme) and with time. The activity increased with increasing concentration of the lead ammonium citrate/acetate up to the concentration used in the present method. There was no inhibition of activity with higher concentrations. The pH optimum was pH 7.6. This is close to that reported for 'microsomal preparations' that include the cell membrane (Pérez-González de la Manna et al, 1980). The reaction was also specific for ATP and was not influenced by the potent inhibitor (Borgers and Thoné, 1975) of alkaline phosphatase, bromotetramizole.

The reaction-product was precipitated along the contra-lumenal boundary of the cells. This is the expected location of the enzyme (Beeuwkes and Rosen, 1975, 1980; Pérez-González de la Manna et al, 1980; Ernst et al, 1980). In the guinea-pig and the rat it was found in greatest concentration in the TAL and in the distal convoluted tubules. It was appreciably

less in the proximal convoluted tubules. These findings agree with those of Katz et al (1979) who assayed ATPase activities microchemically in regions of the nephron of the rat, mouse and rabbit. However, the results of Katz et al (1979) were expressed in terms of picomoles of ATP hydrolyzed per millimetre length of the region of the nephron per hour and cannot be directly related to these cytochemical measurements which give the concentration of the activity per cell. Nonetheless the proportion of the total activity that was due to the specific, ouabain-sensitive, Na^+-K^+-ATPase activity should be similar, whether measured microchemically or cytochemically. In the rat, Katz et al (1979) found that the proportion of the total activity that was due to Na^+-K^+-ATPase activity was 51% (proximal convoluted), 76 - 78% (TAL) and 65% (distal convoluted tubules). The results with the new method were 38%, 64% and 60% respectively. The relative values of the total activity in the three regions were also similar: taking the total ATPase activity of the distal convoluted tubules as 100, the activity in the proximal convoluted tubules, found by Katz et al, was 44 (in comparison with 36 in the present study), and that in the TAL was 59 (as against 66 in the present study). Therefore, these results indicate that the present method, based on a hidden-lead trapping agent, can measure ouabain-sensitive ATPase activity, with relative values in different regions of the nephron

that generally conform with results obtained by micro-chemical methods. The advantages of this presentmethod are that it affords a direct measurement of ATPase activity, rather than depending on the related, or associated, K^+-dependent phosphatase activity. It also seems to be more sensitive than previous methods, as shown by the measurement of activity in the proximal convoluted tubules. It should be possible to adapt this present method to the measurement of a wide range of ATPase activities, such as calcium-dependent ATPase, mitochondrial ATPases and possibly even adenyl cyclase activity.

Recent studies using the new method.

(a) A new bioassay of arginine vasopressin, namely the antidiuretic hormone, has been developed (Bayliss et al, 1980) using the method described in this chapter. It depends on the finding that the Na^+-K^+-ATPase activity, measured in the TAL of the loop of Henlé in rat renal tissue maintained in vitro, responded to increasing concentrations of synthetic arginine vasopressin in a log-dose related fashion.

(b) There is a lot of evidence (e.g. Dikstein, 1971), that inhibition of Na^+-K^+-ATPase is associated with the stimulation of glucose 6-phosphate dehydrogenase, the rate-limiting enzyme in the pentose phosphate pathway. Work done by Fenton et al (1981) has developed a highly

sensitive cytochemical assay that shows the capacity of biological fluids to stimulate renal glucose 6-phosphate dehydrogenase activity in vitro as a marker of their ability to inhibit Na^+-K^+-ATPase activity.

CHAPTER XII

GENERAL DISCUSSION

Problems Concerning the Oxidative Metabolism of Bone.

Although the electrical and biochemical properties of bone have been studied extensively, relatively little work has been done on its biochemistry and general metabolism. This is due largely to the physical nature of bone which is relatively difficult to examine by the procedures of conventional biochemistry. However it was shown, in this laboratory, that thin (e.g. 10 μm) sections of fresh, undemineralized adult bone could be cut with a heavy duty microtone set in a cryostat and equipped with a tungsten-carbide tipped knife (Johnstone et al, 1972; Johnstone, 1976). Consequently bone could now be examined for metabolic and other biochemical features by virtually the same methods of cytochemical analysis as have been used previously for soft tissues.

Studies on the oxidative metabolism of bone were facilitated by the development (by Dr. G.T.B. Frost, for this laboratory) of a new substrate for assaying hydroxyacyl dehydrogenase (HOAD) activity. This enzyme is involved in the β-oxidation of fatty acids and so made possible, cytochemically, the investigation of fatty acid oxidation (Chapter VI). Thus for the first time it was possible to show that bone is capable

of this type of oxidation, with the implication that fatty acids may constitute a considerable source of energy for bone cells. This may have much wider implications in bone pathology. However, the immediate consequence of this finding was that it became possible to suggest the mechanism of the apparent paradox of 'aerobic glycolysis' in bone. Thus by assaying maximal activities of certain key-enzymes, it was apparent that such fatty acid oxidation could supply the needs of the Krebs' cycle and direct the conversion of pyruvate to lactate, even at high oxygen tensions (Chapter VI).

In studying the general oxidative metabolism of bone, in particular in fracture-healing, increased activity of glucose 6-phosphate dehydrogenase was a prominent feature. There is considerable evidence (discussed in Chapter XI) of an inverse relationship between this activity and that of Na^+-K^+-ATPase. There were many reasons why the latter could not be investigated cytochemically. Yet this is such an important enzyme for the normal function of cells that it was worthwile trying to overcome the obstacles to its assay. This was done by the development (by Dr. G.T.B. Frost) of a 'hidden-capture' reagent (as described in Chapter XI). The drawback to the use of this method on sections of bone has been the propensity of the 'hidden' lead to react with the free phosphate of bone. It is likely that this can be overcome by reacting the sections first with material that will bind to these phosphates,

but that is a problem for the future.

Fracture-healing and the Vitamin K_1-cycle

The earlier studies on the metabolism of fracture-healing by Dunham et al (1977) demonstrated that the closed fracture of the metatarsal of the Wistar rat formed a useful and remarkably reproducible model for studying the major changes that occur during fracture-healing. The response to fracture involves both active cell proliferation and biosynthesis of extra-cellular material.

Subsequent to these earlier studies on fracture-healing, it was found (Hauschka et al, 1978) that mineralization might involve the γ-carboxylation of glutamate residues in existing proteins. This γ-carboxylation is produced by the vitamin K_1 cycle, with NADH or NADPH as the reductant, and results in calcium-binding γ-carboxyglutamate (Gla) residues (Fig. III.2).

Although much attention has been focussed on osteocalcin, or on the bone Gla-protein, and although such studies have generated considerable controversy (as discussed in Chapter III), there seems little doubt that the formation of Gla-residues, by the action of the vitamin K_1-cycle, plays an essential role in the formation of new bone. It is fortunate that the function of this cycle can be demonstrated by feeding animals with the anticoagulant Warfarin, or related substances, which inhibit the conversion of the vitamin K epoxide back

to the naphthoquinone, so breaking the cycle (Whitlon et al,1978). However, such experiments have yielded confusing results due largely to the various experimental designs used by the different workers (and as discussed in Chapter III). Thus it seemed advisable to re-examine the effect of such compounds, and so the significance of the vitamin K_1-cycle, in a well studied system (Chapter VIII). For this, I used the closed fracture of the metatarsal in the rat, as had been investigated in some detail by Shedden et al (1976) and by Dunham et al (1977). Since it seems to be virtually impossible to deplete rats of vitamin K_1, I used dicoumarol to inhibit the vitamin K_1-cycle.

The immediate difficulty in using this model was the finding that the Wistar rats used in the model described by Shedden et al, 1976, proved too sensitive to dicoumarol. Consequently, for these studies, male Sprague-Dawley rats were used as they were found to be more resistant to the anticoagulant effect. However, this entailed investigating fracture-healing in this rat to ensure that it was equally reproducible. Chapter VII describes the fracture-healing process and the associated metabolic changes, in the Sprague-Dawley rat, comparing it directly to the earlier work done on the Wistar rat by Shedden et al (1976) and Dunham et al (1977). It compared very closely, both histologically and metabolically, with the Wistar rat model

except that the bones healed considerably faster in the Sprague-Dawley and in all cases the callus was larger on the dorsal side than that on the plantar side in the Sprague-Dawley rats. As in the study by Dunham and colleagues (1977) interest was centred on the activity of glucose 6-phosphate dehydrogenase (G6PD). G6PD is important for supplying NADPH, to be used as the source of reducing equivalents in many biosynthetic reactions, and in producing ribose phosphate for nucleic acid synthesis. As in the study by Dunham et al (1977) there was a striking elevation of periosteal G6PD activity in response to the fracture both at the site of periosteal proliferation and, later, at the site of formation of new bone, suggesting that NADPH plays a role both in the periosteal proliferation to form the callus and in the process of new bone formation on the shaft of the bone.

When dicoumarol was fed to the Sprague-Dawley rats (immediately after fracture) the ossification of the callus was severely retarded. Dicoumarol also decreased G6PD activity selectively at points at which ossification occurred. Thus, not only could dicoumarol be acting as an antagonist of the vitamin K cycle but it also depressed the amount of reducing equivalents, from NADPH, available for the cycle at these points of ossification.

Possible Mechanism of G6PD Activation

The increase in G6PD activity therefore seemed to be fundamental to the process of fracture-healing. Thus it seemed important to investigate the mechanism by which this increase is brought about. From other studies in progress in this laboratory, it seemed possible that G6PD activity may be stimulated by the formation of the polyamine precurser, putrescine, from ornithine decarboxylase (ODC) activity (fully described in Chapter IV). ODC activity is readily stimulated by many hormones acting on their target cells (Bachrach, 1980) so it is possible that the trauma of fracture might act similarly. G6PD can exist in an active aggregated form or it may dissociate into inactive units: by binding to the enzyme at non-catalytic sites, $NADP^+$ can hold the enzyme in this active state (as reviewed by Bonsignore and de Flora, 1972; Chayen and Bitensky, 1982), allowing for a rapid response to stimuli. So it was possible that a positively charged polyamine (such as putrescine) might take the place of $NADP^+$ at these non-catalytic sites. Consequently, a study was made to investigate whether the increased periosteal G6PD activity, observed early in fracture-healing, could be inhibited by inhibiting ODC activity and thus decrease the tissue levels of polyamines(Chapter IX). ODC activity is dependent on the co-enzyme pyridoxal phosphate (vitamin B_6) and it has been demonstrated (Eloranta et al, 1976; Pegg, 1976) that young Wistar rats can be made deficient

in polyamines if fed on a B_6-deficient diet (described in Appendix 3). Thus male Wistar rats (50 g) were fed on a B_6-deficient diet (control rats were fed a similar diet supplemented with B_6) before and after their metatarsals were fractured. A detailed histological and metabolic investigation was made (Chapter IX). The results of these studies conformed with the view that ODC activity might regulate G6PD activity. Thus, of all the enzymes tested only G6PD activity was markedly decreased in the various cell types of the forming callus. This decreased G6PD activity, necessary for proliferation and for bone formation, was also reflected in bizarre histological changes found in the B_6-deficient fractures. The callus appeared flattened and there was a decrease in new bone formation. There was also massive invasion of the periosteum and endosteum into the shaft of the bone and partial replacement of cortical bone by woven bone, producing bone that was remarkably similar to that found in human osteoporosis.

Studies on Osteoporotic Fractures

Osteoporotic fracture of the hip in the elderly is a significant social and medical problem. The fractures are often induced by minimal trauma in osteoporotic patients, and the aim of the study in Chapter X was to try to elucidate the increased susceptibility of the neck of femur to fracture in these osteoporotic

subjects. Inspection of the sections taken from the fracture-site showed the appearance of unexpectedly large crystals, apparently of apatite. The presence of such large crystals, much larger than have been reported from the many cryostallographic studies in normal bone, could account for the increased tendency to fracture: in this respect, these osteoporotic fractures of the neck of femur might resemble the fatigue fractures of metals. However the fundamental question was what caused the growth of such large crystals.

Previous enquiries had focussed on possible roles for the collagen matrix. This was readily examined because the collagen fibres show form birefringence. However it was shown (Chapter X) that the orientation (as measured by the birefringence) of the collagen was unchanged in the fractures. At the time this work was started, there was only scanty information as regards the orientation of the glycosaminoglycans (GAGs) which do not show form-birefringence. However, by making use of the potentially birefringent properties of Alcian blue, a method of 'induced birefringence' was developed. The results showed firstly that the GAGs of normal bone were closely orientated to the collagen, and secondly that, although the total content of GAGs was unaltered, they were relatively disorientated in the osteoporotic bone, even at a considerable distance from the fracture (Chapter X).

Appendix 1

Methods for Determining Enzyme Activity

1. Glucose 6-phosphate dehydrogenase

The reaction medium contained NADP (3 mM; 2.5 mg/ml); glucose 6-phosphate (5 mM; 1.5 mg/ml); chloroform-purified neotetrazolium chloride (5 mM; 0.3%; 0.6% in Chapter VI) in a 30% (w/v) solution of polyvinyl alcohol (grade G04/140) in 0.05M glycylglycine buffer (pH 8.0). The final reaction medium was adjusted to pH 8.0 and saturated with nitrogen before and during use. Phenazine methosulphate (0.7 mM; 0.2 mg/ml) was added to this medium just before use and the sections incubated at 37°C. Perspex rings surrounding the sections were used to contain the reaction medium and the slides were placed in an incubation chamber. The reacted sections were rinsed well with distilled water and mounted in Farrants' medium prior to measurement.

2. Lactate dehydrogenase

The reaction medium contained NAD (2.5 mM; 1.75 mg/ml); sodium lactate (60 mM); chloroform purified neotetrazolium chloride (5 mM; 0.3%; 0.6% in Chapter VI) in a 30% (w/v) solution of polyvinyl alcohol (grade G04/140) in 0.05 M glycylglycine buffer (pH 8.0). The pH of the final reaction medium was adjusted to pH 8.0 and saturated with nitrogen before and during use. Phenazine methosulphate (0.7 mM; 0.2 mg/ml) was added to this medium just before use and the sections incubated at

37°C. The reacted sections were rinsed in distilled water and mounted in Farrants' medium.

3. Glyceraldehyde 3-phosphate dehydrogenase

The reaction medium contained NAD (1.5 mM; 1 mg/ml); aldolase (10 units per ml); fructose 1-6-diphosphate, trisodium salt (5 mM; 3 mg/ml); chloroform-purified neotetrazolium chloride (5 mM; 0.3%; 0.6% in Chapter VI) in a 30% (w/v) solution of polyvinyl alcohol (grade G04/140) in 0.05 M glycylglycine buffer (pH 8.0). The pH of the final reaction medium was adjusted to pH 8.5 and saturated with nitrogen before and during use. Phenazine methosulphate (0.7 mM; 0.2 mg/ml) was added to this medium just before use and the sections incubated at 37°C. The reacted sections were rinsed in distilled water and mounted in Farrants' medium.

4. Succinate dehydrogenase

For demonstrating succinate dehydrogenase activity, which is tightly bound within the mitochondria, the reaction medium contained chloroform-purified neotetrazolium chloride (0.6%) in a 0.1 M phosphate buffer, pH 7.8. Sodium succinate (50 mM; 13.6 mg/ml) was added and the solution saturated with nitrogen before and during use. Phenazine methosulphate (0.7 mM; 0.2 mg/ml) was added to the medium and the sections incubated in a Coplin jar at 37°C. The sections were rinsed in distilled water and mounted in Farrants' medium.

5. Alkaline phosphatase: The Naphthol-phosphate Method.

The reaction medium contained a 10% solution of magnesium chloride, $MgCl_2 6H_2O$ (0.2ml); α naphthol acid phosphate sodium salt (2 mg) in a 2% solution of 5,5 diethylbarbiturate (50 ml). The pH of the medium was adjusted to pH 9.2 and Fast blue RR salt (50 mg) added just prior to use. The reaction was done at room temperature (25°C) in a Coplin jar.

6. β -Hydroxy acyl CoA dehydrogenase

7. Na^+K^+-ATPase

The methods for determining these enzyme activities are described fully in Chapters VI and XI respectively.

Appendix II

Cytochemical Demonstration of Ornithine Decarboxylase

It has proved considerably difficult to demonstrate the products of ornithine decarboxylase (ODC) activity cytochemically. This is because it is unlikely that a way will be found of specifically precipitating the decarboxylated substrate (putrescine), and it is not easy to precipitate the other product of the reaction (CO_2) at the pH at which the enzyme works optimally (about pH 7.1). Consequently histochemical procedures have concentrated on localizing the site of the enzyme itself. Two types of method have been suggested:

1. Use of a labelled suicidal enzyme inhibitor, namely α-difluoromethylornithine (Gilad and Gilad, 1981; Pegg et al, 1982a).

2. Immunohistochemistry (Persson et al, 1982). Both methods are reviewed by Dodds and Chayen (1984).

Preliminary studies towards a quantitative cytochemical method

Neither method mentioned gives quantitative results and are not likely to be able to define changes in ODC activity. Consequently there is a real need for a quantitative cytochemical demonstration for ODC.

In normal cytochemistry, the activity of an enzyme such as a phosphatase or decarboxylase would be measured by precipitating the smaller moiety released, namely either phosphate or, in this case, carbon dioxide. With metal capture reactions, where the metallic ion may be inhibitory to the enzyme, care has to be taken to ensure that the precipitating ion should be sequestered from the active site of the enzyme (Chayen et al, 1981). It was found by Dr. G.T.B. Frost (personal communication) that lead, in the form of lead hydroxyisobutyrate, is sufficiently chelated not to inhibit the enzyme, but can be precipitated, apparently as lead carbonate, by CO_2 at neutral pH. All the solutions have to be prepared in CO_2-free water and care must be taken not to introduce other ions that might compete successfully against the hydroxyisobutyrate.

At present, the provisional method, outlined below, seems to yield a quantitative estimation of ODC activity in the mouse kidney.

Reaction - medium

All solutions have to be prepared in CO_2-free water. To three volumes of 0.2 M triethanolamine buffer, pH 8.0, containing 40% G04/140 grade of polyvinyl alcohol (PVA) (Wacker Chemicals, Mount Felix, Bridge Street, Walton-on-Thames, KT12 1AS, UK) is added 1 volume of the solution of lead hydroxyisobutyrate (17.85% Pb); L-ornithine, 3.4 mg/ml; pyridoxal phosphate, 0.62 mg/ml; D,L-dithiothreitol, 0.08 mg/ml; L-p-bromotetramizole, 0.15 mg/ml (to inhibit alkaline phosphatase acting on the pyridoxal phosphate). The final pH should be adjusted, if necessary, to pH 7.1. Before incubating the sections in this reaction-medium, a pre-rinse is required to remove 'background' colouration, possibly caused by free phosphates retained in, or close to, the sections, by the stabilizer (as discussed in Chapter XI). The pre-rinse consists of 0.2 M triethanolamine buffer, pH 8.0, containing 20% G04/140 PVA. The final pH is 7.1. This medium is poured into Perspex rings surrounding the sections and left for 10 minutes at 37°C after which time it is sucked off and replaced by the reaction-medium.

Procedure

1. Incubate in the full reaction-medium at 37°C (sections of unfixed mouse kidney may require 10 - 30 min).

2. Wash in CO_2 - free water.

3. Immerse in 0.5% aqueous solution of ammonium sulphide (1 min).

4. Rinse in distilled water.

5. Mount in Farrants' medium.

Measurement

The reaction-product is measured by microdensitometry at 580 nm, with a x40 objective and a flying spot that had a diameter of 0.4 μm in the plane of the section.

Results

At present, the provisional method, outlined above, has several drawbacks. With prolonged reaction-times, the nature and intracellular localization of the reaction-product changes. This may be due to the formation of a complex lead precipitate containing the more soluble lead bicarbonate. For all that, measurements of total activity per cell increased (in mouse kidney) linearly with time, irrespective of the localization of the lead precipitate (Fig. A.1). For the optimization of all the reactants, a time of 30 minutes was chosen. Figures A. 2,3 and 4 show the optimizations of substrate (L-ornithine), co-factor (pyridoxal phosphate) and pH. The reactions were always done

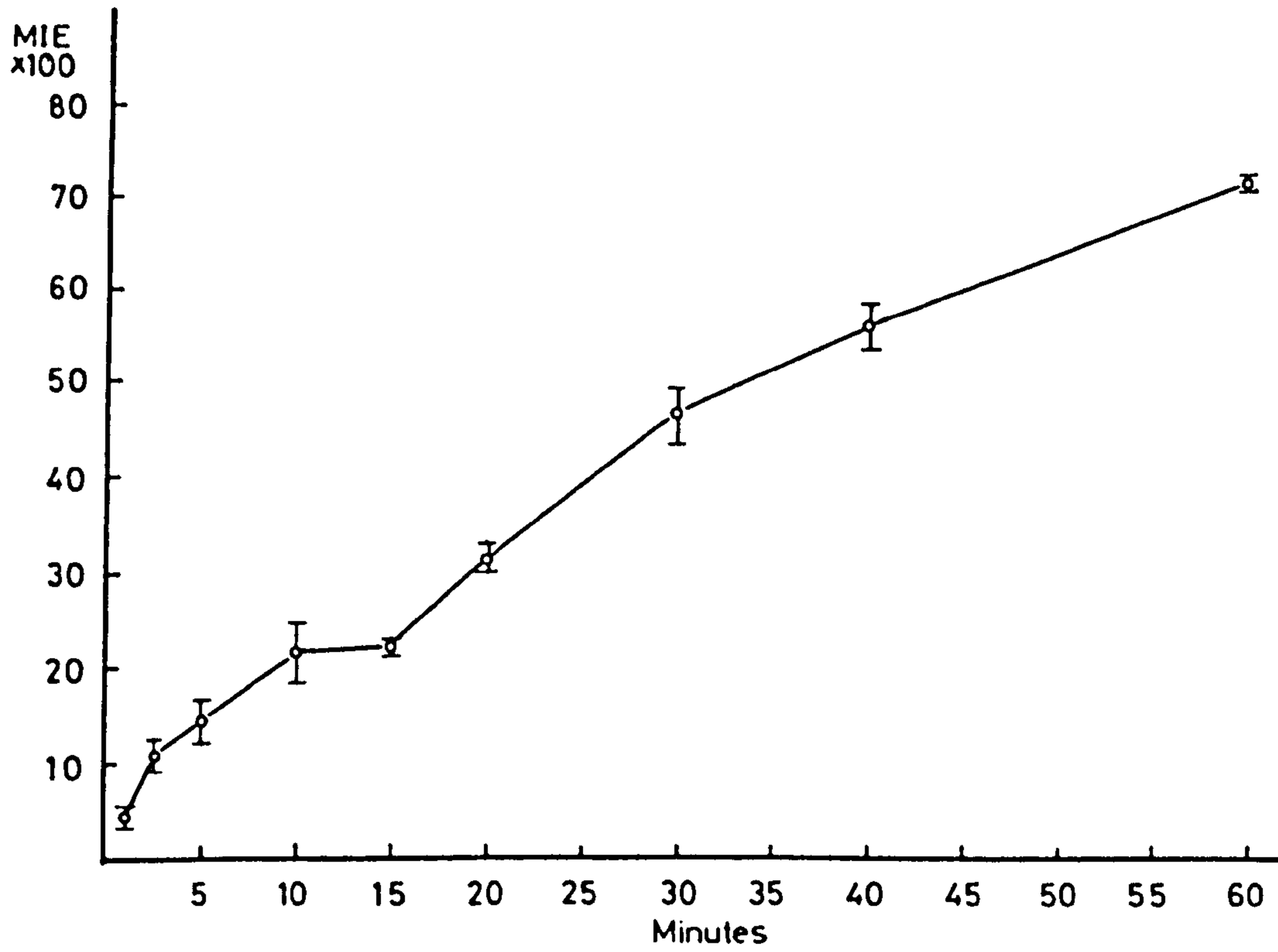

Fig. A. 1 The effect of time of incubation on the activity (MIE x 100; mean ± SEM) of ornithine decarboxylase activity in the proximal convoluted tubules of mouse kidney.

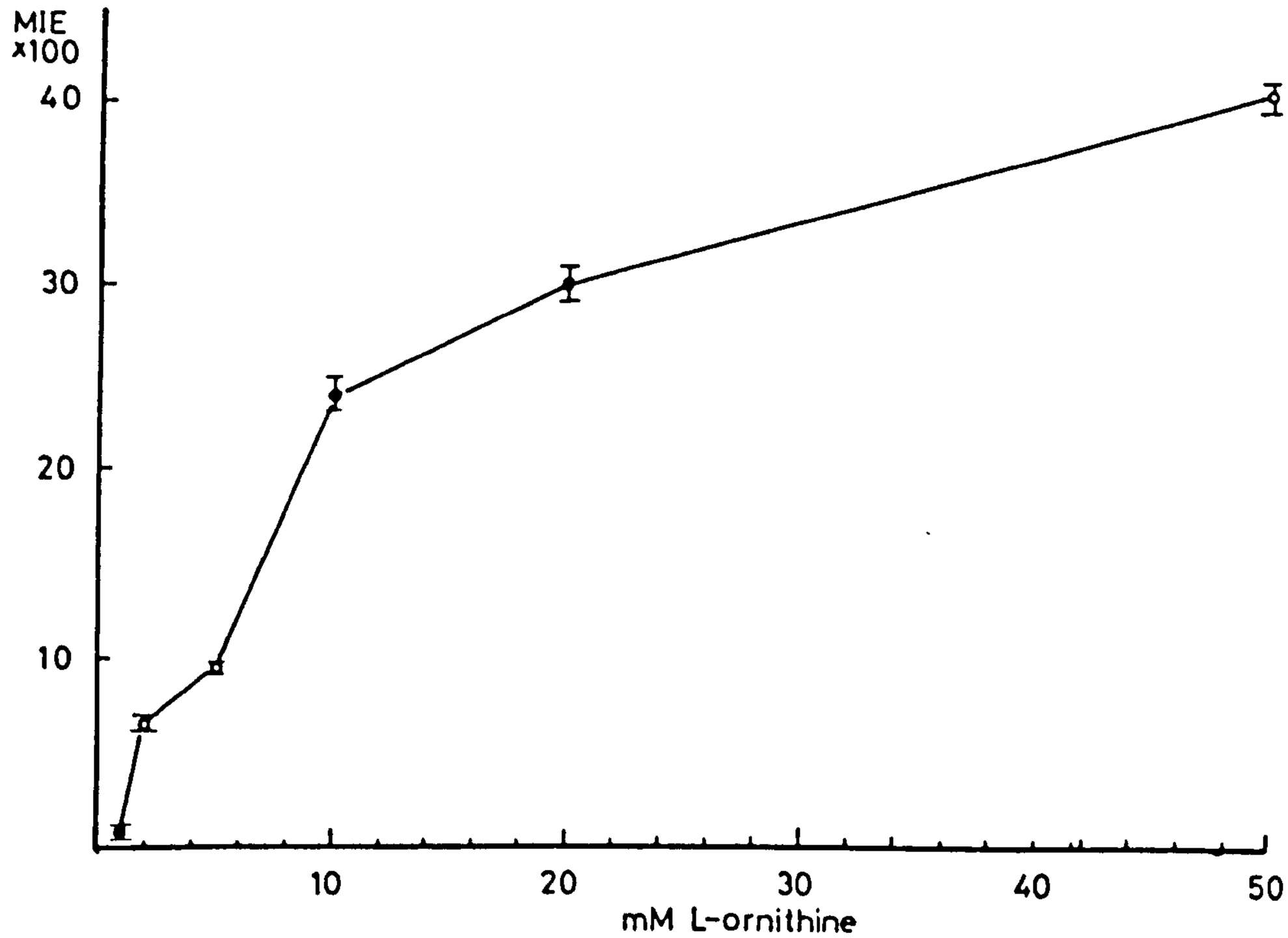

Fig. A. 2 The effect of different concentrations of substrate on the activity (MIE x 100; mean ± SEM) of ornithine decarboxylase.

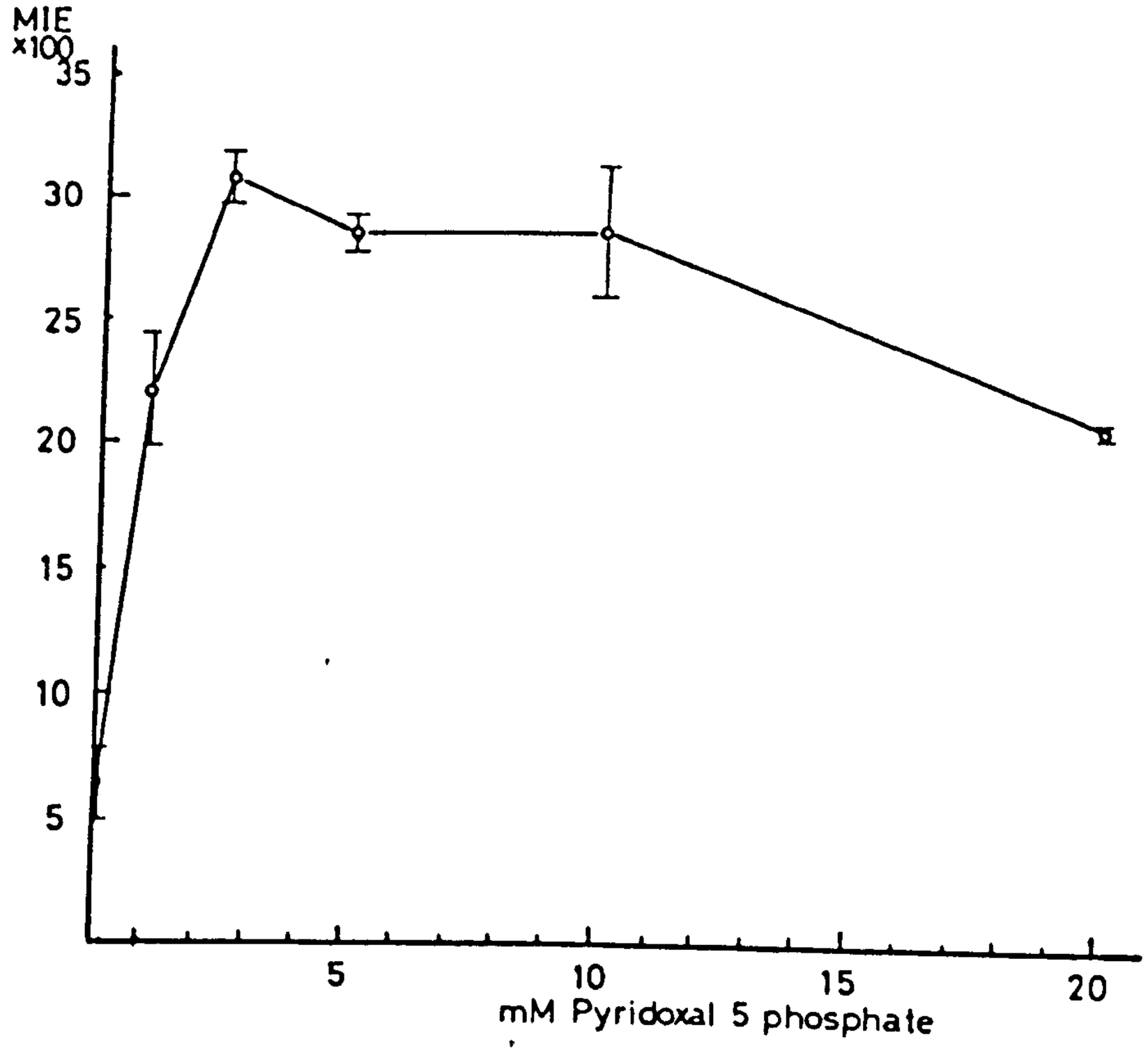

Fig. A. 3 The effect of increasing concentrations of pyridoxal phosphate on ornithine decarboxylase activity (MIE x 100; mean ± SEM).

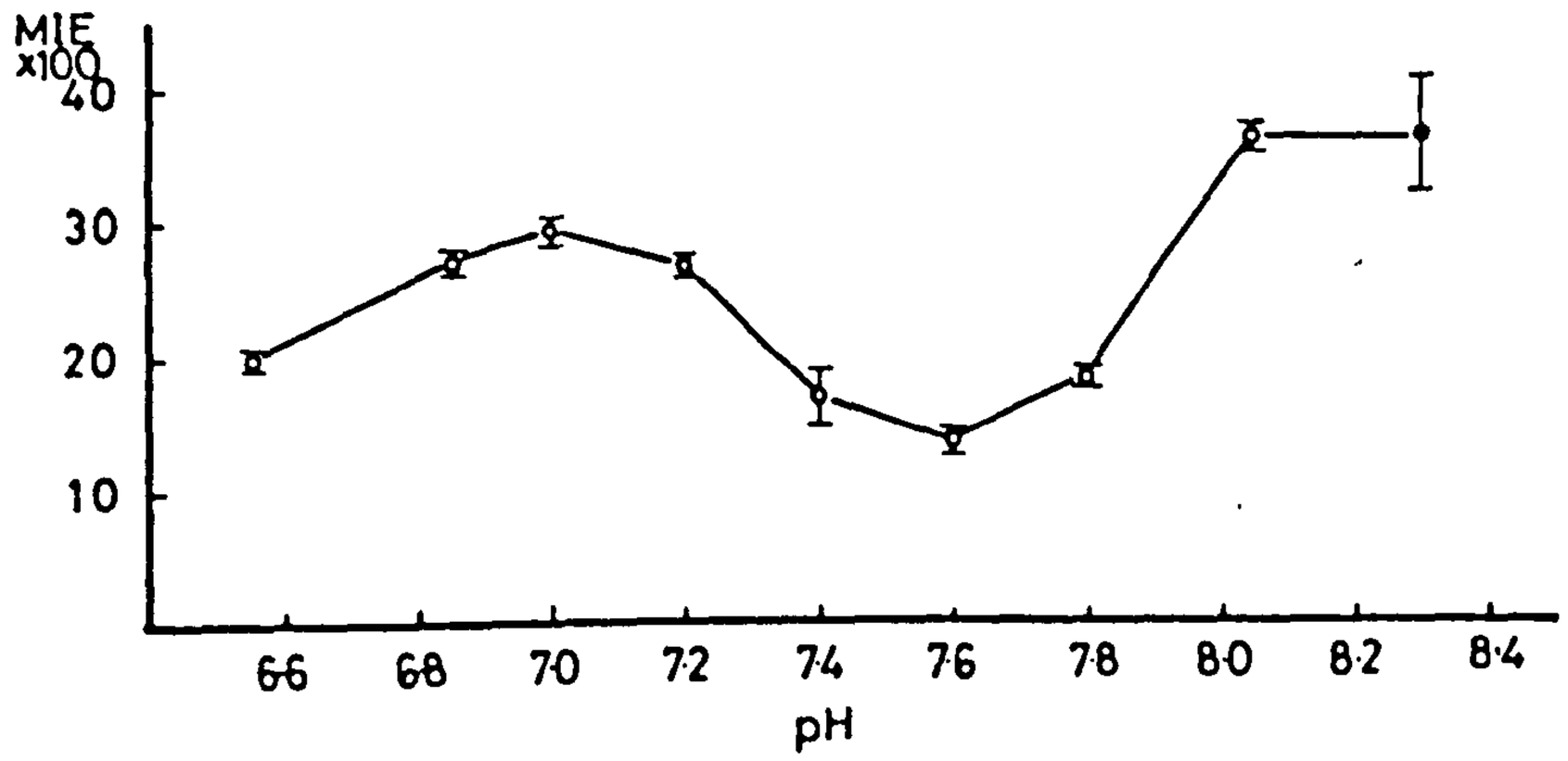

Fig. A. 4 The effect of pH on the activity (MIE x 100; mean ± SEM) of ornithine decarboxylase.

with and without an inhibitor of alkaline phosphatase (L-p-bromotetramizole).

Extensive studies were done to choose the correct grade and concentration of PVA, the amount of lead reagent, and the type of buffer used. Lower concentrations (<40%) of PVA produced extensive nuclear staining. Polypeptide (grade P5115) caused immediate precipitation in the reaction medium.

Specificity

30 mM α-difluoromethyl ornithine (DFMO; gift from Merrill International, Strasbourg) caused up to 42% inhibition of activity in sections of mouse kidney reacted for 30 minutes.

Appendix III

The formula of the B_6 deficient diet

Vitamin/Fat Free Casein	20.0%
Corn Oil	5.0%
Cellulose Powder	5.0%
Cornflour Starch	35.0%
Sugar	30.0%
Premix	5.0%

The premix contributes the following per kilogramme of diet:-

Vitamin A	10000 i.u./kg	Choline	400 mg/kg
" D_3	2000 "	Iron	50.0 "
" E	100 mg/kg	Cobalt	0.5 "
" B_2	10 "	Manganese	50.0 "
" K	10 "	Copper	10.0 "
Nicotinic Acid	20 "	Zinc	20.0 "
Calcium Pantothenate	20 "	Iodine	0.5 "
Folic Acid	1.0 "	Magnesium	100 "
Vitamin B_1	10.0 "	Chlorine	3.0 g/kg
Biotin	40.0 mcg/kg	Sodium	2.0 "
Vitamin B_{12}	10.0 "	Phosphoros	5.0 "
Inositol	500 mg/kg	Calcium	8.0 "
pAminobenzoic Acid	100 "	Potassium	5.0 "
Vitamin C	50.0 "	Selenium	0.05mg/kg

Alffram, P.A. (1964) Acta. Orthop. Scand. Suppl 65 : 1

Allen, J.C. (1983) Cell. Bioch. and Funtion 1: 131 - 139

Anderson, H.C. (1976) In: Bourne, G.H. (Ed) The Biochemistry and Physiology of Bone. Academic Press, New York, Vol 4 p.p. 135 - 157

Ascenzi, A. (1976) In: Bourne, G.H. (Ed) The Biochemistry and Physiology of Bone. Academic Press, New York, Vol 4 p.p. 403 - 441

Bachrach, U. (1980) In: Gaugas, J.M. (Ed) Polyamines in Biomedical Research John Wiley and Sons, London and New York p.p. 81 - 107

Baker, P.F. (1972) In: Hokin, L.E. (Ed) Metabolic Transport 3rd Edition. Academic Press, New York, p.p. 243 - 268

Balogh, K. Dudley, R.H. and Cohen, R.B. (1961) Lab. Invest 10: 839 - 845

Bartl, R. Burkhardt, R. Vondracek, H. Sommerfeld, W. and Hagemeister E. (1978) Klin. Wschr.56: 545 - 550

Baylis, P.H. Pitchford, J. Chayen, J. and Bitensky, L. (1980) Journal of Immunoassay 1: 399 - 411

Beeuwkes, R. 3 and Rosen, S. (1975) J. Histochem. Cytochem. 23: 828 - 839

Beeuwkes, R. and Rosen, S. (1980) Current Top. Memb. Transp. 13: 343 - 354

Bélanger, L.F. (1971) In: Bourne, G.H. (Ed) The Biochemistry and Physiology of Bone. Academic Press, New York, Vol 3 p.p. 240 - 270

Bell, R.G. and Matschiner, J.T. (1972) Nature 237: 32 - 33

Bell, R.G. (1978) Fed. Proc. 37: 2599 - 2604

Bernard, G.W. (1969) J. Dent. Res. 48 Suppl: 781 - 788

Bitensky, L. (1980) In: Evered, D. and O'Connor, M. (Eds) Trends in Enzyme Histochemistry and Cytochemistry. Excerpta Medica, Amersterdam.. p.p. 181 - 202

Blum, E. (1964) Beitr. Klin. Chir. 208: 346

Bocciarelli, D.S. (1970) Calcif. Tissue. Res. 5: 261 - 269

Bonsignore, A. and De Flora, A. (1972) Current Topics in Cell Regulation 6: 21 - 62

Borgers, M. and Thoné, F. (1975) Histochemistry 44: 277 - 280

Boskey, A.L. (1981) Clin. Orthop. 157: 225 - 257

Bourne, G.H. (1972) In: Bourne, G.H. (Ed) The Biochemistry and Physiology of Bone. Academic Press, New York, Vol 2 p.p. 79 - 120

Brommage, R. Neuman, M.W. and Neuman, W.F. (1978) In: Copp, D.H. and Talmage, R.V. (Eds) Endocrinology of Calcium Metabolism. Excerpta Medica, Amersterdam p.p. 79 - 84

Burgess, A.I. Esnouf, M.P. Rose, K. and Offord, R.E. (1983) Biochem. J. 215: 75 - 81

Butcher, R.G. and Altman, F.P. (1973) Histochemie 37: 351 - 363

Cameron, D.A. (1972) In Bourne, G.H. (Ed) The Biochemistry and Physiology of Bone Vol 1: 191 - 236

Cannellakis, E.S. Viceps - Madore, D. Kyriakidis, D.A. Heller, J.S. (1979) Current Topics in Cellular Regulation 15: 155 - 202

Cannellakis, E.S. Heller, J.S. and Kyriakidis, D.A. (1981) In: Calderara, C.M. Zappra, V. and Bachrach, V. (Eds). Advances in Polyamine Research. Raven Press, New York Vol 3: 1 - 13

Carlstromm, D. (1955) Acta Radiol; Suppl. 121: 33 - 76

Carr, S.A. Hauschka, P.V. and Biemann, K. (1981) J. Biol. Chem. 256: 9944 - 9950

Chambers, D.J. Brainbridge, M.V. Frost, G.T.P. Nahir, A.M. and Chayen, J. (1982) Histochemistry 75: 67 - 76

Chatterji, S. Wall, J.C. and Jeffery, J.W. (1981) Calcif. Tissue Int. 33: 567 - 574

Chayen, J. (1978 a) Int. Rev. Cytol. 53: 333 - 396

Chayen, J. (1978 b) In: Slater, T.F. (Ed) Biochemical Mechanism of Liver Injury. Academic Press, London, New York..p.p. 257 - 291

Chayen, J. (1980) The Cytochemical Bioassay of Polypeptide Hormones. Springer, Berlin Heidelburg, New York.

Chayen, J. (1983) Ann . Rheum. Dis. 42 Suppl: 64 - 67

Chayen, J. and Bitensky, L. (1968) In: Bittar, E.E., and Bittar, N. (Eds) The Biological Basis of Medicine. Academic Press, London. Vol 1: p.p. 337

Chayen, J. and Bitensky, L. (1982) Reviews in Pure and Applied Pharmacological Sciences 3: 271 - 317

Chayen, J. Bitensky, L. and Butcher, R.G. (1973) Practical Histochemistry. John Wiley and Sons, London, New York.

Chayen, J. Bitensky, L. and Butcher, R.G. (1975) Histochemie: Grundlagen and Methoden Verlag Chemie Weinheim.

Chayen, J. and Denby, E.F. (1968) Biophysical Technique: as applied to cell biology. London: Methuen.

Chayen J. Frost, G.T.B. Dodds, R.A. Bitensky, L. Pitchfork, J. Baylis, P.H. and Barnett, R.J. (1981) Histochemistry 71: 533 - 541

Chayen, N. (1984) Ph.D. Thesis, Brunel University.

Cohn, D.V. and Forscher, B.K. (1962) J. Biol. Chem. 237: 615 - 618

Couch, M. Woods, D.A. Gallagher, J.A. Poser, J.W. and Russell, R.G.G. (1984) Calcif. Tiss. Int. Suppl. 2: S3

Cook, P.J. Exton - Smith, A.N. Brockelhurst, J.C. and Lempert - Barber, S.M. (1982) J.R. Coll, Physicians, 16: 45 - 49

Coulton, L.A. (1977) Histochemistry 50: 207 - 215

Deftos, L.J. Parthemore, J.G. and Price, P.A. (1982) Calcif. Tissue. Int. 34: 122 - 124

Delmas, P.D. Stenner, D. Wahner. H.W. Mann, K.G. and Riggs, B.L. (1983 a) J. Clin. Invest. 71: 1316 - 1321

Delmas, P.D. Wahner, H.W. Mann, K.G. and Riggs, B.L. (1983 b) J. Lab. Clin. Med. 102: 470 - 476

Delmas, P.D. Russell, P.T. Riggs, L. and Mann, K.G. (1984) Calcif. Tissue. Int. 36: 308 - 316

Dickenson, R.P. Hutten, W.C. and Scott, J.R.R. (1981) J. Bone Jt. Surg. 63B: 233 - 238

Dikstein, S. (1971) Naturwissenschaften 58: 439 - 443

Dixon, T.F. and Perkins, H.R. (1952) Biochem. J. 52: 260 - 264

Dodds, R.A. Catterall, A. Bitensky, L. and Chayen, J. (1984) Calcif. Tissue. Int. 36: 233 - 238

Dodds, R.A. and Chayen, J. (1984) Cell. Biochem. and Funtion 211: 10 - 11

Dunham, J. Shedden, R.G. Catterall, A. Bitensky, L. and Chayen, J. (1977) Calcif. Tissue. Res. 23: 77 - 81

von Ebner, V. (1984) S.B. Akad. Wiss. Wien. 103 Abst 3: 162 - 188

Eigenbrodt, E. and Glossmann, H. (1980) Trends, Pharm. Sci. 1: 240 - 245

Eloranta, T.O. Kajander, E.O. and Raina, A.M. (1976) Biochem. J. 160: 287 - 294

Elsasser, V. Hesp, R. Klenerman, L. and Wooton, R. (1980) Clin. Sci. 59: 393 - 395

Engel, L. and Klingele, H. (1981) An Attas of Metal Damage: Surface Examination by Scanning Electron Microscope. Munich and London. Wolfe Medical and Scientific Publications.

Engström, A. (1972) In: Bourne, G.H. (Ed) The Biochemistry and Physiology of Bone. Academic Press, New York. Vol 1: p.p. 237 - 257

Epstein, S. Poser, J. McClintock, R. Johnston jr, C.C. Bryce, G. and Hui, S. (1984) Lancet i, 307 - 310

Ernst, S.A. (1972 a) J. Histochem. Cytochem. 20: 13 - 22

Ernst, S.A. (1972 b) J. Histochem. Cytochem. 20: 23 - 38

Ernst, S.A. (1975) J. Cell. Biol. 66: 586 - 608

Ernst, S.A. Riddle, C.V. and Karnaky, K.J.jr. (1980) Curr. Top. Memb. Transp. 13: 355 - 385

Ernst, S.A. and Hootman, S.R. (1981) Histochemical Journal 13: 397 - 418

Farquhar, M.G. and Palade, G.E. (1966) J. Cell.Biol. 30: 359 - 379

Fenton, S. Clarkson, E. Mac Gregor, G. Alaghband - Zadeh, J. and de Wardener, H.E. (1982) J Endocrinol. 94: 99 - 110

Firth, J.A. (1974) J. Histochem. Cytochem. 22: 1163 - 1168

Fong, W.E. Heller, J.S. and Cannellakis, E.S, (1976) Biochim. Biphys. Acta. 428: 456 - 465

Fritz, I.B. (1963) Adv. Lipid. Res. 1: 285 - 334

Fritz, I.B. and Yue, K.T.K. (1963) J. Lipid. Res. 4: 279 - 288

Forsyth, P.J.E. (1969) The physical basis of metal fatigue. London. Blackie and Sons Ltd.

Fullmer, H.M. (1966) Clin. Orthop. 48: 285 - 295

Gillad, G.M. and Gillad, H.G. (1981) J. Histochem. Cytochem. 29: 687 - 692

Gundberg, C.M. Lian, J.B. and Gallop, P.M. (1982) Clin. Chim. Acta. 128: 1 - 8

Gundberg, C.M. Lian J. B. Gallop, P.M. and Steinberg, J.J. (1983) J. Clin. Endocrinol. Metab. 57: 1221 - 1225

Guth, L. and Albers, R.W. (1974) J. Histochem. Cytochem. 22: 320 - 326

Hähnel, H. Modis, L. and Levai, G. (1978) Exp. Path. Bd. 15: S 196 - 207

Hall, J.G. Pauli, R.M. and Wilson, K.M. (1980) Am. J. Med. 68: 122

Hartshorne, N.H. and Stuart, A. (1970) Crystals and the Polarising Microscope 4th Ed. Edward Arnold, London.

Ham, A.W. and Harris, W.R. (1971) In: Bourne, G.H. (Ed) The Biochemistry and Physiology of Bone. Academic Press, New York. Vol 3 p.p. 337 - 399

Hancox, N.M. (1972) In: Bourne, G.H. (Ed) The Biochemistry and Physiology of Bone. Academic Press, New York. Vol 1 p.p. 128 - 189

Hardingham, T. (1981) Biochem. Soc. Trans. 9: 489 - 497

Hart, J.P. Catterall, A. Dodds, R.A. Klenerman, L. Shearer, M.J. Bitensky, L. and Chayen, J. (1984) Lancet ii, 283

Hauschka, P.V. Lian, J.B. and Gallop, P.M. (1975) Proc. Natl. Acad. Sci. 72: 3925 - 3929

Hauschka, P.V. Lian, J.B. and Gallop, P.M. (1978) Trends in Biochemical Science 3: 75 - 78

Hauschka, P.V. and Reddi, A.H. (1980) Biochemic. Biophys. Res. Comm. 92: 1037 - 1041

Hauschka, P.V. and Reid, M.L. (1978 a) J. Biol. Chem. 253: 9063 - 9068

Hauschka, P.V. and Reid, M.L. (1978 b) Dev. Biol. 65: 426 - 434

Heby, O. (1981) Differentiation 19: 1 - 20

Heby, O. and Anderson, G. (1980) In: Gaugas, J.M. Polyamines in Biomedical Research. New York. Wiley p.p. 17 - 34

Heby, O. Martin, L.J. Wilson, C.B. and Martinez, H.M. (1982) J. Cell. Physiol. 86: 511 - 522

Hekkelman, J.W. (1973) In Zyphin, (Ed) Biological Mineralization. p.p. 165 - 184

Henderson, B. (1976) Histochemistry 48: 191 - 204

Herring, G.M. (1972) In: Bourne, G.H. (Ed) The Biochemistry and Physiology of Bone. Academic Press, New York. Vol 1 p.p. 128 - 189

Hokin, L.E. and Dahl, J.L. (1972) In: Hokin, L.E. (Ed) Metabolic Transport . 3rd edn. Academic Press, New York, London p.p. 269 - 315

Holtta, E. Janne, J. and Hovit, T. (1979) Biochem. J. 178: 109 - 117

Holtta, E. and Pohjanpelto, P. (1982) Biochem. Biophys. Acta. 721: 321 - 327

Jackson, S.A. Cartwright, A.G. and Lewis, D. (1978) Calcif. Tissue. Res. 25: 217 - 222

Janne, O. Bardin, W. and Jacob, S.T. (1975) Biochemistry 14: 3589 - 3597

Jocelyn, P.C. (1972) Biochemistry of the S.H. Group. Academic Press, London.

Johnstone, J.J. Bitensky, L. and Chayen, J. (1972) J. Clin. Pathol. 25: 742

Johnstone, J.J. (1976) Histochem. J.11: 359 - 365

Junqueira, I.C. Carneiro, J. and Contopoulos, A. (1977) Basic Histology 2nd edn. Lange Los Alots. p.p. 119 - 139

Kamatani, N. and Carson, D.A. (1981) Biochim. Biophys. Acta. 675: 344 - 350

Katz, A.I. Doucet, A. and Morel, F. (1979) Am. J. Physiol. 237: F114 - F120

Kent, G.N. Dodds, R.A. Bitensky, L. Chayen, J. Klenerman, L. and Watts, R.W.E. (1983) J. Bone. Jt. Surg. 65B No. 2: 189 - 194

Kerbey, A.L. Randle, J.P. Cooper, R.H. Whitehouse, S. Pask, H.T. and Denton, R.M. (1976) Biochem, J. 154: 327 - 348

Kinne, R. Keljo, D. Gmaj, P. and Murer, H. (1978) In: Vogel, H.G. and Ullrich, K.J. (Eds) New Aspects of renal function. Excerpta Medica, Amsterdam p.p. 41 - 50

Knoth, E. Und, E. Markgraf. (1976) In: Hrsg, P.F. Matzen (Ed) Callus. Nova. Acta. Leopoldina. N.F. Nr 223 Bd. 44 S. 171, Halle/S.

Knowlden, J. Buhr, A.J. and Dunbar, O. (1964) Br. J. Prev. Soc. Med. 18: 130 - 141

Krebs, H.A. (1972) In: Campbell, P.N. and Dickens, F. (Ed) Essays in Biochemistry. Academic Press, London. Vol. 8: p.p. 1 - 34

Krebs, H.A. and Kornberg, H.L. (1957) Energy Transformation in Living Matter. Springer, Berlin.

Krebs, H.A. and Eggleston, L.V. (1974) Adv. Enzyme Regul. 12: 421 - 434

Kuehn, G.D. and Atmar, V.J. (1982) Fed. Proc. 41: 3078 - 3083

Lees, S. (1979) Calcif. Tissue. Int. 27: 53 - 56

Lehninger, A. (1976) Biochemistry. Worth, New York 2nd edn p. 543, 460.

Lehninger, A. (1982) Biochemistry. Worth, New York 3rd end p. 519

Levy, R.J. and Lian, J.B. (1979) Clin. Pharm. Therap. 25: 562 - 570

Lewinnek, G.E., Kelsy, J., White, A.A. and Krieger, N.I. (1980) Clin. Orthop. 152: 35 - 43

Lewis, A.F. (1981) Br. Med. J. 283: 1217 - 1220

Lian, J.B. and Friedman, P.A. (1978) J. Biol. Chem. 253: 6623 - 6626

Linn, T.C. Pettit, F.H. Hucho, F. and Reed, L.J. (1969) Proc. Natl. Acad. Sci, 64: 227 - 234

Lynch, R. Bitensky, L. and Chayen, J. (1966) J.R. Micr. Soc. 85: 213

Mamont, P.S. Bohlen, P. McCann, P.P. Bey, F. Shuber, F. and Tardif, C. (1976) Proc. Natl. Acad. Sci..73: 1626 - 1630

Mamont, P.S. Duchesne, M.C. Grove, J. and Bey (1978) Biochem, Biophys. Res. Commun, 81: 58 - 66

Mamont, P.S. Bey, P. and Koch - Weser, J. (1981) In: Moris, D.R. and Martin, L.J. Eds). Polyamines in Biology and Medicine. Marcel Dekker, New York. p.p. 147 - 165

Marks, S.C. and Walker, D.G. (1976) In: Bourne, G.H. (Ed) The Biochemistry and Physiology of Bone. Vol 4. p.p. 227 - 301

Maroudas, A. (1980) In: Maroudas, A. and Holborrow, E.J. (Eds) Studies in Joint Disease 1. Pitman Medical, Tunbridge Wells.

Maudsley, D.V. (1979) Bioch. Pharmacol. 28: 153 - 161

Mayahara, H. and Ogawa, K. (1980) Acta. Histochem. Cytochem. 13: 90 - 102

Mayahara, H. Fujimoto, K. Ando, T. and Ogawa, K. (1981) Histochemistry 67: 125 - 138

McCann, P.P. Tardif, C. Mamont, P.S. and Schuber, F. (1975) Biochem. Biophys. Res. Commun. 64: 336 - 341

Merck, (1968) In: Stecher, P.G. (Ed) The Merck Index 9th edn p.p. 548

Mita, M. and Yasamasu, I. (1979) Biochem. Biophys. Res. Commun. 86: 961 - 967

Mita, M. and Yasamasu, I. (1983) Arch. Bioch. Biophys. 226: 19 - 26

Modis, L. (1974) In: Graumann, W. and Neumann, K. (Eds) Handbuch der Histochemie, Vol 2. Part 4. Fischer, Stuttgart.

Muir, H. and Hardingham, T. (1975) M.T.P. Int. Rev. Sci. Biochem. Ser. One. 5: 153 - 220

Nahir, A.M. (1983) Ph.D Thesis. Brunel University.

Neely, J.R. Rovetto, M.J. and Oram, J.F. (1972) Prog, C.V. Dis. 15: 289 - 329

Neely, J.R. and Morgan, H.E. (1974) Ann. Rev. Physiol. 36: 413 - 459

Neuman, W.F. (1977) Calcif. Tissue. Res. Suppl. 22: 169 - 178

Nelsestuen, G.L. (1978) Fed. Proc. 37: 2621 - 2625

Nishimoto, S.K. and Price, P.A. (1979) J. Biol. Chem. 254: 437 - 441

Nishimoto, S.K. and Price, P.A. (1980) J. Biol. Chem. 255: 6579 - 6583

Novikoff, A.B. Drucker, J. Shin, W. and Goldfischer, S.(1961) J. Histochem. Cytochem. 9: 434 - 451

Olson, R.E. Houser, R.M. Seareey, M.T. Gardner, E.J. Scheinbuks, J. Subba Rao, G.N. Jones, J. and Hall, A.L. (1978) Fed. Proc. 37: 2610 - 2614

Owen, M. (1971) In: Bourne, G.H. (Ed) The Biochemistry and Physiology of Bone. Academic Press, New York. Vol. 3. p.p. 271 - 298

Owen, M. (1983) In; Dixon, A. St.J. Russell, R.G.G. and Stamp, T.C.P. (Eds) Osteoporosis, a Multi Disciplinary Problem. Academic Press, London. p.p. 25 - 29

Passonneau, J.V. and Lowry, O.H. (1964) Adv. Enzyme. Regul. 2: 265 - 274

Patterson - Allen, P. Brautigam, C.E. Grindleland, R.E. Willet. Asling, C. and Callahan, P.X. (1982) Anal. Chem. 120: 1 - 7

Peck, W.A. Birge, Jr. S.J. and Brandt, J. (1967) Biochem. Biophys. Acta. 142: 512

Pegg, A.E. (1967) Biochem. J. 166: 81 - 88

Pegg, A.E. (1984) Cell. Bioch. and Function. 2: 11 - 14

Pegg, A.E. Corti, A. and Williams - Ashman, H.G. (1973) Biochem. Biophys. Res. Commun. 52: 696 - 701

Pegg, A.E. Hibasami, H. Matsui, I. and Bethell, D.R. (1981) Adv. Enzyme. Reg. 19: 427 - 451

Pegg, A.E. and Mc Cann, P.P. (1982) Amer, J. Physiol. 243: C212 - C221

Pegg, A.E. Seely, J. and Zagon, I.S. (1982 a) Science 217: 68 - 70

Pegg, A.E. Tang, K - C and Coward, J.K. (1982 b) Biochemistry 21: 5082 - 5089

Pérez - González de la Manna, M. Proverbio, F. and Whittembury, G. (1980) Curr. Top. Memb. Transp. 13: 219 - 226

Persson, L. Rosengre, E. and Sundler, F. (1982) Biochem. Biophys. Res. Commun. 104: 1196 - 1201

Piro, L.D. Whyte, M.P. Murphy, W.A. and Birge, S.J. (1982) J. Clin. Endocrinol. and Metab. 54: 470 - 473

Poser, J.W. and Price, P.A. (1979) J. Biol. Chem. 254: 431 - 436

Posner, A.S. (1969) Physiol. Rev. 49: 760 - 792

Price, P.A. (1983) In: Peck, W.A. (Ed) Bone and Mineral Research Annual 1. Excerpta Medica, Amsterdam. p.p. 157 - 90

Price, P.A. Lothringer, J.W. and Nishimoto, S.K. (1980 a) J. Biol. Chem. 255: 2938 - 2942

Price, P.A. Lothringer, J.W. Baukol, S.A. and Reddi, A.H. (1981 a) J. Biol. Chem. 256: 3781 - 3784

Price, P.A. and Nishimoto, S.K. (1980) Proc. Natl. Acad. Sci. 77: 2234 - 2238

Price, P.A. Otsuka, A.S. Poser, J.W. Kristaponis, J. and Raman, N. (1976 a) Proc. Natl. Acad. Sci. 73: 1447 - 1454

Price, P.A. Parthemore, J.G. and Deftos, L.J. (1980 b) J. Clin. Invest. 66: 878 - 883

Price, P.A. and Williamson, M.K. (1981) J. Biol. Chem. 256: 12754 - 12759

Price, P.A. Williamson, M.K. Haba, T. Dell, R.B. Webster, S. and Jee, S. (1982) Proc. Natl. Acad. Sci. 79: 7734 - 7738

Price, P.A. Williamson, M.K. and Lothringer, J.W. (1981 b) J. Biol. Chem. 256: 12760 - 12766

Raina, A. and Janne, J. (1975) Med. Biol. 53: 121 - 147

Rath, N.C. and Reddi, A.H. (1981) Developmental Biology. 82: 211 - 216

Reynolds, J.J. (1983) In: Dixon A. St.J. Russell, R.G.G. and Stamp, T.C.P. (Eds) Osteoporosis, a Multi Disciplinary Problem. Academic Press, London. p.p. 43 - 50

Robinson, R.A. (1952) J. Bone. Jt. Surg. 35A: 389 - 434

Rokkanen, P. and Slatis, P. (1964) Acta. Orthop. Scand. 35: 21

Russell, D.H. and Manen, C - A. (1982) Biochem. Pharmacol. 31: 3373 - 3378

von Schmidt, W.J. (1938) Handbuch biol. Arb - Meth. 10: 435 - 665

Schmidt, U. and Dubach, U.C. (1969) Pflugers. Arch. 306: 219 - 226

Schmidt, U. Schmidt, H. Funk, B. and Dubach, V.C. (1974) Ann. N.Y. Acad. Sci. 242: 489 - 500

Schwartz, A. Nagano, K. Nakao, M. Lindenmayer, G.E. Allen, J.C. and Matsui, H. (1971) In: Schwartz, A. (Ed) Methods in Pharmacology. Vol. 1. Appleton - Century - Crofts, New York. p.p. 361 - 388

Scott, J.E. (1973) Biochem. Soc. Trans. 1: 787 - 806

Scott, J.E. and Dorling, J. (1965) Histochemie 5: 221 - 233

Sekar, V. Atmar, V.J. Krim, M. and Kvenn, G.D. (1982) Biochem. Biophys. Res. Commun. 106: 305 - 311

Shah, D.V. Tews, N.K. Harper, D.E. and Suttie J.W. (1978) Biochim. Biophys. Acta. 539: 209 - 217

Shedden, R. Dunham, J. Bitensky, L. Catterall, A. and Chayen, J. (1976) Calcif. Tissue. Res. 22: 19 - 25

Sissons, H.A. (1971) In: Bourne, G.H. (Ed) The Biochemistry and Physiology of Bone. Academic Press, New York. Vol. 3: p.p. 145 - 180

Singh, M. Nagrath, A.R. and Maini, P.s. (1970) J. Bone. Jt. Surg. 52A: 457 - 467

Stenflo, J. and Suttie, J.W. (1977) Ann. Rev. Biochem. 46: 157 - 172

Stinchfield, F.E. Sankaran, B. and Samilson, R. (1956) J. Bone. Jt. Surg. 38A: 270 - 282

Stockwell, R.A. (1979) The Biology of Cartilage Cells. Cambridge University Press, Cambridge.

Sunkara, P.S. Pargac, M.B. Nishioka, K. and Rao, P.N. (1979 a) J. Cell. Physiol. 98: 451 - 459

Sunkara, P.S. Rao, P.N. Nishioka, K. and Brinkley, B.R. (1979 b) Exp. Cell. Res. 119: 63 - 68

Suttie, J.W. Larson, A.E. Canfield, L.M. and Carlisle, T.L. (1978) Fed. Proc. 37: 2605 - 2609

Swanson, S.A.W. (1971) Adv. Biomed. Eng. 1: 137

Tabor, C.W. and Tabor, H. (1976) Ann. Rev. Biochem. 45: 285 - 306

Takano, T. Takigawa, M. and Suzuki, F. (1982) J. Biochem. (Tokyo) 93: 591 - 598

Taketa, K. and Pogell, B.M. (1966) J. Biol. Chem. 241: 720 - 726

Tormey, J. Mc. D. (1966) Nature 210: 820 - 822

Urist, M.R. (1976) In: Bourne, G.H. (Ed) The Biochemistry and Physiology of Bone. Academic Press, New York. Vol. 4: p.p. 2 - 57

Vaes, G. (1969) In: Dingle, J.T. and Fell, H.B. (Eds) Lysosomes in Biology and Pathology North Holland, Amsterdam. Vol. 1: p.p. 217 - 253

Van Reen, R. (1959) J. Biol. Chem. 234: 1951 - 1954

Voegel, J.C. and Frank, R.M. (1977) J. Biol. Buccale. 5: 181 - 194

Wachstein, M. amd Meisel, E. (1957) Am. J. Clin. Pathol. 27: 13 - 23

Walker, P.J. (1973) Biochem. Soc. Trans. 1: 62 - 67

Wall, J.C. Chatterji, S. and Jeffery, J.W. (1979) Calcif. Tissue. Int. 27: 105 - 108

Wallin, R. and Suttie, J.W. (1982) Arch. Biochem. Biophys. 214: 155 - 163

Watts, R.W.E. Scott, J.T. Chalmers, R.A. Bitensky, L. and Chayen, J. (1971) Q.J. Med. 40: 1 - 40

Whitlon, D.S. Sadowski, J.A. and Suttie, J.W. (1978) Biochemistry 17: 1371 - 1377

Yoshida, H.K. Nagai, T. Ohashi, and Nakagawa, Y. (1969) Biochim. Biophys. Acta. 171: 178 - 185

Zaman, G. and Chayen J. (1981) J. Clin. Pathol. 34: 567 - 568

Lian, J.B. Skinner, M. Glimcher, M.J. and Gallop P.M. (1976) Biochem. Biophys. Res. Commun. 73: 349 - 355

Lian, J.B. Hauschka, P.V. and Gallop, P.M. (1978) Fed. Proc. 37: 2615 - 2620

Robison, R. (1923) sited in Bourne, G.H. (1972)

Histochemistry (1981) 71:533–541

Histochemistry
© Springer-Verlag 1981

The Use of a Hidden Metal-Capture Reagent for the Measurement of $Na^+ - K^+$-ATPase Activity: A New Concept in Cytochemistry

J. Chayen[1], G.T.B. Frost[2], R.A. Dodds[1], L. Bitensky[1], J. Pitchfork[3], P.H. Baylis[3]*, and R.J. Barrnett[4]

[1] Division of Cellular Biology, Kennedy Institute of Rheumatology, Bute Gardens, London W6 7DW, UK
[2] Sigma London Chemical Company Ltd., Poole, Dorset BH17 7NH, UK
[3] Department of Medicine, University of Birmingham, Queen Elizabeth Hospital, Edgbaston, Birmingham B15 2TH, UK
[4] Section of Cell Biology, Yale University School of Medicine, New Haven, Connecticut 06510, USA

Summary. The original lead-trapping method for demonstrating $Na^+ - K^+$-ATPase activity was discredited because of the effect that lead ions can have on the substrate and on the enzyme. Current methods, that measure this activity by the related K^+-dependent phosphatase activity, do not appear to measure activity that is known, from microchemistry, to occur in proximal convoluted tubules. The disadvantages of using lead appear to have been overcome by the use of a new reagent in which the lead is complexed with ammonium citrate ions; phosphate, liberated enzymatically, successfully competes with these ions. The activities of total ATPase and of the ouabain sensitive $Na^+ - K^+$-ATPase have been measured in three regions of the nephron in the guinea-pig and in the rat. The relative activities found, by this method, in the different regions of the latter, appear to be comparable with results found by others, using microchemical methods applied to isolated regions of the nephron.

Introduction

There seems little doubt that the sodium-potassium dependent, magnesium-stimulated adenosine triphosphatase ($Na^+ - K^+$-ATPase) of cell plasma membranes (Pérez-González de la Manna et al. 1980), equated with the sodium-potassium exchange pump (e.g. Hokin and Dahl 1972; Katz et al. 1979), plays a major role in maintaining the normal ionic concentration and cell volume (Baker 1972) and possibly even in the transport of sugars and amino acids (Hokin and Dahl 1972). Because of the critical importance of this ATPase in cellular physiology, several workers have sought a cytochemical procedure for demonstrating its activity. The earlier methods, based on that of Wachstein and Meisel (1957) which employed lead ions to trap the phosphate liberated by ATPase

* Present address: Department of Medicine, University of Newcastle-upon-Tyne, The Royal Victoria Infirmary, Newcastle-upon-Tyne NE1 4LP, UK

0301-5564/81/0071/0533/$01.80

Histochemistry (1981) 71 : 533–541

Histochemistry
© Springer-Verlag 1981

The Use of a Hidden Metal-Capture Reagent for the Measurement of $Na^+ - K^+$-ATPase Activity: A New Concept in Cytochemistry

J. Chayen[1], G.T.B. Frost[2], R.A. Dodds[1], L. Bitensky[1], J. Pitchfork[3], P.H. Baylis[3]*, and R.J. Barrnett[4]

[1] Division of Cellular Biology, Kennedy Institute of Rheumatology, Bute Gardens, London W6 7DW, UK
[2] Sigma London Chemical Company Ltd., Poole, Dorset BH17 7NH, UK
[3] Department of Medicine, University of Birmingham, Queen Elizabeth Hospital, Edgbaston, Birmingham B15 2TH, UK
[4] Section of Cell Biology, Yale University School of Medicine, New Haven, Connecticut 06510, USA

Summary. The original lead-trapping method for demonstrating $Na^+ - K^+$-ATPase activity was discredited because of the effect that lead ions can have on the substrate and on the enzyme. Current methods, that measure this activity by the related K^+-dependent phosphatase activity, do not appear to measure activity that is known, from microchemistry, to occur in proximal convoluted tubules. The disadvantages of using lead appear to have been overcome by the use of a new reagent in which the lead is complexed with ammonium citrate ions; phosphate, liberated enzymatically, successfully competes with these ions. The activities of total ATPase and of the ouabain sensitive $Na^+ - K^+$-ATPase have been measured in three regions of the nephron in the guinea-pig and in the rat. The relative activities found, by this method, in the different regions of the latter, appear to be comparable with results found by others, using microchemical methods applied to isolated regions of the nephron.

Introduction

There seems little doubt that the sodium-potassium dependent, magnesium-stimulated adenosine triphosphatase ($Na^+ - K^+$-ATPase) of cell plasma membranes (Pérez-González de la Manna et al. 1980), equated with the sodium-potassium exchange pump (e.g. Hokin and Dahl 1972; Katz et al. 1979), plays a major role in maintaining the normal ionic concentration and cell volume (Baker 1972) and possibly even in the transport of sugars and amino acids (Hokin and Dahl 1972). Because of the critical importance of this ATPase in cellular physiology, several workers have sought a cytochemical procedure for demonstrating its activity. The earlier methods, based on that of Wachstein and Meisel (1957) which employed lead ions to trap the phosphate liberated by ATPase

* Present address: Department of Medicine, University of Newcastle-upon-Tyne, The Royal Victoria Infirmary, Newcastle-upon-Tyne NE1 4LP, UK

0301-5564/81/0071/0533/$01.80

activity, fell into disrepute because the lead ions themselves caused a non-enzymatic hydrolysis of the ATP that was used as a substrate, and also because free lead ions strongly inhibit $Na^+ - K^+$-ATPase activity (as reviewed by Ernst 1972a; Beeuwkes and Rosen 1975, 1980). Ernst (1972a, b) introduced the use of the substrate p-nitrophenyl phosphate (PNPP) for demonstrating the potassium-dependent phosphatase activity which is now believed to function as part of the $Na^+ - K^+$-ATPase activity (Ernst 1972a; Hokin and Dahl 1972); he used strontium as the trapping agent and this strongly inhibits the enzymatic activity (Ernst 1972a; Ernst et al. 1980). Guth and Albers (1974) modified this technique in two ways: first, by adding dimethyl sulphoxide to the medium, which, at 30% concentration, changes the optimal pH to 9.0 (Beeuwkes and Rosen 1980), and inhibits alkaline phosphatase activity (Ernst et al. 1980); and secondly, by leaving out the strontium, relying on the phosphate being captured, albeit rather inefficiently, by the magnesium and potassium ions (Beeuwkes and Rosen 1975; Ernst et al. 1980). The precipitated phosphate was converted to cobalt phosphate, by immersion in a solution of cobalt chloride, and thence to cobalt sulphide. This method was used by Beeuwkes and Rosen (1975, 1980) who used electron-probe analysis to quantify the reaction-products. In the kidney, Beeuwkes and Rosen (1975) showed highest activity in the thick ascending limbs of the loop of Henle, and in the distal convoluted tubules, but reported that no PNPPase activity could be discerned in the proximal tubules, even though ATPase activity has been recorded in these tubules by the microchemical, microdissection studies of Schmidt and Dubach (1969) and Schmidt et al. (1974) and of Katz et al. (1979). Beeuwkes and Rosen (1975) considered that their inability to record activity in proximal tubules might have been due to the relative insensitivity of their method.

Thus until recently, this important enzyme, $Na^+ - K^+$-ATPase, has been examined cytochemically only by an indirect method that has a number of disadvantages. Firstly, it does not demonstrate activity in proximal tubules, in which this enzymatic activity appears to fulfil major physiological functions (Kinne et al. 1978) and may be about half that found in the strongly active distal convoluted tubules (Katz et al. 1979). Secondly, although there seems little doubt that the K^+-dependent phosphatase, demonstrable by the PNPP-method, is associated with the $Na^+ - K^+$-ATPase, there are several discrepancies, as reviewed by Hokin and Dahl (1972), that imply that the relationship may not always hold. It would therefore be preferable to have a cytochemical procedure that can demonstrate $Na^+ - K^+$-ATPase activity directly, by its response to its normal substrate (ATP) and in relation to the ions that are known to influence such activity.

The original, direct method of Wachstein and Meisel (1957) failed because lead ions hydrolyze ATP in solution and inhibit the enzyme. Furthermore few, if any, lead salts are readily soluble at the pH at which the reaction should be done for maximal $Na^+ - K^+$-ATPase activity. It was therefore decided to complex the lead with weak acidic moieties which should sequester the lead from the ATP and from the active site of the enzyme, but which would be displaced by the electrochemically more active phosphate ions when these were liberated by the action of the ATPase on ATP. Consequently, a mixture of

lead salts was prepared which, when dissolved in water with the addition of a dilute solution of ammonia, would give a buffered solution of lead ammonium citrate. This lead ammonium citrate/acetate material contained approximately 10% lead in a bound form. This new stable lead ammonium citrate/acetate complex (Sigma) is readily soluble at pH values from 7 to 8 and does not hydrolyze solutions of ATP although it forms a rapid and dense precipitate when free phosphate is present. This communication records its use as the capture-reagent in a method for $Na^+ - K^+$-ATPase activity.

Materials and Methods

Segments (about $5 \times 5 \times 3$ mm) cut from the kidneys of Wistar rats (of either sex) or of guinea-pigs (Hartley strain; either sex) that had been killed by asphyxiation with nitrogen, were chilled to $-70°$ C in n-hexane (BDH: free from aromatic hydrocarbons, boiling range 67–70° C). The tissue was stored in cold dry tubes, at $-70°$ C for up to 2 days. As has been found in biochemical studies on $Na^+ - K^+$-ATPase activity (Pérez-González de la Manna et al. 1980), the activity alters with prolonged storage. For most purposes the tissue was sectioned at 10 µm in a Bright's cryostat, with an automatic cutting device to ensure constancy of thickness (Chayen 1980), with the cabinet temperature between -25 and $-30°$ C and with the knife cooled with solid carbon dioxide. The sections were picked off the knife on to glass slides (Chayen et al. 1973, 1975).

The method for assaying magnesium-activated, $Na^+ - K^+$-ATPase activity was derived from the biochemical procedure of Schwartz et al. (1971) except that all reactants were used at four times the concentrations in order to overcome the lower diffusibility in the viscous polypeptide medium. Thus the final reaction-medium was made as follows: A 40% solution (w/v) of Polypep 5115 (Sigma) was prepared in 0.2 M Tris buffer at pH 7.4 containing sodium acetate (1 mM for sections of rat kidney and 2 mM for the more delicate guinea-pig tissue). Then the following were added sequentially: sodium chloride (24 mg/ml; 410 mM), magnesium chloride (4 mg/ml; 20 mM), potassium chloride (2.8 mg/ml; 37.5 mM) and ATP (disodium adenosine 5′ triphosphate, Boehringer; 10 mg/ml; 16.5 mM). The lead ammonium citrate/acetate complex (Sigma) was dissolved, with constant shaking, in the smallest volume of dilute ammonia (5 drops of 0.88 ammonia per ml) to give a final concentration of 32 mg/ml. The final pH was adjusted to pH 7.5 by the addition either of a mixture of sodium and potassium hydroxides (10:1 on a molar basis; 2.5 mM) or of 0.1 M hydrochloric acid.

To economize on the relatively costly components of the reaction-medium, the reactions were done by placing a small Perspex ring around each section and pouring the medium into the ring (Chayen et al. 1973).

In the final method, but not in some earlier studies, the sections were first immersed for 5 min in a 40% solution of Polypep 5115 in the Tris buffer, pH 7.5, containing 0.1 M potassium acetate. The purpose of this procedure was to remove free phosphate that otherwise produced a strong 'background' colouration. This medium was sucked-off; a little of the full medium was added to each section, and then sucked-off again, to ensure adequate replacement of the initial Polypep medium. Then the full reaction-medium was added to each section to a depth of 2–3 mm.

The medium, and the sections, were at 37° C before these procedures were begun. At 37° C, 15 min were required for reactions that could readily be quantified. The sections were then rinsed, in Coplin jars, in several changes of a 0.2 M Tris buffer, pH 7.4, at 37° C to remove all the Polypep. They were then immersed, at room temperature, in water that had been saturated with hydrogen sulphide (1–2 min). Subsequently they were rinsed several times in distilled water and allowed to dry. They were mounted in the Z5 medium that is based on polyvinyl alcohol (Zaman and Chayen 1981). This contains 12% polyvinyl alcohol (G18/140 grade from Wacker Chemical Co.); 20% glycerine; 20% lactic acid in a 0.4 M sodium acetate:acetic acid buffer, with the final pH of 6.5.

The reaction-product, assumably of lead sulphide, was measured by means of a Vickers M85 microdensitometer, with a $\times 40$ objective, at 585 nm, and with a flying-spot of 0.5 µm diameter in the plane of the section. The size of the mask allowed measurement of the reaction-product in one cell. By suitable calibration (Chayen 1978a, b; Bitensky 1980) the microdensitometric readings

were expressed as the mean ± SEM of the integrated extinction. In general, duplicate sections were measured, with 10 or 20 cells from different tubules from each region of the nephron being measured in each section. The reaction measured in sections exposed to the full medium gave the total $Na^+ - K^+$-ATPase activity. Serial sections were treated with the same medium containing 0.4 mM (0.3 mg/ml) ouabain (ouabain octahydrate; Sigma). Measurements made in these sections recorded the activity of the ouabain-insensitive enzyme or enzymes. Subtraction of this activity from the first (i.e. the total $Na^+ - K^+$-ATPase activity) gave the activity of the specific, ouabain-sensitive, $Na^+ - K^+$-ATPase.

For some studies, where alkaline phosphatase activity was likely to interfere with the measurements, the specific inhibitor (Borgers and Thoné 1975), L-p-bromotetramisole oxalate (Aldrich: 0.4 mM), was included in both reaction-media.

Results

Optimal Concentration of Reactants and Specificity

The optimal pH for the specifically ouabain-sensitive reaction, in the thick ascending limbs (TAL) of the loop of Henle in sections of rat kidney, was pH 7.65 (Fig. 1). The use of different concentrations (0, 5, 10, 15, 20 mg/ml) of ATP in the full reaction-medium (with and without ouabain) used on sections of rat kidney showed that, in this region of the nephron, the optimal concentration was 10 mg/ml for the ouabain-sensitive $Na^+ - K^+$-ATPase activity (Fig. 2).

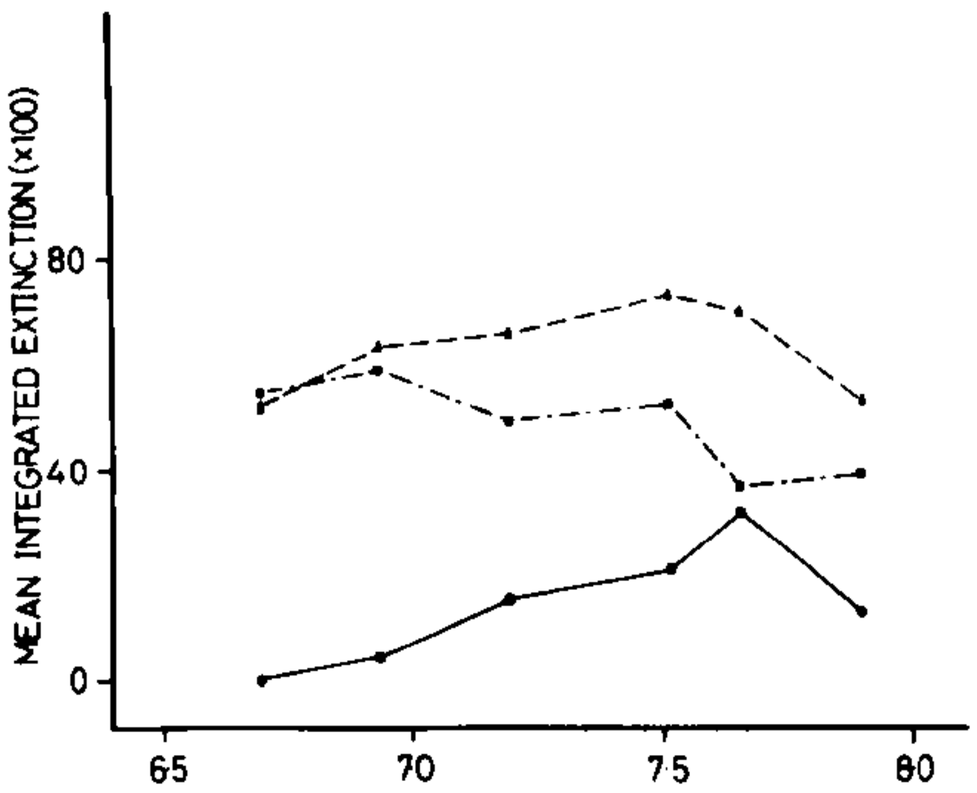

Fig. 1. The effect of pH on the activities of total ATPase (triangles; top graph), ouabain-insensitive ATPase (squares; middle graph) and of the ouabain-sensitive ATPase (by subtraction: circles; bottom graph) in the thick ascending limb of the loop of Henle in the rat. Activity is recorded as mean integrated extinction per unit field per unit time

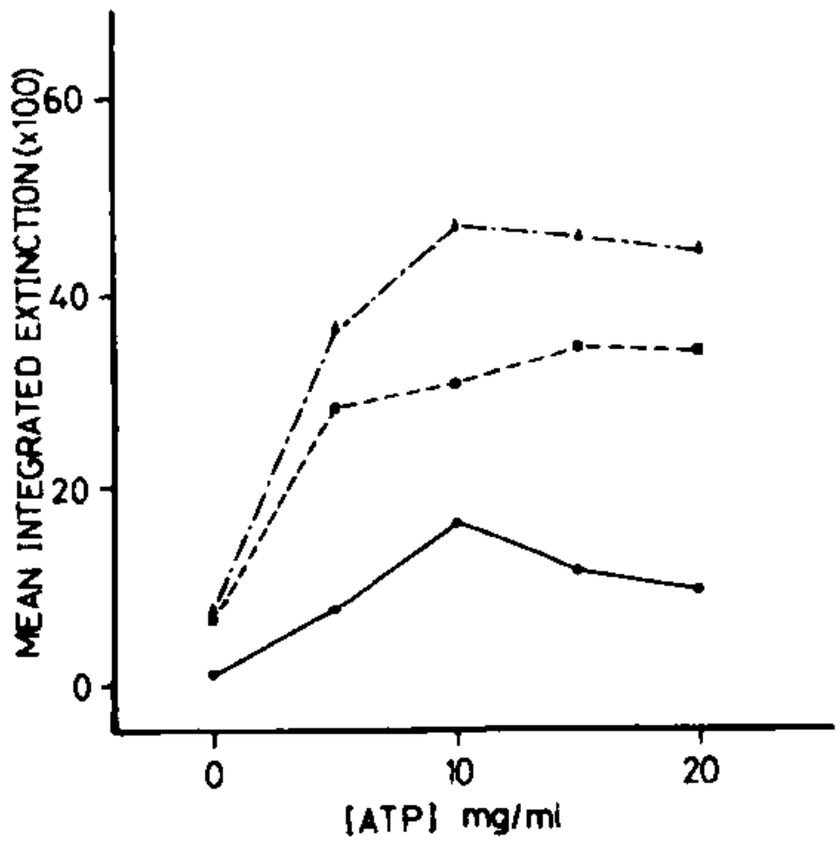

Fig. 2. The effect of the concentration of ATP on the activities (mean integrated extinction × 100) of total ATPase (top), ouabain-insensitive ATPase (middle) and of the ouabain-sensitive ATPase (bottom graph; derived by subtraction of the previous graphs) in the thick ascending limb of the loop of Henle in the rat

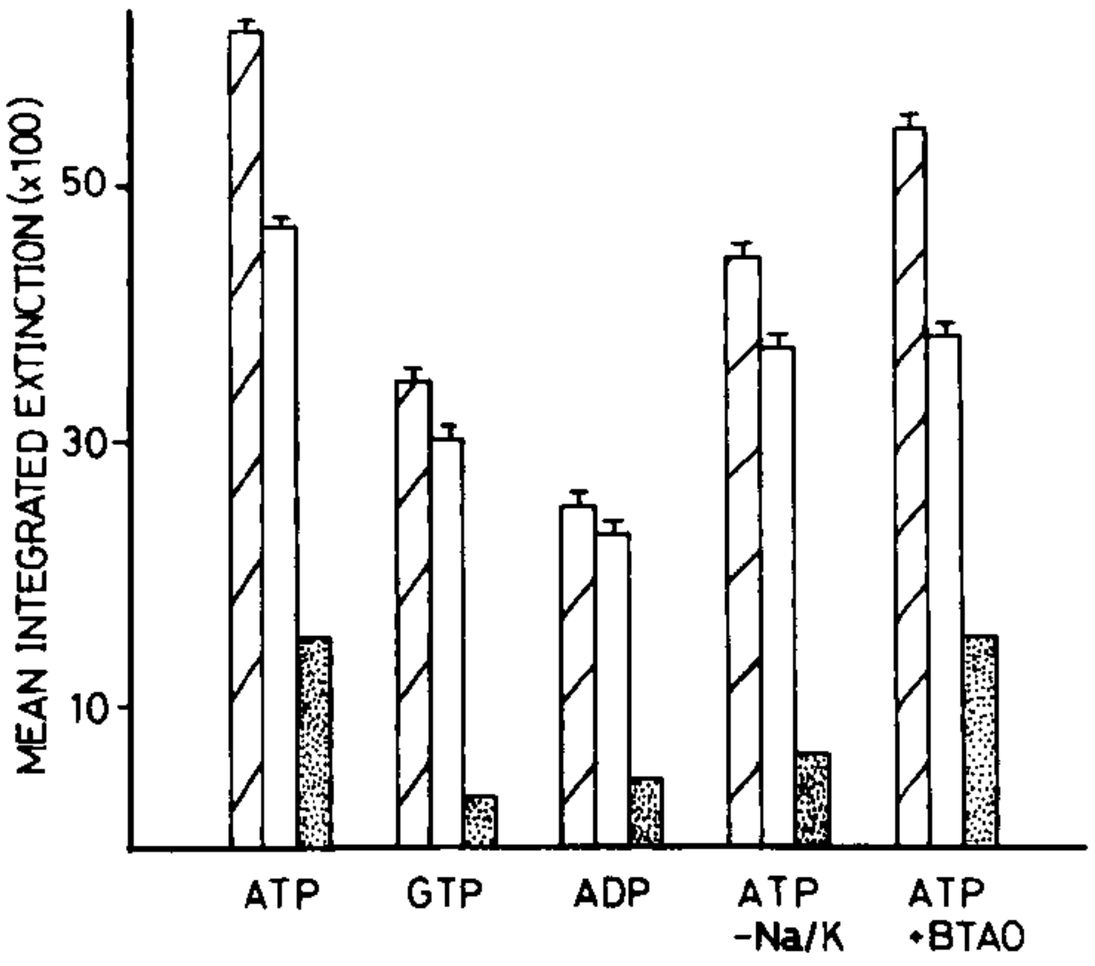

Fig. 3. Specificity of the reaction. Serial sections were tested for activity against ATP, GTP and ADP; others were tested against ATP either with no sodium or potassium added to the reaction-medium, or with bromotetramisole oxalate (BTAO) to inhibit alkaline phosphatase activity. For each treatment, the specific ouabain-sensitive ATPase activity (stippled columns) was derived by subtracting the ouabain-insensitive activity (clear columns) from the total ATPase activity (crossed columns); bars represent the SEM of the readings

Very low specific activity was found when ATP was replaced by trisodium guanosine 5′-phosphate (10 mg/ml: 17 mM), or by adenosine diphosphate at equimolar concentration (Fig. 3). When the sodium and potassium chlorides were excluded from the reaction-medium, the total activity and the ouabain-sensitive activity were depressed, with the ouabain-insensitive activity being unaffected (Fig. 3). It is probable that the residual ouabain-sensitive activity was due to the sodium/potassium hydroxide used to establish the final pH, and to those ions that were endogenous within the section. The addition of L-*p*-bromotetramisole oxalate (0.4 mM; 0.15 mg/ml), to inhibit alkaline phosphatase activity, did not affect the measured $Na^+ - K^+$-ATPase activities in this region of the nephron (Fig. 3). In this region of the nephron, the activity was linear with thickness over the range of thickness tested (5–20 μm); it was linear with time for at least 20 min.

Total and Ouabain-Sensitive $Na^+ - K^+$-ATPase Activities in Different Regions of the Nephron

In both the rat and the guinea-pig, total and ouabain-sensitive $Na^+ - K^+$-ATPase activity was found on the contra-lumenal boundary of the cells of proximal convoluted tubules (characterized by the lumenal alkaline phosphatase activity), of the distal convoluted tubules and in the cells of tubules that were grouped in clusters at the cortico-medullary boundary and extended into the medulla (Fig. 4). Following Beeuwkes and Rosen (1975), these last tubules were taken to be the thick ascending limbs (TAL) of the loop of Henle.

The total and the ouabain-sensitive $Na^+ - K^+$-ATPase activities were measured, at various times, in cells in these three regions in seven guinea-pigs. The total activity (mean integrated extinction × 100; mean ± SEM) in the proximal convoluted, distal convoluted tubules and in the TAL, were 12.4 ± 1.1, 29.5 ± 4.2, and 33.8 ± 2.8, respectively. The percentage of the total activity that was represented by the ouabain-sensitive $Na^+ - K^+$-ATPase activity was 41 ± 5.8, 58 ± 5.9 and 54 ± 4.8, respectively.

In sections of rat kidney, and with the concentration of ouabain increased to 1 mM for comparison with the studies of Katz et al. (1979), the results

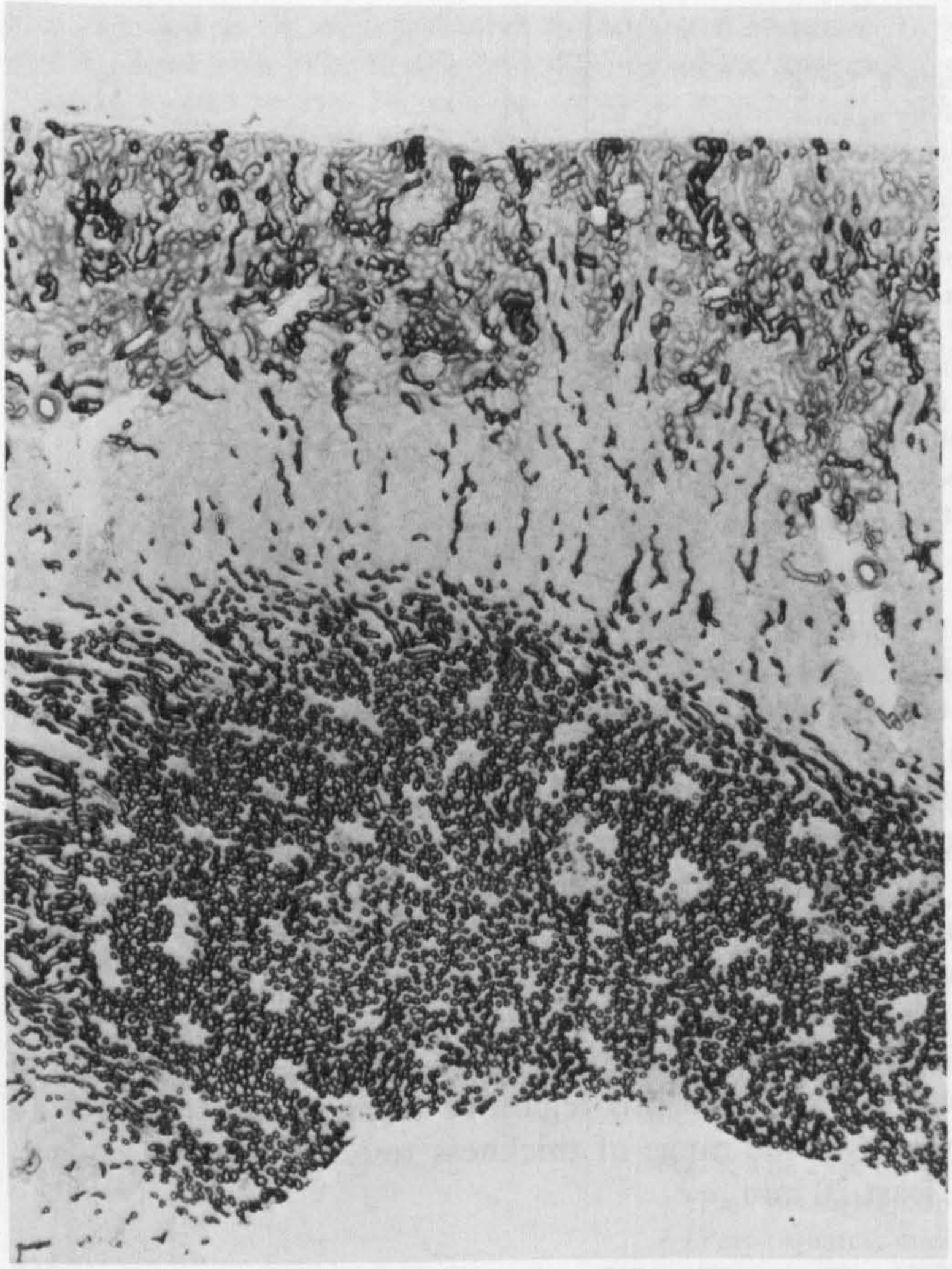

Fig. 4. A low-power view (×21) of a cryostat section of rat kidney reacted for total ATPase activity. The proximal tubules of the cortex can be seen by virtue of their weak, grey staining, the distal tubules being much darker. The thick ascending limbs of the loop of Henle in the medulla stain heavily

for total activity (mean integrated extinction × 100; mean ± SEM), in the presence of bromotetramisole, were 9.2 ± 1.2, 25.4 ± 2.8 and 16.9 ± 2.2 in the proximal convoluted and distal convoluted tubules and in the TAL respectively. The percentage of the total activity that was due to ouabain-sensitive $Na^+ - K^+$-ATPase activity was 38%, 60% and 64%, respectively. The addition of bromotetramisole had no effect on either the total or the $Na^+ - K^+$-ATPase activity in the distal convoluted tubules or in the TAL. Thus the total activity without bromotetramisole in these regions was 24.0 ± 3.3 and 16.1 ± 1.9, respectively.

Discussion

There seems little doubt that enzymes which hydrolyze ATP are of considerable importance in normal cell-function. These include the mitochondrial ATPases,

myosin ATPase activity of muscle, and the various ATPases of the cell surface. Initially it might have been hoped that the procedure of Wachstein and Meisel (1957) could have been used to demonstrate all these enzymes. However, the free lead ions used in this method inhibited the enzymes and hydrolyzed, non-enzymatically, the ATP used as substrate. A huge controversy grew up over the validity of the procedure (as reviewed by Ernst, 1972a). As regards the $Na^+ - K^+$-ATPase activity that is associated with cell membranes, and to avoid the contentious arguments over the validity of the use of lead ions as trapping agents, Ernst (1972a, b) also Guth and Albers (1974) turned to methods for demonstrating the K^+-dependent phosphatase activity. This is related to $Na^+ - K^+$-ATPase activity in that the hydrolysis of ATP by the $Na^+ - K^+$-ATPase is believed to proceed in at least two steps involving a sodium-dependent phosphorylation of the enzyme and a potassium-dependent dephosphorylation (Hokin and Dahl 1972). However, there is considerable evidence that the K^+-dependent phosphatase, responsible for the dephosphorylation, is not specific to the phosphorylated intermediate but can act on a variety of phosphate esters (as reviewed by Ernst 1972a). Beeuwkes and Rosen (1975, 1980) used a modified form of Ernst's (1972a, b) paranitrophenyl phosphate (PNPP) method; following Guth and Albers (1974) they relied on the rather inefficient (Ernst et al. 1980) capture of the liberated phosphate by magnesium and potassium ions. For all that, they showed clear differences in activities in the various parts of the nephron, both by visual inspection and by the use of electron probe analysis to quantify the amount of reaction-product produced in each region. They were able to show high activities in the distal convoluted tubules and in tubules which they considered to be the thick ascending limbs (TAL) of the loop of Henle. These activities were in agreement with microchemical results done after microdissection of the nephron (e.g. Schmidt and Dubach 1969).

The disadvantages of the PNPP method were: (i) it was indirect, measuring the K^+-dependent phosphatase activity that was generally, but not necessarily, related to the $Na^+ - K^+$-ATPase activity; it was of concern that the K^+-dependent phosphatase was not specific for the phosphorylated intermediate generated by $Na^+ - K^+$-ATPase activity; (ii) it did not demonstrate the $Na^+ - K^+$-ATPase activity that was known, from biochemical studies, to be present in the proximal convoluted tubules; thus it was unlikely to be of value in the study of less active ATPases in cells in which this activity was not as great as it is in the distal convoluted tubules and TAL.

We have therefore reverted to the Wachstein and Meisel method but have sought to overcome its deficiencies by ensuring that there are no free lead ions in the reaction-medium. In the lead ammonium citrate/acetate complex, the lead is hidden (and so made soluble in neutral and alkaline solutions) by ammonium citrate. Thus when it is added to a solution of ATP, the solution remains crystal-clear. However free phosphate, either added to the solution or generated by enzymatic hydrolysis, successfully competes with the ammonium citrate moieties and precipitates lead phosphate, which can then be converted to the brown-black lead sulphide. With this trapping agent, the enzymatic activity is linear with thickness (amount of enzyme) and with time. The activity increased with increasing concentration of the lead ammonium citrate/acetate up to the

concentration used in the present method; higher concentrations did not appear to inhibit the activity. The pH optimum of 7.6 recorded with this trapping agent is close to that reported for 'microsomal preparations' that include the cell membrane (Pérez-González de la Manna et al. 1980). The reaction seems to be specific for ATP and is not influenced by bromotetramisole which is a potent inhibitor of alkaline phosphatase (Borgers and Thoné 1975).

The reaction-product is precipitated along the contra-lumenal boundary of the cells, which is the expected location of the enzyme (Beeuwkes and Rosen 1975, 1980; Pérez-González de la Manna et al. 1980; Ernst et al. 1980). It was found in greatest concentration, in the guinea-pig and the rat, in the TAL and in the distal convoluted tubules, and was appreciably less active in the proximal convoluted tubules. These findings agree with those of Katz et al. (1979) who assayed ATPase activities microchemically in regions of the nephron of the rat, mouse and rabbit. Their results were expressed in terms of picomoles of ATP hydrolyzed per millimetre length of the region of the nephron per hour and therefore cannot be directly related to cytochemical measurements which give the concentration of the activity per cell. Nonetheless, the proportion of the total activity that was due to the specific, ouabain-sensitive, $Na^+ - K^+$-ATPase activity should be similar, whether measured microchemically or cytochemically. In the rat, Katz et al. (1979) found that the proportion of the total activity that was due to $Na^+ - K^+$-ATPase activity was 51% (proximal convoluted), 76–78% (TAL) and 65% (distal convoluted tubule). The results of the present method were 38%, 64% and 60% respectively. The relative values of the total activity in the three regions were also similar: taking the total ATPase activity of the distal convoluted tubules as 100, the activity in the proximal convoluted tubules, found by Katz et al. was 44 (in comparison with 36 in the present study), and that in the TAL was 59 (as against 66 in the present study).

The results indicate that the present method, based on a hidden-lead trapping agent, can measure ouabain-sensitive ATPase activity, with relative values in different regions of the nephron that are in general conformity with results obtained by microchemical methods. The advantages of the present method are that it affords a direct measurement of ATPase activity, rather than depending on the related, or associated, K^+-dependent phosphatase activity; it seems to be more sensitive than previous methods, as shown by the measurement of activity in the proximal convoluted tubules; and it should be possible to adapt it to the measurement of a wide range of ATPase activities, such as calcium-dependent ATPase, mitochondrial ATPases and possibly even adenyl cyclase activity.

Acknowledgements. Part of this work was done with the aid of a grant from the Medical Research Council (to PHB) and from the Arthritis and Rheumatism Council for Research (to RAD).

References

Baker PF (1972) The sodium pump in animal tissues and its role in the control of cellular metabolism and function. In: Hokin LE (ed) Metabolic transport. 3rd edn. Academic Press, New York London, pp 243 268

Beeuwkes R III, Rosen S (1975) Renal sodium-potassium adenosine triphosphatase optical localization and X-ray microanalysis. J Histochem Cytochem 23:828 839

Beeuwkes R, Rosen S (1980) Renal $Na^+ - K^+$-ATPase: localization and quantitation by means of its K^+-dependent phosphatase activity. Curr Top Membr Transp 13:343–354

Bitensky L (1980) Microdensitometry. In: Evered D, O'Connor M (eds) Trends in enzyme histochemistry and cytochemistry. Excerpta Medica, Amsterdam, pp 181–202

Borgers M, Thoné F (1975) The inhibition of alkaline phosphatase by L-*p*-bromotetramisole. Histochemistry 44:277–280

Chayen J (1978a) The cytochemical approach to hormone assay. Int Rev Cytol 53:333–396

Chayen J (1978b) Microdensitometry. In: Slater TF (ed) Biochemical mechanisms of liver injury. Academic Press, London New York, pp 257–291

Chayen J (1980) The cytochemical bioassay of polypeptide hormones. Springer, Berlin Heidelberg New York

Chayen J, Bitensky L, Butcher RG (1973) Practical histochemistry. J Wiley, New York London

Chayen J, Bitensky L, Butcher RG (1975) Histochemie: Grundlagen und Methoden. Verlag Chemie, Weinheim

Ernst SA (1972a) Transport adenosine triphosphatase cytochemistry. I. Biochemical characterization of a cytochemical medium for the ultrastructural localization of ouabain-sensitive, potassium-dependent phosphatase activity in the avian salt gland. J Histochem Cytochem 20:13–22

Ernst SA (1972b) Transport adenosine triphosphatase cytochemistry. II. Cytochemical localization of ouabain-sensitive, potassium-dependent phosphatase activity in the secretory epithelium of the avian salt gland. J Histochem Cytochem 20:23–38

Ernst SA, Riddle CV, Karnaky KJ Jr (1980) Relationship between localization of $Na^+ - K^+$-ATPase, cellular fine structure and resorptive and secretory electrolyte transport. Curr Top Membr Transp 13:355–385

Guth L, Albers RW (1974) Histochemical demonstration of $(Na^+ - K^+)$-activated adenosine triphosphatase. J Histochem Cytochem 22:320–326

Hokin LE, Dahl JL (1972) The sodium-potassium adenosine triphosphatase. In: Hokin LE (ed) Metabolic transport. 3rd edn. Academic Press, New York London, pp 269–315

Katz AI, Doucet A, Morel F (1979) Na-K-ATPase activity along the rabbit, rat and mouse nephron. Am J Physiol 237:F114–F120

Kinne R, Keljo D, Gmaj P, Murer H (1978) The energy source of glucose and calcium transport in the renal proximal tubule. In: Vogel HG, Ullrich KJ (eds) New aspects of renal function. Excerpta Medica Foundation, Amsterdam, pp 41–50

Pérez-González de la Manna M, Proverbio F, Whittembury G (1980) ATPases and salt transport in the kidney tubule. Curr Top Membr Transp 13:315–335

Schmidt U, Dubach UC (1969) Activity of (Na^+K^+)-stimulated adenosine triphosphatase in the rat nephron. Pfluegers Arch 306:219–226

Schmidt U, Schmidt H, Funk B, Dubach UC (1974) The function of Na, K-ATPase in single portions of the rat nephron. Ann NY Acad Sci 242:489–500

Schwartz A, Nagano K, Nakao M, Lindenmayer GE, Allen JC, Matsui H (1971) The sodium- and potassium-activated adenosinetriphosphatase system. In: Schwartz A (ed) Methods in pharmacology. vol 1. Appleton-Century-Crofts, New York, pp 361–388

Wachstein M, Meisel E (1957) Histochemistry of hepatic phosphatases at a physiologic pH. Am J Clin Pathol 27:13–23

Zaman G, Chayen J (1981) An aqueous mounting medium. J Clin Pathol (in the press)

Received February 9, 1981

CHANGES IN CRYSTAL SIZE AND ORIENTATION OF ACIDIC GLYCOSAMINOGLYCANS AT THE FRACTURE SITE IN FRACTURED NECKS OF FEMUR

G. N. KENT, PhD
Research Fellow
Division of Inherited Metabolic Diseases
Clinical Research Centre, and Division of Cellular Biology
Mathilda and Terence Kennedy Institute of Rheumatology

R. A. DODDS, BSc (Hons)
Research Fellow
Mathilda and Terence Kennedy Institute of Rheumatology
Bute Gardens, Hammersmith, London W6 7DW, England

LUCILLE BITENSKY, DSc, FRCPath
Head of Medical Histochemistry Laboratory
Mathilda and Terence Kennedy Institute of Rheumatology
Bute Gardens, Hammersmith, London W6 7DW, England

J. CHAYEN, MInstP, DSc
Head of Division of Cellular Biology
Mathilda and Terence Kennedy Institute of Rheumatology
Bute Gardens, Hammersmith, London W6 7DW, England

L. KLENERMAN, ChM, FRCS
Consultant Orthopaedic Surgeon
Department of Orthopaedics, Northwick Park Hospital
Watford Road, Harrow, Middlesex HA1 3UJ, England

and

R. W. E. WATTS, FRCP, FRSC
Consultant Physician
Division of Inherited Metabolic Diseases, MRC Clinical Research Centre
Watford Road, Harrow, Middlesex HA1 3UJ, England

REPRINTED FROM
THE JOURNAL OF BONE AND JOINT SURGERY
BRITISH VOLUME
Number Two 1983
British Editor: R. C. F. Catterall

CHANGES IN CRYSTAL SIZE AND ORIENTATION OF ACIDIC GLYCOSAMINOGLYCANS AT THE FRACTURE SITE IN FRACTURED NECKS OF FEMUR

G. N. KENT, R. A. DODDS, L. KLENERMAN, R. W. E. WATTS, LUCILLE BITENSKY, J. CHAYEN

From the Kennedy Institute of Rheumatology, London, and the Clinical Research Centre and Northwick Park Hospital, Harrow

The aim of this study was to try to elucidate the increased susceptibility of the neck of femur to fracture. Quantitative polarised light microscopy has been applied to fresh, undecalcified sections of samples of bone taken from the site of fracture, in specimens taken at operation from patients with fractures of the femoral neck or osteoarthritic femoral heads or from the equivalent site from otherwise normal subjects at necropsy. In all 21 specimens of fractured necks of femur, but in none of the other specimens, relatively large crystals (up to 2.5 × 0.5 micrometres) were found close to the site of fracture; the properties of these crystals were compatible with their being apatite. Measurement of the natural birefringence of the collagen showed no difference in the orientation of the collagen in all three types of specimen. However, the orientation of acidic glycosaminoglycans, measured by the birefringence of alcian blue bound to these moieties, was 45 per cent lower in the specimens from fractured necks of femur than in the other specimens, even though the total content of acidic glycosaminoglycans was unchanged. Although the decreased orientation was most marked close to the site of fracture, it was still apparent 15 millimetres from that site. These changes were unlikely to be simply the sequelae of fracture since they were not found in traumatic fractures of other bones. Thus it is conceivable that changes in the orientation of the ground substance allow formation of relatively large crystals of apatite and that such crystals, in the microcrystalline mass of apatite, are the cause of the increased fragility of such bones.

The incidence of fractures of the femoral neck rises exponentially after the age of 50 years (Knowelden, Buhr and Dunbar 1964) and the fractures are usually the result of only relatively minor trauma. An estimated 40 000 such fractures occur in the United Kingdom each year (Lewis 1981). They represent a significant social and medical problem in terms of treatment and rehabilitation (Lewinnek *et al.* 1980). It is apparent from the reported studies on the aetiology of fractures of the femoral neck that there is no single cause of the fracture but rather it is associated with a combination of factors such as age, sex, nature and type of fall, and changes in bone fragility (Elsasser *et al.* 1980; Cook *et al.* 1982).

The structural changes that occur in the femoral head before fracture are poorly understood, partly because they may be a result of several sequential or concurrent changes such as osteoporosis, osteomalacia or in the tensile strength of the bone matrix (Wall, Chatterji and Jeffery 1979; Cook *et al.* 1982). Since the decrease in tensile strength of bone with age progresses at a greater rate than the decrease in bone density (Wall *et al.* 1979), a change in structure of the bone or in the interaction between the organic matrix and the mineral phase could explain the increased liability of the femoral neck to fracture in these individuals. In osteoporotic patients who have had a femoral neck fracture, changes in the mechanical properties of machined pieces of the femoral shaft compared to similar pieces prepared from normal subjects have been found by Dickenson, Hutton and Stott (1981). The bone specimens tested under tension from patients who had femoral neck fractures had less stiffness and strength compared with normal bone and these changes were correlated with the degree of osteoporosis. Moreover, these bones had considerably reduced energy absorption before failure and this was not related to changes in mineral content of the bone or to the degree of osteoporosis. Thus this bone has a much

G. N. Kent, PhD, Research Fellow
Division of Inherited Metabolic Diseases, Clinical Research Centre, and Division of Cellular Biology, Mathilda and Terence Kennedy Institute of Rheumatology.
R. A. Dodds, BSc (Hons), Research Fellow
Lucille Bitensky, DSc, FRCPath, Head of Medical Histochemistry Laboratory
J. Chayen, M Inst P, DSc, Head of Division of Cellular Biology
Mathilda and Terence Kennedy Institute of Rheumatology, Bute Gardens, Hammersmith, London W6 7DW, England.
L. Klenerman, ChM, FRCS, Consultant Orthopaedic Surgeon
Department of Orthopaedics, Northwick Park Hospital, Watford Road, Harrow, Middlesex HA1 3UJ, England.
R. W. E. Watts, FRCP, FRSC, Consultant Physician
Division of Inherited Metabolic Diseases, MRC Clinical Research Centre, Watford Road, Harrow, Middlesex HA1 3UJ, England.
Requests for reprints should be sent to Mr L. Klenerman.

© 1983 British Editorial Society of Bone and Joint Surgery
0301–620X/83/2043–0189 $2.00

greater tendency to fracture during the sudden stress of a fall when the work done on the bone is too great to be elastically absorbed.

The three-dimensional structure of bone, especially the morphology of bone mineral, has been studied with techniques such as polarised light microscopy (von Ebner 1894; von Schmidt 1938), x-ray diffraction (Carlström 1955; Engström 1972; Chatterji, Wall and Jeffery 1981), electron microscopy (Robinson 1952; Bernard 1969; Bocciarelli 1970; Voegel and Frank 1977) and scanning electron microscopy (Jackson, Cartwright and Lewis 1978). Although there is some disagreement on the habit of the crystallites (rod- or plate-like) and the orientation of the crystallite c-axis with regard to the long axis of the collagen fibre (parallel or perpendicular) there is very good agreement that the crystals must be small in size (50 nanometres or less in the long axis). Lees (1979) attempted to reconcile the two types of crystallite habit and orientation into one model for the distribution of hydroxyapatite crystals in bone. More recently, Chatterji *et al.* (1981), using x-ray diffraction techniques, measured the orientation and size of crystals in human femoral cortical bone taken from individuals within the age range 13 to 97 years. After the age of 60, there was a marked change in the distribution of crystallites so that older bones had a greater proportion of large crystallites (over 600 nanometres).

In the present study, we have used quantitative polarised light microscopy to identify changes in the microstructure of some of the components of bone at the site of fracture that could explain the increased fragility of the bone in patients who have suffered fracture of the femoral neck. Some of this study has been presented at a meeting of the British Orthopaedic Research Society.

MATERIALS AND METHODS

Femoral heads were obtained from Northwick Park Hospital between December 1980 and October 1981 from patients undergoing total hip replacement for severe osteoarthritis or Thompson replacement for subcapital femoral neck fractures; others were obtained at necropsy from patients whose death was not related to any bone disease.

For studies on crystals, 19 osteoarthritic samples (five male, and 12 female; mean age and standard deviation, 67.6 ± 11.5 years), 16 cadaveric samples (five male, 11 female; mean age and standard deviation, 73.7 ± 8.2 years) and 21 samples of fractured necks of femur (one male; mean age and standard deviation, 76.7 ± 12.6 years) were investigated. For studies on the birefringence of collagen and of the glycosaminoglycans, the number of specimens and the ages of the subjects were eight (62.1 ± 14.7 years), eight (72.3 ± 5.1 years) and 11 (80.4 ± 12.0 years) respectively.

Small blocks of trabecular bone (about 2 × 1 × 3 centimetres) were sawn from the femoral head to include the fracture site or from an equivalent position at the epiphysial region of the osteoarthritic and cadaveric bones. Pieces of bone were also collected at operation from three patients who had suffered traumatic fractures of the tibial or femoral shaft or the neck of humerus. After brief immersion in five per cent (weight/volume) polyvinyl alcohol (GO4/140 Polyviol; Wacker Chemicals) the blocks of bone were chilled to −70 degrees Celsius in *n*-hexane.

Cryostat sections (10 micrometres thick) of the unfixed, undemineralised bone were prepared as previously described (Johnstone 1979). The sections were cut from the blocks orientated in such a way that one side of the section was at the fracture surface or the equivalent surface from the osteoarthritic or cadaveric specimens. All sections were dried overnight at 37 degrees Celsius. They were then inspected, under crossed polars, either unstained or after staining with alcian blue by the critical electrolyte concentration method of Scott and Dorling (1965) as described by Chayen, Bitensky and Butcher (1973). These methods depend on the fact that whereas collagen fibres naturally show form birefringence, the orientation of the acidic glycosaminoglycans and related molecules can be demonstrated only after a birefringent dye has been attached to them (Módis 1974). All microscopic examinations and birefringence measurements, using a Brace-Köhler $\lambda/30$ compensator, were done on a Zeiss universal microscope equipped with a range of polarising objectives (16×, 0.32 NA; 40×, 0.85 NA; 63×, 0.9 NA). Birefringence was expressed as nanometres of optical path difference (R_{obj}) after conversion of the angle of rotation of the Brace-Köhler compensator (ψ_{comp}) according to the equation

$$R_{obj} = R_{comp} \sin 2\psi_{comp}$$

where R_{comp} is the optical path difference imposed by the compensator (Chayen and Denby 1968). The refractive index of crystals was determined by the method described by Watts *et al.* (1971). The amount of alcian blue staining in the areas used for birefringence measurements was quantified with a Zeiss photometer head fitted to the microscope; the optical density was determined with a standard mask-aperture with light from a mercury-vapour lamp. The photometer was calibrated with a series of neutral density filters.

RESULTS

Reproducibility of measurements of birefringence. On six occasions, the birefringence (optical path difference) was measured five times by each of two of us. The overall coefficient of variance was 9.5 per cent.

Appearance of sections under crossed polars. All sections from all 35 osteoarthritic or cadaveric specimens, either mounted in air or in benzaldehyde (refractive index 1.545), showed highly birefringent lamellae of collagen, often with the haversian systems in the plane of the section. In between these arrays of collagen, the section appeared to be as black as the background, indicating an apparent lack of suitably orientated birefringent material (Figs 1 and 2). Such sections, which were fully mineralised, were indistinguishable from sections of bone that had been chemically fixed, decalcified, embedded in paraffin and sectioned in a routine histological laboratory. An exactly similar image was obtained when the sections of undemineralised bone were treated with EDTA (0.1M) at pH7 for 16 hours to remove the mineral component. These results implied that the crystals of mineral, in the undecalcified sections, were too small, and too disorientated, to be detected in this microscopic system.

In marked contrast, in all 21 samples of fractured necks of femur, discrete crystalline material was found, particularly close to the site of fracture, in between the collagen lamellae (Figs 3 and 4). The incidence of crystals decreased with distance (up to three centimetres) from the site of fracture. These crystals showed true crystalline birefringence in that their birefringence was virtually unaffected by the refractive index of the medium in which the sections were mounted. They showed straight

extinction, positive birefringence and appeared to be hexagonal. Although many were small, about 0.5 micrometres long, many were 2.5 by 0.5 micrometres. The optical path difference through such large crystals was only 19 nanometres; assuming a thickness of 0.5 micrometres, this indicates a birefringence of 3.8×10^{-2}.

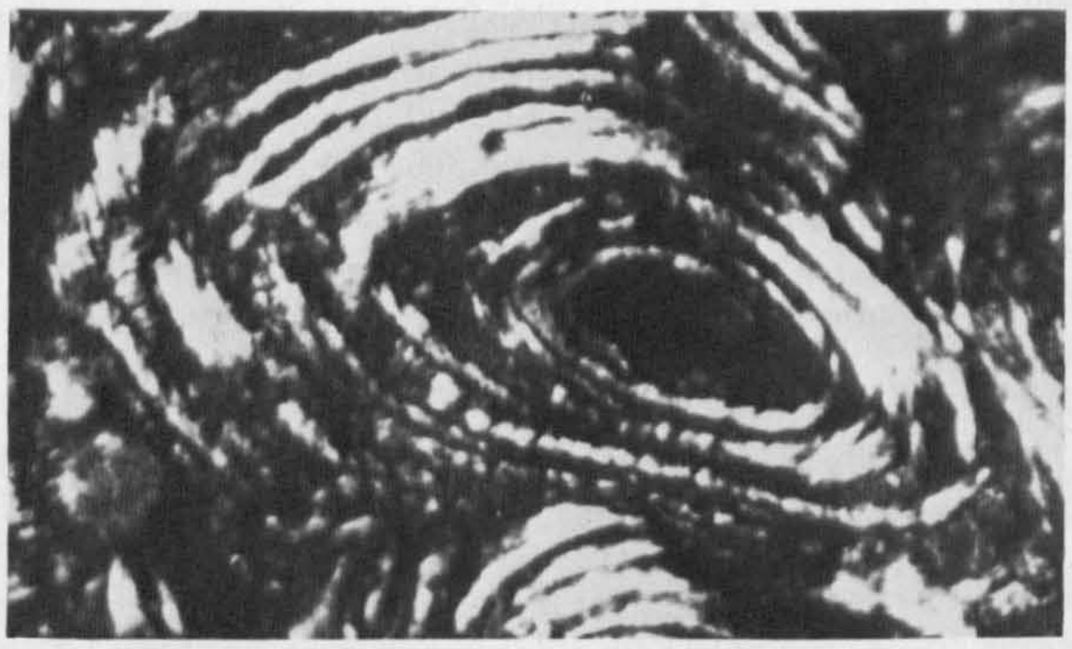

Fig. 1

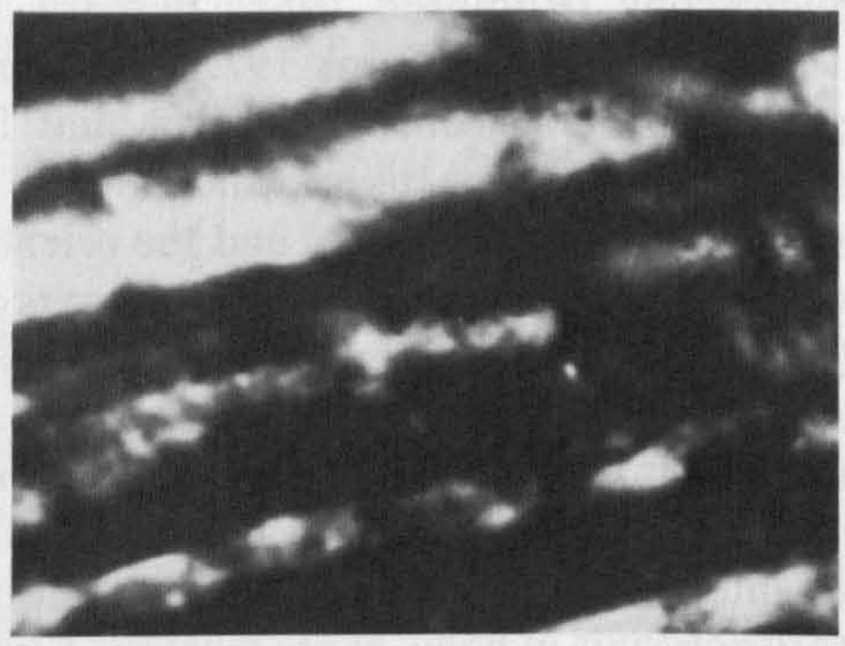

Fig. 2

Section of undecalcified osteoarthritic bone, viewed between crossed polars. Figure 1—The spaces between the birefringent collagen bundles of the haversian system are clear of birefringent material (×440). Figure 2—The space between the birefringent (white) collagen is devoid of crystalline material (×1750).

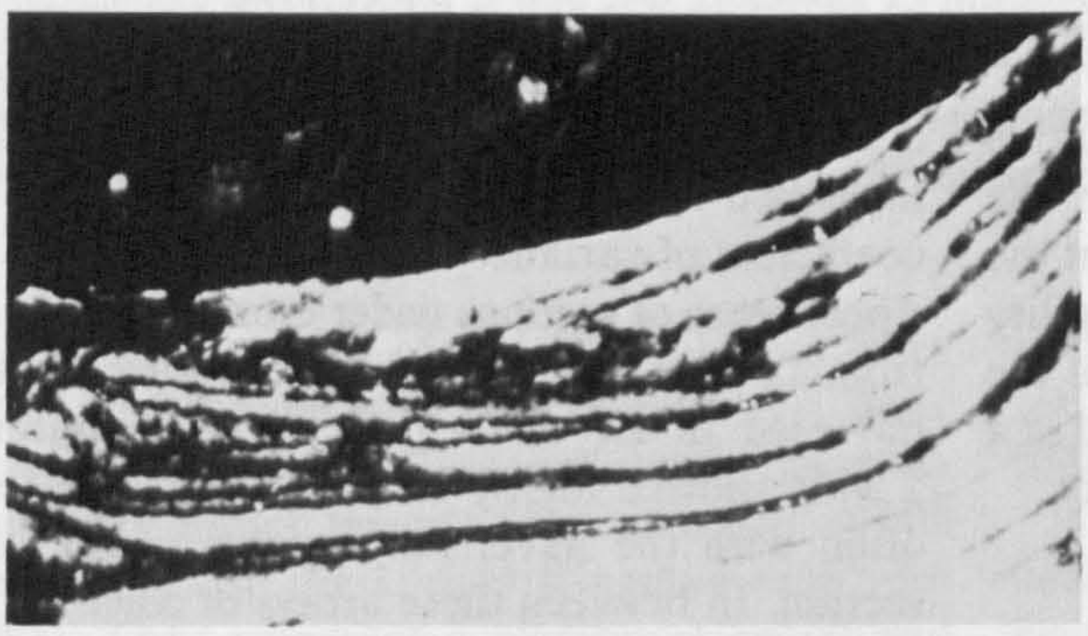

Fig. 3

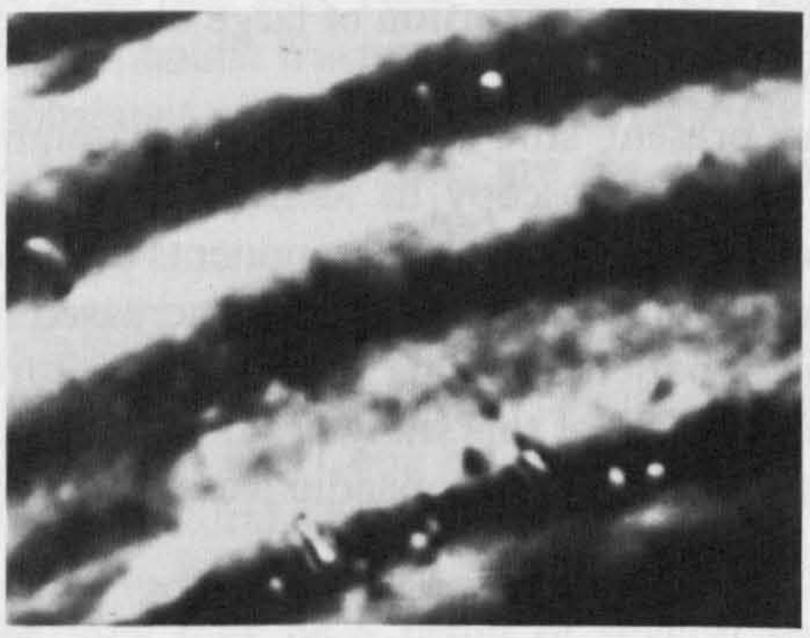

Fig. 4

Section of undecalcified bone from the area of the fracture of a fractured neck of femur. Even in the low-power photograph (Fig. 3: ×440), and more discretely in the higher power view (Fig. 4: ×1750), birefringent and apparently crystalline material can be seen in between, and on, the birefringent (white) collagen.

The refractive index was greater than 1.545. Thus in all features, these crystals corresponded to crystals of apatite.

Birefringence of collagen and acidic glycosaminoglycans. Untreated sections were examined by polarised light microscopy. The optical path difference measured in the collagen lamellae was the same in all three types of specimen (Table I).

Sections stained with alcian blue, in the presence of either concentration of magnesium chloride, and examined by polarised light microscopy showed blue birefringent matter apparently coincident with the collagen lamellae. The white birefringence of the latter was largely obscured by the blue birefringence. The optical path difference induced by this blue birefringence in sections of osteoarthritic and cadaveric samples, stained by alcian blue in the presence of 0.025M-$MgCl_2$ was identical. It was markedly less in the sections from the fractured necks of femur (Table I): it was least when close to the site of fracture and rose to higher values up to 15 millimetres from the fracture (Fig. 5); however, even at this distance from the fracture, the values did not achieve

Table I. Birefringence (optical path difference) of collagen and sections of bone stained with alcian blue, measured in nanometres of retardation (mean ±SEM)

Treatment	Osteo-arthritic ($n=8$)	Cadaveric ($n=8$)	Fractured neck of femur ($n=11$)	Traumatic fractures ($n=2$ or 3)
Unstained collagen	17.4 ± 0.5	17.2 ± 0.6	16.7 ± 0.2	14.7, 16.9
Alcian blue + 0.025M-$MgCl_2$	20.3 ± 0.4	20.2 ± 0.3	11.2 ± 0.4*	19.1, 21.0
Alcian blue + 0.5M-$MgCl_2$	15.2 ± 0.6	15.8 ± 0.6	7.8 ± 0.5*	17.3, 15.8, 15.1

*Significantly different ($P<0.001$) from osteoarthritic and cadaveric groups; Student's t-test

normal levels. Although the higher concentration of magnesium chloride decreased the amount of alcian blue birefringence, essentially similar results were obtained (Table I; Fig. 5).

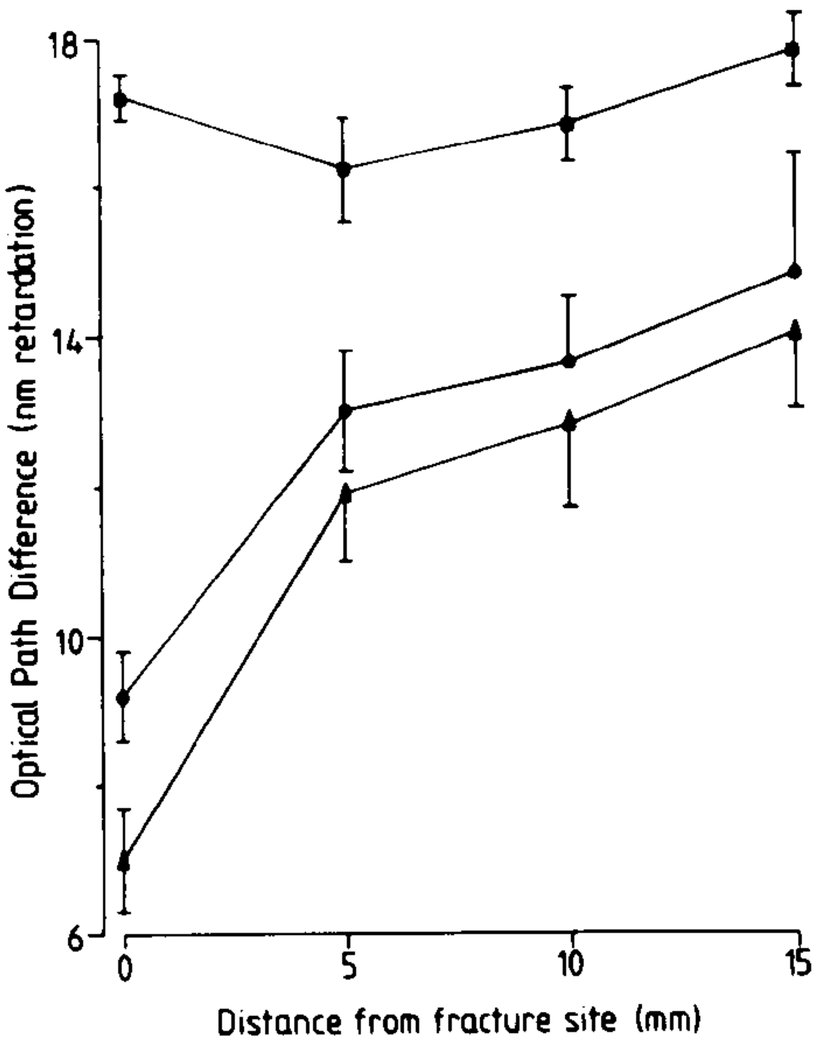

Fig. 5

The amount of birefringence (optical path difference, measured as nanometres of retardation of the polarised light) found in the collagen (squares), in the material that was stained with alcian blue either with the low (circles) or the high (triangles) concentration of magnesium chloride, at different distances from the fracture site. The results represent the mean ± SEM measured in two sections from each of five specimens, each measured five times independently by two observers.

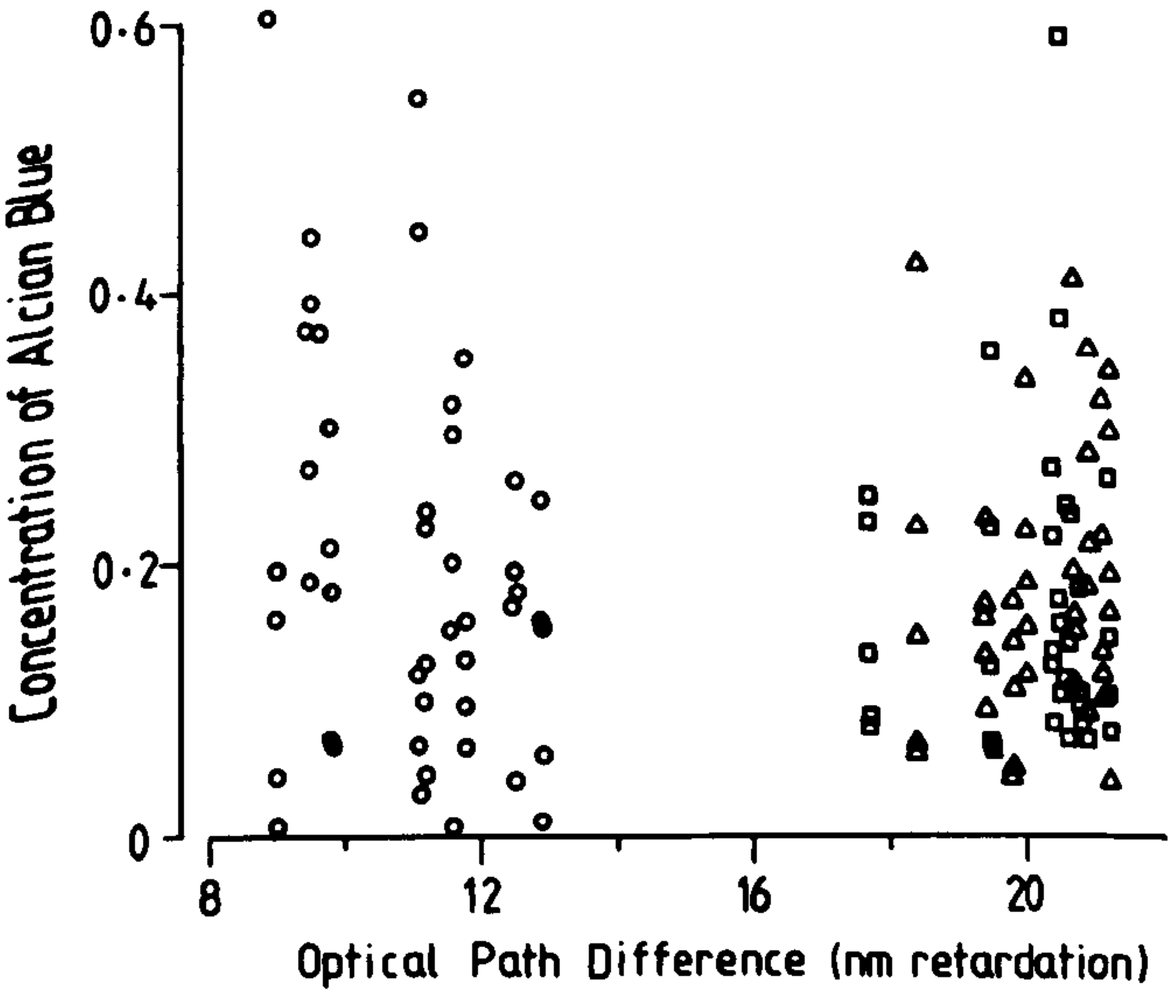

Fig. 6

The concentration of alcian blue stain, measured by direct microscopic photometry (as extinction of the dye) measured in the same microscopic field as the birefringence of oriented dye (optical path difference) in sections of fractured necks of femur (circles), of cadaveric (triangles) and of osteoarthritic (squares) specimens. Although there is a clear difference in the degree of orientation (optical path difference), this is not reflected in the total amount of dye present.

Content of acidic glycosaminoglycans. In a few sections, the amount of alcian blue stain present was measured by direct photometry in the same regions as had been selected for birefringence measurements. These results (Fig. 6) showed that the content of acidic glycosaminoglycans through the thickness of the section was equivalent in all three types of specimen even though the amount of birefringence in the individual lamellae in sections from the fractured necks of femur was decreased by about 45 per cent.

Results with traumatic fractures. No crystals were found in several serial sections taken from these fractures. The optical path difference measured in the native collagen and the alcian blue birefringence in sections stained at both concentrations of magnesium chloride agreed closely with the values found in the non-fractured specimens (Fig. 7).

DISCUSSION

The relationship between applied tensile load and resultant strain in normal and osteoporotic bone (Dickenson *et al.* 1981) shows the elastic component, presumably related to collagen, is virtually identical. The difference between these types of bone lies in the plastic loading region so that the latter will break at lower load; this region is presumably related to the properties of the mineral component. In agreement with these findings, the degree of orientation of the collagen has been the same in the specimens of fractured neck of femur as in the other two categories. However, the mineral phase has been found to be different in that, close to the site of fracture, some of the mineral phase occurred in the form of crystals of the size that could readily be resolved by normal, polarised light microscopy. Such crystals were not seen in the few traumatic fractures that have been available for study so that the crystals seen in the fractured necks of femur were unlikely to be due simply to the fracture process.

The use of the potential birefringent properties of alcian blue allowed studies to be made on the orientation of acidic glycosaminoglycans. Under the conditions used in this study, as defined by Scott and Dorling (1965), in the presence of 0.025M-$MgCl_2$ this dye will stain all acidic glycosaminoglycans and other acidic molecules, such as hyaluronic acid and acidic proteins. Although such acidic molecules may not be birefringent, even when orientated, the stain that is bound to such orientated molecules will exhibit birefringence (Módis 1974). At the higher concentration of magnesium chloride, the binding of the dye is restricted to highly sulphated, long-chain moieties, mainly chondroitin and keratan sulphates (Scott and Dorling 1965; Scott 1973).

The total content of acidic glycosaminoglycans was the same in all samples tested in this study. However, the degree of orientation, both of the "non-specific" acidic moieties (stained in the presence of the lower concentration of magnesium chloride) and of the chondroitin and

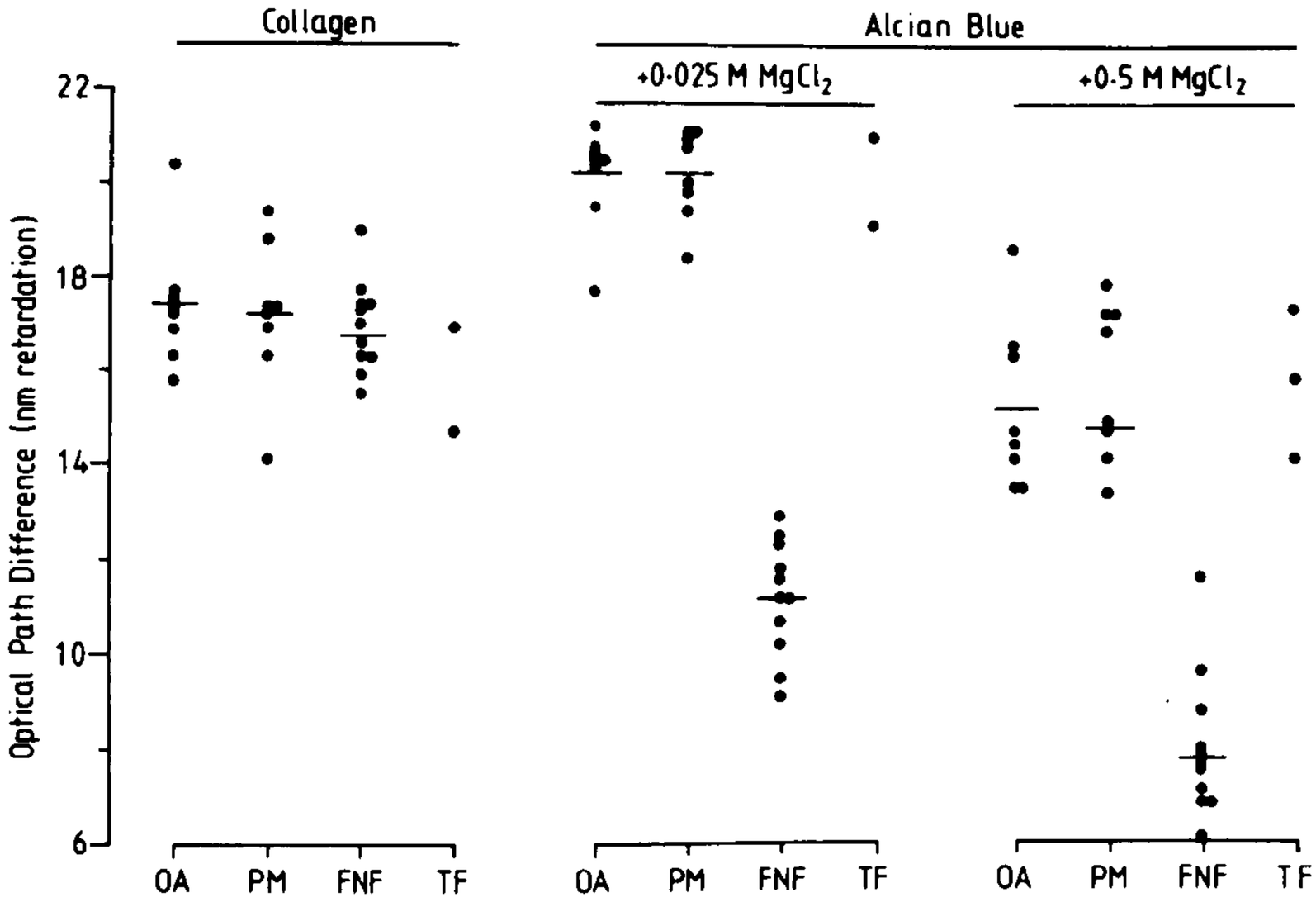

Fig. 7

Scattergram showing the degree of orientation (optical path difference) in the collagen and in the ground substance (stained with alcian blue with either 0.025M- or 0.5M-$MgCl_2$) in sections from osteoarthritic (OA) cadaveric (PM), fractured necks of femur (FNF) and traumatic fractures (TF). The bar indicates the mean value for each group. (The statistical significance of these results is given in Table I).

keratan sulphate-like moieties, was about 45 per cent less in the bone from the fractured necks of femur than in the osteoarthritic or cadaveric specimens. This decreased orientation was maximal close to the site of fracture and tended towards more normal values further from the fracture. But it was noteworthy that the birefringence was subnormal even 15 millimetres from the fracture (Fig. 5). This effect was also unlikely to be a direct consequence of fracture since the orientation of alcian blue-stained material in the lamellae of the traumatic fractures was the same as in the "control" specimens (Fig. 7).

Thus this study has shown that, close to the fracture, relatively large crystals, that appear to have the optical properties of apatite, have been detected in all 21 cases of fractured necks of femur and in none of the 35 other control specimens or in the three traumatic fractures. This finding is in keeping with the observations of Wall *et al.* (1979) and of Chatterji *et al.* (1981) that, with advancing age, some microstructural change occurs in bone and that the density of the bone is not the sole determining factor in its resistance to fracture. The development of crystals, of the size found in the present study, would be in keeping with a microstructural change that could predispose the bone to fracture. It is well known (Forsyth 1969; Engel and Klingele 1981) that the presence of such crystals in otherwise microcrystalline metals can be a source of structural failure or fracture.

The finding that the orientation of ordered components of the non-collagenous ground substance is also decreased in the fractured necks of femur may indicate a cause for the development of such anomalously large crystals of apatite in the microcrystalline mineral phase. This arises from the fact that the crystallisation of apatite can be modulated by glycosaminoglycans (Boskey 1981). The fact that these changes, and the appearance of crystals, occur only at a specific locus may be related to the fact that this region is the site of greatest shear; it is the site of greatest tension, as calculated by Singh, Nagrath and Maini (1970).

We are grateful for a grant from the Percy Bilton Charity that allowed this work to be done. Specific and general support from the Arthritis and Rheumatism Council for Research is also gratefully acknowledged.

REFERENCES

Bernard GW. The ultrastructural interface of bone crystals and organic matrix in woven and lamellar endochondral bone. *J Dent Res* 1969;**48** (5) Suppl:781–8.

Bocciarelli DS. Morphology of crystallites in bone. *Calcif Tissue Res* 1970;**5**:261–9.

Boskey AL. Current concepts of the physiology and biochemistry of calcification. *Clin Orthop* 1981;**157**:225–57.

Carlström D. X-ray crystallographic studies on apatites and calcified structures. *Acta Radiol* 1955;Suppl 121:33–7.

Chayen J, Bitensky L, Butcher RG. *Practical histochemistry*. London, New York, Sydney, Toronto: John Wiley & Sons, 1973:75–6.

Chayen J, Denby EF. *Biophysical technique: as applied to cell biology*. London: Methuen, 1968.

Chatterji S, Wall JC, Jeffery JW. Age-related changes in the orientation and particle size of the mineral phase in human femoral cortical bone. *Calcif Tissue Int* 1981;**33**:567–74.

Cook PJ, Exton-Smith AN, Brockelhurst JC, Lempert-Barber SM. Fractured femurs, falls and bone disorders. *J R Coll Physicians* 1982;**16**:45–9.

Dickenson RP, Hutton WC, Stott JRR. The mechanical properties of bone in osteoporosis. *J Bone Joint Surg [Br]* 1981;**63–B**:233–8.

Elsasser U, Hesp R, Klenerman L, Wooton R. Deficit of trabecular and cortical bone in elderly women with fracture of the femoral neck. *Clin Sci* 1980;**59**:393–5.

Engel L, Klingele H. *An atlas of metal damage: surface examination by scanning electron microscope.* Munich and London: Wolfe Medical and Scientific Publications, 1981.

Engström A. Aspects of the molecular structure of bone. In: Bourne GH, ed. *The biochemistry and physiology of bone.* Vol I, 2nd ed. New York, San Francisco and London: Academic Press, 1972:237–57.

Forsyth PJE. *The physical basis of metal fatigue.* London: Blackie & Sons Ltd, 1969.

Jackson SA, Cartwright AG, Lewis D. The morphology of bone mineral crystals. *Calcif Tissue Int* 1978;**25**:217–22.

Johnstone JJ. The routine sectioning of undecalcified bone for cytochemical studies. *Histochem J* 1979;**11**:359–65.

Knowelden J, Buhr AJ, Dunbar O. Incidence of fractures in persons over 35 years of age: a report to the MRC Working Party on fractures in the elderly. *Br J Prev Soc Med* 1964;**18**:130–41.

Lees S. A model for the distribution of HAP crystallites in bone: an hypothesis. *Calcif Tissue Int* 1979;**27**:53–6.

Lewinnek GE, Kelsey J, White AA III, Krieger NJ. The significance and a comparative analysis of the epidemiology of hip fractures. *Clin Orthop* 1980; **152**:35–43.

Lewis AF. Fracture of neck of the femur: changing incidence. *Br Med J* 1981;**283**:1217–20.

Módis L. Topo-optical investigations of mucopolysaccharides (acid glycosaminoglycans). In: Graumann W, Neumann K, eds. *Handbuch der Histochemie*, Vol. II. Polysaccharides Part 4. Stuttgart: G. Fischer Verlag, 1974.

Robinson RA. An electron microscopic study of the crystalline inorganic component of bone and its relationship to organic matric. *J Bone Joint Surg [Am]* 1952;**34–A**:389–434.

Scott JE. Affinity, competition and specific interactions in the biochemistry and histochemistry of polyelectrolytes. *Biochem Soc Trans* 1973;**1**: 787–806.

Scott JE, Dorling J. Differential staining of acid glycosaminoglycans (mucopolysaccharides) by alcian blue in salt solutions. *Histochemie* 1965;**5**: 221–33.

Singh M, Nagrath AR, Maini PS. Changes in the trabecular pattern of the upper end of the femur as an index of osteoporosis. *J Bone Joint Surg [Am]* 1970;**52–A**:457–67.

Voegel JC, Frank RM. Ultrastructural study of apatite crystal dissolution in human dentine and bone. *J Biol Buccale* 1977;**5**:181–94.

von Ebner V. Über eine optische Reaction der Bindesubstanzen auf Phenole. *S B Akad Wiss Wien* 1894;103:Abt 3, 162–88.

von Schmidt WJ. Polarisationoptische Analyse des submikrsoskopischen Baues von Zellen und Geweben. *Handbuch biol Arb-meth* 1938;Abt 5 Teil 10:435–665.

Wall JC, Chatterji S, Jeffery JW. Age related changes in the density and strength of human femoral cortical bone. *Calcif Tissue Int* 1979;**27**: 105–8.

Watts RWE, Scott JT, Chalmers RA, Bitensky L, Chayen J. Microscopic studies on skeletal muscle in gout patients treated with allopurinol. *Q J Med* 1971;NS **40**:1–14.

ly occurring indoles of cruciferous plants *J. Natl. Cancer Inst.* **54**, 985–988
9 Pantuck, E. J., Hsiao, K. C., Kuntzman, R. and Conney, A. H. (1975) Intestinal metabolism of phenacetin in the rat: Effect of charcoal-broiled beef and rat chow *Science* **187**, 744–746
10 Hietanen, E. (1980) Oxidation and subsequent glucuronidation of 3,4-benzopyrene in everted intestinal sacs in control and 3-methylcholanthrene-pretreated rats *Pharmacology* **21**, 233–243
11 Hietanen, E. and Lang, M. (1978) Conjugation reactions in drug biotransformation (Aitio, A., Ed.) Elsevier, Amsterdam, pp. 399–408
12 Aitio, A., Vainio, H. and Hänninen, O. (1972) Enhancement of drug oxidation and conjugation by carcinogens in different rat tissues *FEBS Lett.* **24**, 237–240
13 Hietanen, E. (1981) Gastrointestinal defence mechanisms. (Moszik, G. Hänninen, O. and Jávor, T., Eds) Pergamon Press, London, pp. 373–384
14 Turner, J. G., Shanks, V., Kelly, W. J. and Green, R. S. (1977) The effect of sodium phenobarbital and 3,4-benzpyrene on the glucuronidation of 1-naphthol in rat small intestinal loops *in vivo Gen. Pharmacol.* **8**, 51–53
15 Hook, G. E. R., Haseman, J. K. and Lucier, G. W. (1975) Induction and suppression of hepatic and extrahepatic microsomal foreign-compound-metabolizing enzyme systems by 2,3,7,8-tetrachlorodibenzo-*p*-dioxin *Chem. Biol. Interact.* **10**, 199–214
16 Schiller, C. M. and Lucier, G. W. (1978) The differential response of isolated intestinal crypt and tip cells to the inductive actions of 2,3,7,8-tetrachlorodibenzo-*p*-dioxin *Chem. Biol. Interact.* **22**, 199–209
17 Pantuck, E. J., Hsiao, K. C., Kaplan, S. A., Kuntzman, R. and Conney, A. H. (1974) Effects of enzyme induction on intestinal phenacetin metabolism in the rat *J. Pharmacol. Exp. Ther.* **191**, 45–52
18 Pekas, J. C. (1974) Naphthol metabolism: glucuronide conjugation and transport by the rat intestine *in vitro Toxicol. Appl. Pharmacol.* **29**, 404–419
19 Barr, W. H. and Riegelman, S. (1970) Intestinal drug absorption and metabolism. I. Comparison of methods and models to study physiological factors of *in vitro* and *in vivo* intestinal absorption *J. Pharm. Sci.* **59**, 154–163
20 Dawson, J. R. and Bridges, J. W. (1979) Conjugation and excretion of metabolites of 7-hydroxycoumarin in the small intestine of rats and guinea pigs *Biochem. Pharmacol.* **28**, 3291–3297
21 Stohs, S. J., Grafström, R. C., Burke, M. D. and Orrenius, S. (1977) Benzo(α)pyrene metabolism by isolated rat intestinal epithelial cells. *Archs. Biochem. Biophys.* **179**, 71–80
22 Shirkey, R. S., Kao, J., Fry, J. R. and Bridges, J. W. (1979) A comparison of xenobiotic metabolism in cells isolated from rat liver and small intestinal mucosa *Biochem. Pharmacol.* **28**, 1461–1466
23 Grafström, R., Moldéus, P., Andersson, B. and Orrenius, S. (1979) Xenobiotic metabolism by isolated rat small intestinal cells *Medical Biol.* **57**, 287–293
24 Dawson, J. R. and Bridges, J. W. (1979) Xenobiotic metabolism by isolated intestinal epithelial cells from guinea-pigs *Biochem. Pharmacol.* **28**, 3299–3305
25 Dawson, J. R. and Bridges, J. W. (1981) Intestinal microsomal drug metabolism. A comparison of rat and guinea-pig enzymes, and of rat crypt and villous cell enzymes *Biochem. Pharmacol.* **30**, 2415–2420
26 Stohs, S. J., Grafström, R. C., Burke, M. D., Moldéus, P. W. and Orrenius, S. G. (1976) The isolation of rat intestinal microsomes with stable cytochrome P_{450} and their metabolism of benzo(α)pyrene *Arch. Biochem. Biophys.* **177**, 105–116
27 Toivonen, L., Hänninen, O. and Hartiala, K. (1973) Drug metabolism in canine duodenum *Ann. Med. Exp. Biol. Fenn.* **51**, 8–10
28 Moog, F. (1981) The lining of small intestine *Sci Am.* **245**, 116–125
29 Leblond, C. P. and Stevens, C. E. (1948) The constant renewal of the intestinal epithelium in the albino rat *Anat. Rec.* **100**, 357–378
30 Hülsmann, W. C., van den Berg, J. W. O. and de Jonge, H. R. (1973) Isolation of intestinal mucosa cells *Methods Enzymol.* **32**, 665–673
31 Harrison, D. D. and Webster, H. L. (1969) The preparation of isolated intestinal crypt cells *Exp. Cell Res.* **55**, 257–260
32 Greenlee, W. F. and Poland, A. (1978) An improved assay of 7-ethoxycoumarin *O*-deethylase activity: induction of hepatic enzyme activity in C57BL/6J and DBA/2J mice by phenobarbital, 3-methylcholanthrene and 2,3,7,8-tetrachlorodibenzo-*p*-dioxin *J. Pharmacol. Exp. Therap.* **205**, 596–605
33 Estabrook, R. W., Peterson, J. A., Baron, J. and Hildebrandt, A. (1972) Methods in Pharmacology, vol. 2: Physical Methods (Chignell, C. F., Ed.) Appleton-Century-Crofts, New York, pp. 303–350
34 Lowry, A. H., Rosebrough, N. J., Farr, A. L. and Randall, R. J. (1951) Protein measurement with folin phenol reagent *J. Biol. Chem.* **193**, 265–275
35 Jones, G. M. and Mayer, R. J. (1973) Hexokinase in isolated epithelial cells from rat intestine *Biochem. Biophys. Acta* **304**, 634–641
36 Eade, O. E., Andre-Ukena, S. St. and Beeken, W. L. (1981) Comparative viabilities of rat intestinal epithelial cells prepared by mechanical, enzymatic and chelating methods *Digestion* **21**, 25–32
37 Stern, B. K. and Jensen, W. E. (1966) Active transport of glucose by suspensions of isolated rat intestinal epithelial cells *Nature* **209**, 789–790
38 Jones, D. P., Grafström, E. and Orrenius, S. (1980) Quantitation of hemoproteins in rat small intestinal mucosa with identification of mitochondrial cytochrome P_{450} *J. Biol. Chem.* **255**, 2383–2390
39 Borm, P. J. A., Frankhuijzen-Sierevogel, A. and Noordhoek, J. (1982) Time and dose dependence of 3-methylcholanthrene induced metabolism in intestinal mucosal cells and microsomes *Biochem. Pharmacol.* **31**, 3703–3710
40 Lawson, A. J., Smit, R. A., Jeffers, N. A. and Osborne, J. W. (1982) Isolation of rat intestinal crypt cells *Cell Tissue Kinet.* **15**, 69–80
41 Iemhoff, W. G. J., van den Berg, J. W. O., de Pijper, A. M. and Hülsmann, W. C. (1970) Metabolic aspects of isolated cells from rat small intestinal epithelium *Biochim. Biophys. Acta* **215**, 229–241
42 Shirkey, R. S., Chakraborty, J. and Bridges, J. W. (1979) Comparison of the drug metabolizing ability of rat intestinal mucosal microsomes with that of the liver *Biochem. Pharmacol.* **28**, 2835–2839
43 Hietanen, E. and Pelkonen, K. (1979) Hepatic and extrahepatic induction of drug-metabolizing enzymes in specific pathogen free and germ-free rats. *Gen. Pharmacol.* **10**, 239–247
44 Borm, P. J. A., Frankhuijzen-Sierevogel, A. and Noordhoek, J. (1983) Kinetics of *in vitro O*-deethylation of phenacetin and 7-ethoxycoumarin by rat intestinal mucosal cells and microsomes *Biochem. Pharmacol.* **32**, 1573–1580
45 Koster, A. Sj. and Noordhoek, J. (1983) Glucuronidation in the rat intestinal wall. Comparison of isolated mucosal cells, latent microsomes and activated microsomes *Biochem. Pharmacol.* **32**, 895–900
46 Klippert, P. J. M., Borm, P. J. A. and Noordhoek, J. (1982) Prediction of intestinal first-pass effect of phenacetin in the rat from enzyme kinetic data — Correlation with *in vivo* data using mucosal blood flow *Biochem. Pharmacol.* **31**, 2542–2548

Aerobic glycolysis of bone and cartilage: the possible involvement of fatty acid oxidation

Jane Dunham, R. A. Dodds, A. M. Nahir, G. T. B. Frost*, A. Catterall†, Lucille Bitensky and J. Chayen

*Division of Cellular Biology, Kennedy Institute of Rheumatology, Hammersmith, London W6 7DW, UK; *Sigma London Chemical Company Ltd, Production Division, Gate 2, Fancy Road, Poole, Dorset BH17 7NZ, UK; †Charing Cross Hospital, Fulham Palace Road, London W6 8RF, UK*
(Received 17 January 1983)

The apparent paradox of aerobic glycolysis has been investigated in bone and in cartilage. A new cytochemical procedure for hydroxyacyl dehydrogenase (HOAD) activity showed that the maximal activity of this enzyme in both tissues was equivalent to the maximal activity of glyceraldehyde 3-phosphate dehydrogenase (GAPD). The sum of these activities gave a measure of the maximum amount of acetyl-coenzyme A that could be produced. In these tissues, but not in liver which does not exhibit aerobic glycolysis, this summed value exceeded the maximal activity of succinate dehydrogenase (SDH). Consequently, it suggested that where fatty acid oxidation is sufficient to supply all the acetyl-coenzyme A required for the Krebs' cycle, that derived from fatty acid oxidation may inhibit pyruvate dehydrogenase causing accumulation of pyruvate which must be converted to lactate if pentose-shunt activity is to be maintained.

Keywords: Bone, aerobic glycolysis, fatty acid oxidation, cartilage

Introduction

Cartilage (as reviewed in Refs 1 and 2) and bone[3,4] produce considerable amounts of lactic acid from glucose, indicating a dependence on glycolysis. This might be expected of cartilage which can be relatively anaerobic because of its avascular nature, but this argument cannot be applied to bone which is a highly vascular tissue. Moreover, both show the phenomenon of 'aerobic glycolysis' namely a high rate of formation of lactic acid from glucose, even when studied *in vitro* at high oxygen tensions in the medium. This apparent paradox of aerobic glycolysis has been found to occur in many cell-types, and is particularly marked in growing malignant cells[5].

Both cartilage and bone are difficult to study by conventional biochemical procedures. Bone, in particular, is recalcitrant to conventional biochemical procedures. Both contain relatively few cells per mass of tissue; the cells may be of different cell-types so that, even when they have been harvested, the population may be heterogeneous and each subpopulation may have characteristic metabolic activities. An approach to the study of the oxidative metabolism of bone and cartilage, that overcomes these difficulties is afforded by the development of methods for cutting serial sections of adult unfixed, undemineralized bone[6,7]. Such sections can be examined by conventional methods of quantitative cytochemistry so that biochemical activities can be related to histology, so avoiding problems of tissue heterogeneity.

In considering the question of lactic acid production by these tissues, it is obvious that the pyruvate dehydrogenase complex could play a crucial role (*Figure 1*). There is considerable evidence that the behaviour of this multi-enzyme complex is fundamental in determining the fate of pyruvate produced by the Embden-Meyerhof pathway. It has been studied particularly in alloxan-diabetes where pyruvate oxidation is inhibited[8]. The activity of the complex is inhibited by the products of fatty acid oxidation (as reviewed in Ref. 8), particularly by acetyl co-enzyme A (Ref. 9). It therefore seemed appropriate to try to evaluate the oxidative metabolism of the various cellular components of bone and of cartilage to determine whether these tissues could oxidize fatty acids at such a rate that the acetyl coenzyme A, so produced, might become a factor in controlling the pyruvate dehydrogenase activity.

This study became feasible with the synthesis of a new substrate for hydroxyacyl dehydrogenase (HOAD) activity, namely DL-*S*-β-hydroxybutyryl-*N*-acetyl cysteamine[10].

Materials and methods

Female Wistar rats weighing ~ 50 g were killed by cervical dislocation. The metatarsals were cut in

0263–6484/83/030168–05$03.00
© 1983 Butterworth & Co. (Publishers) Ltd

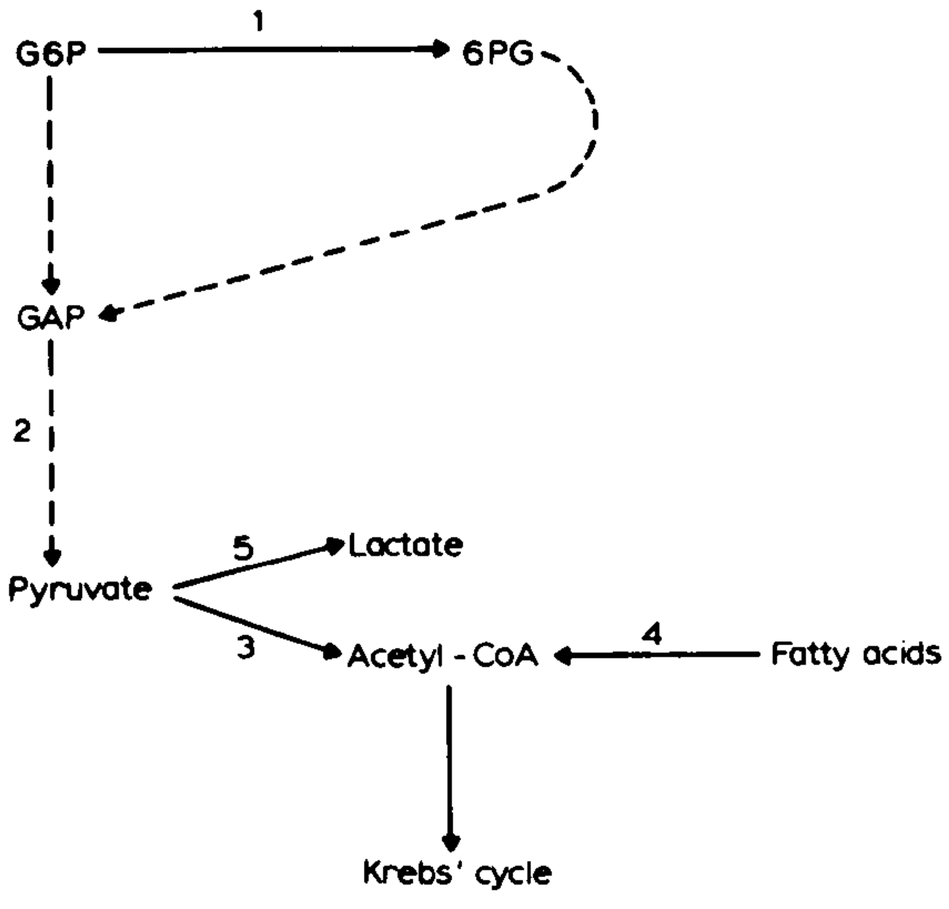

Figure 1 The main oxidative enzymes involved in the generation of acetyl-coenzyme A for the Krebs' cycle, and in the production of lactic acid. 1, glucose 6-phosphate dehydrogenase; 2, glyceraldehyde 3-phosphate dehydrogenase; 3, the pyruvate dehydrogenase complex; 4, hydroxyacyl dehydrogenase; 5, lactate dehydrogenase (pyruvate reductase)

half and the distal half, with the epiphyseal plate, was removed. Two metatarsals from each of six rats were used for all the enzyme studies except for the study of succinate dehydrogenase where three metatarsals from each of two rats were used. The bones were dipped in 5% polyvinyl alcohol before being chilled in n-hexane at −65 to −70°C. These techniques have been fully described by Chayen *et al.*[11] The bones were sectioned (10 μm) on a Jung 1130 rotary microtome set in a Bright's cryostat (cabinet temperature −25 to −30°C with the knife cooled with solid carbon dioxide[6,12]). To test the oxidative activity in a tissue that does not show 'aerobic glycolysis', small pieces (3 × 3 × 3 mm) of the liver from three female Wistar rats (body weight 200 g) were chilled in hexane at −65 to −70°C and sectioned at 10 μm in a Bright's cryostat[11]. The same reactions were carried out on these sections as on those from the metatarsals.

Except for the studies on succinate dehydrogenase activity, all the reaction-media contained 0.6% (10 mM) chloroform-purified neotetrazolium chloride (Serva) in a 30% (w/v) solution of polyvinyl alcohol (grade G04/140; Wacker Chemicals Ltd, Walton-on-Thames, Surrey, UK) in glycyl glycine buffer (50 mM; pH 8.0). For demonstrating the activity of succinate dehydrogenase, which is tightly bound within the mitochondria, a 0.1 M phosphate buffer, pH 7.8 was used. Except for the demonstration of hydroxyacyl dehydrogenase activity (see below), the media contained the intermediate hydrogen-acceptor, phenazine methosulphate (0.7 mM added to the medium just before use).

The specific reactants were as follows. Lactate dehydrogenase activity: sodium lactate, 60 mM; NAD, 2.5 mM. Glucose 6-phosphate dehydrogenase activity: glucose 6-phosphate, monosodium salt, 5 mM; NADP, 3 mM. Glyceraldehyde 3-phosphate dehydrogenase activity: fructose 1-6-diphosphate, 5 mM; aldolase, 10 units ml^{-1}; NAD, 1.5 mM. The reaction medium was left for 20 min at 37°C before it was used in order to convert sufficient fructose diphosphate to glyceraldehyde 3-phosphate[13]. Succinate dehydrogenase activity: sodium succinate, 50 mM. β-Hydroxyacyl dehydrogenase[10]: the reaction-medium contained NAD (2 mM); sodium nitroprusside (5 mM) to inhibit the effects of any acetyl cysteamine liberated by non-enzymatic hydrolysis of the substrate; menadione (2-methyl-1,4-naphthoquinone, 3 mM) as the preferred intermediate hydrogen-acceptor for this reaction[10]; and either the substrate, DL-*S*-β-hydroxybutyryl-*N*-acetyl cysteamine (50 mM) or cysteamine (β-mercaptoethylamine; 5 mM) in a 0.05 M glycyl glycine buffer at pH 8.0. The menadione and the substrate were first dissolved in a small volume of ethanol so that, when added to the reaction medium, the final concentration of alcohol in the test and control medium was 1%. The pH of the medium was adjusted to pH 8.9 before the substrate, or cysteamine, was added to it. After this addition, the pH was again checked and adjusted to pH 8.5 when necessary. Unless otherwise specified, all chemicals were obtained from Sigma, London, UK.

All the reactions were performed at 37°C in an atmosphere of nitrogen, since oxygen competes with neotetrazolium chloride for reducing equivalents. The reactions were run for 45 min except for that for lactate dehydrogenase activity which was run for 10 min, the results from this being multiplied by 4.5 for comparison with the results from the other tests. Over these reaction times, the responses were linear with time.

Measurement

The coloured formazan produced in the sections was measured with a Vickers M85 scanning and integrating microdensitometer with a × 40 objective and a flying spot that had a diameter of 0.5 μm in the plane of the section, and at a wavelength of 585 nm[14]. The mask encompassed one cell of each type studied and the results were expressed in absolute units of extinction (mean integrated extinction × 100) per cell. The cell-types measured were: chondrocytes in the resting, proliferating, and hypertrophic zones of the growth plate; and osteoblasts and osteocytes in the metaphysis.

Results

Validation of the HOAD reaction

The optimal pH for osteoblasts was pH 8.5 and for chondrocytes was pH 8.0 (*Figure 2*). The graph relating activity to concentration of coenzyme was broad, with 2 mM giving maximal activity, and little sign of inhibition at greater concentrations. The concentration of the final hydrogen-acceptor, neotetrazolium chloride, had a strong influence on the activity recorded: the activity (mean extinction for a reaction-time of 45 min) was 0.29 at 0.6% (10 mM); maximal (0.32) at 0.9% (15 mM): with some inhibition (0.23) at 1.2% (20 mM). To ensure freedom from inhibitory effects, 0.6% was used in all subsequent studies. Nitroprusside increased activity

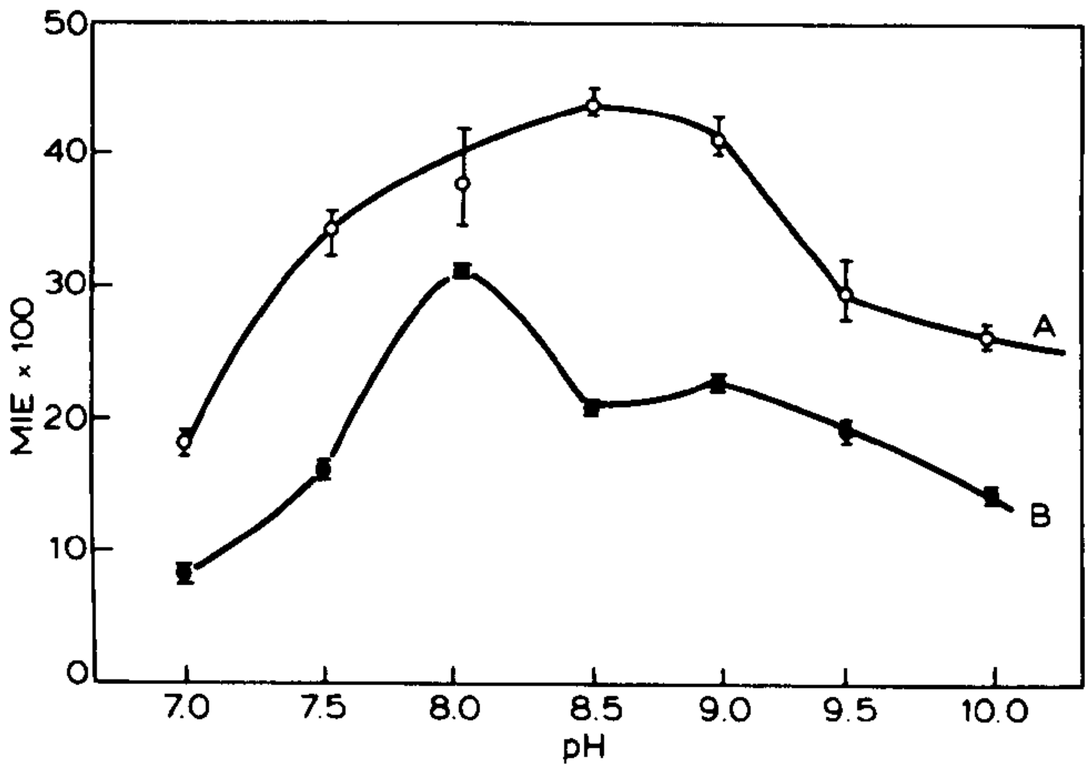

Figure 2 Variation in activity with pH of hydroxyacyl dehydrogenase in (A) osteoblasts, and (B) chondrocytes. The activity is represented by the mean integrated extinction (MIE) × 100 per cell in a 45 min reaction; the bars represent the s.e.m. of 20 measurements

in osteoblasts and in chondrocytes up to a concentration of 5 mM with considerable inhibition thereafter; 50 mM nitroprusside caused total inhibition. Increasing concentrations of substrate produced typical substrate-activity graphs with a rapid initial rise in activity at lower concentrations (up to 5–10 mM) with a much slower rise in activity at higher concentrations, up to 100 mM. Considering the cost of the substrate, and the small difference found at higher concentrations, 50 mM was taken as an adequate compromise. The substrate has the potential to become hydrolysed spontaneously, at the pH of the reaction, to yield free *N*-acetylcysteamine that, in the presence of menadione, could reduce the neotetrazolium salt. Spectrophotometric determinations[15] of the cysteamine liberated in the reaction-medium, after 30 and 90 min, gave values equivalent to 3.1, 4.0 and 2.7 mM of free cysteamine. When sections were reacted with various concentrations of cysteamine instead of the substrate, the 'activity' recorded was maximal with 2.5 mM cysteamine, this level of activity was maintained up to 10 mM; higher concentrations gave less activity, with no reaction at 50 mM. Consequently control sections were reacted with 5 mM cysteamine replacing the substrate. This was over-cautious since dithionite reduction of the neotetrazolium in the reaction-medium did not produce formazan deposits in the chondrocytes.

Increasing the concentration of the intermediate hydrogen-acceptor, menadione, up to 3 mM, increased the activity with no further increase, or inhibition, at concentrations up to 5 mM.

The reaction was linear with time over the first 45 min; the activity increased less rapidly over the subsequent 20 min and did not increase with longer reaction-times. This may reflect the rate of hydrolysis of the substrate.

Sections of bone, incubated in the final reaction-medium for 45 min at 37°C, showed reaction-product in all cell-types of normal bone, including the osteocytes deeply embedded in adult bone.

Oxidative activities in the various cell-types of the bone and cartilage

The activities of one oxidative enzyme of each of the major pathways (*Figure 1*) were measured in the region of the growth plate of the metatarsals. The selected enzymes were as follows: Embden–Meyerhof pathway: glyceraldehyde 3-phosphate dehydrogenase (GAPD); pentose-shunt: glucose 6-phosphate dehydrogenase (G6PD); the tricarboxylic acid cycle: succinate dehydrogenase (SDH); fatty acid oxidation: hydroxyacyl dehydrogenase (HOAD); and lactate dehydrogenase activity (LDH). The results (*Table 1*) showed first, that under the conditions of the tests, in all cell-types the HOAD activity was equivalent to that of GAPD; secondly, that the SDH activity was too small to accommodate the combined GAPD plus HOAD activities; and thirdly, that there was a direct correlation ($r = 0.85$; $p = 0.02$) between the LDH activities and the value of (GAPD + HOAD) − SDH. The activities recorded when these reactions were done in the absence of the substrate were so low that they have not been taken into account.

Oxidative activities in rat liver

In the liver, with its stores of endogenous substrates, the activities recorded when the reaction-medium lacked exogenous substrate were appreciable (*Table 2*). However, whether or not these 'control' values were taken into account, the combined activities recorded for glyceraldehyde 3-phosphate dehydrogenase and for hydroxyacyl dehydrogenase (GAPD + HOAD; *Table 2*) were far less than that recorded for succinate dehydrogenase activity. Thus the value (GAPD + HOAD) − SDH was negative (*Table 2*).

Discussion

The development of a new substrate and a new method for measuring fatty acid oxidation has allowed the demonstration that all the cells of the growth-plate, even the differentiated osteocytes, are capable of oxidizing fatty acids. It is recognized that although cells show a particular metabolic activity in such tests, this does not prove that the cells have the same activity in life, as they are not necessarily supplied with optimal concentrations of substrate, cofactor and other reactants. Equally, the activities of enzymes that support 'near-equilibrium' or 'non-equilibrium' reactions cannot be taken to indicate the flux through the system or pathway in which they occur. However, the results of these tests can be taken as an indication of the potential activities of the different pathways, and of their maximal capacities.

The pentose-shunt involves the oxidation of glucose 6-phosphate, where NADP is the obligate cofactor. However, for the system to remain active as a cycle, it must feed-back into the normal glycolytic (Embden-Meyerhof) pathway, supplying either fructose 6-phosphate or glyceraldehyde 3-phosphate[16]. Thus, the maximum activity of GAPD must be considered to be rate-limiting both for the

Table 1 Enzymatic activities, expressed as the mean integrated extinction × 100 ± s.e.m./cell/45 min reaction, in various cell-types of the bone and cartilage of the growth-plate

Enzyme	Osteocytes	Osteoblasts	Chondrocytes from		
			Hypertrophic zone	Proliferating zone	Resting zone
G6PD	12.0 ± 1.0	54.2 ± 2.6	29.4 ± 0.9	21.0 ± 0.9	13.4 ± 0.6
LDH	32.3 ± 1.0	63.2 ± 1.0	95.6 ± 1.0	81.9 ± 2.0	45.8 ± 1.0
GAPD	14.0 ± 1.0	24.2 ± 1.1	20.7 ± 1.3	11.6 ± 0.9	8.6 ± 2.9
HOAD	8.9 ± 1.9	19.6 ± 1.6	19.6 ± 2.6	14.2 ± 1.5	10.1 ± 3.2
SDH	13.0 ± 0.7	32.0 ± 2.0	9.0 ± 0.6	9.0 ± 0.5	6.0 ± 0.5
GADP + HOAD	22.9	43.8	40.3	25.8	18.7
(GAPD + HOAD) − SDH	9.9	11.8	31.3	16.8	12.7

Table 2 Mean (± s.e.m.) of the oxidative activities measured in the liver of three rats

	Activity (mean integrated extinction × 100/unit field/10 min reaction)						
	G6PD	LDH	GAPD	HOAD	SDH	GAPD + HOAD	(GAPD + HOAD) − SDH
Activity ($n = 3$)	52 + 0.7	45 + 0.5	67 + 1.0	32 + 0.4	160 + 4.0	99	−61
Control[a]	(9 + 0.4)	(16 + 0.4)	(27 + 0.6)	(16 + 0.3)	(0)	–	–

[a]The 'control' activities were measured either in the absence of substrate or, for HOAD activity, with cysteamine instead of the substrate. The different 'control' activities recorded for the two NAD-dependent enzymes are due to the different pH values at which these are done, in accordance with the different pH optima of the enzymes

pentose-shunt and for the Embden-Meyerhof pathway. That is, it reflects the maximum oxidation produced from glucose 6-phosphate from either route, and therefore is an indication of the maximum capability of the cells to use glucose as a substrate for the energy-requirements of the cells. On this basis the results show that the capacity of the cells of the growth-plate to oxidize sugar or fatty acids is roughly equivalent, indicating that as much as 50% of the 'energy' of these cells could come from the oxidation of fatty acids. Thus, for example, the osteoblasts were capable of 24.2 units of GAPD activity, and 19.6 units of HOAD activity. Chondrocytes of the resting zone were capable of 8.6 units of GAPD activity and 10.1 units of HOAD activity.

In the Embden-Meyerhof pathway, the substrate-products of GAPD activity are finally converted to pyruvate. For this to be utilized in the Krebs' cycle, and so to be used for the generation of ATP for the energy-requirements of the cell, it must be converted to acetate and linked to coenzyme A (CoA) to form acetyl-CoA. It is noteworthy that the oxidation of fatty acids yields acetyl-CoA directly. Thus the amount of activity of GAPD and of HOAD is a measure of the total amount of acetyl-CoA that could be available to be fed into the Krebs' cycle. However, the SDH activity can be taken as the maximum Krebs' cycle activity of which the cell is capable[17]. Thus the calculation (*Tables 1* and *2*) of (GAPD activity plus HOAD activity) − SDH activity gives a measure of whether there could be sufficient, or excessive amounts of acetyl-CoA produced in the cells, relative to the maximum amount that could be dealt with by the Krebs' cycle. It is clear (*Table 1*) that in all the skeletal cells studied, particularly the osteoblasts and the chondrocytes of the hypertrophic region, excessive amounts of acetyl-CoA could be produced over and above what could be accommodated by the Krebs' cycle activity. If such conditions were to occur in life, the acetyl-CoA produced directly by fatty acid oxidation, and produced within the mitochondria close to the site of most of the Krebs' cycle enzymes, might be expected to be favoured. Moreover, the conversion of pyruvate to acetyl-CoA is very readily inhibited by acetyl-CoA[8,9]. It follows, therefore, that fatty acid oxidation, producing acetyl-CoA, could inhibit the conversion of pyruvate (*Figure 1*). Blockage of the Embden-Meyerhof pathway at the level of pyruvate would stop not only the normal glycolytic pathway, but also the pentose shunt (*Figure 1*). This blockade would be relieved if the pyruvate were to be converted into lactate (by the pyruvate-reductase/LDH enzyme), with loss of lactic acid from the cells. This hypothesis is supported by the finding (*Table 1*) that there was a direct relationship between the LDH activity in these cells and the excess of (GAPD + HOAD) activities over the SDH activity, i.e. (GAPD + HOAD) − SDH.

In contrast to cartilage and bone, liver does not normally produce lactic acid. The results with rat liver (*Table 2*) showed that the value of (GAPD activity + HOAD activity) − SDH activity gave a negative value. This implies that the maximal activity of the succinate dehydrogenase was well in excess of the combined activities of the glycolytic pathway and of fatty acid oxidation.

If these results reflect something of what might

occur in life, the hypothesis would explain the apparent paradox of 'aerobic glycolysis' in bone and cartilage. This phenomen could be due to normal aerobic respiration, using the acetyl-CoA provided by fatty acid oxidation, with the removal of excess pyruvate (as lactate) produced by the glycolytic pathways. Thus lactic acid would be produced even though the cells showed full oxidative metabolism.

References

1 Stockwell, R. A. (1979) The Biology of Cartilage Cells. Cambridge University Press, Cambridge
2 Maroudas, A. and Holborow, E. J. (Eds) (1980) Studies in Joint Disease 1. Pitman Medical, Tunbridge Wells
3 Hekkelman, J. W. (1973) Biological Mineralization (Ziphin, I., Ed.) Wiley, pp. 165–184
4 Neuman, W. F. (1977) Aerobic glycolysis in bone in the context of membrane-comparmentalization *Calcif. Tiss. Res. Suppl.* **22**, 169–178
5 Eigenbrodt, E. and Glossmann, H. (1980) Glycolysis — one of the keys to cancer? *Trends Pharm. Sci.* **1**, 240–245
6 Johnston, J., Bitensky, L. and Chayen, J. (1972) Cryostat sections of undemineralized bone *J. Clin. Pathol.* **25**, 742
7 Shedden, R., Dunham, J., Bitensky, L., Catterall, A. and Chayen, J. (1976) Changes in alkaline phosphatase activity in periosteal cells in healing fractures *Calcif. Tiss. Res.* **22**, 19–25
8 Kerbey, A. L., Randle, J. P., Cooper, R. H., Whitehouse, S., Pask, H. T. and Denton, R. M. (1976) Regulation of pyruvate dehydrogenase in rat heart *Biochem. J.* **154**, 327–348
9 Linn, T. C., Pettit, F. H., Hucho, F. and Reed, L. J. (1969) α-Keto acid dehydrogenase complexes, XI. Comparative studies of regulatory properties of the pyruvate dehydrogenase complexes from kidney, heart and liver mitochondria *Proc. Natl. Acad. Sci. USA* **64**, 227–234
10 Chambers, D. J., Braimbridge, M. V., Frost, G. T. B., Nahir, A. M. and Chayen, J. (1982) A quantitative cytochemical method for the measurement of β-hydroxyacyl Co-A dehydrogenase activity in rat heart muscle *Histochemistry* **75**, 67–76
11 Chayen, J., Bitensky, L. and Butcher, R. G. (1973) Practical Histochemistry. Wiley, New York and London
12 Johnstone, J. J. A. (1979) The routine sectioning of undecalcified bone for cytochemical studies *Histochem. J.* **11**, 359–365
13 Henderson, B. (1976) Quantitative cytochemical measurement of glyceraldehyde 3-phosphate dehydrogenase activity *Histochemistry* **48**, 191–204
14 Butcher, R. G. and Altman, F. P. (1973) Studies on the reduction of tetrazolium salts. II. The measurement of the half-reduced and fully reduced formazans of neotetrazolium chloride in tissue sections *Histochemie* **37**, 351–363
15 Jocelyn, P. C. (1972) Biochemistry of the SH Group. Academic Press, London and New York
16 Krebs, H. A. and Kornberg, H. L. (1957) Energy Transformations in Living Matter. Springer-Verlag, Berlin-Gottingen-Heidelberg
17 Lehninger, A. . (1975) Biochemistry. Worth, New York, 2nd edition, p. 460

Calcif Tissue Int (1984) 36:233–238

Calcified Tissue International
© 1984 by Springer-Verlag

Effects on Fracture Healing of an Antagonist of the Vitamin K Cycle

R. A. Dodds, A. Catterall,[1] Lucille Bitensky, and J. Chayen

Division of Cellular Biology, Kennedy Institute of Rheumatology, Bute Gardens, London W6 7DW, UK; and [1]Department of Orthopaedic Surgery, Charing Cross Hospital, London W6 8RF, UK

Summary. The anticoagulant, dicumarol, inhibits the vitamin K cycle by blocking the conversion of the vitamin K epoxide. The effects of dicumarol on ossification have been tested by feeding it to rats in which a closed fracture of the metatarsals had been induced; the effects were studied up to 12 days postfracture. At 12 days, treatment with dicumarol caused a highly significant decrease in the amount of bone produced, without affecting the total size of the callus. Quantitative cytochemistry of unfixed, undemineralized sections showed that dicumarol also markedly affected the periosteal activities of glucose 6-phosphate dehydrogenase and of alkaline phosphatase in the first 2 mm from the fracture measured at 3 and 5 days postfracture when normally, new bone is first formed. In contrast, dicumarol had little effect on these activities in the fully formed callus.

Key Words: Vitamin K cycle — Anticoagulant therapy — Experimental fracture healing — Quantitative cytochemistry.

There is considerable evidence that calcification of bone may involve the γ-carboxylation of glutamate residues, as is found in osteocalcin [1–3]. The production of these calcium-binding γ-carboxyglutamate (Gla) residues is effected by a microsomal mixed-function oxidation-carboxylation reaction in which vitamin K_1, or a similar naphthoquinone substituted at the 3 position [4], is reduced by NAD(P)H [5, 6]. The reoxidation of the quinol is required for the process in which a proton is abstracted from the γ-methylene of a glutamate residue [5]; the resulting carbanion fixes carbon dioxide to form the γ-carboxyglutamate residue [3, 4].

Previous studies on cellular metabolic activities in healing fractures in rats [7] had shown that there was a marked increase in periosteal glucose 6-phosphate dehydrogenase (G6PD) activity at the site at which new bone formed on the shaft. This activity preceded the first signs of new bone. The simple assumption would be that the NADPH, generated by this stimulated G6PD activity at this site, would be used in the vitamin K cycle for ossification. This assumption has now been tested by treating the rats with dicumarol (chemically related to warfarin) which antagonizes the effect of vitamin K_1 in the vitamin K cycle by blocking the reversible conversion of vitamin K to the vitamin K epoxide [8].

Materials and Methods

Animals

For these studies, male Sprague-Dawley rats (230–250 g) were used instead of the Wistar rats used in previous studies [7] because the latter were too sensitive to dicumarol. The rats were anesthetized with pentobarbitone sodium given intraperitoneally. Closed fractures were imposed by digital pressure on two metatarsals of one hind limb. The rats were allowed to revive and were killed up to 6 weeks later. Those rats that were treated with dicumarol received it in the drinking water as soon as they revived. A standard dose was achieved by giving each rat, daily, 25 ml of drinking water containing 0.125 mg bis hydroxycumarin (Sigma) after which the water bottle was replenished with ordinary water. To obtain a "solution" of dicumarol, 25 mg of dicumarol was dissolved initially in 10 ml of 1 M sodium hydroxide, the pH was decreased to pH 10 with 5 M HCl; this solution was diluted 1:500 with tap water, giving it a final pH of between 8 and 9. It proved palatable to the rats. The control rats were given ordinary water only. The clotting time of normal rats was 2.0 min; in the dicumarol-treated rats it became prolonged from day 4, to reach 7.5 min on day 10 and 9 min on day 12.

Send offprint requests to J. Chayen at the above address.

Experimental Procedures

At suitable times, the rats were killed by asphyxiation with nitrogen. The fractured bone, with its associated plantar muscle, was dissected free and immersed briefly in a 5% (w/v) solution of polyvinyl alcohol (GO4/140). The bone was then chilled to −70°C in hexane (BDH "low in aromatic hydrocarbons" grade, boiling range 67–70°C), as described previously [7, 9], and stored in dry tubes at this temperature for up to 7 days. The bones were sectioned at 10 μm in a Bright's bone cryostat equipped with a tungsten-tipped steel knife (Autoradiographic Products, Cheshire) with the haft packed around with solid carbon dioxide [7, 10].

Cytochemical Reactions

The sections were reacted in triplicate for a number of enzymatic activities. Serial sections were stained with toluidine blue [9] for histological study. For G6PD activity, the reaction medium contained glucose 6-phosphate (5 mM), $NADP^+$ (3 mM), phenazine methosulphate (0.7 mM) and 0.3% (5 mM) purified neotetrazolium chloride in a 0.05 M glycyl glycine buffer, pH 8.0, containing 30% (w/v) of the GO4/140 grade of polyvinyl alcohol (Wacker Chemicals, Mount Felix, Bridge St., Walton-on-Thames, KT12 1AS, UK).

The medium for demonstrating alkaline phosphatase activity contained α-naphthyl acid phosphate (Sigma, 2 mg), Fast blue RR (Sigma, 50 mg), with 0.2 ml of a 10% solution of magnesium chloride, in 50 ml of a 2% solution of sodium 5,5-diethylbarbiturate at a final pH of pH 9.2. For demonstrating hydroxyacyl-coenzyme A dehydrogenase activity [11], the medium contained DL-S-β-hydroxybutyryl-*N*-acetyl cysteamine (Sigma, 37 mM, or 5 mM cysteamine, as control), NAD^+ (2 mM), menadione (3 mM), sodium nitroprusside (5 mM), and 0.6% (10 mM) of purified neotetrazolium chloride in a 0.05 M glycyl glycine buffer containing 30% of the polyvinyl alcohol with a final pH of 8.5.

The colored reaction product of these cytochemical reactions was measured in the periosteum, and in histologically defined cell types in the developing callus, by means of a Vickers M85 scanning and integrating microdensitometer. It had a ×40 objective, spot size 1 (equivalent to 0.4 μm in the plane of the specimen), with light corresponding to the absorption maximum of the chromophore for the alkaline phosphatase reaction (580 nm) and to the isobestic point for the formazan from the dehydrogenase methods (585 nm). The reaction times required to obtain ideal concentrations of the colored reaction product for measurement were 10 min for G6PD, 45 min for hydroxyacyl dehydrogenase (HOAD), and 3 min for alkaline phosphatase activity.

For histological examination, sections were selected that passed through approximately the mid-axis of the endosteal space. To confirm that this gave a good representation of the distribution of the various cellular components, one bone was sectioned serially from side to side, and the relative size of each component was ascertained at different levels. The image of the selected sections was thrown onto a screen; the enlarged image was traced onto tracing paper, and the areas of the selected tissue components were measured by planimetry.

Table 1. Total area and area of new bone formation (mean ± SD) of dorsal and plantar callus in sections through the greatest diameter (midshaft) of fractured rat metatarsals 12 days post-fracture

	Control (n = 16)		Dicumarol-treated (n = 13)	
	Dorsal	Plantar	Dorsal	Plantar
Area (mm^2 × 16)	29 ± 13	6 ± 4	25 ± 9	9 ± 6
New bone	15 ± 6	4 ± 3	10 ± 4	3 ± 3
New bone %	56 ± 14[a]	45 ± 10[a]	39 ± 5	30 ± 6

[a] $P < 0.001$ as compared with dicumarol-treated: Student's *t* test

Results

Histological Results

In all cases, the callus on the dorsal side of the fracture was considerably larger than that on the plantar side (Table 1). The total projected area of the dorsal callus in the treated and control animals was very similar (Table 1). However, the callus in the dicumarol-treated rats appeared to be less advanced in terms of the degree of differentiation that it achieved (Fig. 1). As a test of this suggestion, the area occupied by new bone was expressed as a percentage of the total area of the callus. When expressed in this way (Table 1), 12 days after fracture, the proportion of the callus occupied by new bone was significantly higher ($P < 0.001$) in the control rats (e.g. 56% ± 10; mean ± SD) than in those treated with dicumarol (38% ± 6). In the controls, the center of the callus around the fracture site (Fig. 1) was occupied by fibrocartilagelike material, differentiating into mature cartilage further from the fracture. In the rats treated with dicumarol, the region which should have contained fibrocartilagelike material contained effete, fibrous material with few cells. At 6 weeks, the fracture in the control rats was fully united, but union was still incomplete in those given dicumarol.

Glucose 6-Phosphate Dehydrogenase Activity in the Periosteum

The activity was measured in individual periosteal cells at measured distances from the fracture. In 3 control rats, 3 days postfracture, there was considerable activity close to the fracture, reaching a mean extinction value of 22 units at 0.4 mm from the fracture, and rising to 27 units 1.2 mm from the fracture. In contrast, the activity in the dicumarol-

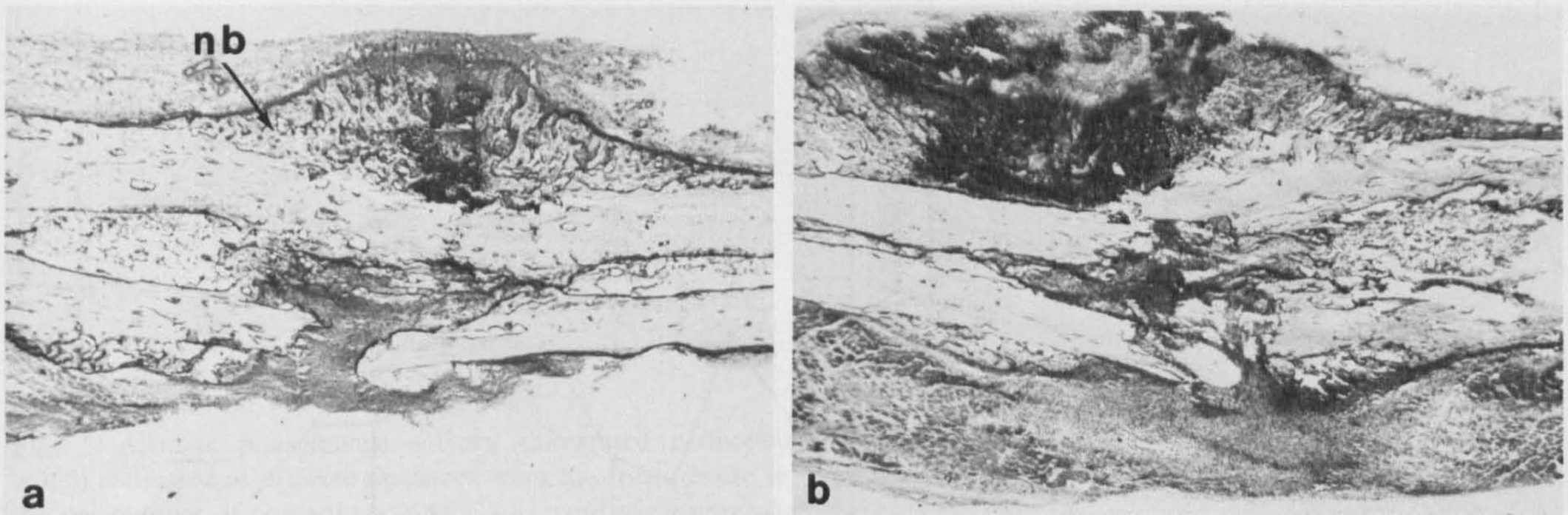

Fig. 1. Sections of fractures, 12 days postfracture, stained with toluidine blue. In the control bone **(a)**, the upper part of the callus has been largely converted to new bone (*nb*) with very little residual cartilage. In the fracture from the animal treated with dicumarol **(b)**, most of the callus consists of cartilage, staining dark. Magnification ×24.

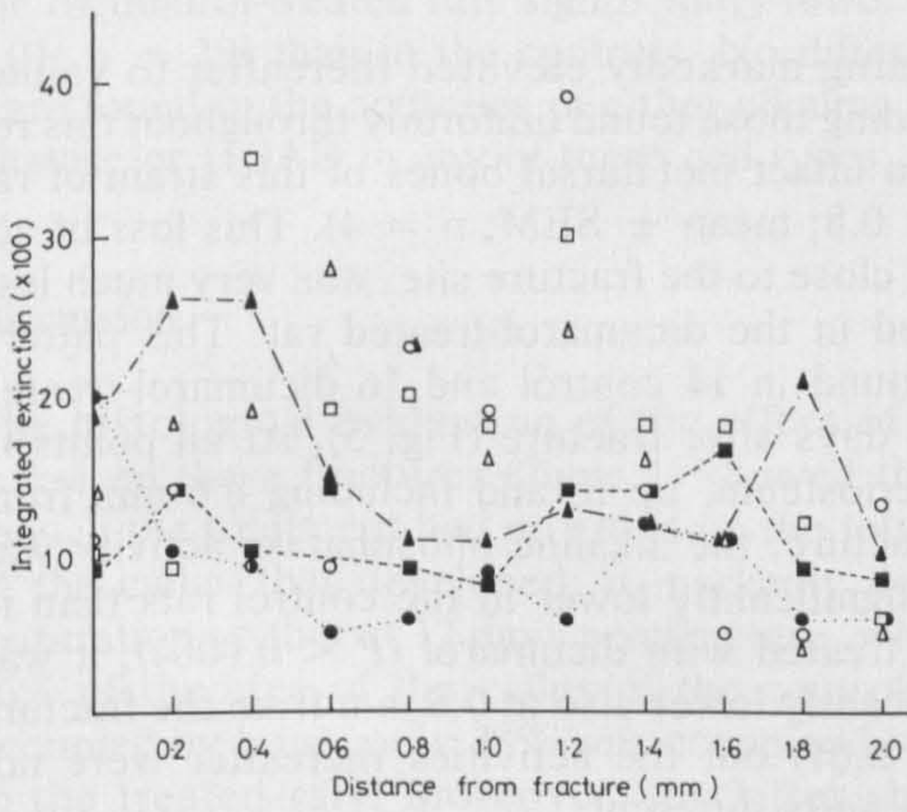

Fig. 2. G6PD activity (integrated extinction ×100) at discrete distances from the fracture in the periosteum of 3 control rats (*open symbols*) and of 3 rats treated with dicumarol (*closed symbols*) 3 days postfracture.

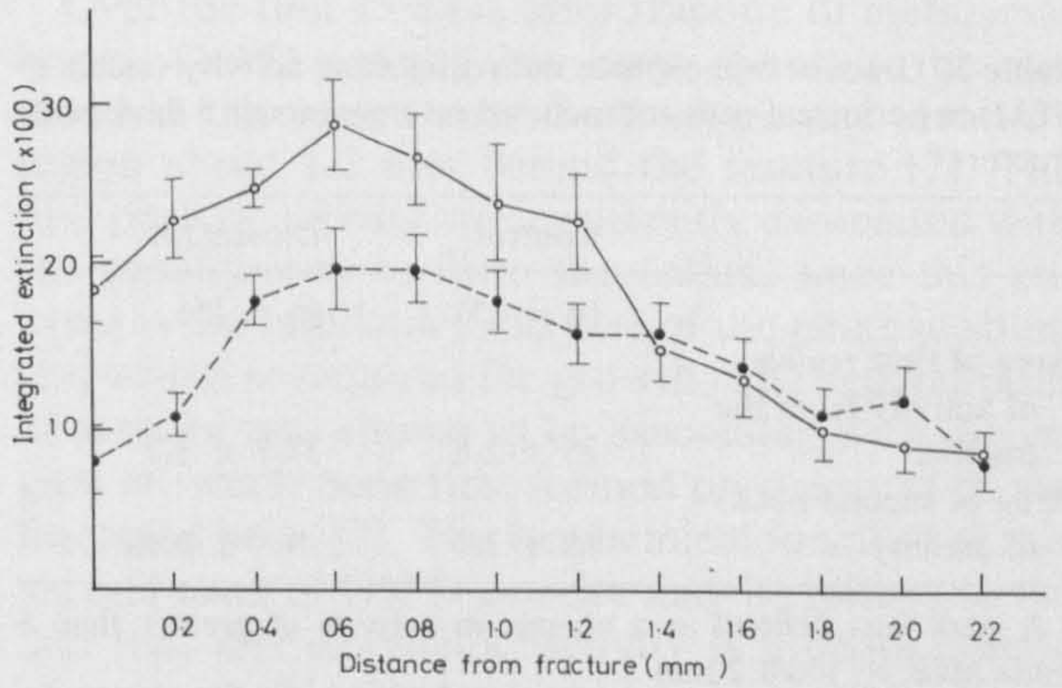

Fig. 3. The mean G6PD activity (integrated extinction ×100) at discrete points from the site of fracture in the periosteum of 15 control rats (*solid line*) and 14 rats, 5 days after fracture, that had been treated with dicumarol (*broken line*). The *bars* represent the standard error of the means.

treated rats declined over this region of the periosteum (Fig. 2).

In the periosteum of the fractured bones from 15 otherwise untreated and 14 dicumarol-treated rats taken 5 days after fracture, the mean activity was depressed in the latter and was found even in the face of wide individual variations (Fig. 3). The differences at 0, 0.2, and 0.4 mm from the fracture site were significant at the level of $P \leq 0.02$; at 0.6 mm the difference was significant at $P = 0.03$.

Because the precise location of the peaks of activities varied slightly in the different animals, the mean results did not adequately represent the changes in activity either along the periosteum of any one animal, or the differences induced by the treatment. In general, all the bones from the control rats, and most of the bones from the treated rats, showed two regions of elevated G6PD activity (Fig. 4). The region closest to the fracture had relatively low activity, with higher activities over part or all of the first 0.8 mm from the fracture. Particularly in the controls, another peak of activity occurred in the region of 1.0–1.8 mm from the fracture. However, because the precise location of these elevated activities varied from one rat to the next, the overall mean values (Fig. 3) did not clearly show these variations. Thus, to express the first of these activities numerically, the activity in each section was plotted against the distance from the fracture, as in Fig. 4, and the area under the graph up to the beginning of the second peak was measured by planimetry.

The results (Table 2) showed that there was a

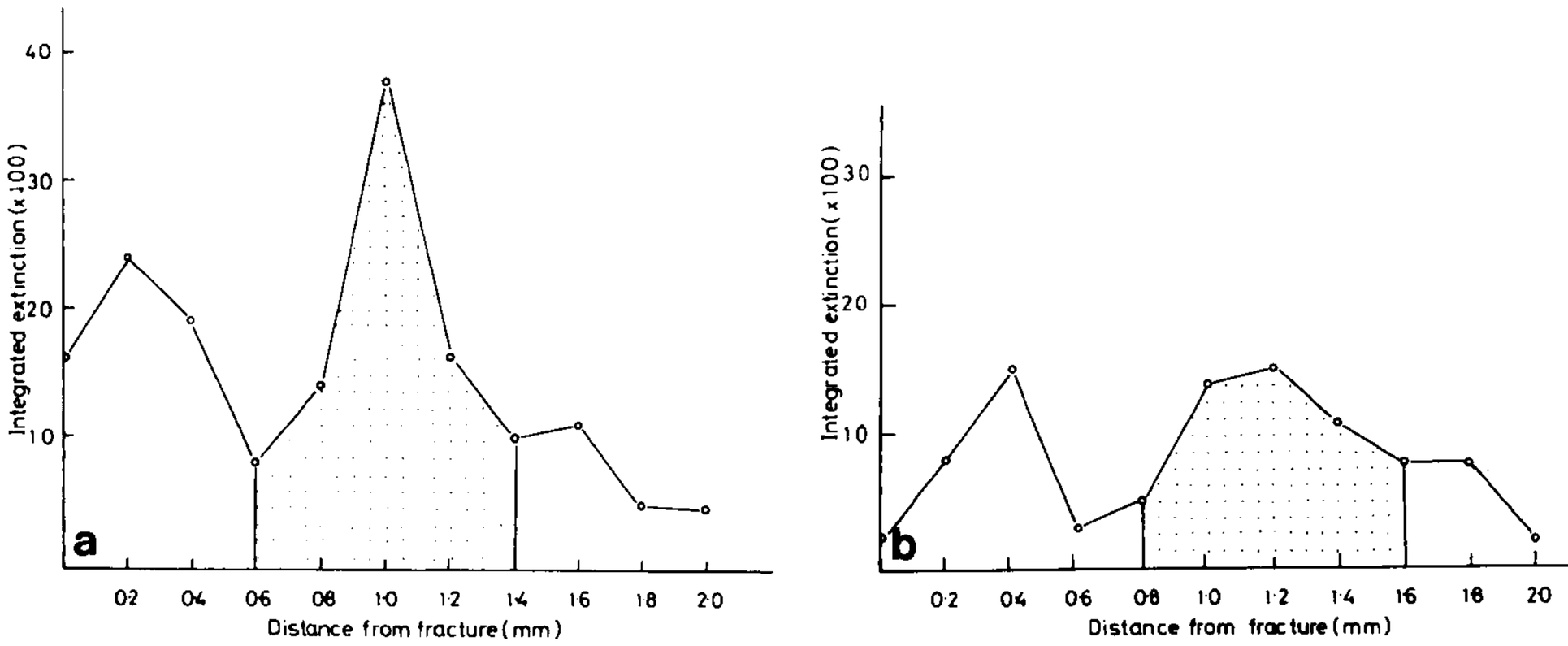

Fig. 4. Examples of how the G6PD activity (integrated extinction $\times 100$) was measured at different sites in the periosteum, 5 days postfracture (**a** control rat; **b** dicumarol-treated rat). The first measurement merely involved measuring the area under the graph up to the beginning of the second peak. The second measurement was of the area under the graph for the second peak of activity (stippled).

Table 2. Glucose 6-phosphate dehydrogenase activity (mean ± SEM) in periosteal cells of fractured rat metatarsals 5 days postfracture

	Control	Dicumarol
	(n = 15)	(n = 15)
Area of first region of activity from the fracture	25 ± 2.8[b]	17.7 ± 1.7
Area of second peak[a] of activity	16 ± 2.7[c]	3 ± 0.98

[a] A peak was defined as a change in activity of greater than 5 units MIE × 100/0.2 mm
[b] $0.05 > P > 0.02$ and [c] $P < 0.001$ as compared with dicoumarol-treated rats: Student's t test

barely significant depression of G6PD activity over this region of the periosteum in the dorsal callus of the rats treated with dicumarol ($0.05 > P > 0.02$). A similar device was used to achieve a numerical representation of how the treatment influenced the second peak of activity in the region of 0.8–1.8 mm from the fracture. For this purpose, an increase from one measurement to the next (a distance of 0.2 mm) of more than 5 units of mean integrated extinction $\times 100$ (corresponding to 0.05 of absolute extinction) was defined as a "peak." The area of such peaks was marked on the graphs (as in Fig. 4); these were measured by planimetry. The results (Table 2) showed that treatment with dicumarol had markedly suppressed this second peak ($P < 0.001$).

Alkaline Phosphatase Activity in the Periosteum

In a control rat, 3 days after fracture, there was very low activity up to 0.8 mm from the fracture site, becoming markedly elevated thereafter to values exceeding those found uniformly throughout this region in intact metatarsal bones of this strain of rat (38 ± 0.8; mean ± SEM; n = 4). This loss of activity, close to the fracture site, was very much less marked in the dicumarol-treated rat. This pattern was found in 14 control and 16 dicumarol-treated rats 5 days after fracture (Fig. 5). At all points in the periosteum, up to and including 0.6 mm from the fracture, the alkaline phosphatase activity was very significantly lower in the control rats than in those treated with dicumarol ($P < 0.0004$); it was significantly lower also at 0.8 mm from the fracture ($P = 0.01$) but the activities thereafter were not significantly different.

HOAD Activity in the Periosteum

This enzymatic activity was measured in the periosteum from the fractures of 10 control rats and of 11 rats that had been treated with dicumarol. Because inspection of the graphs of activity/distance for individual bones disclosed no obvious patterns, the results from all the specimens were plotted (Fig. 6). There was no difference in activity as a consequence of treatment with dicumarol.

Enzymatic Activity in the Cells of the Callus

Glucose 6-phosphate dehydrogenase activity was measured in 5 specified cell types in the callus of the fractures of 9 or 10 control, and 6–8 dicumarol-treated rats, 12 days postfracture. Only in the cells of the mature cartilage (Table 3) was the activity in

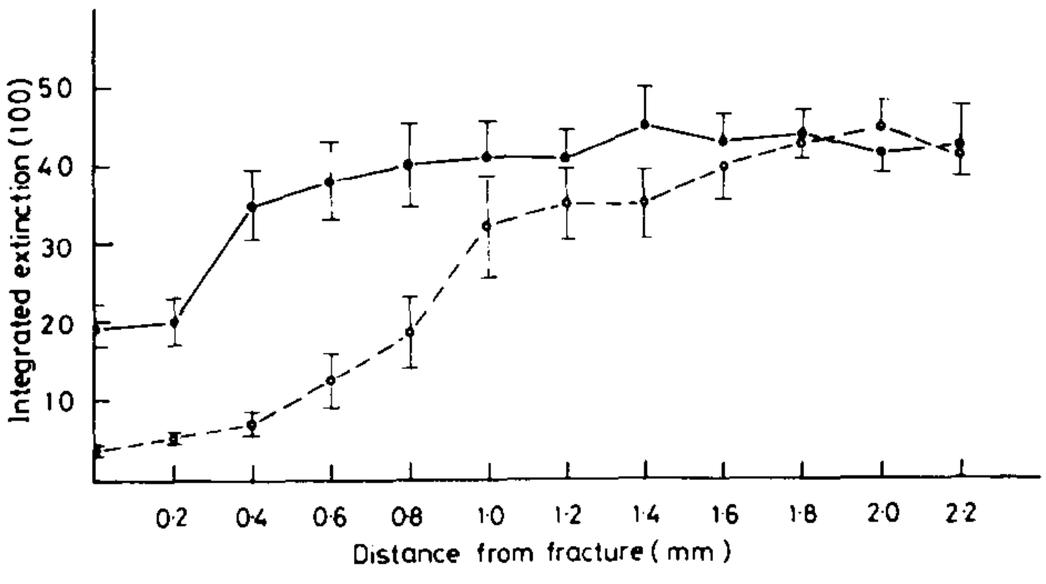

Fig. 5. Alkaline phosphatase activity (integrated extinction $\times 100$) measured at discrete distances from the fracture site in the periosteum of control rats (*solid line*) and of dicumarol-treated rats 5 days postfracture. The mean values (*solid or empty circles*) and SEM of 14 control and 16 dicumarol-treated rats are shown.

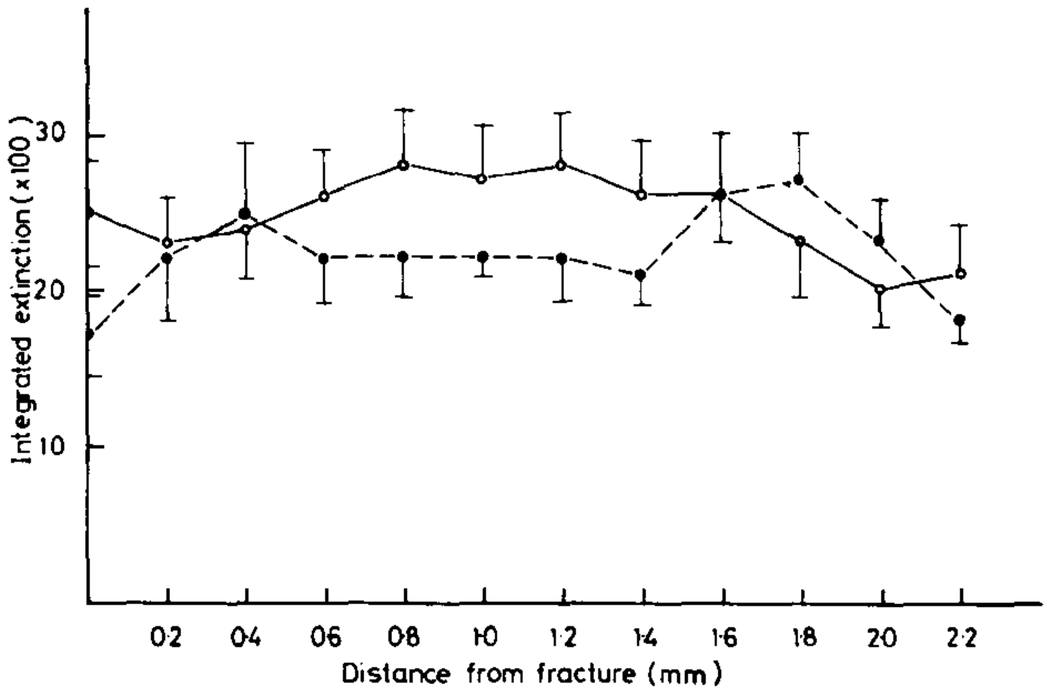

Fig. 6. HOAD activity (integrated extinction $\times 100$; mean $\pm$ SEM) at discrete distances from the fracture site, 5 days post-fracture, in 10 control rats (*solid line*) and 11 rats that had been treated with dicumarol (*broken line*).

the dicumarol-treated rats significantly lower ($P = 0.01$; n = 19) than in the controls. No differences were found in the activities of either alkaline phosphatase or HOAD in any of these cell types.

Discussion

The histological evaluation of the effect of dicumarol on these fractures (Table 1) showed that although the treatment had no effect on the total size of the callus that developed, it markedly delayed maturation so that at 12 days postfracture, whereas 56% of the area of the callus of the controls was occupied by bone, only 38% was occupied by bone in the treated rats. Moreover, the latter showed large regions of cartilaginous material (Fig. 1) and effete, fibrous material. This is in keeping with the earlier studies, for example, by Stinchfield et al [12] who found fibrous tissue and immature bone in the healing fractures of rabbits and a dog given dicumarol at the rate of 2 mg/kg body weight each day.

Superficially, the results reported here seem to be at variance with the results of Price and Williamson [13] who detected no abnormality in the repair of fractures in rats fed with warfarin. However, these workers studied young rats, in which the radius was fractured at 17 days of age. Because the amount of warfarin given was apparently toxic, vitamin K_1 was also administered simultaneously. Thus, the conditions were very different from those used in the present study. Moreover, evidence of repair was obtained radiologically and not histologically, thus allowing for the possibility that an outer cuff of bone, overlying a region of unossified cartilage (as found in the present study), could have confused the radiological evidence.

Over the first 15 days after fracture of metatarsal bones, G6PD activity has been shown to be elevated in the region near the fracture and also in a region about 1.2 mm behind the fracture [7]. The first peak of activity was apparently associated with the proliferation to form the callus, since this enzyme is the regulatory enzyme of the pentose shunt [14] which is required for growth. The second peak of activity was shown to be associated with the region at which bone first formed on the shaft of the fractured bone [7]. The biochemical function of this second peak of G6PD activity may be related to the fact that this enzymatic activity is a major source of cytosolic NADPH which may be used in the vitamin K cycle [6].

The results in the present study indicated that treatment with dicumarol only slightly depressed G6PD activity in the first region of the periosteum (Tables 2 and 3), but virtually obliterated the second peak. Moreover, it depressed G6PD activity in the cells of the mature cartilage. Thus, not only could it be acting as an antagonist of the vitamin K cycle, blocking the conversion of the epoxide to the naphthoquinol, but it also depressed the amount of reducing equivalents, from NADPH, available for the cycle at these points of ossification.

This action of dicumarol was not a universal effect in that it had no influence on the G6PD activity of the other cells of the callus (and therefore on the proliferative capacity of the callus or its ultimate size); nor did it influence fatty acid oxidation, as shown by the hydroxyacyl dehydrogenase activity. Furthermore, it enhanced periosteal alkaline phosphatase activity (Fig. 5) and left that of the various cells of the callus unaltered (Table 3). Thus it would seem, from the histological results, that it retarded the ossification of the callus; this would be consis-

Table 3. Enzyme activities (MIE × 100/10 min) in the various cell types of the callus 12 days postfracture

Cell Type		Enzyme		
		G6PD	HOAD	Alk. phos
Mature chondrocytes	Control	28 ± 2	5.3 ± 0.5	107 ± 6.3
	Dicumarol	20 ± 2	5.5 ± 0.4	100 ± 8.3
Chondrocytes in calcified cartilage	Control	11 ± 1.2	2.5 ± 0.2	53 ± 8.3
	Dicumarol	10 ± 1.0	3.0 ± 0.2	53 ± 6.0
Cellular granulation tissue	Control	51 ± 6.0	7 ± 1.2	70 ± 6.7
	Dicumarol	32 ± 7.0	7 ± 1.0	73 ± 7.0
Loose granulation tissue	Control	18 ± 1.7	3.0 ± 0.4	3.3 ± 2.2
	Dicumarol	14 ± 1.5	3.0 ± 0.3	3.3 ± 3.2
Osteoblasts	Control	37 ± 3.7	9.0 ± 0.8	140 ± 7.3
	Dicumarol	20 ± 3.0	9.0 ± 0.9	123 ± 12

G6PD: glucose 6-phosphate dehydrogenase; HOAD: hydroxyacyl dehydrogenase; Alk. phos: alkaline phosphatase

tent with its having an antagonistic effect against vitamin K_1 in the vitamin K cycle. In addition, dicumarol decreased the amount of reducing equivalents for this cycle selectively at points at which ossification should have occurred.

Acknowledgment: We are grateful to the Arthritis and Rheumatism Council for Research for a grant for this work.

References

1. Hauschka PV, Lian JB, Gallop PM (1975) Direct identification of the calcium-binding amino acid, γ-carboxyglutamate, in mineralised tissue. Proc Natl Acad Sci 72:3925–3929
2. Price PA, Otsuka AS, Poser JW, Kristaponis J, Raman N (1976) Characterization of a γ-carboxyglutamic acid-containing protein from bone. Proc Natl Acad Sci 73:1447–1451
3. Hauschka PV, Lian JB, Gallop PM (1978) Vitamin K and mineralization. Trends in Biochemical Science 3:75–78
4. Olson RE, Houser RM, Searcey MT, Gardner EJ, Scheinbuks J, Subba Rao GN, Jones J, Hall AL (1978) Nature of the vitamin K-dependent CO_2 fixation in microsomal membranes. Fed Proc 37:2610–2614
5. Stenflo J, Suttie JW (1977) Vitamin K-dependent formation of γ-carboxyglutamic acid. Ann Rev Biochem 46:157–172
6. Suttie JW, Larson AE, Canfield LM, Carlisle TL (1978) Relationship between vitamin K-dependent carboxylation and vitamin K epoxidation. Fed Proc 37:2605–2609
7. Dunham J, Shedden RG, Catterall A, Bitensky L, Chayen J (1977) Pentose-shunt oxidation in the periosteal cells in healing fractures. Calcif Tissue Res 23:77–81
8. Whitlon DS, Sadowski JA, Suttie JW (1978) Mechanism of coumarin action: significance of vitamin K epoxide reductase inhibition. Biochemistry 17:1371–1377
9. Chayen J, Bitensky L, Butcher RG (1973) Practical histochemistry. John Wiley & Sons, London, New York
10. Johnstone JJA (1979) The routine sectioning of undecalcified bone for cytochemical studies. Histochem J 11:359–365
11. Chambers DJ, Braimbridge MV, Frost GTB, Nahir AM, Chayen J (1982) A quantitative cytochemical method for the measurement of β-hydroxyacyl CoA dehydrogenase activity in rat heart muscle. Histochemistry 75:67–76
12. Stinchfield FE, Sankaran B, Samilson R (1956) The effect of anticoagulant therapy on bone repair. J Bone Jt Surg 38A:270–282
13. Price PA, Williamson MK (1981) Effects of warfarin on bone. J Biol Chem 256:12754–12759
14. Krebs HA, Eggleston LV (1974) The regulation of the pentose phosphate cycle. Adv Enzyme Regul 12:421–434

the testis of immature rats. *Biochem. Biophys. Res. Commun.* **65**, 1350–1354
30 Grahn, B., Henningsson, S. S. G., Kahlson, G. and Rosengren, E. (1973) Alterations in the activities of ornithine and nistidine decarboxylases provoked by testosterone in mice. *Br. J. Pharmacol.* **48**, 113–120
31 Pass, K. A., Bintz, J. E. and Postulka, D. D. (1982) Effects of testosterone on renal ornithine decarboxylase and kidney function. *Enzyme* **27**, 108–113
32 Younglai, E. (1982) Relationship of ornithine decarboxylase activity to HGG induced androgen production by rabbit testis. *Experientia* **38**, 973–974
33 Anderson, T. R. and Schanberg, S. M. (1975) Effect of thyroxine and cortisol on brain ornithine decarboxylase activity and swimming behaviour in developing rat. *Biochem. Pharmacol.* **24**, 495–501
34 Richman, R., Dobbins, C., Voina, S., Underwood, L., Mahaffee, D., Gitelman, H. J. Van Wyk, J. and Ney, R. L (1973) Regulation of adrenal ornithine decarboxylase by adrenocorticotropic hormone and cylic AMP. *J. Clin. Invest.* **52**, 2007–2015
35 Levine, J. H., Nicholson, W. E., Peytremann, A. and Orth, D. N. (1975) The mechanism of ACTH stimulation of adrenal ornithine decarboxylase activity. *Endocrinology* **97**, 136–144
36 Gaza, D. J., Short, J. and Lieberman, I. (1973) On the possibility that the prereplicative increases in ornithine decarboxylase activity are related to DNA synthesis in liver. *FEBS Lett.* **32**, 251–253
37 Mallette, L. E. and Exton, J. H. (1973) Stimulation by insulin and glucagon of ornithine decarboxylase activity in perfused rat livers. *Endocrinology* **93**, 640–644
38 Aisbitt, R. P. G. and Barry, J. M. (1973) Stimulation by insulin of ornithine decarboxylase activity in cultured mammary tissue. *Biochim. Biophys. Acta* **320**, 610–616
39 Maudsley, D. V., Leif, J. and Kobayashi, Y. (1976) Ornithine decarboxylase in rat small intestine: Stimulation with food or insulin. *Am. J. Physiol.* **231**, 1557–1561
40 Haselbacher, G. K. and Humbel, R. E. (1976) Stimulation of ornithine decarboxylase activity in chick fibroblasts by non supressible insulin-like activity (NSILA) insulin and serum. *J. Cell Physiol.* **88**, 239–246
41 Matsuzaki, S. and Suzuki, M. (1974) Thyroid function and polyamines. I. Rapid fluctuation of thyroid ornithine decarboxylase activity in response to change in circulating thyrotropin level in the rat. *Endocrinol. Jpn.* **21**, 529–537
42 Richman, R., Park, S., Akbar, M., Yu, S. and Burke, G. (1975) Regulation of thyroid ornithine decarboxylase (ODC) by thyrotropin. I: The rat. *Endocrinology* **96**, 1403–1412
43 Scalabrino, G. and Ferioli, M. E. (1976) *In vivo* hormonal induction of ornithine decarboxylase in rat kidney. *Endocrinology* **99**, 1085–1090
44 MacDonnell, P. C., Nagaiah, K., Lakshmanan, J. and Guroff, S. (1977) Nerve growth factor increases activity of ornithine decarboxylase in superior cervical ganglia of young rats. *Proc. Natl. Acad. Sci. USA* **74**, 4681–4684
45 Stastny, M. and Cohen, S. (1970) Epidermal growth factor IV. The induction of ornithine decarboxlyase. *Biochim. Biophys. Acta* **204**, 578–589
46 Nissley, S. P., Passamani, J. and Short, P. (1977) Stimulation of DNA synthesis, cell multiplication and ornithine decarboxylase in 3T3 cells by multiplication stimulation activity (MSA). *J. Cell Physiol.* **89**, 393–402
47 Byus, C. V., Costa, M., Sipes, I. G., Brodie, B. B. and Russell, D. H. (1976) Activation of 3:5′ cyclic AMP dependent protein kinase and induction of ornithine decarboxylase as early events in induction of mixed function oxygenases. *Proc. Natl. Acad. Sci. USA* **73**, 1241–1245
48 Wyatt, G. R., Rothaus, K., Lawler, D. and Herbst, E. J. (1973) Ornithine decarboxylase and polyamines in silkmoth pupal tissues: Effects of ecdysone and injury. *Biochim. Biophys. Acta* **304**, 482–494
49 Murty, C. M., Hornseth, R., Verney, E. and Sidarsky, H. (1982) Ethanol-induced stimulation of hepatic ornithine decarboxylase activity in the rat. *Alcoholism* **6**, 80–88
50 Van Dyke, R. A., Baihly, C. D. and Nelson, R. M. (1982) Elevated ornithine decarboxylase activity in the rat liver following exposure to halothane, enflurane and isoflurane. *Life Sci.* **30**, 1893–1898
51 Vinores, J. A., Marangos, P. J. and Ko, L. (1982) Butyrate–induced increase in neuron-specific enolase and ornithine decarboxylase in anaplastic glioma cells. *Dev. Brain Res.* **5**, 23–28
52 Otani, S., Kuramoto, A., Matsui, I. and Morisawa, S. (1982) Induction of ornithine decarboxylase in guinea pig lymphocytes by the divalent cation ionophore A23187. *Eur. J. Biochem.* **125**, 35–40
53 Mizrahi, Y. and Heimer, Y. M. (1982) Increased activity of ornithine decarboxylase in tomato ovaries induced by auxin. *Phys. Plantarum* **54**, 367–368
54 Beck, W. T., Bellatone, R. A. and Canellakis, E. S. (1972) The *in vivo* stimulation of rat liver ornithine decarboxylase activity by dibutyryl cylic adenosine 3′,5′-monophosphate, theophylline and dexamethasone. *Biochem. Biophys. Res. Commun.* **48**, 1649–1655
55 Hölttä, E. and Raina, A. (1973) Stimulation of ornithine decarboxylase and nuclear RNA polymerase activity in rat liver by glucagon and dibutyryl cyclic AMP. *Acta Endocrinol.* **73**, 794–800
56 Eloranta, T. and Raina, A. (1975) Involvement of hyophysis in the stimulation of liver ornithine decarboxylase by dibutyryl cyclic AMP. *FEBS Lett.* **55**, 22–26
57 Byus, C. V. and Russell, D. H. (1974) Effects of methyl xanthine derivatives on cyclic AMP levels and ornithine decarboxylase activity of rat tissues. *Life Sci.* **15**, 1991–1997
58 Mizoguchi, Y.,Otani, S., Matsui, I. and Morisawa, S. (1975) Control of ornithine decarboxylase activity by cyclic nucleotides in phytohemagglutinin induced lymphocyte transformation. *Biochem. Biophys. Res. Commun.* **66**, 328–335
59 Canellakis, Z. N. and Theoharides, T. C. (1976) Stimulation of ornithine decarboxylase synthesis and its control by polyamines in regenerating rat liver and cultured rat hepatoma cells. *J. Biol. Chem.* **251**, 4436–4411
60 Byus, C. V., Wicks, W. D. and Russell, D. H. (1976) Induction of ornithine decarboxylase in Reuber H35 rat hepatoma cells. *J. Cycl. Nucl. Res.* **2**, 241–250
61 McCann, P. P. (1980) Polyamines in Biomedical Research, (Gaugas, J. M. Ed.), Wiley, New York, pp. 109–123.
62 Heller, J. S., Fong, W. F. and Canellakis, E. S. (1976) Induction of a protein inhibitor to ornithine decarboxylase by the end products of its reaction. *Proc. Natl. Acad. Sci. USA* **73**, 1858–1862
63 McCann, P. P., Tardif, C. and Mamont, P. S. (1977) Regulation of ornithine decarboxylase by ODC-antizyme in the HTC cells. *Biochem. Biophys. Res. Commun.* **75**, 948–954
64 Heller, J. S., Chen, K. Y. Kyriakidis, D. A., Fong, W. F.. and Canellakis, E. S. (1978) The modulation of the induction of ornithine decarboxylase by spermine, spermidine and diamines. *J. Cell Physiol.* **96**, 225–236
65 Kyriakidis, D. A., Heller, J. S. and Canellakis, E. S. (1978) Modulations of ornithine decarboxylase in *Escherichia coli* by positive and negative effectors. *Proc. Natl. Acad. Sci. USA* **75**, 4699–4703
66 Fujita, K., Murakami, Y. and Hayashi, S-I (1982) A macromolecular inhibitor of the antizyme to ornithine decarboxylase. *Biochem. J.* **204**, 647–652
67 Atmar, V. J., Daniels, G. R. and Kuehn, G. D. (1978) Polyamine stimulation of phosphorylation of nonhistone acidic protein in nuclei and nucleoli from *Physarum polycephalum. Eur. J. Biochem.* **90**, 29–37
68 Atmar, V. J. and Kuehn, G. D. (1981) Phosphorylation of ornithine decarboxylase by a polyamine-dependent protein kinase. *Proc. Natl. Acad. Sci. USA* **78**, 5518–5522
69 Kuehn, G. D. and Atmar, V. J. (1982) Posttranslational control on ornithine decarboxylase by a polyamine-dependent protein kinase. *Fed. Proc.* **41**, 3078–3083
70 Kuehn, G. D. and Atmar, V. J. (1973) New perspectives on polyamine dependent protein kinase and the regulation of ornithine decarboxylase by reversible phosphorylation. *Adv. Polyamine Res.* **4**, 615–629
71 Tyagi, A. K., Tabor, C. W. and Tabor, H. (1981) Ornithine decarboxylase from *Saccharomyces cerevisiae.* Purification properties and the regulation of activity. *J. Biol. Chem.* **256**, 12156–12163
72 Costa, M. and Nye, J. S. (1978) Calcium, asparagine and cAMP are required for ornithine decarboxylase activation in intact chinese hamster ovary cells. *Biochem. Biophys. Res. Commun.* **85**, 1156–1164
73 Daniels, G. R., Atmar, V. J. and Kuehn, G. D. (1981) Polyamine-activated protein kinase reaction from nuclei and nucleoli of *Physarum polycephalum* which phosphorylates a unique M_r 70 000 nonhistone protein. *Biochemistry* **20**, 2525–2532
74 Criss, W. E., Yamamoto, U., Takai, Y., Nishizuka, Y. and Morris, H. P. (1978) Requirement of polycations for the enzymatic activity of a new protein kinase-substrate complex from Morris Hepatoma 3924A *Cancer Res.* **38**, 3532–3539
75 Leiderman, L. J., Criss, W. E., Morishita, Y. and Oka, T. (1983) Hormonal regulation and function of polyamine responsive protein kinase activity in the mouse mammary gland. *Adv. Polyamine Res.* **4**, 655–666
76 Criss, W. E., Morishita, Y., Watanabe, Q., Akogyeram, C., Sahai, A., Deu, B. and Oka, T. (1983) Multiple-protein complex with [calmodulin]-polyamine responsive protein kinase activity. *Adv. Polyamine Res.* **4**, 647–654
77 Morishita, Y., Watanabe, K., Akogyeram, C., Deu, B. and Criss, W. E. (1983) Calmodulin stimulates polyamine-responsive protein kinase in the absence of Ca^{2+}. *Biochim. Biophys. Acta* **755**, 352–357
78 Morishita, Y., Sahai, A., Akogyeram, C., Hollis, V., Oka, T. and Criss, W. E. (1982) Identification and characterization of endogenous inhibitors of polyamine-responsive protein kinase activity. *J. Cycl. Nucl. Res.* **8**, 173–179
79 Morishita, Y., Akogyeram, C., Deu, B. and Criss, W. E. (1983) Regulation of polyamine-responsive protein kinase by certain highly specific polyamines and charged carbohydrates. *Biochim. Biophys. Acta* **755**, 358–362
80 Russell, D. H. (1981) Posttranslational modification of ornithine decarboxylase by its product putrescine. *Biochem. Biophys. Res. Commun.* **99**, 1167–1172
81 Russell, D. H. and Manen, C-A (1982) Posttranslationally modified ornithine decarboxylase may regulate RNA polymerase I activity. *Biochem. Pharmacol.* **31**, 3373–3378
82 Haddox, M. K. and Russell, D. H. (1981) Increased nuclear conjugated polyamines and transglutaminase during liver regeneration. *Proc. Natl. Acad. Sci. USA* **78**, 1712–1716
83 Manen, C-A and Russell, D. H. (1977) Ornithine decarboxylase may

function as an initiation factor for RNA polymerase I. *Science* **195**, 505–506
84 Russell, D. H. (1983) Microinjection of purified ornithine decarboxylase into *Xenopus* oocytes selectively stimulates ribosomal RNA synthesis. *Proc. Natl. Acad. Sci. USA* **80**, 1318–1321
85 Rose, K. M., Stetler, D. A. and Jacob, S. T. (1981) Protein kinase activity of RNA polymerase I purified from rat hepatoma. Probable function of M_r 42 000 and 24 6000 polypeptides. *Proc. Natl. Acad. Sci. USA* **78**, 2833–2837
86 Jacob, S. T., Duceman, B. W. and Rose, K. M. (1981) Spermine-mediated phosphorlation of RNA polymerase I and its effect on transcription. *Med. Biol.* **59**, 381–388
87 Jacob, S. T., Rose, K. M. and Canellakis, Z. N. (1983) Effects of spermidine and its monoacetylated derivatives on phosphorlyation by nuclear protein kinase NII. *Adv. Polyamine Res.* **4**, 631–646
88 Hovanessian, A. G. and Kerr, I. M. (1979) The (2'-5') oligoadenylate (pppA2'-5'A2-5'A) synthetase and protein kinase(s) from interferon-treated cells. *Eur. J. Biochem.* **93**, 515–526
89 Lee, E. J., Larkin, P. C. and Sreevalsan, T. (1980) Differential effect of interferon on ornithine decarboxylase activation in quiscent swiss 3T3 cells. *Biochem. Biophys. Res. Commun.* **97**, 301–308
90 Sreevalsan, T., Taylor-Papadimitriou, J. and Rozengurt, E. (1979) Selective inhibition by interferon of serum-stimulated biochemical events in 3T3 cells. *Biochem. Biophys. Res. Commun.* **87**, 679–685

Histochemical and cytochemical demonstration of ornithine decarboxylase

It has proved remarkably difficult to demonstrate the products of ornithine decarboxlyase (ODC) activity cytochemically. This is because it is unlikely that a way will be found of specifically precipitating the decarboxylated substrate, namely putrescine, and it is not easy to precipitate the other product of the reaction, namely CO_2, at the pH at which the enzyme works optimally. Consequently histochemical procedures have concentrated on localizing the site of the enzyme itself. Two types of method have been suggested.

Use of a labelled suicidal enzyme inhibitor

The more direct histochemical approach to localizing the site of the enzyme has been to use an enzyme-activated irreversible inhibitor, or 'suicidal inhibitor', namely α-difluoromethylornithine[1]. In one procedure, the inhibitor is linked to a fluorescent moiety, such as rhodamine[2]; the site of the inhibitor–rhodamine conjugate, and presumably that of the enzyme, is demonstrable by fluorescence microscopy. In the other procedure[3], the inhibitor is labelled radioactively with ^{14}C and its site in sections is determined by autoradiography. The results obtained by the autoradiographic technique correlated quantitatively with previous biochemical results in that the ODC staining was high in the kidney and was lost rapidly when protein-synthesis was inhibited.

Neither method has been used quantitatively. Both require more validation. As far as can be seen, neither is likely to define changes in ODC activity, although further validation may dispel this criticism. A major criticism of both procedures is the methods used for preparing the sections. The histochemical localization of many 'soluble proteins' can vary greatly according to the procedures used for fixing, embedding, sectioning and removing the embedding wax. Moreover, water-soluble material can move considerable distances when such processed sections are immersed in aqueous media or aqueous autoradiographic film.

Immunohistochemistry

The second type of histochemical procedure[4] involved the preparation and purification of the enzyme; the production of a rabbit antibody to it; and then the use of goat-anti-rabbit IgG conjugated with fluorescein isothiocyanate. After specificity tests, the localization of the goat-anti-rabbit IgG, and presumably of the ODC, was detected by fluoresence microscopy.

No quantitative results have been presented for this procedure. Moreover, assuming complete specificity, the anti-ODC antibody may be expected to react with any molecule that has sufficient antigenicity to yield an appreciable response to this antibody. Thus, at best, the method probably could not distinguish between active and inactive enzyme; nor would it demonstrate the enzyme if the antigenic sites were masked, for example by binding to some other protein, or were not immediately available to the antigen. As before, the localization of the enzyme will also depend critically on the conditions under which the sections are prepared and treated with the primary and secondary antibodies. Clearly much work remains to be done even to validate the localization produced by this procedure.

Preliminary studies towards a quantitative cytochemical method

In normal cytochemistry, the activity of an enzyme such as a phosphatase or decarboxylase would be measured by precipitating the smaller moiety released, namely either phosphate or carbon dioxide. Care has to be taken that the precipitating ion should be sequestered from the active site of the enzyme so as to avoid inhibition[5]. The localization of the enzyme is not the primary concern of such techniques as long as the products of the enzyme-activity are retained within the cell that contains that activity. However, a series of procedures has been developed, designed to stop the movement of 'soluble' enzymes. These include particular ways of chilling and sectioning tissues; flash-drying the sections; and the use of inert colloid stabilizers to protect the sections, and stop diffusion, during the chromogenic reaction[6].

It was found by Frost (personal communication) that lead, in the form of lead hydroxyisobutyrate, is sufficiently chelated not to inhibit the enzyme, but can be precipitated, apparently as lead carbonate, by CO_2 at neutral pH values. This, therefore, could act as the precipitating agent. All the solutions have to be prepared in CO_2-free water and care must be taken not to introduce other ions that could compete successfully against the hydroxyisobutyrate for the lead. At present, the provisional method, outlined below, seems to yield a quantitative estimation of ODC activity in tissues, showing inhibition with α-difluoromethylornithine, and stimulation by relevant hormones in tissues that respond to these hormones. However, the method is not finalized because, with prolonged reaction-times, the nature and intracellular localization of the reaction-product changes. This may be due to the formation of a complex lead precipitate containing the more soluble lead bicarbonate. For all that, measurement of total activity per cell increases linearly with time, irrespective of the localization of the lead-precipitate. The lead carbonate is converted to the brown-black lead sulphide which is measured by microdensitometry.

0263–6484/84/010010–02$03.00
© 1984 Butterworth & Co. (Publishers) Ltd

Reaction-medium

All solutions have to be prepared in CO_2-free water. To three volumes of 0.2 M triethanolamine buffer, pH 8.0, containing 40% G04/140 grade of polyvinyl alcohol (PVA) (Wacker Chemicals, Mount Felix, Bridge Street, Walton-on-Thames KT12 1AS, UK) is added 1 volume of the solution of lead hydroxyisobutyrate (17.85% Pb); L-ornithine, 3.4 mg ml^{-1}; pyridoxal-5-phosphate, 0.62 mg ml^{-1}; D,L-dithiothreitol, 0.08 mg ml^{-1}; L-P-bromotetramizole, 0.15 mg ml^{-1} (to inhibit alkaline phosphatase activity). The final pH should be adjusted, if necessary, to pH 7.1. Before incubating the sections in this reaction medium, a pre-rinse is required to remove 'background' colouration, possibly caused by free phosphates retained in, or close to, the sections, by the stabilizer. The pre-rinse consists of 0.2 M triethanolamine buffer, pH 8.0, containing 20% G04/140 PVA. The final pH is pH 7.1. This medium is poured into Perspex rings surrounding the sections and left for 10 min at 37°C after which time it is sucked off and replaced by the reaction medium.

Procedure

(1) Incubate in the medium at 37°C, (cryostat sections of unfixed mouse kidney may require 10–30 min).
(2) Wash in CO_2-free water.
(3) Immerse in a 0.5% aqueous solution of ammonium sulphide (1 min).
(4) Rinse in distilled water.
(5) Mount in an aqueous mounting medium (e.g. Farrants' medium).

Measurement

By microdensitometry at 580 nm.

Specificity

30 mM α-difluoromethyl ornithine caused up to 42% inhibition of the activity in cryostat sections (10 μm) of unfixed mouse kidney reacted for 30 min.

Acknowledgements

We are indebted to Mr G. T. B. Frost (Sigma, London) for his exploration of possible trapping agents; for the synthesis of lead isohydroxybutyrate; and for kindly supplying the reagent. The α-difluoromethylornithine was a gift from Merrell International, Strasbourg. We thank the Arthritis and Rheumatism Council for Research for support.

R. A. Dodds and J. Chayen,
Kennedy Institute of Rheumatology,
6, Bute Gardens,
London W6 7DW

References

1 Mamont, P. S., Duchesne, M.-C., Grove, J. and Bey, P. (1978) Antiproliferative properties of D,L-α difluoromethylornithine in cultured cells: A consequence of the irreversible inhibition of ornithine decarboxylase. *Biochem. Biophys. Res. Commun.* **81**, 58–66
2 Gilad, G. M. and Gilad, H. G. (1981) Cytochemical localization of ornithine decarboxylase with rhodamine or biotin-labelled α-difluoromethylornithine. *J. Histochem. Cytochem.* **29**, 687–692
3 Pegg, A. E., Seely, J. and Zagon, I. S. (1982) Autoradiographic identification of ornithine decarboxylase in mouse kidney by means of α-{5-^{14}C} difluoromethylornithine. *Science* **217**, 68–70
4 Persson, L., Rosengren, E. and Sundler, F. (1982) Localization of ornithine decarboxylase by immunocytochemistry. *Biochem. Biophys. Res. Commun.* **104**, 1196–1201
5 Chayen, J., Frost, G. T. B., Dodds, R. A., Bitensky, L., Pitchfork, J., Baylis, P. H. and Barrnett, R. J. (1981) The use of a hidden metal-capture reagent for the measurement of Na^+-K^+-ATPase activity – a new concept in cytochemistry. *Histochemistry* **71**, 533–541
6 Chayen, J., Bitensky, L. and Butcher, R. G. (1973) Practical histochemistry, Wiley, London.

S-Adenosylmethionine decarboxylase: a brief review

An outline of the pathway for polyamine biosynthesis in mammalian cells is shown in *Figure 1*. It can be seen that *S*-adenosyl-L-methionine (AdoMet) plays a key role in this pathway. In most living organisms AdoMet is the precursor of the aminopropyl groups of spermidine and spermine[1–3]. Before it can be used as an aminopropyl donor, AdoMet must be decarboxylated. The enzyme (EC 4.1.1.50) which catalyses this reaction was first discovered by H. and C. W. Tabor[1] in *E. coli* and is termed AdoMet decarboxylase (AdoMetDC). This enzyme is an important regulatory step in polyamine bosynthesis and in AdoMet metabolism since decarboxylated AdoMet is virtually inactive as a methyl donor; once the decarboxylation has occurred AdoMet is irreversibly committed to polyamine biosynthesis. In mammalian cells AdoMetDC is the rate limiting step in the synthesis of polyamines and the normal cellular content of decarboxylated AdoMet is very low amounting to less that 5% of the AdoMet concentration[4–9].

This review covers the properties and regulation of AdoMetDC, describes briefly work on inhibitors of its activity and concludes with a description of the changes in AdoMetDC activity and AdoMet levels brought about by inhibition of other steps in the polyamine biosynthetic pathway. No attempt has been made to cover all of the voluminous literature on this enzyme and many early references can be obtained from previous reviews[1–3].

Purification and properties of AdoMetDC

Homogeneous preparations of AdoMetDC have been obtained from *E. coli*[10–12], *S. cerevisiae*[12,13], rat liver[14–17], rat psoas muscle[17], mouse liver and mammary gland[18] and bovine liver[19]. Partial purifications and characterizations of the enzyme from other sources including plants have also been reported (see[2,12,20–23]). The most convenient purification step involves affinity chromatography on MGBG-Sepharose[14]. Methylglyoxal bis(guanylhydrazone) (MGBG) is a powerful competitive inhibitor and the enzyme binds to MGBG-Sepharose even in the presence of a high salt concentration which can be used to wash off contaminating proteins. All of the homogeneous preparations of AdoMetDC from eukaryotes have been obtained with the aid of this methodology[12–19]. More recently, it has been observed that the bacterial AdoMetDC can also be purified on MGBG-Sepharose even though MGBG is a weaker inhibitor of the bacterial enzyme[11,12].

AdoMetDCs from *E. coli*[10,11], yeast[13] and rat liver[14] have been shown to contain a covalently linked pyruvate which is essential for enzyme activity. Presumably this pyruvoyl residue forms a Schiff base with the substrate and thus facilitates the decarboxylation. A small class of amino acid decarboxylases having pyruvate rather than pyridoxal phosphate for this purpose is now known[24].

0263–6484/84/010011–05$03.00
© 1984 Butterworth & Co. (Publishers) Ltd

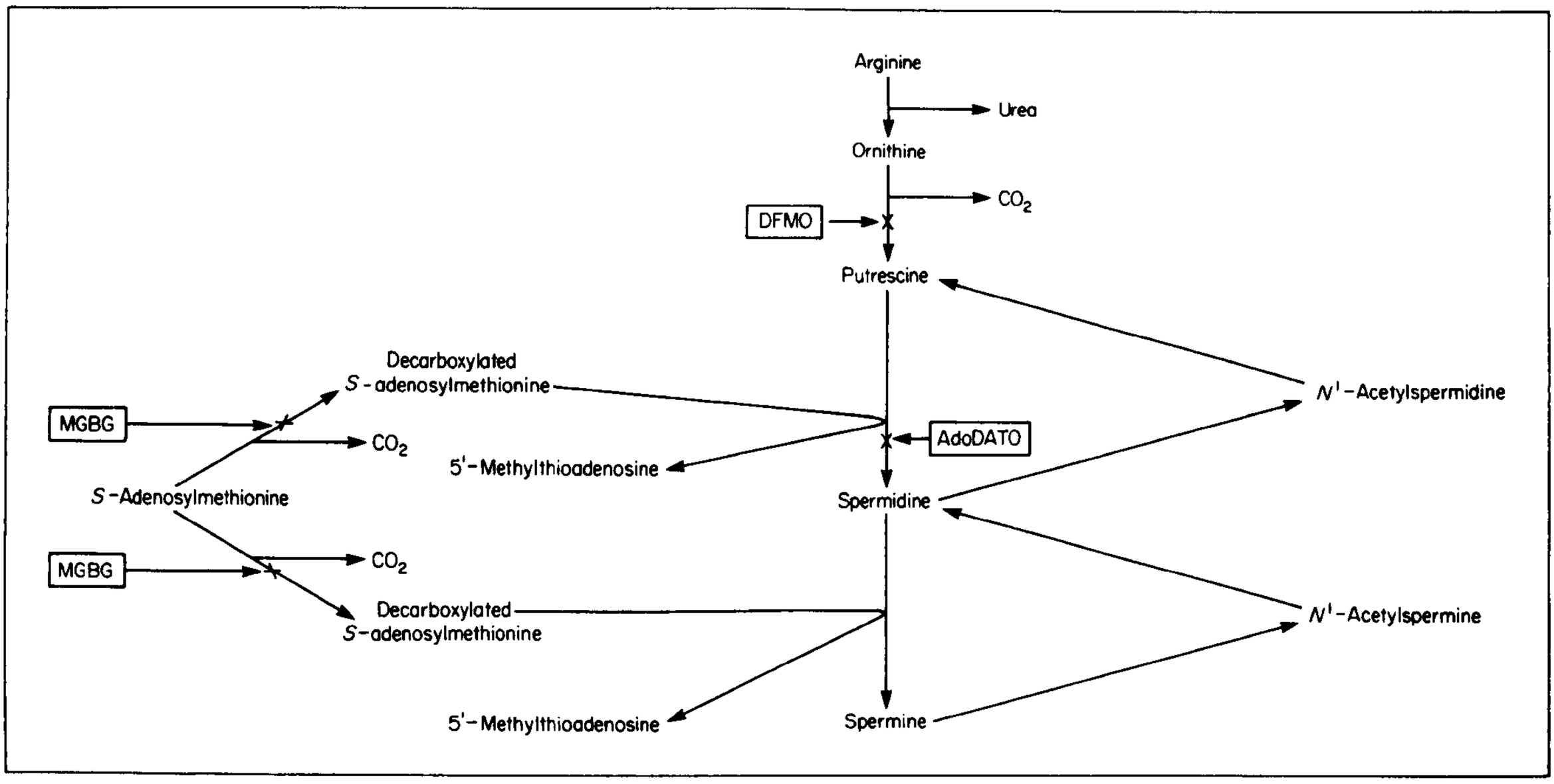

Figure 1 Pathway of polyamine biosynthesis in mammalian cells. The reactions involved and their inhibition are described in detail in Ref. 3. Inhibition of the steps shown is brought by α-difluoromethylornithine (DFMO), methylglyoxal bis(guanylhydrazone) (MGBG) and *S*-adenosyl-1,8-diamino-octane (AdoDATO).

Mammalian AdoMetDC has a subunit *MW* of about 32 000 and is normally present as a dimer of *MW* about 65–70 000, although larger aggregates occur quite readily[2,15–19]. AdoMetDC from *S. cerevisiae* is also a dimer with a subunit *MW* of about 41 000[13], but the enzyme from *E. coli*[11] has six subunits of *MW* 17 000. Although the first determinations of pyruvate in the latter enzyme showed only one molecule per molecule of enzyme[10], more recent preparations produced with less harsh isolation conditions give one pyruvate per subunit and have a 5–6 fold higher activity[11].

The stereochemistry and kinetic isotope effects in the decarboxylation of AdoMetDC were investigated and it was shown that the reaction proceeds with retention of the configuration at the 1C and a tritium isotope effect of 4.5[25].

The gene coding for the *E. coli* AdoMetDC has been mapped at 2.7 minutes and deletion mutants lacking this enzyme constructed[26]. *S. cerevisiae* mutants lacking AdoMetDC are also known and are closely linked to arg1 which is on chromosome xv[27]. The AdoMetDC mutants are unable to produce spermidine confirming the absolute requirement for decarboxylated AdoMet in these organisms. No mammalian mutants lacking AdoMetDC are yet available. Convincing evidence that at least two forms of AdoMetDC occur in mammalian cells was obtained by Pösö and Pegg[17,28] who purified the enzyme to homogeneity from rat liver and rat psoas. The enzymes from these sources differed with respect to activation by putrescine, K_m for AdoMet, inhibition by MGBG and repression by spermidine[17,28,29]. They also differed in isoelectric point and could readily be separated by polyacrylamide gel electrophoresis under isoelectric focusing conditions[17,29]. However, the nature of the difference is not yet known and could relate to post-translational modifications rather than to the presence of multiple genes for AdoMetDC in mammalian cells.

AdoMetDC preparations from *E. coli*, certain plants and some other microorganisms require Mg^{2+} for activity[1,2,10–12,20,21]. AdoMetDC from other micro-organisms including the slime moulds, *Physarum polycephalum* and *Dictyostelium discoideum*, and the protozoan, *Tetrahymena pyriformis* did not require cations for maximal activity[2,12,20,23,30].

In contrast, the enzyme from all higher eukaryotes (including invertebrates, reptiles, amphibia, and mammals) and from many yeasts including *S. cerevisiae* are activated by putrescine[2,12–14,17–20,22,23,29–31]. This activation which was first noted by Pegg and Williams-Ashman[31] is an important regulatory mechanism which ensures that the synthesis of decarboxylated AdoMet is increased in response to increased availability of putrescine[5,6]. Therefore, an increase in ornithine decarboxylase activity brings about an increased synthesis of spermidine (see *Figure 1*). Similarly, spermidine and spermine rather than putrescine are the predominant polyamines in those organisms with a putrescine-activated AdoMetDC. It has been suggested[22,30] that the presence of a putrescine-activated AdoMetDC correlates with the ability to synthesize spermine (which is not normally present in many micro-organisms), but the generality of this correlation is not fully established.

Putrescine can be partially replaced as an activator of AdoMetDC by a variety of other diamines although these are not as potent[2,20,29,31–34]. The activation is pH dependent and is considerably greater at pH 6.5 than 8.5[2,29,33]. Early reports that spermidine was able to activate AdoMetDC could not be confirmed with highly purified spermidine and the homogeneous enzyme[29]. A minor spermidine-activated AdoMetDC could be present in crude extracts and would explain the earlier results, but another explanation is that putrescine or another diamine was a contaminant of the spermidine used for activation.

Inhibition of AdoMetDC activity

Williams-Ashman and colleagues[31,33] made the extremely important discovery that MGBG was a potent inhibitor of the putrescine-activated AdoMetDC. This observation has been repeated and confirmed by many subsequent experiments[1–7,12–19,35–37]. MGBG is a competitive inhibitor with respect to AdoMet and has a K_i of less than 1 μM[2,12]. A number of congeners of MGBG are also strong inhibitors[2,12,17,33] and the ethyl analogue, EGBG is about

DAMAGED
TEXT
IN
ORIGINAL

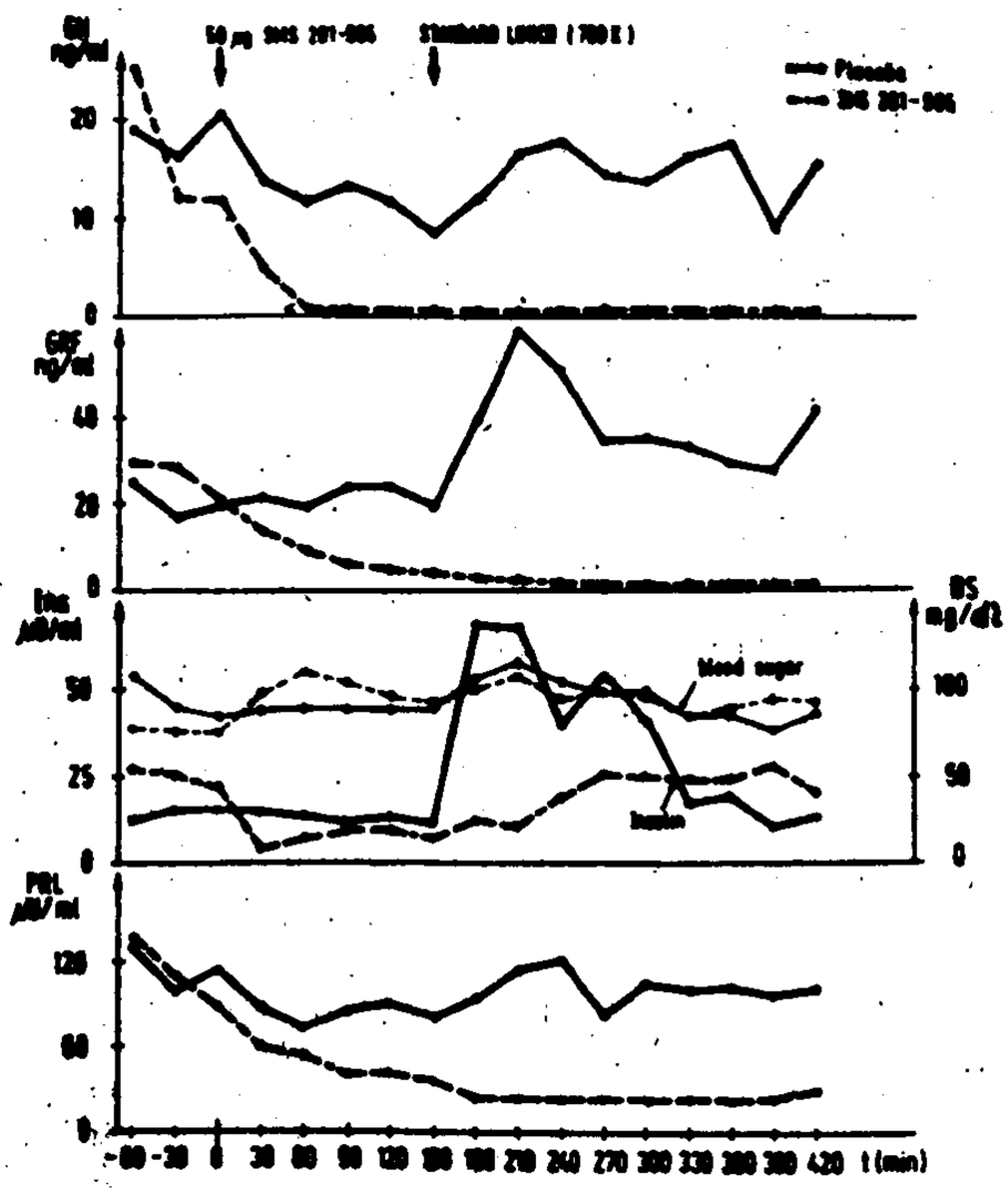

GH, GRF, insulin (fine), and prolactin (PRL) levels after subcutaneous injection of 50 μg SMS 201–995.

Somatostatin analogue injected at 0900 hours and hormone levels were monitored from 0800 to 1700 and compared with those from a control day (placebo). All four hormones were significantly suppressed. Blood sugar (BS) was not significantly influenced by the insulin suppression, which may be due to elimination of GH-induced insulin antagonism.

somatostatin analogue may inhibit not only GRF secretion but also tumour growth, as in the patient with a metastatic vipoma.[1]

Medizinische Klinik Innenstadt,
University of Munich,
8000 Munich 2, West Germany

KLAUS VON WERDER
MARCO LOSA
O. ALBRECHT MÜLLER

Chirurgische Klinik Innenstadt,
University of Munich

LEONHARD SCHWEIBERER

Department of Neurosurgery,
University of Erlangen

RUDOLF FAHLBUSCH

Sandoz Ltd,
Basle, Switzerland

EMILIO DEL POZO

1. Kreenzlin ME, Ch'ng JC, Wood SM, Bloom SR. Can inhibition of hormone secretion be associated with endocrine tumour shrinkage? *Lancet* 1983; ii: 1501.
2. Losa M, Stalla GK, Müller OA, von Werder K. Human pancreatic growth hormone releasing factor (hpGRF): Dose response of GRF- and GH-levels. *Klin Wochenschr* 1983; 61: 1249–53.
3. Bauer W, Briner U, Doepfner W, et al. SMS 201–995: a very potent and selective octapeptide analogue of somatostatin with prolonged action. *Life Sci* 1982; 31: 1133–40.
4. Lamberts SWJ, Uitterlinden P, Zuiderwijk J, Verleun T, Neufeld M, Del Pozo E. The effects of a long-acting somatostatin analog on pituitary tumour growth and hormone secretion in rat and man. In: 7th International Congress of Endocrinology, (Quebec City). Amsterdam: Excerpta Medica. 1984: 847.
5. Guillemin R, Brazeau P, Böhlen P, Esch F, Ling N, Wehrenberg WB. Growth hormone-releasing factor from a human pancreatic tumor that caused acromegaly. *Science* 1982; 218: 585–87.
6. Thorner MO, Perryman RL, Cronin MJ, et al. Somatotroph hyperplasia: Successful treatment of acromegaly by removal of a pancreatic islet tumour secreting a growth hormone-releasing factor. *J Clin Invest* 1982; 70: 965–77.

CIRCULATING VITAMIN K_1 LEVELS IN FRACTURED NECK OF FEMUR

SIR,—Vitamin K cycle plays a significant part in calcification.[1] When glutamate (Glu) residues are carboxylated to γ-carboxyglutamate (Gla), this carboxylation is mediated by the hydroquinone form of vitamin K_1 (phylloquinone) which is oxidised to the epoxide and then reduced back to the quinone form. Vitamin K_1 antagonists inhibit the conversion of epoxide to quinone,[2] so blocking the cycle and retarding new bone formation.[3] The role of osteocalcin (bone Gla-protein) in bone formation is less clear.[4] A critical factor in the maintenance of normal bone may thus be the circulating level of vitamin K_1, and this can now be measured.[5,6] We have compared circulating levels of vitamin K_1 in normal subjects and in elderly osteoporotic subjects with fractures of the neck of femur.

Estimates of normal circulating levels were obtained from 34 controls (14 males, 20 females) aged 15–81 at Guy's, Northwick Park, and Charing Cross Hospitals. Blood was also taken at operation, within 48 h of fracture, from 16 patients (1 male, 15 females) aged 63–88 with fractured neck of femur.

20 ml blood was withdrawn into lithium-heparin tubes. The plasma was separated after minimal delay and stored at −20°C. For the normal circulating levels 10 ml or 3 ml of plasma was extracted twice with ethanol-hexane (1:2:4; plasma:ethanol:hexane); 5 ml was required for the samples from the osteoporotic patients. The dried extract was dissolved in hexane and passed through a 'Sep-Pak' cartridge (Waters Associates). The fraction containing the vitamin K_1 was eluted in a 3% solution of diethyl ether in hexane and purified by HPLC with a 'Partisil-5' column. The final stage of the assay was by HPLC, with a 'Spherisorb' octyl column with 95% methanol/50 mmol/l acetate buffer (pH 3·0) as the mobile phase.[4] The vitamin was detected either by means of a glassy carbon flow-through cell (TL5) with an LC4B amperometric detector, in the reductive mode[5] (Bioanalytical Systems), or by the use of a Coulochem model 5100A electrochemical detector, equipped with two porous graphite electrodes in series (model 5011) operated in the redox mode (Environmental Science Associates).

In the controls the mean plasma vitamin K_1 was 340 pg/ml; after exclusion of two outriders (950 and 1240 pg/ml) the mean (and SEM) was 299 (32) pg/ml.

The value in 16 osteoporotic patients with fractures was 98 (20) pg/ml. We compared this result with the data from the 10 controls at Northwick Park Hospital (274±62 pg/ml, excluding the outrider), whose ages were more comparable with those of patients with fractured neck of femur. The difference was significant ($p<0·01$). When 4 other controls aged 57, 59, 72, and 81 were included the results were significant at $p<0·001$.

The circulating level of vitamin K_1, in patients with fractured neck of femur, seems to be about one-third of normal. We cannot say whether these low values are related solely to the fracture or to the osteoporosis although, since the blood was taken at operation, it is likely that the osteoporosis is decisive in respect of the circulating level of this vitamin. These patients do seem to have a deficit of circulating vitamin K_1, and this may be significant in view of the importance of the vitamin K_1 cycle in the maintenance of normal bone and in fracture healing.

We thank Miss R. Yaakub for assistance and acknowledge support from the Percy Bilton Charity and the Arthritis and Rheumatism Council for Research.

Division of Cell Biology,
Kennedy Institute of Rheumatology,
London W6 7DW

J. P. HART

Department of Orthopaedics,
Charing Cross Hospital

A. CATTERALL

Division of Cell Biology,
Kennedy Institute of Rheumatology

R. A. DODDS

Department of Orthopaedics,
Northwick Park Hospital

L. KLENERMAN

Department of Haematology,
Guy's Hospital

M. J. SHEARER

Division of Cell Biology,
Kennedy Institute of Rheumatology

LUCILLE BITENSKY
J. CHAYEN

1. Hauschka PV, Lian JB, Gallop PM. Vitamin K and mineralization. *Trends Biochem Sci* 1978; 3: 75–78.
2. Whitlon DS, Sadowski JA, Suttie JW. Mechanism of coumarin action: significance of vitamin K epoxide reductase inhibition. *Biochemistry* 1978; 17: 1371–77.
3. Dodds RA, Catterall A, Bitensky L, Chayen J. Effects on fracture healing of an antagonist of the vitamin K cycle. *Calcif Tissue Int* 1984; 36: 233–38.
4. Price PA. Osteocalcin. In: Peck WA, ed. Bone and mineral research annual 1. Amsterdam: Excerpta Medica, 1983: 157–90.
5. Shearer MJ, Barkhan P, Rahim S, Stimmler L. Plasma vitamin K_1 in mothers and their newborn babies. *Lancet* 1982; ii: 460–63.
6. Hart JP, Shearer MJ, McCarthy PT, Rahim S. Voltammetric behaviour of phylloquinone (vitamin K_1) at a glassy-carbon electrode and determination of the vitamin in plasma using high-performance liquid chromatography with electrochemical detection. *Analyst* 1984; 109: 477–81.